The Application of a Linear Photodiode Array as a Multichannel Detector for Inductively Coupled Plasma Atomic Emission Spectroscopy

by

Scott W. McGeorge

A thesis submitted to the Faculty of Graduate Studies and Research in partial fulfillment of the requirements for the degree of PhD.

Department of Chemistry
McGill University
Montreal, Quebec
CANADA

March 1985

Application of a Photodiode Array as a Detector for ICP Spectroscopy

To my parents for getting me started and to my wife, Antoinette for seeing me to the finish

Abstract

A multichannel detection system based on a linear photodiode array (PDA) is described. The design and construction of the detection system and a rapid slew-scan computer-controlled stepping motor grating drive system is detailed. The theoretical performance of an optimized PDA system is contrasted with the performance of photomultiplier tubes. A technique is described which allows the dynamic range of the PDA to be extended by one order of magnitude towards higher light levels. A wavelength calibration procedure is outlined which results in a wavelength prediction accuracy of ± 0.003 nm. A theory for high resolution spatial image positioning is presented and the ability to detect varying degrees of spectral overlap is evaluated. Applications of the PDA to the measurement and characterization of transient signals is described.

Résumé

Un système de détection à canaux multiples, conçu à base d'un vecteur d'éléments photodiodiques (PDA), est décrit. Les détails de la conception et de la construction de ce système de détection et d'un spectromètre à réseau utilisant un moteur pas-à-pas sous commande d'ordinateur pour le balayage rapide sont présentés. Une comparaison du rendement théorique d'un système PDA optimisé et d'un système à tubes photo-multiplicateurs est présentée. Une technique pour l'accroissement, vers des intensités lumineuses supérieures, du champ linéaire utile du PDA est décrite. Une procédure de calibration est décrite par laquelle une précision de ± 0.003 nm dans la longeur d'onde peut être obtenue. Une théorie pour la haute résolution de l'emplacement d'images est présentée et la possibilité d'identifier divers niveaux de superpositions spectrales est evaluée. L'application du PDA à la mesure et à la charactérisation de signaux transients est décrite.

Original Contributions

1. A determination of the best theoretical performance of a PDA for inductively coupled plasma (ICP) atomic emission spectrometry compared to that of photomultiplier tubes, based on fundamental characterisics of the device and the ICP source.

2. A method which can be used to select and configure a data acquisition system optimized for operation with the PDA detector.

3. A calibration technique that furnishes a wavelength prediction accuracy of ± 0.003 nm using only one calibration line.

4. A theory for spatial resolution enhancement and experimental verification. The use of this theory to detect partial and direct spectral overlaps which cannot be resolved by the PDA directly.

5. The application of the PDA to temporally characterize multielement spectra produced by a transient sample introduction method. Enhancement of measurement precision of transient signals using the method of internal standardization.

Preface

In the middle 1970's there was a great deal of interest among spectroscopists regarding the use of electronic imaging sensors, like the television camera, as detectors for multielement spectroscopy. The number of publications in this area have diminished somewhat in recent years, partly due to the fact that these systems are now well characterized and, perhaps more importantly, instrument companies are getting involved to a significant degree. The linear photodiode array (PDA) has emerged as a preferred detector for atomic emission spectroscopy and several instrument companies are marketing or contemplating production of detection systems based on this technology.

When we first started working with a PDA in 1980 much of the basic characterization of the device for atomic and molecular spectroscopy had been done. However, the more we contemplated its features and limitations, the more we realized that several unexplored avenues of research remained. This thesis is a collection of several projects which explore capabilities and features of the PDA not yet addressed in the literature.

I would like to express my warmest thanks to my supervisor, Dr. Eric Salin, for his continued support and imaginative resources. Working with him has been rewarding, stimulating and a heck of a lot of fun. I would also like to thank Robert Sing, a colleague with whom I have had numerous discussions about software, hardware, and almost everthing else that is contained

in these pages. Many thanks are also due to Magdi Habib, the other member of the "original 3", for supportive discussions and contributions to my somewhat limited knowledge of electrochemistry.

I would also like to express my gratitude to Dr. Sam McClintock who provided valued insight on issues ranging from the "research approach" to the perfectly barbecued steak and to Tom Belliveau for his invaluable contributions in virtually every aspect of this work. Thanks are also due to Mr. Fred Kluck and Mr. Bill Bastian of the Departmental Machine Shop. Their help in building portions of the detection system was extremely valuable.

Table of Contents

List of Figures

List of Tables

Chapter 5

Chapter 6

1. Introduction

Inductively coupled plasma (ICP) atomic emission spectrometry (AES) has been established as a superior method for multielement and trace element analysis for many sample types and is currently in a state of rapid maturation [1]. The primary advantages of the ICP are its convenience for multielement analysis and a minimization of certain types of matrix effects. Both of these advantages stem, in part, from the high energy nature of the plasma. Because it is a high energy excitation source, the plasma provides an environment in which many elements are excited with a subsequent emission of radiation. This excitation takes place without the use of additional radiation sources, thus providing an apparent simplicity of apparatus and theory that is not present with multielement absorption or fluorescence techniques. The plasma also provides sufficient energy for the complete decomposition of many sample matrices, thus reducing the sample to an atomic state suitable for analysis without elaborate compensation or digestion techniques.

While it might appear initially that the ICP has provided an almost ideal source for multielement analysis, the reality has yet to match the rhetoric. There exist several major areas which still need substantial work for the ICP to reach its full potential. These deficiencies exist in the areas of sample introduction [2,3] and detection systems [4]. The focus of this thesis is the exploration of a new detection system for ICP atomic emission spectroscopy which utilizes a solid state

photodiode array imaging detector as the sensing device. Before detailing the research, it would be useful to review the development of atomic spectroscopic detection systems.

The characteristics of the plasma which make it such a good emission source are also responsible for many of the problems inherent in its application. The plasma achieves a very high excitation temperature and thus causes emission from many, if not most, of the components of the sample [5]. This can cause a large number of spectral lines and bands to be emitted by the plasma and the sample. Nitrogen from the atmosphere, argon from the plasma, and hydroxyl bands from water are just a few of the sources of non-analyte radiation which may appear in the analyst's spectrum [6]. Intense radiation from a component of the sample may cause extraneous (stray) light to appear at the detector [7] and, finally, overlap of spectral lines from sample components is far more likely in a high energy environment which can cause numerous lines to appear from only one element.

The analyst is therefore confronted with the problem that certain desired spectral information is convoluted with unwanted information or other desired spectral information. With most common arrangements for atomic fluorescence, emission and absorption measurements, analyte radiation from the atom cell (flame, plasma, etc.) travels the same optical path as radiation from the background and other analyte(s). Therefore, a deconvolution of the radiation following the optical path must be made. This process is carried out by the detection system. A detection system converts radiation from the

experiment into a directly measurable signal, usually electrical in nature. The system may consist of several different subsystems including one or more computers to carry out the functions of control and data acquisition.

1.1 Detection Strategies

The basic strategies for multielement detection can be categorized as follows:

1. temporal (single channel)
2. spatial (multichannel)
3. multiplex (single channel)

For each of the above detection approaches a dispersive or nondispersive optical system may be employed. Table 1.1 illustrates the breakdown of detection schemes.

Detection Scheme	Dispersive	Nondispersive
Temporal	Sequential Linear Scan	Rotating Filters
	Sequential Slew Scan	
	Image Dissector PMT	
Spatial	Spectrograph	Resonant Detection
	Direct Reader	
	Vidicon Image Tubes	
	Semiconductor Arrays	
Multiplex	Hadamard Transform	Fourier Transform
		Correlation

Table 1.1 : Detection Techniques for Atomic Spectroscopy.

Temporal devices extract individual spectral features from the entire spectrum and record this information in the time domain. This is commonly achieved by dispersing a slit image of the polychromatic radiation, using a grating or prism, into multiple monochromatic slit images. The term monochromatic in this sense refers to a very narrow range of wavelengths as opposed to a single wavelength. By rotating the dispersing optic, the monochromatic radiation can be scanned across an exit slit to be recorded by the detector. In non-dispersive systems the encoding may be done by rotating a series of bandpass filters into the optical path. This results in a time dependent isolation of the wavelength bands of interest. The image dissector photomultiplier tube (IDPMT) is fundamentally a temporal device; however, it possesses the ability to rapidly interrogate a spectral region by electronic scanning and is often referred to as a spatial, multichannel detector.

Spatial detectors are those which are able to simultaneously monitor entire spectral regions (sometimes called windows), or several discreet wavelengths. Direct readers and resonant systems are examples of the latter. The direct reader usually consists of a long focal length spectrometer in which the dispersing element is held stationary. At several positions along the exit focal plane, corresponding to the analytical wavelengths of interest, discrete detector modules are placed. Resonant detection systems are non-dispersive and employ multiple light sources such as hollow cathode lamps which are multiplexed in the time domain. This approach can be applied to

atomic fluorescence and atomic absorption spectrometry. In contrast, photographic systems, image tubes and semiconductor arrays interrogate a contiguous wavelength window. If the detector is not physically wide enough to monitor the window of interest then the dispersing optic must be repositioned for the acquisition of a new window containing the additional spectral information.

Multiplex systems use a single detector and are capable of simultaneous multielement detection. This is achieved [8] by encoding the spectral information in the frequency domain using Fourier transform methods or as a matrix of N equations in N unknowns using the Hadamard transform. The obvious advantage of the multiplex approach is that a single detector like a photomultiplier tube (PMT) can be used. Other advantages include the fact that absolute wavelengths can be determined and a very high degree of resolution is theoretically possible. Also, if the measurement system is detector noise limited the Fellget [9] advantage can be realized, but this is not normally the case in atomic spectroscopy. In fact, if background or analyte noise is dominant then multiplex methods are disadvantageous because an inherently poorer signal to noise ratio (SNR) results when compared to multichannel or temporal systems [10]. Another problem in applying multiplex methods to atomic spectroscopy is that severe aliasing can occur which can cause more overlap than existed before the encoding step. For the above reasons conventional detection systems have evolved around the temporal or spatial schemes.

1.2 Conventional Temporal Detection Systems

Earlier scanning systems consisted of a conventional monochromator with a sine-bar grating drive which could be driven at various rates or stopped at a particular wavelength. The detector was normally a PMT which was situated at the exit slit of the monochromator. The grating could be positioned at a wavelength of interest or scanned in a linear fashion to produce a complete spectrum of the sample.

Modern scanning systems utilize much faster and more precise scanning hardware such as stepping motors, synchronous motors and galvanic drive mechanisms. The rapid and accurate movement of a dispersion element, usually a grating, in a spectrometer is a non-trivial problem. Modern computer-controlled rapid slew scan spectrometers often utilize stepping motors or synchronous motors to position the grating. Stepping motors offer the advantage that they are easily interfaced to digital systems which can be controlled directly by computer. The precision and accuracy of wavelength selection is enhanced if some sort of feedback is employed that is independent of the driving motor. This is often accomplished by using an optical or electromagnetic encoder coupled to the drive shaft which generates a stream of electrical pulses as the grating is rotated [11]. Without this feedback the precision of the drive system is dependent on the characteristics of the motor and the errors introduced during acceleration and deceleration. In either case, considerable care must be exercised to ensure that

backlash in the threads or gears of the drive mechanism is compensated and that stepping motor pulses are not missed by accelerating or decelerating the drive too rapidly. This calls for relatively sophisticated software. Galvanic drive systems are extremely fast and precise for the positioning of relatively small dispersing optics. One commercial spectrometer can cover 400 nm in about one second [12] with a very high degree of precision.

These more modern systems are designated sequential slew scan (SSS) spectrometers because they can rapidly slew from one wavelength to another. In addition to their rapid scanning ability these spectrometers can reduce their scanning speed radically as the wavelength of interest approaches so that the line may be slowly profiled or simply centered on the exit slit. Because these systems are sequential in nature, they cannot observe more than one transient signal simultaneously or utilize certain ratioing or internal standard techniques [13] to enhance analytical precision. The analysis time can be estimated to be $T=N(S+A)$, where T is the total analysis time, N is the number of lines to be recorded, S is the average slew time and A is the average analysis time including any time required for background correction. For many analytical applications sample throughput is of prime importance and the analysis rate of temporal detection systems is inadequate. Of course, the prime advantage of SSS systems is that any wavelength can be selected for analysis. For unknown samples additional lines can be measured to ensure that spectral overlap is not present and for confirmation of qualitative analysis.

1.3 Conventional Multichannel Detection Systems

Multichannel detectors are systems which are capable of recording multiwavelength information simultaneously, or, are capable of scanning a multiwavelength region so quickly that the readout time can be considered to be virtually instantaneous. A number of publications have appeared [4,10,14-22] which discuss the potential applications of these systems or review their use in atomic spectrochemical analysis. Two books devoted to multichannel image detectors [23,24] have been edited by Talmi, and Pardue has published a book chapter [25] outlining applications of imaging devices for analytical spectroscopy.

The first multichannel detector used in atomic spectroscopy was the photographic plate. In fact, other than naked eye measurements, the photographic emulsion was the first detector type ever employed. Following the development of the PMT in the 1940's [26] direct reader spectrometers were developed. They used a series of PMTs arranged as discrete detectors along the focal plane of a spectrometer. Modern imaging detectors such as the vidicon camera tube and linear photodiode arrays are electronic analogs to the photographic plate. These devices have been developed within the last 20 years and are most likely to develop as the multichannel detectors of the future.

1.3.1 Spectrograph Systems

The earliest multiwavelength detection systems dispersed the input radiation using a prism or concave grating and

focussed the radiation onto a focal plane. The surface of a photographic plate or film was positioned to coincide with this focal plane. The active detection area could be made large enough to cover the entire spectral region normally interrogated in atomic work. The spectrograph is still actively in use in some laboratories, particularly for qualitative analysis.

The fine grain emulsions used today provide more than enough spectral resolution for spectroscopic applications. The biggest advantage of photographic detection is that an extremely wide spectral window can be monitored. If the required region is too wide for one plate then a series of plates can be placed side by side in the detection focal plane. Alternatively, plates of sufficient width can be prepared as needed. The photographic plate is an integrating detector and can be exposed for as long as is needed to obtain a usable spectrum. Another attractive feature of photographic plates is that they are quite inexpensive, however the cost accumulates depending on the number of spectra acquired and the associated quantity of film or emulsion used. Typically 5 to 40 spectra are recorded by one plate. This is done by exposing the emulsion as a series of horizontal strips stacked in the vertical direction.

Some of the major drawbacks to photographic detection are low efficiency (sensitivity), limited dynamic range and nonlinearity. Silver halide emulsions are sensitive to blue, violet and ultraviolet light. Sensitizing compounds must be added to the emulsion to detect light at wavelengths in the green and beyond. The spectral range of photographic plates using sensitized emulsions is from 240 nm to about 1300 nm.

Although the silver halide emulsion is sensitive down into the X-ray region, the gelatin surrounding the grains is opaque to radiation at shorter wavelengths. The spectral response of these emulsions is relatively flat from 250 to 450 nm which is highly desirable for atomic work. The dynamic range of photographic emulsions is between 1 and 2 orders of magnitude, which severely limits the ability to quantitate sample components which are present in widely varying concentrations. The total dynamic range spans approximately 8 orders of magnitude when different integration times are used. The response of the emulsion to a given wavelength of light is nonlinear, therefore, calibration plots for response vs. intensity and response vs. integration time must be prepared for quantitative applications involving very high and very low intensity lines.

Perhaps the greatest disadvantage of photographic detection is the development and processing time. The exposure of the emulsion may only consume a few minutes, but the plate or film cassette has to be physically removed from the spectrometer and developed. After development, the emulsion may be scanned by a microdensitometer which quantitates the line spacings and corresponding intensities. Computer controlled microdensitometers have been used for many years [14], however the number of steps required to transform information from the spectral domain to a human readable format increases the analysis time to well over 15 minutes per spectrum.

1.3.2 Direct Reader Systems

Following the commercial availability of reliable, high gain PMTs in the 1940's, instrument manufacturers started to employ photoelectric detection for atomic spectroscopy. A direct reader spectrometer is similar to a spectrograph except that the photographic plate is replaced by a series of PMTs. The location of spectral lines on the focal plane is very accurately determined, and, at those locations, individual detector modules are positioned. Each detector module consists of a slit assembly and a PMT. The exit slits are usually larger than the entrance slit to accommodate line shifts caused by thermal expansion or contraction of the instrument.

The greatest asset of the direct reader is that it is the most sensitive multichannel detection system available. This is due to the very high sensitivity of PMTs which exhibit an internal gain of up to 10^7 depending on the bias voltage. The best detection limits for multielement atomic emission spectroscopy are usually obtained using direct reader systems and they have also been used to advantage in atomic absorption work [27]. The linear dynamic range of a PMT is about 10^7 which is another one of its superior characteristics. Cooled PMTs are commonly used for photon counting measurements. The PMT is inherently a low noise detector due to its internal gain characteristic [28]. Spectrometers employing PMT detection for atomic spectroscopy are seldom detector noise limited.

The spectral response of a PMT is dependent on the composition of the photocathode. There are over 30 different photocathodic materials to choose from, many of which were

classified by the pioneering work of A.H. Sommer during the 1950's and 1960's [29]. The most commonly used PMTs for atomic spectroscopy employ a cesium antimonide or a bialkali antimonide photocathode. The quantum efficiency of these materials is just over 10% at 250 nm and 450 nm and reaches a maximum of 16% at 350 nm. The quantum efficiency refers to the ratio of photoelectrons generated by the photocathode to the photon flux incident on the detector. The spectral response drops off very rapidly below 250 nm and above 450 nm. Gallium arsenide photocathodes exhibit a flat spectral response from 300 nm to 800 nm but the absolute sensitivity of this material to UV radiation is not as high as alkali antimonide photocathodes.

One disadvantage of the direct reader is that it does not monitor the entire spectral window, rather, each PMT monitors a single narrow region of the spectrum. This means that there is limited flexibility of wavelength selection since the repositioning of a detector module can be a tedious and time consuming process. Therefore, alternate line selection is not an available recourse to quickly resolve spectral interference problems. Secondly, simultaneous background correction is not possible. To correct for background contributions some systems employ a refractor plate in the optical path, usually between the entrance slit and first internal optic of the spectrometer. By rotating the refractor plate through a small angle the spectrum can be shifted from side to side. The amount of spectral shifting is dependent on the angle of rotation and the thickness of the plate. If the angle of rotation is large or a

relatively thick plate is used the focal length of the spectrometer will be slightly changed. This will defocus radiation impinging on the focal plane as well as decrease the light throughput of the spectrometer. The simplest implementation of this method of background correction is to place a single refractor plate just behind the entrance slit. This means that all detector channels will simultaneously view the same degree of spectral shifting. Another method of spectral shifting involves moving the entrance slit from side to side. This also has the effect of simultaneously shifting the spectrum by the same amount at all detector modules but is not as mechanically simple as the refractor plate technique.

The output from a PMT is a current which is usually in the nanoampere to microampere range. Often, the output from each channel is integrated by a storage capacitor. If a computer is used for data acquisition this integrated charge must be converted to a voltage before being digitized by an analog to digital conversion (ADC) system. The PMT has a fast response time of about 1 ns and each channel can be independently addressed by the computer. This allows widely varying integration times to be distributed among the detector channels as required.

One of the greatest disadvantages of direct reading spectrometers is their high cost. This cost is related to the number of elements which are to be simultaneously measured since a separate PMT and exit slit assembly is needed for each spectral line. Most direct reader systems are physically large with focal lengths of 0.75 meters or more. Large focal length

spectrometers provide a higher degree of dispersion than smaller focal length systems using gratings or prisms of similar dispersing power. High dispersion spectrometers are required to ensure that spectral lines are far enough apart to accommodate the relatively bulky detector modules.

1.4 Ideal Detection System Requirements

Although SSS and direct reader systems currently enjoy wide application in atomic spectroscopy, they lack certain features which would define an ideal system. What is needed for ICP emission spectroscopy to realize its full potential is a detection system which boasts the following capabilities:

1. Simultaneous integration of multiple wavelengths;
2. Wide spectral coverage with adequate resolution;
3. High uniform spectral response;
4. High signal to noise ratio;
5. Large dynamic range;
6. Linear response;
7. Flexible channel addressing;
8. Ease of implementation;
9. Rapid data readout;
10. Stability;
11. Durability; and
12. Low cost.

Obviously these criteria can only be satisfied by a multichannel detector system.

1.4.1 Simultaneous Integration of Multiple Wavelengths

Apart from the obvious advantage of simultaneous multielement analysis, there are other advantages to monitoring information in addition to the elemental line during a determination. A multichannel detector can provide intensity information for spectral regions adjacent to the analytical line of interest and is therefore ideally suited for background correction procedures. In some cases it is possible to correct for wing or direct line overlap using ratioing techniques.

The use of internal standards in atomic spectrometry has been popular for at least half a century [30]. When the excitation conditions during analysis change irreproducibly, such as those of a direct current (DC) arc experiment, then the excitation conditions can be monitored by simultaneously observing the emission from an element which has been placed in the sample at a known concentration. This technique has been used for many years with spectrometer systems which record entire spectra on photographic plates.

It is also advantageous if the multichannel detector measures energy (integrates current) rather than power (outputs current). The SNR of integrating detectors is superior to that of power detectors of the same type because signal averaging occurs simultaneously over all channels.

1.4.2 Spectral Range and Resolution

The spectral resolution must normally be adequate to resolve the different signals of analytical interest both from

each other and from other signals which are not of interest. The spectral requirements will vary with the experiment. Multielement atomic fluorescence experiments usually produce very few lines, primarily those of the species of interest, thus the resolution requirements of a fluorescence experiment are usually not inordinately stringent. One generally observes that the resolution requirements of atomic absorption are higher than those of atomic fluorescence though usually not as demanding as those of high energy atomic emission spectroscopy. Atomic emission spectroscopy with high energy excitation sources such as the ICP, DC and microwave plasmas, arcs and sparks will often generate tremendous numbers of spectral lines from many of the elements found in the sample.

Certain photosensitive subsystems lend themselves well to a geometric characterization. In this case the photometrically responsive surface area can be considered to consist of a number of independent, individually addressable areas. These areas are independent if radiation falling on a given surface region does not cause a signal to be generated in an adjacent region.

For any fixed geometry multichannel detector there is a trade-off between resolution and wavelength coverage. The degree of dispersion must be carefully matched to the sensor geometry to provide adequate resolution. The ideal detection system for ICP analysis would exhibit a resolution of approximately 0.003 nm over a spectral window at least 400 nm wide.

1.4.3 Spectral Response

A detector system should provide the analyst with the potential for utilizing all of the spectral information provided by the experiment. In atomic spectroscopy this region extends from 800 to below 200 nm. The spectral response of a detector or detector element is dependent on the material used as the photoelectric transducer. A uniform response is desirable, but not absolutely required, because it will allow the convenient absolute determination of the spectral radiation level from the source. If the response is uniform, a single calibration at any wavelength will suffice; however, if this is not the case the device must be calibrated over the desired spectral region. For routine analytical analysis, the instrument is usually calibrated using standards and absolute spectral power levels are not determined or required.

1.4.4 Signal to Noise Ratio

The SNR is a very important measurement criterion because it indicates the precision of a determination. For the purposes of this discussion there are two major categories of noise which adversely affect detection limits and measurement precision: signal generated noise and detector system noise.

These noise sources can be further characterized as being shot noise or flicker noise. Shot noise consists of random fluctuations and is due to the quantum nature of matter and energy. It has uniform intensity over the frequency spectrum and is often called white or quantum noise. Flicker noise is nonfundamental noise and its cause is not generally well

understood. It is called pink or 1/F noise because it often displays an intensity which is inversely proportional to frequency.

One might argue that the ideal detector system should be noiseless; this is, however, not necessary. It is only necessary that the ideal system be able to detect a single photon with a reasonable degree of confidence. If the noise introduced into the experiment by the detector system is much smaller than the noise of the lowest intensity signal, then the detector system will not be a limiting factor in the analysis procedure.

1.4.5 Dynamic Range

The ideal multichannel detector system should be able to simultaneously evaluate small signals in the presence of large signals so that it will be able to provide information about the trace, minor and major constituents of a sample. Only the most ideal of samples would have analyte concentrations which result in signals of the same intensities, and in many cases it is not unreasonable to observe signal levels which differ by several orders of magnitude.

There are essentially four different dynamic range definitions that are used to describe multichannel detection systems. The most common definition is that which is applied to single channel detectors. This is the range of intensities that can be detected by a single sensor element (pixel) with a given degree of linearity and is called the single pixel dynamic

range. For multichannel detectors the "intraspectral" or "intrascenic" dynamic range is a more useful criterion [31]. This is the ratio of the most intense to the least intense spectral feature that can be simultaneously detected within a single readout. For an ideal multichannel detector this would be the same as the single pixel dynamic range.

In some commercial systems the data is acquired from the detector and stored for oscilloscope viewing or subsequent processing by an optical multichannel analyzer (OMA). If the OMA has a fixed word length then we may define the "sum" dynamic range as the largest number that can be represented by a channel of the OMA's memory. If the OMA is interfaced to a general purpose computer, then the sum dynamic range can be increased by employing multiple word storage and processing techniques.

For integrating detectors there is the "time" dynamic range. This is the ratio of the longest to shortest integration periods that can be employed for a given sensor. The shortest integration time may be imposed by the readout rate of the sensor or the maximum rate of data acquisition. The longest period may be limited by the dark current of the detector or its long term stability.

1.4.6 Linearity

While not a requirement for functionality, the ideal detector system should have a linear response. A linear response will be one in which a change in the number of photons at a given wavelength will result in a directly proportional change in the measured output. Linear response from the

detector system will minimize the calculation and calibration requirements of the analysis and may allow rapid realization of instrumental malfunctions. If the instrumental response is not linear, then calibration over the dynamic range used will be required.

1.4.7 Channel Addressing

Detector addressing refers to the methods available to interrogate individual sensor regions, or pixels in the case of discreet multichannel systems. An ideal detector would be able to randomly access any region at a given point in time. This would allow an efficient readout of spectral information which is confined to a small fraction of the total sensor region. Furthermore, these regions should be accessible in any order. This would prove valuable for transient analyses in which various analyte lines appeared at different points in time.

1.4.8 Ease of Implementation

Ease of implementation can be subdivided into three different domains: electrical, mechanical and data. If the detector can be controlled and read out by simple electronics, or better, by a small computer then the system will be easy to install, maintain, and repair. Mechanical ease of use refers to the physical ease with which the detector system can be set up and maintained. One must take into consideration the physical changes that must be made when analysis conditions change and a new set of analytical lines must be examined. Data domain ease

of use relates to both the size of the data set generated by the system and to the manipulation of this data. If numerous difficult calculations are required by the operator, then the instrument is not easy to use and sample throughput will be operator dependent if the procedure cannot be conveniently automated. The detector system may be automated and yet still require active intelligent monitoring by a well-trained operator to supervise either the mechanical or data handling aspects of the system. This type of system cannot be considered easy to use.

1.4.9 Speed of Operation

While certain measurement time requirements may be placed on the total experiment due to the SNR requirements of the experiment, the ideal detector system will not be the limiting factor in the sample throughput rate. The calculational real-time requirements of the system must be such that they can be quickly satisfied. If the detector readout and data acquisition phase is fast compared with the integration times used then the sample throughput rate will not be hampered. If complex and time consuming calculations are required to furnish an analytical result, then it may be necessary to store the raw data for future processing or employ parallel processing techniques.

1.4.10 Stability, Durability and Cost

The ideal detector system will be stable with respect to time. If this is not the case, then recalibration will be

necessary at a time interval determined by the accuracy requirements of the experiment and the rate of change of the system.

The detection system should be rugged enough to survive in the environment in which it is going to be used. Laboratories are usually relatively hostile environments with corrosive fumes and electrical transients. Instruments may find themselves in hot foundries with a high solids content in the air or in satellites or aircraft operating at low temperatures. In addition, one should be able to install and maintain the instrument without a high probability of damaging either the electronics or optics of the system.

Both the cost of the initial purchase and the subsequent operation and maintenance of the system must be taken into account. One must also consider the consequences of system breakdown with respect to loss of revenue and required time to return the system to a fully operational status. Support electronics and other ancillary components should be considered part of the detector system; these peripherals often account for a significant portion of the total system cost.

1.5 Review of Electronic Multichannel Detector Applications

Presently, the ideal multichannel detector does not exist; however, there are a few devices which incorporate many of the required features. Essentially, what is needed is an electronic analog of the photographic plate. The photographic plate can be

physically wide enough to cover the entire atomic spectral region with adequate resolution. Unfortunately, the response characteristics and processing time of photographic emulsions clearly eliminate them from consideration.

The first electronic multichannel detectors were essentially television cameras which were based on IDPMT or vidicon technologies. Within the past ten years solid state photodiode arrays (PDA), charge-coupled devices (CCD) and charge injection devices (CID) have been applied for spectroscopic measurements. Systems based on the above sensors will probably evolve as the multichannel detectors of the future.

1.5.1 Image Dissector Photomultiplier Tubes

The image dissector photomultiplier tube (IDPMT) is actually a scanning detector and not a true simultaneous, multichannel imaging device. The IDPMT is considered to be an imaging type detector because it is capable of scanning the actual image formed on its photocathode in 100 microseconds or less. At such high scan rates the IDPMT should be able to monitor transient signals from furnace sample introduction techniques, flow injection analysis, high performance liquid chromatography, and other direct sample introduction methods. The first practical image dissector was developed in 1928 by Philo T. Farnsworth [32]. The name stems from the process by which the optical image was cut up, or dissected, for time sequenced electrical transmission. In 1935 Farnsworth added an electron multiplier stage to the image dissector which enhanced its sensitivity tremendously.

The IDPMT quickly became one of the most widely used television cameras.

The operation of an IDPMT, as shown in Fig. 1.1, is very similar to that of a conventional PMT.

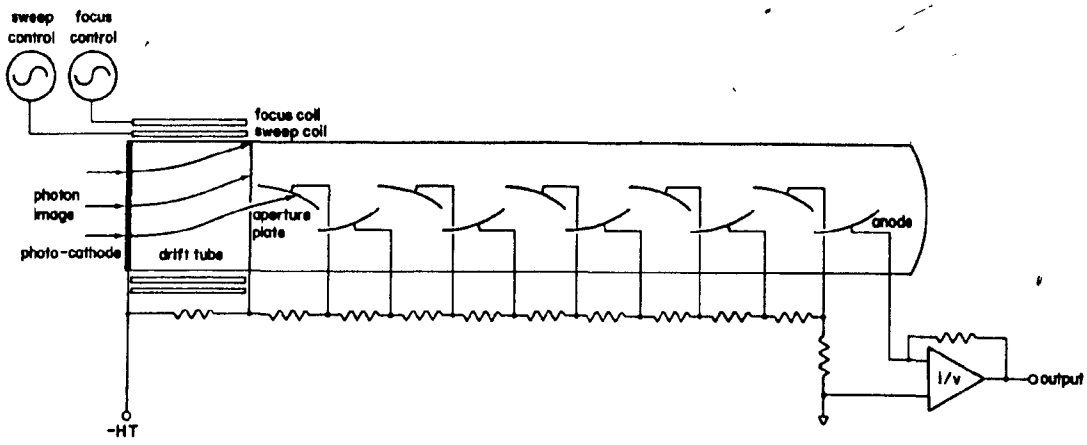

Figure 1.1: Image dissector photomultiplier tube (IDPMT)

Photons which strike the front surface of the photocathode cause photoelectrons to be ejected from the other side. These photoelectrons are accelerated toward the aperture plate which is held at a positive potential of between 200 and 600 volts with respect to the photocathode. In the center of the aperture plate is a circular or slit shaped aperture and photoelectrons which drift through this aperture will strike the first dynode of a conventional PMT electron multiplier dynode chain. By varying the voltages on the focus and sweep coils which surround the drift tube region of the IDPMT, photoelectrons which are emitted from any region of the photocathode can be steered through the

aperture. If a spectral region is focussed onto the front surface of the photocathode, any portion of the image can be interrogated by setting the appropriate voltages on the control coils. In addition, the entire optical image can be reconstructed electronically by repetitively ramping the control voltages and monitoring the output current with respect to photocathode position.

Spectrometer systems based on the IDPMT have been around since the mid 1960's [33]. An important feature of the IDPMT is that its photosensitive region is two-dimensional. for this reason a number of researchers have coupled the IDPMT to echelle optical systems [33-37]. An echelle spectrometer is one in which a grating blazed for high orders is used to disperse radiation in, say, the horizontal direction and a prism is used to separate the different overlapping orders in the vertical direction. What results is a two-dimensional "echellogram" which can be focussed onto the relatively small sensor area of the IDPMT.

With an echelle IDPMT system a wide spectral coverage of 600 nm has been achieved with reciprocal dispersions of 0.16 nm/mm at 200 nm and 0.63 nm/mm at 800 nm [35]. This dispersion is generally regarded as adequate for medium resolution atomic spectrometry. Golightly et. al. [38] reported on the use of an IDPMT as a replacement for the PMT-slit assembly of a conventional direct reader. The advantage of this approach is that the IDPMT can provide background information and can periodically re-center the analytical line which will drift across the focal plane slightly with thermal expansion of the

spectrometer.

1.5.2 Vidicon Image Tubes

The silicon vidicon (SV) is a semiconductor based two-dimensional imaging device which was initially designed for use as a television camera tube. It belongs to a group of devices which can be classified as electron beam imagers. Two comprehensive reviews of TV-type detectors have been written by Talmi [18,19] which describe the instrumentation and applicability of these devices for spectroscopic measurements.

Signal generating electron beam imagers can be divided into two groups. The first group of devices utilizes a photocathode which transduces the photon image into an electron image that is intensified and stored on a target. The target is subsequently read out by an electron beam furnishing the electronic signal. Image tubes that operate in this fashion include the orthicon, isocon, secondary electron conduction (SEC) tube, silicon intensified target (SIT) vidicon and electrostatic camera systems (ECS). The other group of devices utilize a target which functions as the photoelectric transducer and the charge storage medium. The vidicon, plumbicon and silicon vidicon belong to this second group of imagers. The earliest use of an electron beam imaging tube for spectroscopic measurements was reported in 1949 [39,40]. Orthicon tubes have been used [41-43] but these detectors have an inherently low SNR and limited

dynamic range.

The first vidicon camera tube was introduced in 1951 [44], but it wasn't until 1967 [45] that Bell Labs reported on a vidicon which used a silicon based target. The target material of a vidicon must exhibit a relaxation time of about 1/30 second [46,47] if it is to "store" the optical image long enough to be read out by the scanning electron beam. Materials with bandgaps below 1.8 eV cannot meet this specification at room temperature and silicon by itself, with a bandgap of 1.08 eV, is six orders of magnitude too low in bulk resistivity at room temperature to be used as a photoconductive target [48]. Fortunately, a reverse-biased p-n junction diode can be designed which provides a room temperature charge storage time long enough to be used as a vidicon camera tube element. The silicon p-n photodiode has a wide spectral response, high quantum efficiency, linear transfer characteristics and a response time of less than 10 microseconds. Ingenious fabrication techniques have aided in the design of targets which exhibit improved characteristics [49]. Other materials with bandgaps too low to be used as target elements can be used as long as they can form junction diodes. Vidicon camera tubes employing phototransistor storage elements have also been designed and constructed [50].

The operation of the SV is illustrated in Figure 1.2.

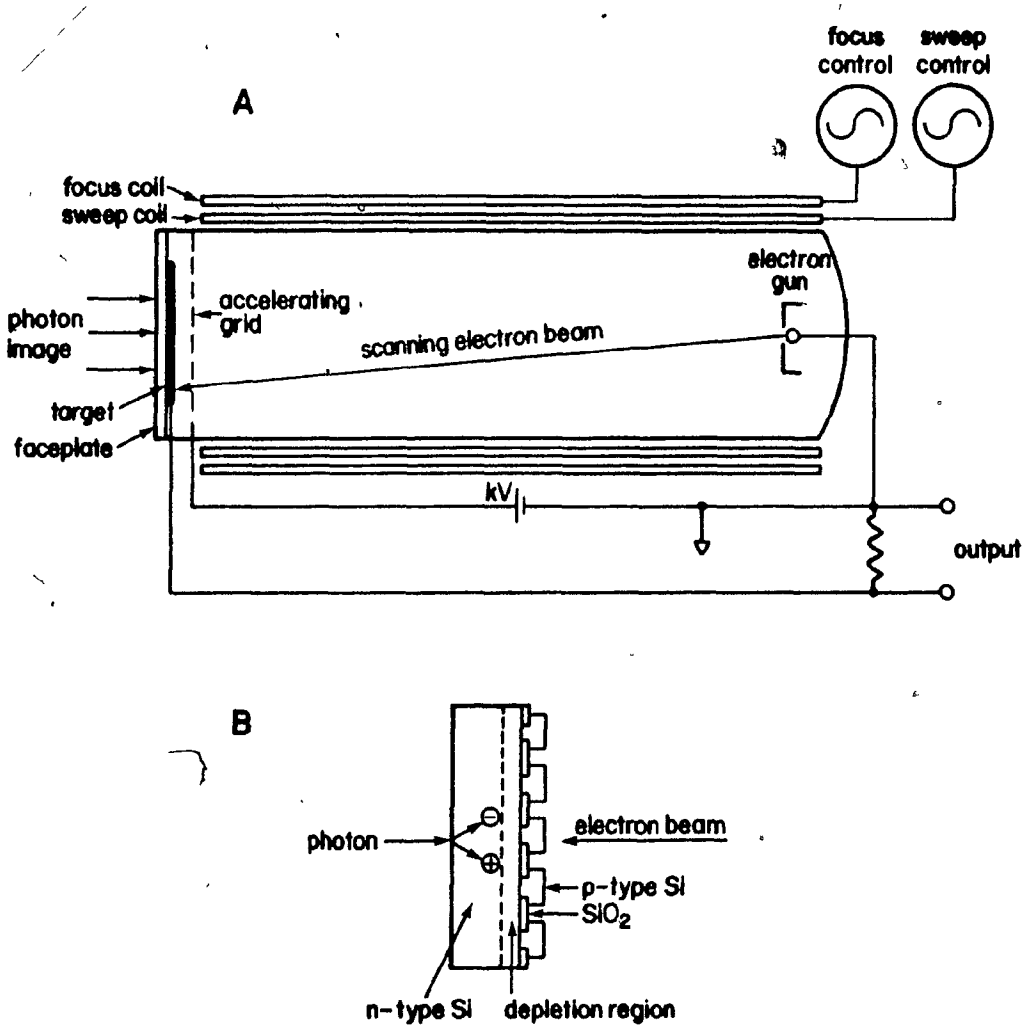

Figure 1.2: Silicon vidicon (SV) image tube.

The target is analogous to the photocathode of a PMT and consists of a wafer of n-type silicon, one side of which is populated by a two-dimensional mosaic of p-type silicon islands. Typically the p-n junctions are organized as a two-dimensional array with a center to center spacing of the diodes of about 10 micrometers. During normal operation of the vidicon an electron beam is swept over the p-type islands and charges them to a negative potential. The n-type substrate is held at ground potential and the region between the islands is shielded from the electron beam by a coating of silicon dioxide. Therefore, the charged islands form a two-dimensional array of reverse-biased photodiodes

which act as miniature storage capacitors. These photodiodes can be discharged by electron-hole pair production in the n-type substrate. The two mechanisms for electron-hole production in the semiconductor are thermal population of the conduction band (leakage or dark current) and absorption of photons of energy greater than 1.1 eV (ie. wavelengths less than 1100 nm).

The electrons generated by either of these two mechanisms discharge rapidly to ground but the holes migrate to the negatively charged p-type islands where they are annihilated. This electron-hole recombination process serves to deplete the charge stored on the p-type islands. The more intense the photon flux is on one side of the wafer the greater is the charge depletion of the photodiodes on the opposite side. Statistically, most of the holes that reach a particular diode will have travelled the shortest distance across the wafer so that an intensity distribution of photons on the irradiated n-type side will generate a corresponding charge pattern on the photodiode surface. When the electron beam is systematically scanned over the p-type islands the amount of current required to recharge the photodiodes is a measure of the intensity distribution of the image.

The above discussion assumes that only one sweep is required to fully restore the pixels. In fact, the vidicon suffers from a phenomenon called lag which refers to the incomplete recharging of the photodiodes after a

scan. To completely recharge the photodiode mosaic, several scans may be required. This is a technical problem which is inherent in the operation of the vidicon detector and is one of its drawbacks.

The design, construction and evaluation of detection systems employing vidicon cameras has been discussed by many research groups [51-64]. It was quickly realized that the limiting resolution of the SV was determined by the width of the electron beam [51] which covers several pixels at any given time.

Felkel and Pardue evaluated a vidicon based echelle spectrometer system [52] for multielement flame atomic absorption spectrometry. In contrast to a previous report [53], where a conventional optical system was used, the detection limits for lines below 300 nm were relatively poor. The discrepancy was ascribed, in part, to the decreased light throughput of the echelle optics. A comparison between an IDPMT and an SV [54] revealed that the IDPMT was shot-noise limited at low light levels while the SV was essentially preamplifier noise limited. Based on the inherently greater sensitivity of the IDPMT, its detection limits were a factor of 20 lower than those of the vidicon detector.

In an attempt to gain improved sensitivity using vidicon systems Howell and Morrison employed a silicon intensified target (SIT) vidicon [55]. A SIT vidicon is a SV tube with a photocathode based electrostatic intensifier prior to the silicon photodiode mosaic. The photocathode is operated at a bias voltage of 5 to 10 kilovolts and forms an electron image

which is stored by the silicon photodiode array. The gain of the SIT tube is controlled by the photocathode bias voltage. It was determined that the SIT was a factor of 100 more responsive than a conventional SV below 350 nm. A comparison of detection limits for 23 elements revealed that the SV results were about 10 times higher than those for a PMT, while above 380 nm the detection limits for the SIT vidicon were essentially the same as for the PMT.

A SIT vidicon has been used for ICP emission spectrometry [56]; however, since the ICP produces such complex spectra, a high resolution spectrometer was required. The detector window was only 5 nm wide but spectral interferences were minimized while still allowing for simultaneous background correction. The fact that it was unreasonable to expect that the entire atomic region could be viewed simultaneously using conventional optical systems prompted Bush et. al. [57] to suggest that perhaps the best solution would be to rapidly slew from one wavelength region to another. The electrostatic image intensification stage of the SIT vidicon provides the capability of time gating the optical information impinging on the photocathode. This ability, in conjuction with the two-dimensional nature of the detector has enabled the measurement of time and space integrated spectra [65]. The readout flexibility of the SIT vidicon allowed time gating for submicrosecond periods and time integration for up to 20 seconds. Spatial information was integrated over distances of 2 mm or resolved on the order of 100 µm.

Several accounts have been published describing analytical determinations of "real samples" [66-69]. The determination of electrolytes in serum [66,67] was found to be a good application of a SV detector because the analysis lines for sodium and potassium are in the visible region of the spectrum where the vidicon is more sensitive. A further advantage was gained due to the rapid sample throughput afforded by multichannel operation. A judicious selection of the wavelength window [66] enabled two Na lines to be viewed in the first order and a Ca and two K lines to be viewed in the second order simultaneously. Other real sample measurements include a determination of trace metals in lubricating oils [68] and potable water [69].

A series of papers detailing novel applications have illustrated the capabilities of imaging detection systems employing SV hardware [70-76]. The enhancement of analysis precision has been demonstrated using spectral stripping [70] and internal standardization [71]. Combining both techniques has resulted in reducing a positive error of 40 to 50% in the analysis of Mg in blood serum to less than 3% using Mn as the internal standard.

Innovative instrument modifications have enhanced certain systems [72,73]. In one case [73] a high frequency signal was superimposed on the lower frequency horizontal ramp scan which resulted in the generation of first derivative spectra directly. The same authors tackled the trade-off problem between spectral range and resolution [74] by stacking 6 mirrors at different angles in a Czerny-Turner monochromator. The result was a resolution of 1 nm from 200 to 800 nm, however, the dynamic

range was severely degraded due to stray light from the multiple mirrors. A totally different solution to the same problem employed multiple entrance slits [75] to simultaneously focus several 40 nm windows onto a SIT vidicon.

1.5.3 Linear Self-Scanning Photodiode Arrays

The silicon photodiode array (PDA) was introduced about 20 years ago and since then has undergone considerable development. It was apparent that if these new solid state arrays were to compete with vidicons and other electron beam imagers, they would have to be able to integrate light flux in a comparable manner. Weckler was the first to describe a photodiode array operating in the charge storage mode and later published a description of arrays of MOS transistors which could integrate photon flux [77]. Even at this early stage of development it was realized that these solid state devices could exhibit a wide dynamic range. A comprehensive review of silicon photodiode arrays which discusses the historical development of these sensors, their theory of operation, and various non-spectroscopic applications has been published by Fry [78].

A schematic diagram of a linear PDA is shown in Figure 1.3. The charge integration pixels of photodiode arrays are reverse biased p-n junctions which operate in an analogous fashion to the pixel elements of the vidicon. However, instead of being charged to an initial potential by a scanning electron beam, the photodiodes of the PDA are individually charged via metal-oxide-semiconductor (MOS) transistor switches. In self-scanning PDAs

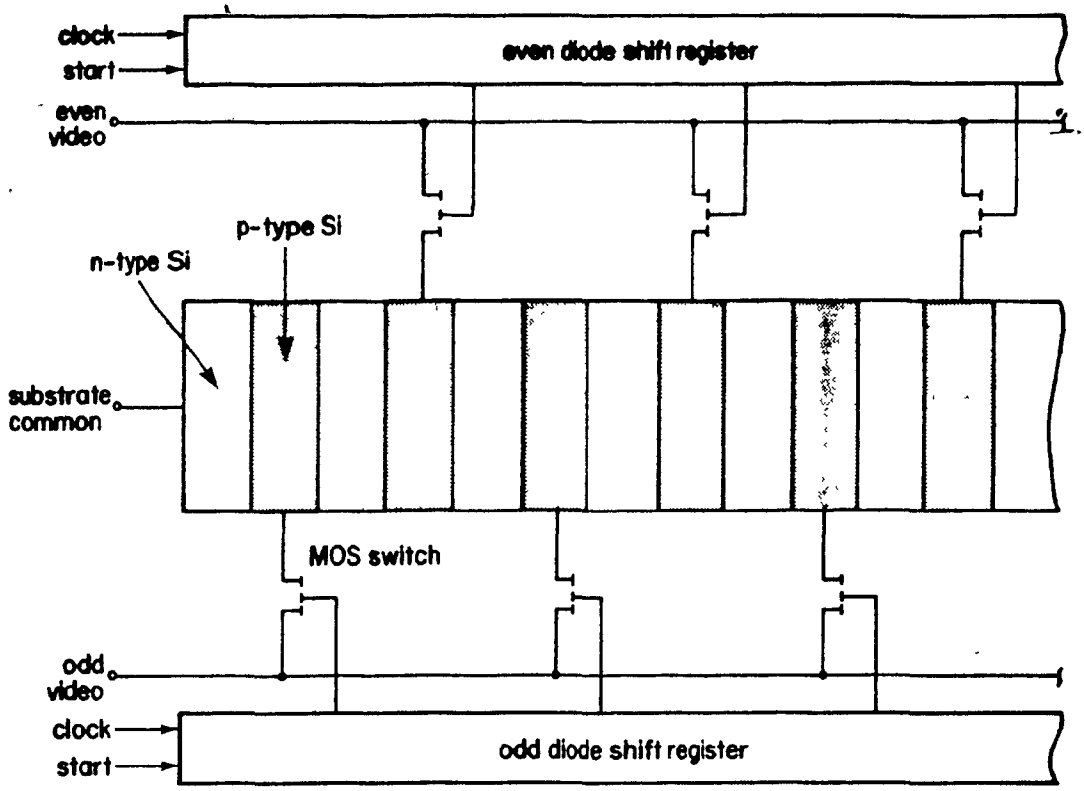

Figure 1.3: Linear photodiode array (PDA).

the charging process is controlled by an on-chip shift register which sequentially connects each photodiode to the charging potential by turning on the MOS switches in a linear sequence. Once the reverse-biased diodes are primed there are two ways in which the stored charge can leak across the junction. At room temperature a small number of electron-hole pairs exist in the conduction band which serve to deplete the stored charge. This process is called dark leakage. In addition, photons with energy greater than 1.1 eV (wavelengths less than 1100 nm) which are absorbed by the semiconductor are capable of populating the conduction band with electron-hole pairs. The greater the flux impinging on a charged photodiode the greater the photon-induced current across the junction. Therefore, the quantity of charge required to reset the photodiode to its initial potential is a

measure of the amount of light which was integrated in the previous scan frame. The PDA readout consists of a serial train of charge pulses which are produced as the shift register sequentially accesses the photodiodes. Due to the sequential self-scanning nature of the PDA, it is not possible to randomly address the various pixel elements as is possible with scanning electron beam imagers.

The maximum integration time of the PDA pixels is limited by the magnitude of the thermally induced dark current and the capacitance of the p-n junctions. At room temperature charge depletion, or saturation as it is commonly referred to, occurs in about 1 second for a typical PDA device. Since many spectroscopic applications require integration periods of 10 seconds or more, it is often necessary to cool the PDA to reduce the dark current. PDA sensors used for astronomical spectroscopy have been cooled to liquid nitrogen temperature permitting integration times of several hours [79]. For atomic measurements simple thermoelectric refrigeration is generally adequate. For one of the commonly used PDAs it has been found that the dark current decreases by a factor of 2 for every 6.7 C of cooling [31].

The maximum spectral response of silicon photodiodes occurs between 700 nm and 800 nm depending on the particular device [78,80]. This is related to the fact that the absorption coefficient of silicon is inversely proportional to wavelength. High energy photons are absorbed very near the surface of the silicon in the p-type region of the photodiode. Electron-hole

pairs generated in this region produce a photocurrent only when electrons, the minority carriers, flow from the p- to the n-type silicon. Since there already exist a large number of holes in the p-type silicon the photon induced current is reduced due to recombination of generated electrons with already existing holes. Low energy photons which penetrate deeper, into the n-type silicon, produce a photocurrent only when generated holes cross the junction into the p-type silicon. Recombination diminishes this current in exactly the same manner as above. Photons of medium energy (600-800 nm) penetrate into the depletion region and immediately give rise to a photocurrent which is not hampered by recombination effects.

One of the first studies of solid state multichannel arrays for atomic spectrometry was published by Boumans and Brouwer [81]. Phototransistors were used instead of photodiodes because of their gain characteristic; however, instead of being used in the charge storage mode like the Reticon self-scanned PDA, the phototransistors were forward biased. The resulting photocurrent was passed through a high resistance to provide an output voltage. This phototransistor technology was later abandoned by the same authors in favour of a photodiode array [82] because the transistor output was non-linear with respect to incident light flux. The photodiodes were also forward biased and exhibited a single pixel dynamic range of 10^3 when synchronous amplification was employed.

The first evaluation of a commercially available self-

scanning PDA for spectrochemical analysis was presented by Horlick and Codding [83]. They used a 256 element linear array. The individual pixels were only 25 by 25 micrometers in size, however, the photodiodes were designed to operate in the charge storage mode. Using variable integration times in conjunction with neutral density filters the linear dynamic range was found to be 3.5 orders of magnitude when the 632.8 nm emission of a He-Ne laser was monitored.

In 1976, with the availability of 256, 512 and 1024 element arrays, Horlick published a more comprehensive characterization [84] of PDA sensors for atomic spectrometry. For this study the arrays were cooled using a Peltier cooler to about -15 C. The electronic background was determined to consist of the expected dark current combined with a fixed pattern signal. Fortunately this pattern was highly reproducible and could be eliminated by simple background subtraction. The PDA sensors did not exhibit lag or bloom, two problems inherent to vidicons.

One of the best discussions of the operational characteristics of earlier arrays was an evaluation of a 1024 element device for high dispersion panoramic astronomical spectroscopy by Vogt et. al. [79]. This paper includes an excellent discussion of the prominent noise sources and furnishes a detailed description of the detector system components with special attention to design considerations for optimizing the electronic performance of the PDA.

Recently, E.G. and G. Reticon Corp. has marketed a new 1024 element linear self-scanning photodiode array which was designed

expressly for spectroscopic applications. The new device, an RL1024S PDA is similar to earlier products with the important exception that the height of the diodes has been increased to 2.5 mm. Since the pixel elements are 25 micrometers wide this results in an aspect ratio of 100:1, which is comparable to that of a conventional polychromator entrance slit. This device was first evaluated for its multichannel spectrometric utility by Talmi and Simpson [31] using an E.G. and G. PARC optical multichannel analyzer. The UV response of the PDA was excellent with a quantum efficiency of 35 to 50% from 200 to 400 nm. The new PDA was found to be lag-free; each diode was fully recharged in less than 1 microsecond. No significant blooming was observed when two adjacent images with a 1000:1 intensity ratio were recorded. The geometric accuracy of the individual diode spacings was so good that the wavelength accuracy of a measurement would be limited by the stability of the source. The PDA was found to be linear over 4 orders of magnitude. The intrascenic dynamic range appeared to span 3 orders of magnitude and was limited by stray light caused by a combination of the wedge filter used for the experiment, the focussing lens and reflections between the surface of the PDA and the quartz faceplate.

Simpson has produced equations [85] for the random noise of self-scanning arrays which includes the shot noise of the dark current, preamplifier noise and the reset noise of the pixels. The fixed pattern noise was not considered because it can be removed by background subtraction. The results of applying these calculations indicate that the taller S-series array is only

slightly noisier than earlier devices and, due to its larger aperture, is theoretically capable of detecting much smaller intensities.

It is possible to enhance the sensitivity of a PDA by coupling a microchannel plate image intensifier to the face of the sensor. Commercially developed systems exhibiting adjustable gains of 10^3 to 10^4 [86,87] are available. The intensifier will degrade the resolution of the PDA but the resulting resolution is not strongly dependent on the magnitude of the gain.

Several publications have addressed the applicability of PDA detectors for atomic absorption spectrometry [88-90]. It has been pointed out [88] that the combined absorbance measurements from all analyte lines of a particular element found in a given window can be used to generate an analytical curve. In addition, the linear concentration range can be extended if two lines of different sensitivities for a given element fall within the spectral range of the detector [89]. The more sensitive line will exhibit linear behavior towards lower concentrations while the less sensitive line will extend the linear range towards the upper concentration region. A detailed examination of the noise characteristics of a PDA based atomic absorption spectrophotometer by Codding et. al. [90] has revealed that the system was readout noise limited for all elements studied except one. However, the PDA was used in conjunction with an evaluation board supplied by the manufacturer which does not employ the highest quality

electronic components and may have contributed to the detector readout noise. Normally all of the diodes in the peak are summed to obtain the peak intensity; however, if the wing diodes are less than $1/(2)^{1/2}$ the height of the peak diode(s) then they will contribute proportionately more noise than signal and should therefore be excluded from the peak.

The first application of a PDA to simultaneous multielement emission analysis [91] involved the measurement of 7 elements by DC arc spectrometry in 1974. It was found that an internal standard was not required to produce linear calibration curves because the simultaneous background correction capabilities of the PDA were effective. The slopes of log-log plots of intensity vs. concentration deviated from unity which suggested that considerable self-absorption was occurring. A qualitative study of C,H,N and O emissions in the red and near infrared has been made [92] using an ICP as the excitation source. PDA detectors should be able to provide good detection limits for these species because their analysis wavelengths lie in the region where photodiodes are most sensitive. It was pointed out that a spectral window of 80 to 100 nm could be viewed because the spectra were fairly simple and spectral overlap was not a problem.

The most comprehensive discussion of PDA detection for multielement ICP emission spectrometry has been published as a book chapter by Grabau and Talmi [93]. Three multichannel detectors were used including a SIT vidicon, an RL1024S photodiode array and a microchannel plate intensified photodiode array. The PDA systems were computer controlled and employed

very high quality amplification electronics. The SIT was not cooled while the PDA detectors were cooled to -20 C with a precision of 0.002 C. Using a 14-bit ADC the single pixel dynamic range of the PDA was found to be 1.6×10^4. When variable integration times were employed an overall dynamic range of 1.6×10^7 was achieved which is similar in magnitude to the dynamic range of the ICP.

The same authors demonstrated a spectral stripping technique identical to that discussed by McGeorge and Salin [94] which can correct for direct spectral overlap. The detection limits for 17 elements whose analysis lines ranged from 193.7 nm to 403.0 nm were determined using the three multichannel detectors and contrasted with PMT values which were obtained using a 10 s integration period. SIT detection limits were about one order of magnitude worse which is expected based on the fact that the SIT was not cooled. The intensified PDA detector provided virtually identical detection limits for integration periods of 16 s. However, the most striking result was that the unintensified PDA also yielded comparable PMT detection when variable integration times were used. Integration times as long as 164 s were required for lines below 220 nm and 16.4 s integrations were adequate above 300 nm. The explanation for this PDA performance was based on the SNR considerations for both detectors. The ICP/PMT detection limits are relatively wavelength independent because the measurements are always either source shot or flicker noise limited. In contrast, the ICP/PDA detection limits get worse at lower

wavelengths because the line intensity decreases but the noise is readout limited, or essentially constant. Fortunately, a nearly linear improvement in SNR can be obtained by increasing the integration time.

One of the most widespread uses of the PDA sensor for applications other than multiwavelength spectroscopic measurement involves rotating the detector by 90 degrees in the focal plane so that the array of photodiodes is parallel and coincident with the dispersed line image. This enables the measurement of vertical spatial profiles with very high spatial resolution. While vertical profiles of analyte emission in flames have been studied [95], most profiling work has been carried out using the ICP as the source.

Profiles obtained for atom and ion lines in the ICP have shown that ion lines generally peak higher in the plasma than atom lines [96]. Lines which peak low in the plasma were found to be spatially affected by forward power and nebulizer flow rate and have been categorized as "soft" lines [97]. Lines which peaked high in the plasma and were spatially insensitive to operating parameters were called "hard" lines. An understanding of analyte spatial behavior has helped to clarify a number of inconsistencies between results published by different laboratories which have tried to categorize intensity variations as a function of varying operating conditions [98]. Matrix effects are also important [99,100] which is illustrated by the dramatic enhancement of the Ca 422.7 nm atom line when high concentrations of an easily ionizable element such as Li is present while the 393.3 nm ion line is affected minimally.

Radial profiles have been obtained by Blades and Horlick [101] after converting lateral intensity measurements into radial information using the Abel inversion technique. These experiments have shown that the region of maximum analyte intensity in the ICP is confined to a doughnut shaped region which ranges from 0 to 1 mm radially outward from the center of the discharge.

Other novel applications of linear PDA detectors include spectral characterization after implementing AND and XOR (exclusive OR) logic operations [102] and spectral enhancement using cross-correlation techniques [103,104]. Temporal information has also been obtained for DC arc transient signals [105] enabling the selection of an optimal observation time. Transient spectra have also been measured for laser microprobe [106] and high energy laser ablation [107] sampling methods.

1.5.4 Charge Coupled and Charge Injection Devices

The concept of charge coupling was introduced in 1970 [108] and has since developed into a well defined technology which is very amenable to imaging applications. The charge coupled device (CCD) is comprised of a one or two-dimensional array of gate electrodes on a semiconductor substrate. The electrodes can be individually charged to a potential. This attracts charge carriers to shallow regions below the gate in the semiconductor substrate. Light incident on the device is absorbed and generates electron-hole pairs. Holes (or electrons) are attracted to the regions under those gates which

are held at an appropriate potential. The pockets of accumulated charge can be shifted from one gate to another by multiphase clocking of the gate electrodes, which eventually results in pockets of charge being shifted onto the video readout line of the device. Detailed descriptions of the operation of CCDs [109,110], their sensitivity and resolution characteristics [111] and design considerations [112] have been published previously.

Ratzlaff has described a spectrophotometer based on a CCD detector [113] which incorporated a linear array of 1728 elements on 13 micrometer centers. The device did not exhibit lag or bloom, unless saturated, and could be read out in 8 ms. Unfortunately the device was relatively insensitive to UV radiation severely limiting its applications to atomic spectroscopy.

The limited sensitivity of CCD arrays is well understood [114] and is due to the fact that UV photons are absorbed at or near the gate electrode surface. This inhibits minority carriers from reaching the electrode potential wells. Commercially available "backside" devices are illuminated from the semiconductor side, but these arrays normally include a glass window which is opaque below about 350 nm. Denton has experimented with a custom prepared CCD [114] which had the glass window etched away and found that the quantum efficiency was enhanced from less than 5% to about 30% at 300 nm. Various sensitization techniques have been discussed [115] for improvement of CCD UV response, but applications to atomic spectroscopy have not been presented in the literature.

CCDs are capable of high SNR performance, especially if pixels are grouped together to form a "super pixel". This necessarily results in a degraded spatial resolution which may be undesirable if complex spectra are being measured. The dynamic range of CCD arrays is limited by the on-chip preamplifier. This is disadvantageous for wide dynamic range spectral sources.

Recently, the charge injection device (CID) has been demonstrated as having excellent characteristics for atomic spectroscopy [116]. The CID offers a quantum efficiency ranging from 8 to 10% in the UV. Two dimensional CIDs can be fabricated providing for random pixel addressing. This poses a direct advantage over most solid state imagers where the entire device must be read out in a sequential fashion. However, the single most attractive new feature of the CID is that selected pixels can be read out nondestructively. Therefore it is possible to monitor the signal accumulating on a pixel so that it can be read out just before is saturates. The SNR can be further increased by repeatedly reading out the pixel nondestructively to gain a signal averaging improvement if the readout noise is random.

The dynamic range of the CID can be extended by mixing destructive with nondestructive readouts. Preliminary detection limit data show that for wavelengths longer than 400 nm the CID is as good as a PMT when used in the same spectrometer configuration. For wavelengths in the UV the detection limits for the PMT are about a factor of 10 lower.

Since the CID is normally manufactured in a two-dimensional format, echelle dispersion systems can be employed to provide a wide spectral window. Using an echelle system with a 244 X 248 pixel CID [116] a resolution of 0.1 nm has been achieved over a spectral window ranging from 200 to 800 nm. Newer devices are expected to offer up to 500 X 500 pixels. This will provide enough detector area to achieve medium to high resolution for atomic spectroscopy.

1.6 Summary of Multichannel Detector Characteristics

The characteristics of the detectors discussed above are summarized in the following sections. The discussions are based on the ideal detector criteria outlined in section 1.4.

1.6.1 Image Dissector Photomultiplier Tubes

The IDPMT has been shown to be an acceptable imaging detector for atomic spectrometry. It is not capable of simultaneous multiwavelength integration; however, using an echelle optical system wide spectral coverage with adequate resolution can be obtained. The important trade-off between resolution and spectral range is determined primarily by the size and shape of the photoelectron aperture. A small circular aperture provides the most electronic resolution elements but may require longer integration times for photon shot noise limited measurements.

The IDPMT exhibits excellent sensitivity based on the fact that it employs the high gain, low noise electron multiplier

dynode chain of a conventional PMT. The dynamic range of the image dissector can match those of standard PMTs spanning 6 or 7 orders of magnitude. This is misleading however, because it refers to the least intense and most intense single image that can be detected according to the inherent transfer function of the device. The intrascenic dynamic range of the IDPMT can be as low as 100:1 depending on the amount of veiling glare and the physical proximity on the photocathode of images of different intensity.

The IDPMT can statically address any region on the photosensitive surface or continually scan over a portion of it. Unfortunately, the image dissector is not an integrating device and can only accumulate spectral information while it is addressed by the deflection coils. This shortcoming is partially offset by the excellent sensitivity of the device compared to other unintensified detectors. Partial integration can be achieved using what is called a smoothing dissector [18].

A detection system based on the IDPMT will be relatively expensive compared with other alternatives. The cost of the tube itself is about $10,000. This does not include the scanning and data acquisition circuitry and computer hardware. If spectral information is encoded as an echellogram the software required to interpret the spectrum will be complex. This eliminates the possibility of using a small inexpensive microcomputer as the main processor. Most of the IDPMT systems to date have employed minicomputers for data acquisition and control. Using multiple IDPMTs in a direct reader configuration

would be prohibitively expensive.

1.6.2 Vidicons

An important feature of the vidicon which distinguishes it from the IDPMT is that it is an integrating detector. Therefore, unlike the IDPMT, the vidicon is a true simultaneous multichannel sensor. While the speed and sensitivity of the IDPMT may compensate in some circumstances, it is reasonable to expect that under certain conditions true simultaneous multiwavelength information collection will be advantageous. One example of this is an application where transient spectra were recorded by a carbon-cup sample introduction and vidicon detection system [76]. Imaging detectors that are integrating in nature are particularly suited to the measurement of transient signals and many sample introduction methods now exist for atomic spectrometry which produce such time dependent spectra.

With conventional linear dispersion spectrometers vidicons have been used to simultaneously monitor regions from 5 to 40 nm in width. The only way to cover the 200 to 400 nm range, where most atomic lines are found, with moderate resolution appears to be by using an echelle dispersion system. Unfortunately, the decreased light throughput can severely degrade detection limits. The spectral response of an SV has been shown [55] to start at about 250 nm and rise sharply to a maximum near 400 nm. From 400 to 800 nm the response curve is relatively flat and then drops off to zero at 1100 nm. The spectral response of a SIT vidicon is less constant but is one to three orders of

magnitude higher than the unintensified device above 350 nm. The photocathode of a SIT vidicon is curved so an optical fiber faceplate is required. This faceplate severely attenuates light below 350 nm [117]. Sensitivity in the UV region can be enhanced by coating the faceplate with an organic fluorescing compound (scintillator) which will result in a quantum efficiency of 1 to 2% down to about 100 nm. The response of a typical SV is linear over about 4 orders of magnitude [60].

The quantum efficiency of silicon ranges from 10 to 80% in the UV to near IR region. This is superior to that of typical PMT photocathodic surfaces in this region. However, because the readout noise of a vidicon is about 1800 electrons RMS, the smallest detectable signals are a few thousand photons in magnitude [20]. The SIT vidicon, with a gain of 2000 to 3000, can detect a few photoelectrons. Using this device it is possible to approach the detection limits achieved using a PMT for lines which are in the visible region of the spectrum. For the majority of analytically useful lines which occur in the UV the SIT has been shown to be 1 to 2 orders of magnitude inferior to conventional PMT detectors. It should be possible to approach the detection capabilities of a PMT using the intensified SIT (ISIT) vidicon but this has not yet been sufficiently explored.

The imaging resolution of all vidicons is limited by the diameter of the scanning electron beam and the size of the target. At any given instant in time the beam partially or fully impinges on about 10 pixels. In practice a number

of pixels are grouped together by selective addressing where each group represents a channel. The addressing accuracy of a typical SV is better than 3% of the sensor area with a precision of better than 0.1% [54]. The power and flexibility of a system is related to the powerful addressing capabilities of the device when coupled to a computer system. The channels can be scanned sequentially, randomly or by any mixture of the two modes. Random access addressing poses the advantage of reading out only those spectral regions of interest, ignoring all other information. The resolution of the detector can be severely degraded by a phenomenon called blooming. This occurs when a high intensity image causes charge depletion over a much larger area of the photodiode mosaic than the actual area of the image. This is particularly disturbing if an intense spectral line is adjacent to a weaker but analytically useful line.

The silicon target is the major source of dark current in all types of vidicons and therefore the detector must be cooled if integration periods longer than about 100 ms are to be employed [20]. Unfortunately vidicons are mechanically difficult to cool [93] and exhibit degraded linearity at lower temperature. If the detector is successfully cooled, the lag is greatly increased [117]. This requires careful signal erasure and target preparation. Attempts have been made [118] to eliminate lag by employing pulsed illumination techniques. Unfortunately, vidicons exhibit lag by nature and no degree of readout control can eliminate this effect.

Like the IDPMT the vidicon requires rather sophisticated control circuitry compared to the simpler self-scanning solid state arrays. This increases the cost and complexity of the computer interface. Although it is feasible to use a microcomputer system, most interfaces to date have relied on minicomputers. The readout from the vidicon can be very rapid but can be conveniently digitized using conventional amplification and acquisition electronics. To avoid being readout limited it is wise to use an ADC with at least 12-bits of resolution. A packaged vidicon system including the detector, a controller, and an OMA configured for operation without an external computer system will range in price from about $30,000 to $50,000 (U.S.) depending on the actual components selected.

1.6.3 Linear Photodiode Arrays

Linear self-scanning photodiode arrays satisfy some of the characteristics outlined earlier for an ideal multichannel detector. One of the major advantages of PDAs is that they are solid state devices. For this reason they are more compact and rugged than detectors incorporating a tube structure. Also, because PDAs are fabricated the same way as other large scale integrated (LSI) circuits, they should be less expensive. Unfortunately, until the demand for these devices increases they will remain expensive. A 1024 element PDA for spectroscopic applications costs between $2000 and $4000 (US). With a commercially available OMA and detector controller, a packaged

PDA system will range in cost from about $20,000 to $50,000 (US).

PDA sensors exhibit true simultaneous multichannel integrating characteristics in much the same way as vidicon image tubes. The geometric registration of the individual photodiodes is extremely precise, and, because the pixels do not bloom, the spectral resolution of the array is dependent only on the optical fidelity of the spectrometer. However, since photons which fall between diodes can be collected by either pixel the best resolution is about half that of a conventional system which uses a PMT and exit slit arrangement.

The one-dimensional nature of linear PDAs does not permit the use of conventional echelle dispersion, which limits the spectral coverage to a maximum of about 20 nm if medium resolution in the atomic sense is to be achieved. For ICP spectrometry it has been argued that the spectral range should be limited to about 8 nm [93] to minimize spectral overlap. Recently, Reticon has started to manufacture a 4096 element PDA which increases the range by a factor of four; however, the aspect ratio of the pixels is only 34:1 which reduces the sensitivity and SNR of the array when compared to the RL1024S device discussed in this report.

The spectral response of the PDA is superior to that of vidicon and CCD detectors in the UV with a quantum efficiency of 40 to 50% from 200 to 400 nm. Although PDA systems are generally readout noise limited, their high spectral response coupled with on-chip integration has resulted in detection limits for lines in the UV which match those obtained using a

PMT [93]. A discussion of PDA noise considerations [119] has indicated that the RL1024S device readout noise will degrade detection limits below 225 nm if the ICP flicker factor (precision) is 3% or below 300 nm if the flicker factor is 0.2% compared to a PMT for 1 second integrations. Greater sensitivity can be achieved using commercially available microchannel plate intensifiers which result in PMT-like detection limits for similar integration periods.

The single pixel dynamic range is at least 10^4 while the time dynamic range can be as high as 10^7. Unfortunately the intrascenic dynamic range is inherently less than the single pixel value due to veiling glare within the detector enclosure. Stray light can be reduced by removing the PDA window and placing the detector in a suitable enclosure which is coupled directly to the spectrometer. Good linearity can be achieved over the full dynamic range of the device.

One of the disadvantages of linear self-scanning PDAs is that the pixels are not independently addressable. Thus, the entire array must be read out to access the spectral regions of interest. There is no reason why future PDAs cannot be designed differently to allow for addressing flexibility. A method for pseudo-random access has been discussed [120] which involves rapidly clocking out the pixels that are not of interest and then switching to a slower clock for data acquisition. This technique also increases the dynamic range of the PDA toward higher light levels by an order of magnitude.

Of all the multichannel systems discussed so far, the PDA

is the most easily controlled by a small computer. Single board microcomputers are relatively inexpensive compared to the detector itself and can therefore be made an integral part of the detection system. Data can be read out at rates ranging from 10 to 50 kHz depending on the central processor used. Certain real-time and delayed resident processing can be carried on the microcomputer by both high and low level software.

1.6.4 Charge Coupled and Charge Injection Devices

CCD imagers are not sensitive enough in the UV to be seriously considered for atomic spectroscopy, but CID devices exhibit much improved response characteristics. The spectral response of CIDs is still inferior to that of PDAs; however, CIDs are solid-state two-dimensional detectors which provide random pixel addressing. Therefore, using echelle dispersion, CID based detection systems can cover a much larger spectral window with adequate resolution. An additional advantage stems from the nondestructive readout mode which can provide square root of N SNR improvement. A great deal of work remains to be done using CID sensors, however the future of these devices for atomic spectroscopic application is very promising.

1.7 Thesis Approach

A number of preliminary decisions were instrumental in determining the direction of subsequent research. An RL1024S PDA was selected as the multichannel detector. The IDPMT was considered too expensive and was not capable of simultaneous

multichannel integration. The vidicon has been successfully used for atomic spectroscopy but inherent problems such as lag, bloom, cooling efficiency and complex readout requirements promoted the investigation of solid state sensors. CCD detectors were not considered because they are not very sensitive to UV radiation and CID sensors were viewed as a relatively new technology with many unknown characteristics.

The linear PDA chosen has been designed expressly for spectroscopic applications. It has a wide sensor area, exhibits high quantum efficiency in the UV region and is a solid state device which is rugged and does not incorporate a tube structure. In addition, a precise geometric registration and unambiguous readout method provide for excellent resolution with no lag or bloom. During the past four years several detection sytems based on the RL1024S PDA have emerged as commercially viable products. The one dimensional nature of the PDA restricts the width of the wavelength window which can be simultaneously monitored. This fact led to the development of a hybrid detection strategy that incorporates a rapid slew scan spectrometer. The original synchronous motor drive system on a one meter Czerny-Turner spectrometer was replaced by a computer controlled stepping motor drive system which can slew at speeds ranging up to 6 nm/s. Chapter 2 describes the exerimental configuration, spectrometer modifications, and the hardware and software designs which were integrated to assemble the detection system.

The first stage analog processing of the PDA video signal

is accomplished using an evaluation board purchased from Reticon. This board does not employ the low noise electronics available with some commercially available PDA ensembles. These systems range in cost from $15,000 to $50,000 (US) as opposed to the $4400 (US) price of the PDA/evaluation board combination. The design of a new PDA board was beyond the scope of the intended research. Fortunately, the noise characteristics of the PDA are quantitatively known, and it was possible to theoretically determine the expected SNR performance of PDA detection systems in comparison to conventional PMT based systems. Chapter 3 deals with this evaluation and includes a discussion of data acquisition considerations.

Other aspects addressed by this thesis include dynamic range extension towards higher light levels, spatial resolution enhancement and the detection of transient signals from sample introduction methods such as the direct sample insertion device (DSID). These topics are pursued in the final chapters with an emphasis on the spatial resolution theory which is potentially the most important development.

2. Instrumentation

The experimental apparatus comprised several commercially available pieces of equipment and some custom designed instrumentation. A complete equipment list with associated suppliers is contained in Appendix A. A block diagram of the experimental configuration is shown in Fig. 2.1.

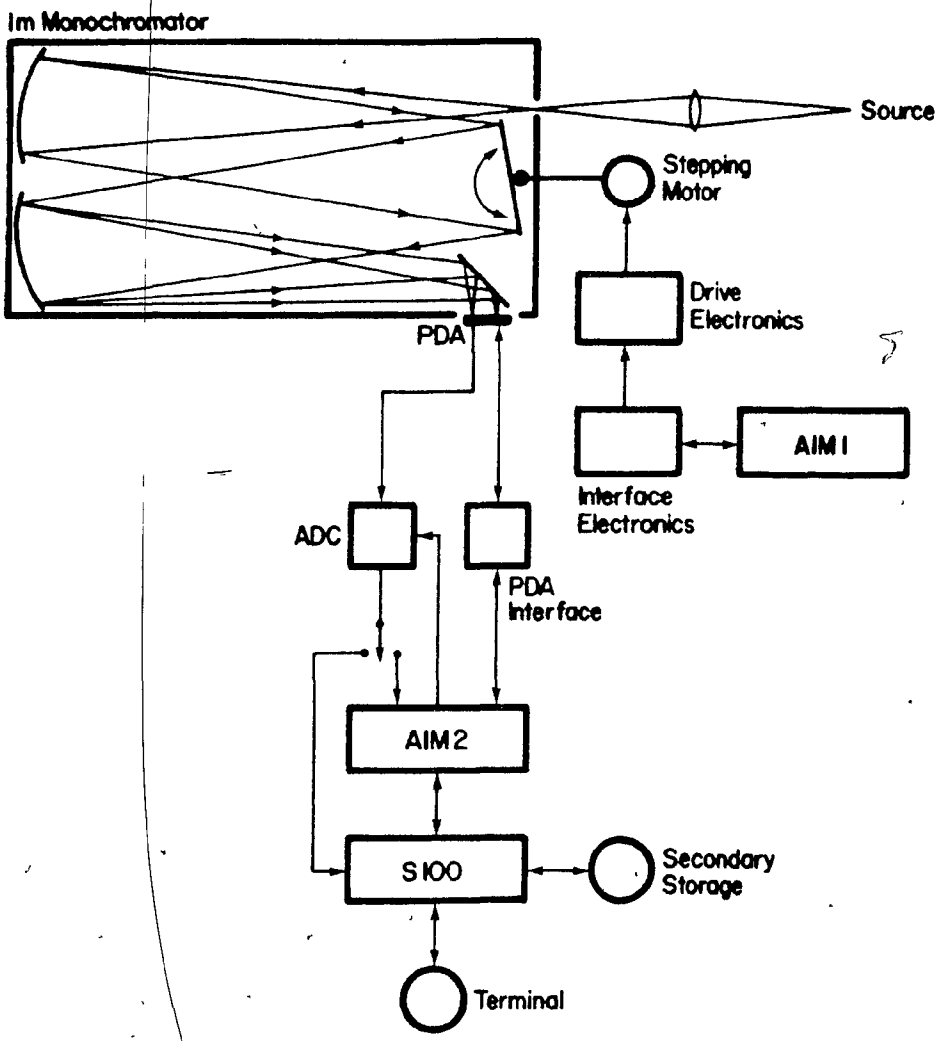

Figure 2.1: Block diagram of experimental configuration.

Radiation is collected by a quartz lens situated at a distance of 2F (40 cm) from the spectral source and entrance slit of the monochromator. The diffracted radiation is focussed onto the PDA by a swing-in mirror situated prior to the exit slit. The PDA is mounted on a positioning mechanism that provides the adjustments necessary to focus the line radiation on the sensor surface.

Selection of a spectral region to be viewed by the detector is carried out by a single-board Rockwell AIM-65 microcomputer (AIM1). Software running on this system accepts commands from the user and translates them into digital control signals to be sent to the stepping motor interface. The interface is responsible for converting the digital information received from the computer into the synchronous 4-phase pulse sequence used to drive the power transistors supplying current to the stepping motor windings. The interface is also responsible for recording the wavelength on a 6-digit numeric display.

Control of the PDA and data acquisition is performed by a second single-board AIM microcomputer (AIM2). This system has been expanded to accommodate additional memory and input/output hardware. AIM2 is responsible for initializing the PDA interface, controlling the readout of the detector, providing the integration period, detecting the presence of valid analog data and triggering the analog to digital converter (ADC) to digitize the data. The bidirectional paths between AIM2, the PDA interface and the PDA detector illustrate the control/feedback network. The unidirectional path from AIM2 to the ADC represents the trigger to initiate a conversion of the

data from the PDA.

The digitized data is routed to one of two possible destinations. Initially, data was collected by AIM2 where it could be processed before being sent to the disk based S-100 laboratory computer. While the AIM is capable of acquiring 1024 spectral points in less than a second, the transmission of 1024 points to the S-100 computer takes about one minute using a serial RS-232 link.

This "throughput" limitation was solved by routing digitized data directly to the S-100 computer. AIM2 triggers the ADC when valid data is sent from the PDA. The S100 system waits for an "end-of-conversion" signal from the ADC and then reads the data directly into memory. An additional advantage is gained because the AIM computer is no longer required to read the data. Since the functions are partitioned between the two computers the readout rate can be increased from 10 kHz to 18 kHz. The PDA is noticeably more stable at this higher readout rate.

The S-100 provides other functions including development and disk storage of programs to be executed by the AIM computers, processing of spectral information, plotting of data on a video screen or X-Y plotter, and word processing for the generation of reports and documentation.

2.1 Optical System

2.1.1 Optical Rail

The foundation for the optical components is a four-rail (quad) optical rail system based on a previous design by Walters et. al. [121]. The stainless steel rails were purchased in 17 ft. lengths with a diameter of 2.5 in. Each rail rests on 5 equally spaced supports. Each support consists of a U-shaped bracket and two cylindrical pieces of aluminum. The rails rest between, and parallel to, the cylindrical aluminum supports which can be independently moved at right angles to the rail length. Moving both supports laterally by the same amount shifts the rail in the same direction and moving the supports toward or away from one another raises or lowers the rail. The support brackets are bolted to I-beams which are perpendicular to the rails. The I-beams are supported by the frame of a Jarrell-Ash 3.4 meter monochromator which had previously been scrapped and salvaged for useful parts. The frame is extremely rigid and provides the torsional stability of the entire optical system. Finally, the frame is held off the floor by two supports constructed out of channel iron and welded in the Departmental Machine Shop.

Optical components are mounted on stainless steel riders that have a trapezoidal groove cut at one end and a flat cut at the other. The riders follow the contour of the rail that is mated with the groove. The riders are 18 in. long and are either 3.875 or 2.875 in. wide. The top surface of each rider consists of a two-dimensional matrix of 1/4-20 tapped holes with

center to center spacings of one inch.

2.1.2 Optical Rail Alignment

The advantage of the rail system over methods that support optical components independently is that once the rails are properly aligned components can be moved along the rails on the riders without disturbing their relative alignment. It is also possible to remove a rider from the rails and replace it without disturbing the optical alignment because the groove-and-flat design is a self-centering kinematic system. However, alignment of the rail system is a nontrivial task. Ideally, all four rails should be level along their lengths to within a few thousandths of an inch. Equally important is the specification that the rails are straight and do not "snake". This is very important if lateral alignment is to be retained while sliding riders along the rails.

The rail system was aligned with the help of Prof. D. Selby of the Civil Engineering Department of McGill University. He suggested that we choose one of the four rails, level and straighten it first, then proceed with the rest of the system. The rails were labelled 1 to 4 from left to right when viewed from the north end of the laboratory. Rail 2 was designated as the starting point. It is important to note that rails 2 or 3 were the best starting points because a rider would later be used to straighten the outside rails. This point will become clear later in the discussion.

A theodolite was used to measure the horizontal level of

the system. The procedure was to mount a vertical surveyor's target on one of the riders. The target was essentially a ruler scaled in inches with clear, sharply contrasting markings. The rider was then positioned above each of the rail supports and the rail moved up or down depending on the theodolite reading. This process was repeated in an iterative fashion until the entire rail was level to about 5/1000 in. This same procedure was used to level the other three rails.

Once the rails were level they had to be straightened. Prof. Selby suggested that we have the shop manufacture two V supports to be mounted next to the support brackets at each end of rail 2. The V was accurately milled along a 1 in. rectangular block of aluminum. It was imperative that the bottoms of the V grooves were the same distance away from the center of rail 2. A length of uninsulated Ni-chrome wire was strung between the grooves and pulled taut by weights hanging at both ends. This resulted in a straight reference line running the length of rail 2. Figure 2.2 illustrates the configuration. Some of the hidden views have been omitted from this illustration to simplify the diagram.

To straighten the rail a rider was placed between rails 2 and 3 such that the groove in the rider mated with rail 2. A bracket and rod assembly was mounted over the edge of the rider such that the bracket was electrically insulated from the rider. The rider, rail, V grooves and wire were all electrically connected and formed a path for electrical current. A digital ohmmeter was connected between the rod and the rider. When the rod contacted the wire the circuit was closed as indicated by

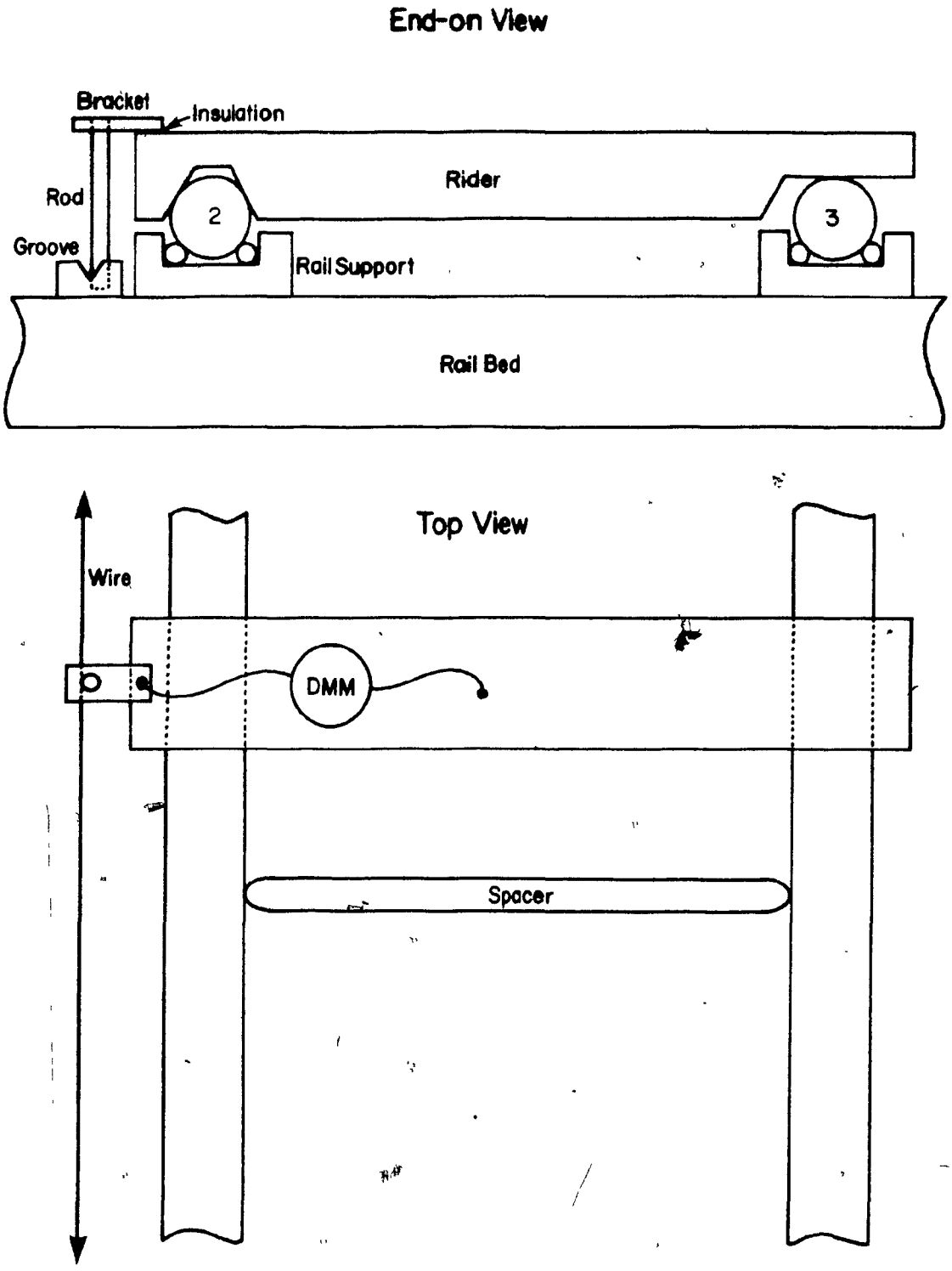

Figure 2.2: Optical rail alignment configuration.

the ohmmeter. Since the rod followed the contour of the rail it was possible to move the rider to each of the rail supports and adjust the rail from side to side until the rod just barely touched the wire. Rail 2 was straightened and relevelled iteratively until a satisfactory alignment resulted.

It was not necessary to employ this procedure for the other rails. Instead, the shop manufactured a spacer of aluminum that was 2.0 in. wide, 0.5 in. thick and exactly 12.500 in. long. This latter dimension is the specified center to center distance between the rails of 15.0 in. minus one rail diameter. Therefore the spacer should fit between the rails with no gap. By positioning the spacer between rails 1 and 2 and 2 and 3 along their lengths, rails 1 and 3 were straightened. Rail 4 was straightened last, using rail 3 as a reference. It was necessary to iterate between the leveling procedure and straightening procedure to arrive at a well aligned system. The result was that all four rails were level and straight to about 5/1000 in. After loading the rail system with heavy optical equipment the rail separations were checked with the spacer and no significant side to side deviations were observed.

2.1.3 Spectroscopic Radiation Sources

The ICP was the primary source of radiation for analytical application experiments. This system consists of a 2.5 kW, 27.12 MHz crystal-controlled RF generator with an automatic impedance matching unit and conventional torch enclosure. Three different torch designs were employed. Two standard 18 mm O.D. Fassel-type torches were used; one was the original torch

supplied with the ICP and the second was made in the glassblowing shop of the Department of Chemistry at McGill University. The second type of torch was a MAK low flow design which was used exclusively with the MAK nebulizer. The third torch design was a standard torch that had the central aerosol injector removed. This torch was used for all studies incorporating the direct sample insertion device (DSID). Argon flow rates and other commonly employed operating parameters are listed in Appendix B under "Standard Operating Conditions".

For some experiments other radiation sources were adequate. A Helium-Neon laser was employed for optical alignment and for those studies requiring an intense, monochromatic beam of light. A mercury pen-lamp was used as a multiple-line source and was very useful for calibrating the drive system of the monochromator. When a stable, narrow line width source was required several hollow cathode lamps could be selected, depending on the wavelengths or elements of interest.

2.1.4 Sample Introduction Systems

Two methods of sample introduction were used with the ICP. Conventional pneumatic nebulizers were employed for the analysis of most liquid samples. A pneumatically driven DSID was used for microsample introduction.

Three different pneumatic nebulizer and spray chamber combinations were available. Meinhard concentric nebulizers were coupled to a standard Scott spray chamber. A Jarrell-Ash (JA) fixed cross-flow nebulizer was used with a JA spray chamber

that was slightly modified so that it would fit into the torch enclosure. This modification required that the aerosol delivery tube be moved from its position at the end of the chamber to a position 2 cm towards the nebulizer. In addition, the ground glass joint which mates with the torch was changed so that it would couple with the torches used. The third system was a MAK-200 assembly which included a MAK-10 fixed cross-flow nebulizer and a MAK spray chamber. The MAK spray chamber, like the Scott chamber, employs a double pass baffle while the JA chamber utilizes an impactor type baffle. A discussion of the DSID used in this work has been published [122]. Operating details concerning the application of the DSID are dealt with in Chapter 6.

2.1.5 Spectrometer Optics

Light emanating from the ICP or other optical source is collected by a quartz lens 4.8 cm in diameter with a focal length of 20 cm (Na D line). The lens is normally placed at a distance corresponding to 2F, or 40 cm from the monochromator so that an inverted 1:1 image is focussed on the entrance slit. The monochromator is a 1.0 meter Czerny-Turner design with a swing-in mirror prior to the exit slit enabling spectrum viewing at the photographic focal plane at the side of the instrument. The photographic plate racking mechanism was removed and replaced by the multichannel detector system. The basic spectrometer specifications are listed in Appendix C.

The spectrometer was originally equipped with an IR grating. This was replaced by a 5 in. X 5 in. holographic

grating optimized for UV operation. The groove spacing of 1200 g/mm results in a reciprocal dispersion of approximately 0.8 nm/mm in the first order UV region. The monochromator is approximately 15 years old and it was discovered that the collimating and camera mirrors had corroded slightly. These mirrors were recoated with Al and overcoated with magnesium fluoride by 3B Optical Co. (Gibsonia PA). When the recoated mirrors were received it was necessary to refocus the spectrometer. Generally the procedures outlined in the instruction manual [123] were followed except for the following changes.

The method for collimating the mirrors called for illumination of the mirrors, cross-hairs and "normal holes" from outside the spectrometer through the exit and entrance apertures. This method did not produce enough optical contrast for this procedure to be effective. Instead, a 100 W light bulb was placed at the grating access port to illuminate the inside of the spectrometer directly. The resulting contrast was excellent and both mirrors were collimated with no problem.

The focus of the collimating mirror is critical for high resolution spectroscopy. No matter how well the camera mirror is focussed, the resulting image fidelity is limited by the focus of the collimating mirror. Unfortunately, the instruction manual did not provide a method for this adjustment. The following procedure for focussing the collimating mirror was suggested by H. Zeeburg of Jarrell-Ash.

The image for this adjustment was provided by the end of a

fiber optic bundle which had been cleaved with a razor blade to ensure that all of the individual light guides were flush with one another. The slits were opened to about 1.5 mm and the end of the bundle was placed flush against the slit jaws. Then the grating was rotated to the zero order so that it reflected the image of the fiber optic bundle back to the entrance slit. The fiber optic was placed at the bottom of the slit aperture so that the inverted image appeared at the top of the aperture. This will occur if the mirror has been collimated properly; otherwise the vertical mirror adjustment can be adjusted to correct the vertical positioning.

A microscope was placed in front of the entrance slit to view the image of the fiber bundle. The microscope was adjusted so that the slit jaws were in sharp focus. By moving the collimating mirror back and forth it was possible to bring the image of the optical fiber bundles into sharp focus as well. Initially the image was viewed with an optical comparator. This did not work well because the eye focusses independently of the comparator and one cannot trust ones judgment that both the slit jaws and the image are coincidently focussed at the exact same spot. The microscope produces an objective image which will focus at one point irrespective of the eye.

It was found that the image was focussed outside of the spectrometer. This meant that the mirror was too close to the entrance slit. Movement of the mirror must be carried out very carefully, otherwise collimation of the mirror can be lost. To move the mirror away from the slit, the center screw on the mirror assembly was turned counter-clockwise between 1/16 and

1/32 of a turn. Then the horizontal and vertical screws were turned the same amount. Two people should carry out the adjustment; one to move the mirror and one to monitor the image movement. This observation was made with an optical comparator because the microscope provided too much magnification. To move the mirror 1/2 mm the screws had to be turned approximately 1/2 a revolution. Thus a large number of individual adjustments were required to move the mirror the appropriate distance.

2.1.6 Stepping Motor Drive System

The reciprocal dispersion of the spectrometer coupled with the 25.6 mm width of the PDA sensor limits the spectral window to 20.5 nm. To achieve high sample throughput and fast access to different windows the conventional synchronous motor/gear train drive was replaced by a stepping motor grating drive system. The stepping motor system was designed to scan faster than the original drive system but the prime advantage, computer control, was realized by dedicating a powerful single-board computer to the control of the spectrometer enabling sophisticated control of the scanning process.

The complete drive system consists of four major components: the stepping motor and reducing gear, the current switching drive unit, the logic interface and the computer. The stepping motor specifications and related technical information are shown in Appendix D. Using an 8-step sequence 400 steps are required to produce one full revolution of the motor shaft. One complete turn of the sine bar drive screw corresponds to a 10 nm

wavelength change. If the motor had been coupled directly to the sine bar a resolution of 0.025 nm/step would have resulted which was considered inadequate. Instead, a 1:8 gear ratio was chosen resulting in a resolution of 0.0031 nm/step. The large gear is coupled directly to the sine bar drive screw. This gear communicates with the smaller gear on the motor drive shaft via a triple-wire nylon coated belt.

The motor is driven by the custom built switching circuit referred to as the drive unit. The switches are controlled by the stepping motor logic interface designed and constructed by Dr. W. Alex Whitla of Mount Alison University as a sabbatical research project. Schematic diagrams for the drive unit and logic interface are included in Appendix D. The 8-step sequence generated by the logic interface turns on the drive unit power transistors supplying approximately 1.3 A of current to the 4 motor windings. At full speed, corresponding to a slewing rate of about 6 nm/s, the power transistors switch this current at 313 Hz. The transistors dissipate about 23 W each through a single, large heat sink, cooled by a fan blowing 52 cu.ft./min of ambient air directly over the drive unit. From time to time one of the power transistors fails and has to be replaced. The diagnosis and replacement procedure is described at the end of Appendix D.

The stepping rate and direction of motor shaft rotation is dictated by AIM1. The computer can also read and modify the wavelength display, slew from one wavelength to another automatically and accelerate and decelerate the motor in a highly controlled fashion. A complete description of the

control program will be discussed later in the software development section.

2.2 Detection System

The heart of the detection system is an E.G. & G. Reticon RL1024S 1024 element linear self-scanning photodiode array [124]. The S-series PDAs were developed expressly for applications in spectroscopy. The pixels consist of diffused p-type silicon bars in an n-type silicon substrate. The p-type regions are 13 microns wide and 2.5 mm high with a center to center spacing of 25 microns. The pixels operate in a reverse-biased charge-storage mode. Therefore, the PDA is an energy detector, capable of integrating photon flux over time. The PDA is packaged as a 22-pin dual-in-line integrated circuit. The electro-optical characteristics of the array are listed in Appendix E. The sensor was originally purchased with a removable quartz window. This window was later permanently attached in a dry nitrogen atmosphere to prevent condensation of water onto the sensor surface when the PDA was cooled.

An E.G. & G. Reticon RC-1024SA evaluation board was used to provide the first stage analog processing of the video signal. This circuit does not incorporate the low-noise electronics necessary to provide the best SNR that can be achieved with the RL1024S PDA. It was decided that in-house design and construction of an optimized analog processing circuit was beyond the scope of the intended research. High quality

commercially available electronics for the RL1024S already exist [125-127] but these systems are costly. Therefore a decision was made to modify the evaluation board for computer control and pursue other interesting avenues of research using this detector.

2.2.1 Modifications to the RC-1024SA Evaluation Board

The operation of the unmodified evaluation board [128] is illustrated in Fig. 2.3.

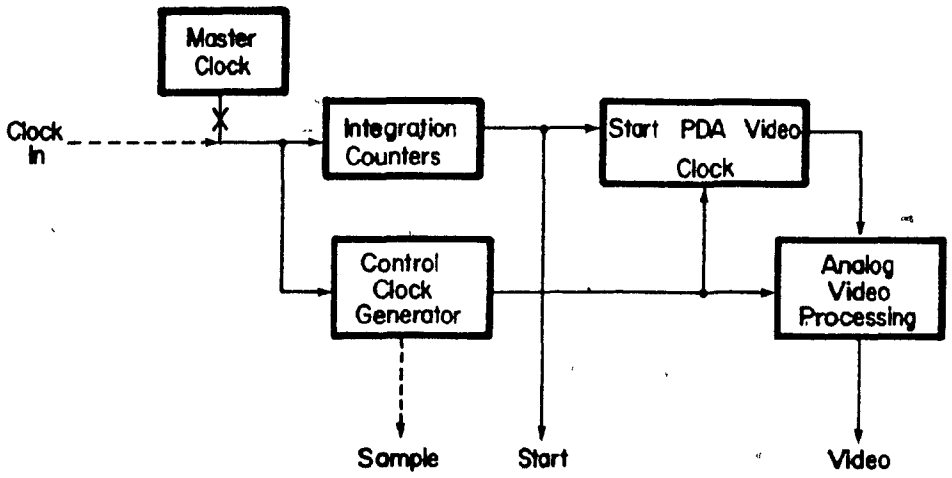

Figure 2.3: Block diagram of RC-1024SA evaluation board operation.

The integration counters are preset using on-board switches to a value corresponding to the desired integration time of the PDA at a particular master clock frequency. During the integration period the control clock generator continues to run but the PDA does not begin reading out until the integration counters reach

zero and the Start signal is asserted. After receiving the Start pulse the PDA begins reading out pixels at a rate determined by the control clock generator. The processed video signal is presented as a serial stream of "sampled-and-held" voltage levels. Using the Start pulse as a trigger the PDA readout can be easily viewed by an oscilloscope and might appear as shown in Fig 2.4.

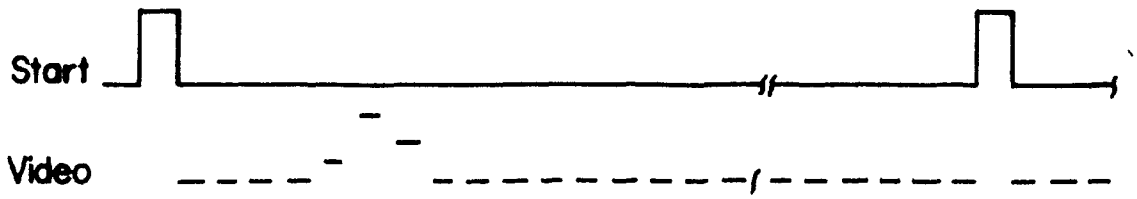

Figure 2.4: Example oscilloscope trace of Start and Video lines.

Each "blip" on the Video line corresponds to the signal generated by a pixel. Fig. 2.4 illustrates an example where diodes 5, 6 and 7 are integrating significantly more light flux than the other pixels. The video output signal ranges from 0 to approximately 3 volts full scale using the RC-1024SA circuit.

The first modification was simply to extend the potentiometers used for adjusting and optimizing the video output from their original position on the printed circuit board to a platform attached to the top edge of the board. This was necessary to allow for the adjustment of the video output while the detector was installed in the focal plane of the spectrometer.

The second modification is illustrated by the dashed lines in Fig 2.3. Two changes were required to provide for computer control and data acquisition. First, the on-board master clock was disconnected so that the clocking of the array could be controlled by a computer generated clock. The integration counters were permanently set at the minimum value of 258 [128]. Variable integration was achieved by simply stopping the clock for the desired period of time [129]. This method of signal integration is superior to the original method because one of the major sources of readout noise is signal cross-talk from the clocking signals [85]. The stopped clock method only contributes clock noise during the readout period when it is unavoidable.

To enable computer data acquisition a method was required to determine when to sample the video line for a pixel signal. This information was not present on the edge connector of the evaluation board but was present within the circuit. The video signal actually consists of the combined odd-even pixel readout, so odd and even sampling pulses were brought out to the edge connector. The clock modification and sample pulse extraction technique is described in Appendix E.

The last board modification was needed to accommodate the cooling system for the detector. It was decided that the most efficient method would be to bring the cooling system in contact with the PDA through the back of the printed circuit board. The machine shop milled an oblong hole underneath the PDA and removed the middle portion of the PDA socket. The wiring traces that occupied this space were rerouted using small gauge wire.

2.2.2 Cooling System

The amount of charge that can be initially "stored" on a reverse biased photodiode of the RL1024S PDA is reported by the manufacturer to be about 14 pCoul. This is often called the saturation charge. At 25 C the dark leakage current of a typical photodiode is 5 pA. Therefore complete charge depletion, termed saturation, will occur for an integration time of 2.8 seconds. It has been demonstrated [93] that integration periods as long as 160 s are required for trace analysis of some elements with an unintensified RL1024S PDA. Talmi and Simpson have measured the dark current as a function of temperature [31] and found that the dark current drops by a factor of 2 for every 6.7 C decrease in temperature. Cooling the PDA to about -30 C will increase the dark current saturation time to about 12 minutes. This is not an inordinately stringent cooling criterion because the dark current will still contribute 10% of the full scale signal for integration periods of only 1.2 minutes.

The cooling system is based on the 4-stage thermoelectric heat pump illustrated in Fig. 2.5. The first stage is a water cooled, hollow core brass heat sink. The surface of the brass heat sink was machined as flat as possible so that it would make efficient thermal contact with stage 2. Stages 2 and 3 are Peltier thermoelectric cooling modules. Technical data for the Peltier modules is listed in Appendix F. These modules can be thought of as thermocouples running in reverse. The "cooling couples" are made of n-type and p-type Bismuth Telluride. The quantity of heat pumped from the hot junction to the cold

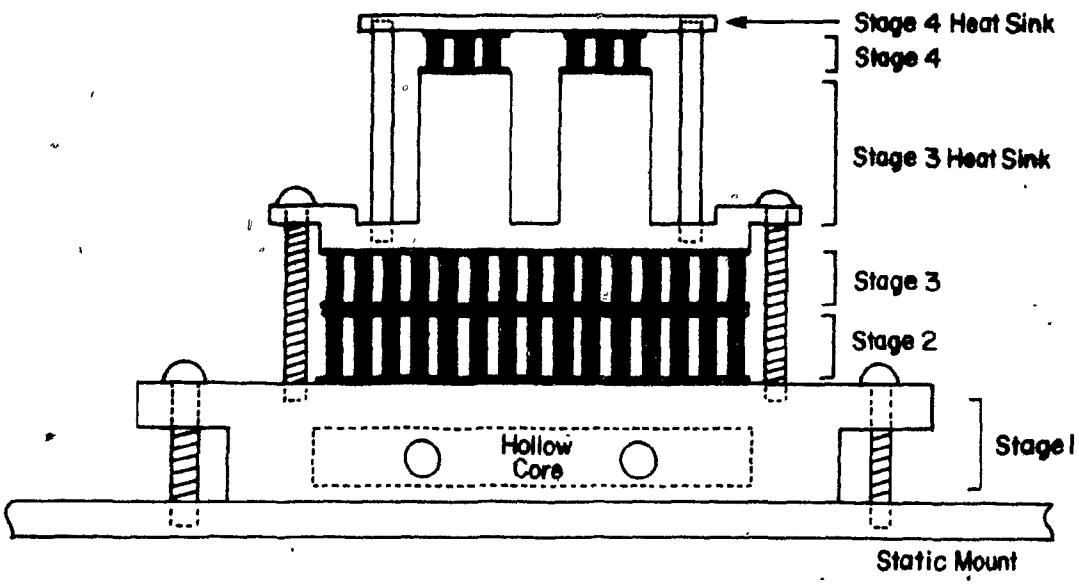

Figure 2.5: Schematic of four stage Peltier cooling system.

junction is proportional to the current passing through the device and the number of couples [130]. Stage 2 has a higher capacity than stage 3. This arrangement is necessary because some heat is generated by the electrical current passing through the device and two coolers of the same capacity offer no further advantage.

Between stage 3 and the stage 4 miniature Peltier elements is a solid copper heat sink constructed with two pillars tall enough to pass through the printed circuit board. The two pillars have the same cross-sectional area as the stage 4 miniature coolers. A rectangular copper plate forms the fourth stage heat sink and ultimately makes direct contact with the bottom of the PDA integrated circuit. This copper plate is held down on the third stage heat sink using thermally insulating fiber standoffs. All thermal junctions were coated with heat

sink compound to optimize the heat transfer efficiency. When the cooling system is mounted, the fourth stage heat sink lies about 1 mm higher than the top of the PDA socket. The clamping force of the socket receptacles is sufficient to hold the PDA firmly against the heat sink.

The coolers are driven by a dual, adjustable 1.25 to 15 V, 10 A power supply. Stages 2 and 3 are driven in series as are the two miniature Peltier elements comprising stage 4. The three Peltier stages can be driven separately if the appropriate connections are made to the terminal strip adjacent to the cooling system. The maximum voltage that can be applied to each of the larger Peltier modules is 8.6 V. The maximum rating of the miniature coolers is 0.97 V.

2.2.3 Detector Mount

The PDA is positioned in the focal plane of the monochromator by the mounting mechanism illustrated in Fig. 2.6. A 15 in. square plate was machined from 1/4 in. aluminum with a 2 in. by 4 in. rectangular hole cut at a position corresponding to the viewing region of the focal plane (FP). Four 1/4 in. stainless steel rods (R1-R4) were attached at right angles to the plate on which the entire mounting assembly eventually rests. The PDA sensor resides on the side of the RC1024SA printed circuit board (PCB) facing the focal plane. The PCB was bolted to the static mount (SM) with aluminum standoffs (dotted lines). The cooling system was also mounted on the static plate (see Fig. 2.5) and the standoffs were cut such that the fourth

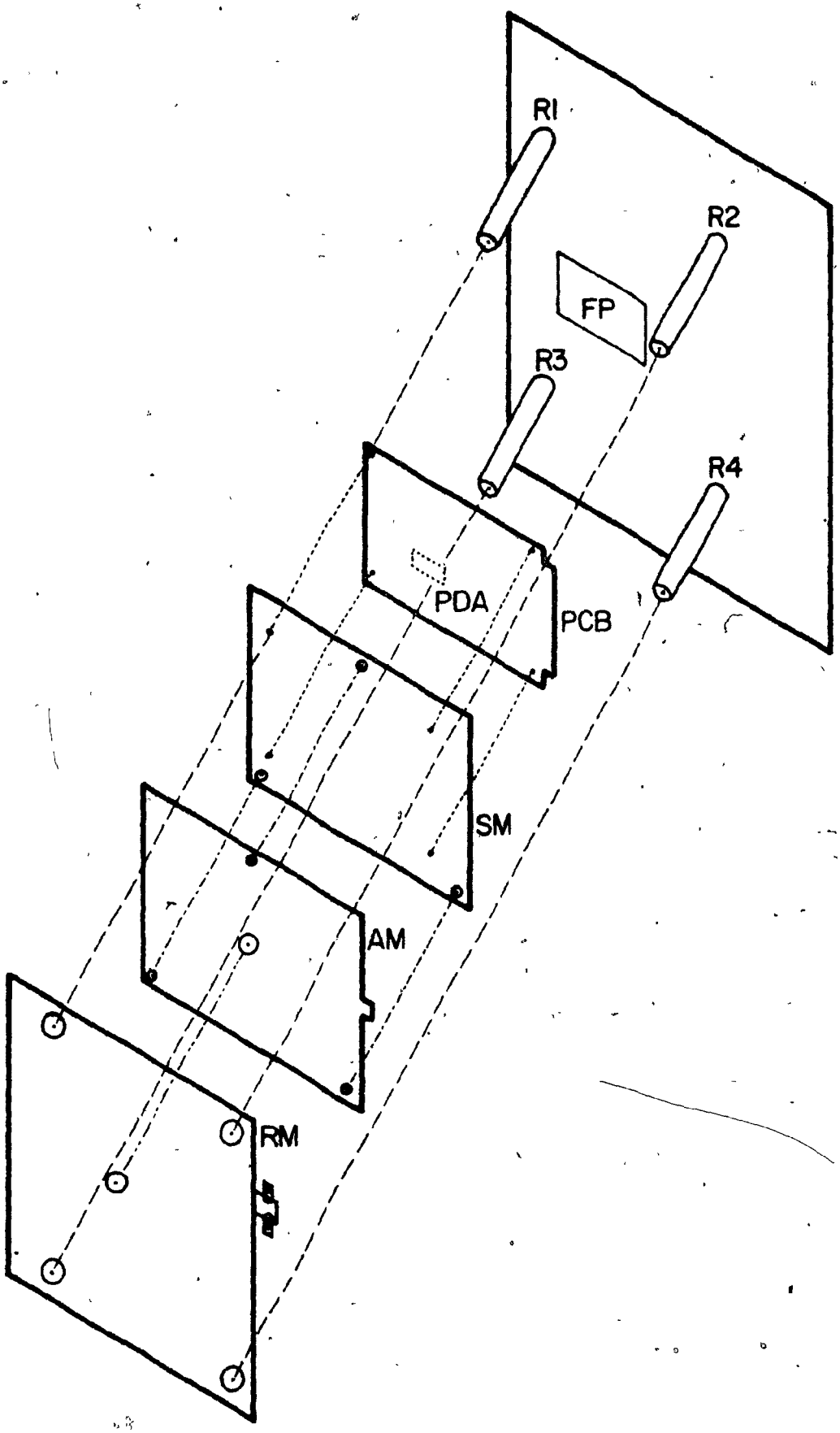

Figure 2.6: Expanded view of detector mount.

stage heat sink passed through the PCB to make contact with the PDA.

The static mount was connected to the adjustment mount (AM) using three spring loaded screws (dash-dot-dash lines) with knurled heads to facilitate manual adjustment. These adjustment screws provide for forward/backward and side-to-side pitch. The adjustment mount was bolted to the rail mount (RM) in one place (dash-dot-dot-dash line). This allows the adjustment mount to be rotated using the set screws indicated at the right hand side of the rail mount. The position of the rotation hole was chosen so that the center of rotation corresponded to the center of the PDA. The rail mount is slid onto the four rails such that the PDA is situated near the focal plane.

The detector was focussed by scanning the grating to a position such that an intense line appeared at the focal plane within the boundary of the PDA. The rail mount was then moved back and forth to achieve a rough focus. The spring loaded screws were then used for fine focussing. In addition to the straight forward and backward movement of the detector, four additional degrees of freedom are available for alignment as shown in Fig. 2.7. The top and side views indicate how the PDA and printed circuit board can be rotated about the vertical and horizontal axes to place the detector parallel to the 2-dimensional focal plane. These adjustments were made using the spring loaded screws. Once the PDA was parallel to the focal plane it was rotated to orient the diodes parallel to the vertical line image furnished by the spectrometer. The PDA can also be moved from side to side because the static mount has

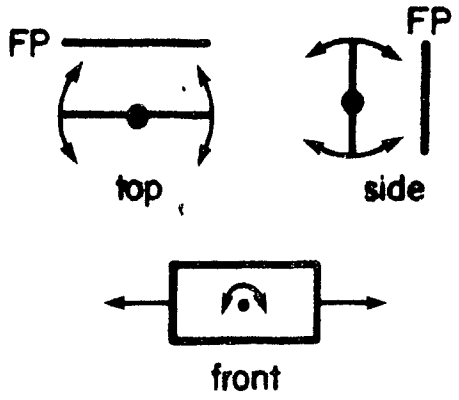

Figure 2.7: Spatial degrees of freedom for PDA detector in spectrometer focal plane.

slotted holes where the the circuit board connects to it. This additional degree of freedom is not crucial to the alignment of the detector.

2.2.4 PDA Interface

The PDA interface is a custom designed circuit that controls the readout process and detects pixel data from the array. The clocking portion of the system is summarized by the block diagram shown in Fig. 2.8. The complete schematic is included as Appendix G.

The only control variables applied to the PDA detector are the readout rate and the integration time. The PDA interface was designed to provide for a wide range of clock frequencies. A crystal controlled 8.000 MHz Master Clock is generated on the interface board and is subsequently fed into a Frequency Divider consisting of a simple 4-bit binary counter. The master frequency is divided by powers of two to provide clock

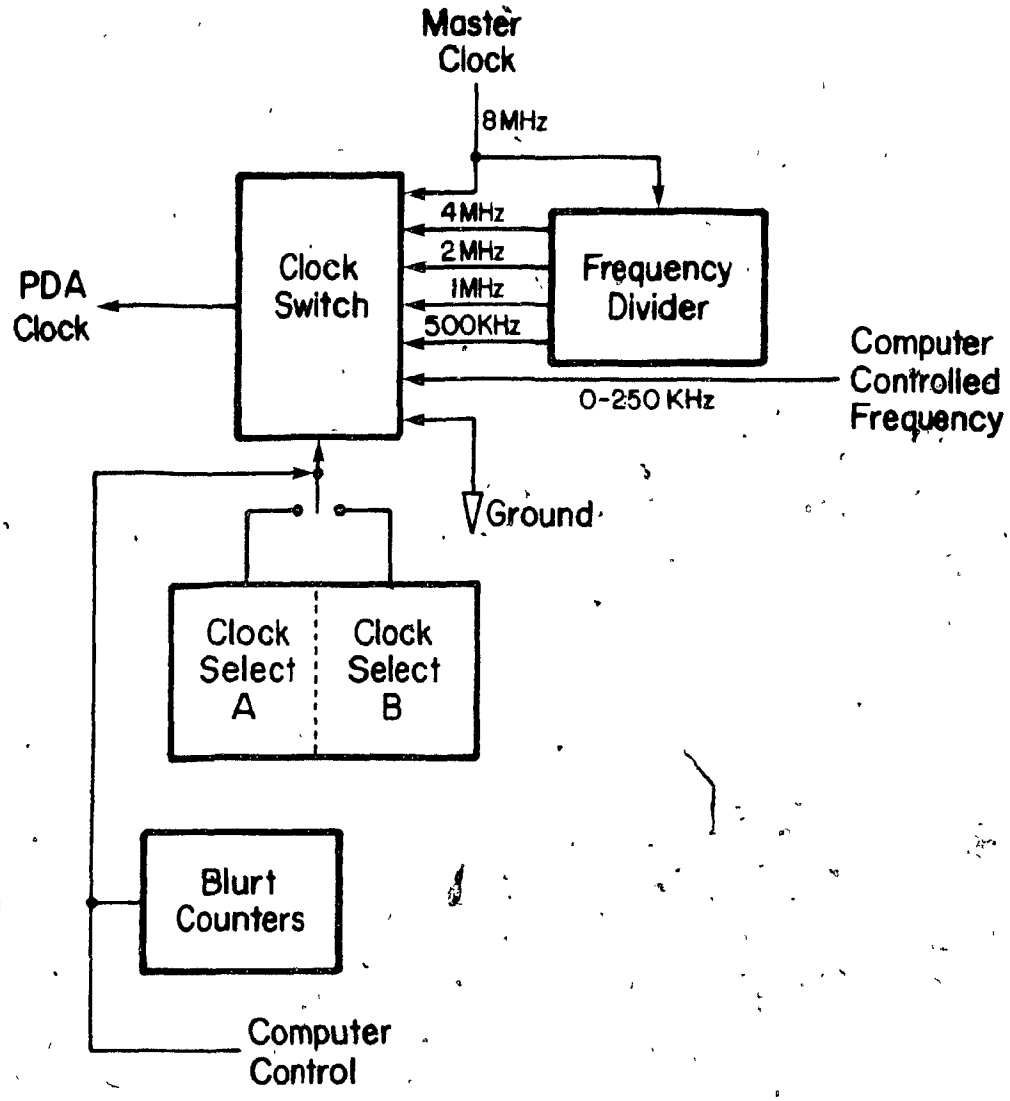

Figure 2.8: Block diagram of clocking portion of PDA interface.

frequencies of 4, 2, 1 and 0.5 MHz. Another clock source is provided by AIM2. The AIM is configured with five 6522 Versatile Interface Adapters (VIA) which are multifunction input/output (I/O) devices. The I/O devices each contain two 16-bit timers; one of which can be programmed to produce an output frequency of 1 to 250 KHz on bit 7 (PB7) of one of the I/O ports. This clock source controls the readout process

during data acquisition periods. The six clock sources and a ground line are connected to the Clock Switch, a standard 8-line to 1-line decoder. At a given time only one clock source is passed through this switch to the PDA board. The clock frequency supplied to the PDA board is translated into a four-phase clock to drive the PDA so the actual readout rate is the clock frequency passing through the Clock Switch divided by four. Therefore, the maximum readout rate that can be provided by the interface is 2 MHz. The practical limit is 1 MHz (4 MHz master clock). This limitation is imposed by the circuitry of the RC1024SA evaluation board.

Integration is achieved by switching to the ground line as the clock source. When the clock is not running the PDA pixels discharge at a rate proportional to the production of photon generated and thermally generated electron-hole pairs. The integration period specified by the user is determined by software running on the AIM. Restarting the clock causes the PDA to resume the readout process. The control software ensures that the clock is only stopped at the end of a readout (ie. after the 1024th pixel). The selection of the clock source for routine situations is carried out by Clock Select A which is directly controlled by AIM2.

The remaining interface circuitry is used to implement a fast access readout method called the "Blurt mode" [120]. The maximum 16-bit data acquisition rate of small computers is generally between 20 and 50 KHz. Therefore the minimum integration time is between 50 and 20 ms. These integration

times will be fast enough for most analyses; however, strong emitters like calcium and magnesium will cause pixel saturation in concentrations of 10 to 100 ppm when the ICP is used as the spectral source. The Blurt mode is appreciated when one considers that usually only a small percentage of the 1024 photodiodes provide useful spectral information within a given readout. Using a 25 μm entrance slit about 5 pixels per line image are excited. If 5 pixels either side of the line are selected for background correction then a total of 15 pixels are required to quantitate a single line. The Blurt mode functions by switching to a fast clock during the readout of pixels containing unwanted spectral information. When the first pixel of a desired group is reached the clock is switched to the acquisition rate and the desired pixels are collected via the data acquisition system. If 15 pixels are acquired at a rate of 20 KHz and the remaining 1009 pixels are Blurted at 1 MHz (using the 4 MHz source from the interface) the resulting integration time will be about 2 ms. This decrease in integration time translates into a dynamic range extension towards higher light levels of a factor of 25.

The operation of the Blurt mode can be understood with the aid of Fig. 2.8. Initially the PDA is read out by the AIM at 10 to 18 KHz, depending on the system software used. The saturated peak is identified by the user and the computer determines which pixels correspond to the peak and associated background. The number of pixels to ignore is loaded into the Blurt Counters. The code for the clock source to be used for the fast clock is loaded into Clock Select B while the PDA is still running under

the AIM generated clock indicated by Clock Select A. When the last pixel of the group of interest is read out the AIM causes the Clock Switch to recognize Clock Select B as the indicator of the desired clock source. The clock rate is switched from the readout source to the Blurt source in a matter of microseconds. When the fast clock is activated the Blurt Counters start to count pixels but no data acquisition occurs. The Blurt Counters will reach zero after the pixels following the peak group are read out, the PDA "wraps around" to the beginning of the array, and the pixels before the peak group are read out. When the Blurt Counters reach zero Clock Select A is chosen as the clock source identifier, the readout clock is switched back to the nominal readout rate and the pixels corresponding the peak group are recorded via the data acquisition system. Specific examples of dynamic range extension using the Blurt mode are given in Chapter 4.

The interface is also responsible for detecting sample pulses generated by the PDA board indicating when valid analog data is present on the video line. Figure 2.9 illustrates the data detection and acquisition portion of the PDA interface in relation to the entire detection system. The PDA is a self-scanning device and therefore provides information in a continuous, sequential fashion as long as it is supplied with the appropriate clock pulses. When the on-chip scanning circuitry finishes accessing the last photodiode it is reset and starts scanning from the beginning of the array again. At the beginning of the readout period a digital Start pulse is

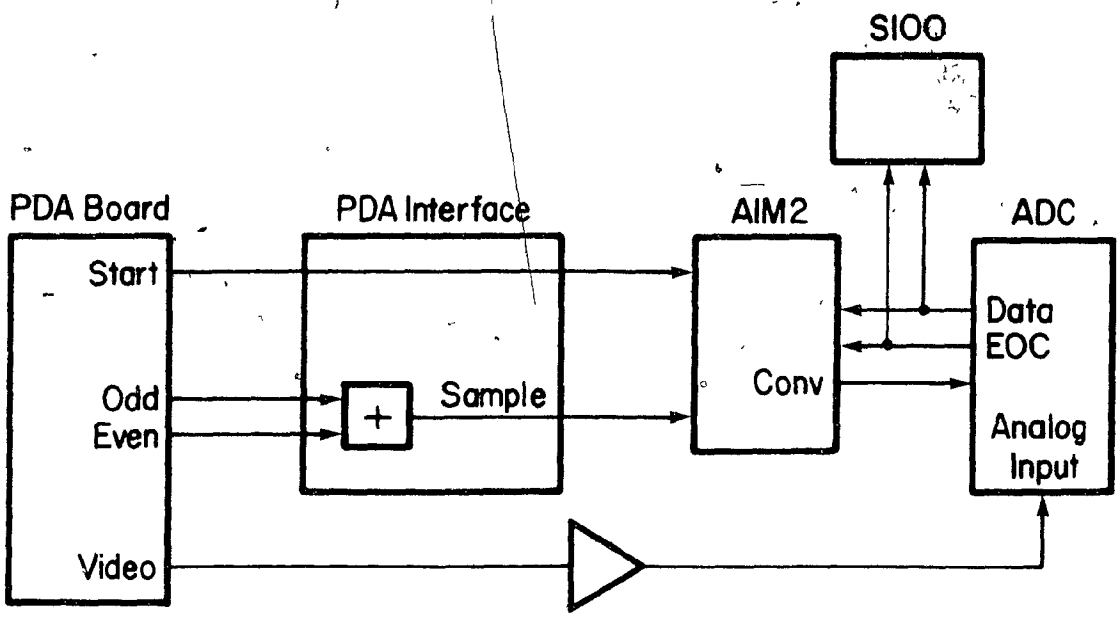

Figure 2.9: Block diagram of detection system configuration.

generated. This signal is passed unmodified through the interface to the AIM computer.

The actual "diode array" is organized as two separate circuits: odd and even. The odd and even charge pulses produced when the array is read out are combined into a single stream of charge pulses and subsequently voltage pulses by the RC1024SA board. The odd and even sample pulses extracted from the PDA board are "ORed" together at the interface and the resulting single stream of digital pulses is sent to the AIM computer. Figure 2.10 indicates the waveforms produced.

When the computer detects a Start pulse, it begins to monitor the Sample line. When the voltage level on this line makes a low (ground) to high (5 volts) transition, the computer activates the ADC system. The computer instructs the ADC to digitize the video signal by asserting a "convert pulse" (Conv).

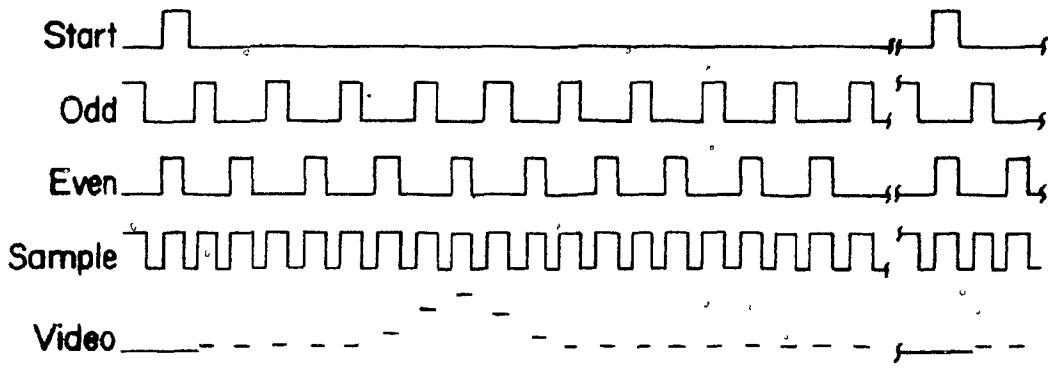

Figure 2.10: Signals used to interface RC-1024SA evaluation board with remaining detection system hardware. The 'Sample' pulses are produced by ORing the 'Odd' and 'Even' signals extracted from the evaluation board.

This signal causes the ADC to perform a successive approximation analog to digital conversion which takes approximately 30 microseconds. When the conversion is completed, the ADC asserts the "end of conversion" (EOC) signal. This signal may be detected by the AIM computer or the S100 computer, depending on the application software chosen by the user. The EOC signal indicates that a valid binary data value is available and the computer simply reads this value via an input port.

The ADC input range is 10 volts but the full scale video output is only 3 volts. Therefore, the video signal is amplified to match the input range of the ADC. The precision instrumentation amplifier illustrated in Fig. 2.11 provides a variable gain ranging from 2.3 to 3.7.

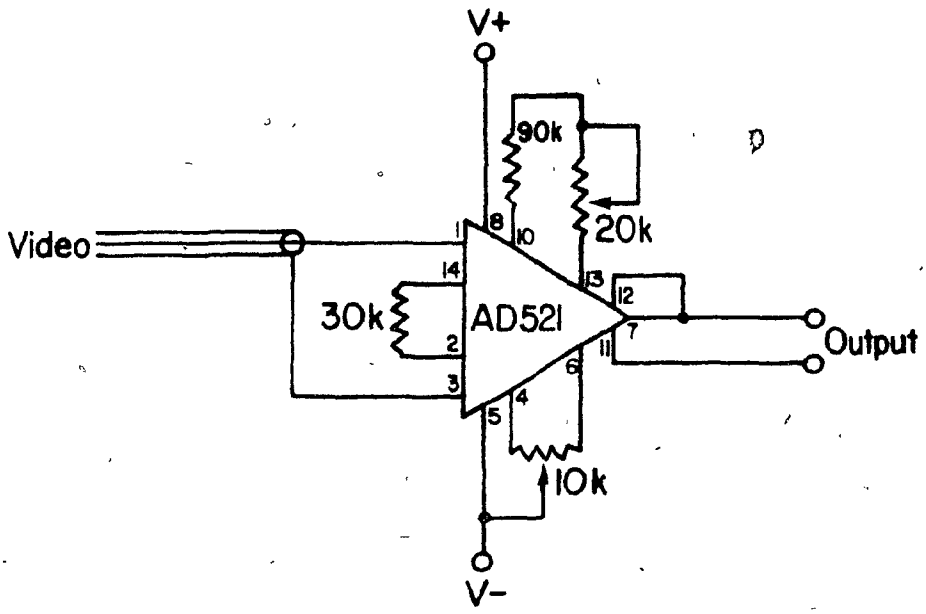

Figure 2.11: Wiring diagram for precision instrumentation amplifier used to amplify PDA video signal to produce 0 to 10 Volt output.

2.2.5 Detector Enclosure

The PDA must be maintained in a dry atmosphere while it is cooled to avoid moisture condensation on the window surface and surrounding electronic components. This was accomplished by building a detector enclosure consisting of a simple 5 sided box. The sixth side is the focal plane plate which is bolted to the monochromator. The box was fabricated out of 1/4 in. aluminum plate because a sturdy enclosure and a firm support for electrical connectors and plumbing fittings was desired. Water is conducted into and out of the enclosure via two 1/4 in. Swagelok bulkhead receptacles located at the bottom of the enclosure. The dry nitrogen inlet is also located at the

bottom. All of the remaining electrical connectors, indicators and adjustments are located on the left hand side of the enclosure. This panel includes the following:

1. Power indicators (+15, -15, +5 V);
2. Raw video and amplified video outputs;
3. Start signal, clock in and clock out connections;
4. Amplifier gain control;
5. Supply voltage inputs for cooling system; and
6. Temperature monitor.

The power source for the detector system is a triple output, overvoltage protected supply. Technical data for this power supply and a schematic of the laboratory constructed cooler power supply are included as Appendix H. The raw video signal can be connected to an oscilloscope and using the Start pulse as a trigger, the output of the detector can be viewed in real time. The amplified video signal is connected to channel 1 of the ADC.

The temperature monitor is based on two AD594 thermocouple amplifier chips. These integrated circuits incorporate internal cold junction compensation and furnish 10 mV per degree C as an output. One of the devices was intended to monitor the temperature of the PDA and the other was configured to act as a set point alarm. If the temperature of the PDA rises above 30 C, indicating cooler failure, the device sounds an audible alarm located at the bottom of the enclosure. Unfortunately, the temperature monitor does not function properly when the ICP is running. This may be due to the fact that the AD594 must

amplify the sub-millivolt signals produced by the thermocouple by a large amount. Electrical noise generated by the ICP is also amplified by the same amount effectively washing out the small signal from the thermocouple. Temperature measurements were subsequently made using a traditional two junction thermocouple with ice water as the reference.

The top, front and right hand side of the enclosure were not used as component supports so that they could be completely removed to provide clear access to the detector mount, interface electronics and adjustment potentiometers. A ribbon cable descends from the lower right hand side of the enclosure. This cable connects the PDA interface to the AIM2 computer via the Port 2 50-pin connector on the expansion board.

2.3 Data Acquisition System

The data acquisition hardware consists of a laboratory built 3-channel differential 12-bit analog to digital conversion system. The ADC chip is an Analog Devices AD574KD integrated circuit that can produce a successive approximation digitization in approximately 30 microseconds. Four analog input ranges can be switch selected from the front panel of the ADC module: 0-10 V, 0-20 V, +/- 5 V and +/- 10 V. The system was rewired so that the BNC connector designated to input an analog signal to channel 4 could be used to input a remotely generated convert signal. This posed no real disadvantage because one analog input was sufficient for virtually all experiments. A block diagram of the ADC system is shown in Fig 2.12. The

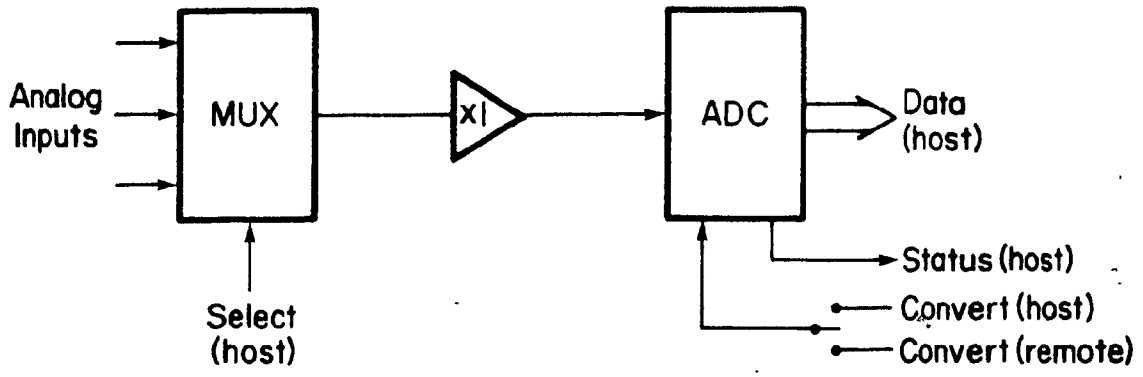

Figure 2.12: Block diagram of ADC system.

specifications for the ADC chip and the analog multiplexer chip, and the schematic for the entire circuit is contained in Appendix I.

The ADC module consists of a wire-wrap circuit board enclosed in a rectangular aluminum box. This box plugs into a "Vector cage" which can accommodate up to 7 other modules at a given time. Other modules include a digital to analog converter and numerous amplifiers. At the rear of the Vector cage, 8 44-pin edge connectors are mounted. The 44-pin card edge of each module extends through the back of the module so that when the module is plugged into the Vector cage the card edge inserts into an edge connector. The 8 edge connectors are wired in parallel to form a 44-wire "bus". The bus provides power to the modules and was initially intended to provide a communication path to a remote computer system. This latter feature has not been implemented, but could be by simply providing a suitable connector, connecting the systems and writing appropriate software for the remote computer.

The ADC was designed so that two computers could

communicate with the system. At present the remote computer can only generate a convert signal. This signal is not conducted by the bus; instead it is conducted via the channel 4 BNC connector on the front panel of the ADC module. The remote communication path is enabled using the BUS switch on the front panel. At the back of the ADC module a 25-pin D-type connector is mounted adjacent to the point where the card edge protrudes. This provides a communication path to the host computer. The host can initiate a conversion, detect the end of a conversion and read the 12-bit data produced. The host communication path is enabled using the EXT switch on the front panel.

The need for combined host/remote computer interaction evolved when large amounts of spectral information were required to be stored on the S100 machine. The expanded AIM computer is ideal for control of the PDA system because it has a well developed I/O capability and can be completely dedicated to the detection system. The S100 computer has too many important resources to be dedicated to the detection system. The AIM computer was originally configured as the host computer for the ADC system. Spectral information was transferred to the S100 system for disk storage and further processing using a relatively slow serial network [130]. This configuration was adequate for the acquisition of up to 200 pixels. However, when it became necessary to transfer multiple sets of 1024 pixels the serial transmission rate produced an unacceptable bottle neck.

The solution was to continue to use the AIM computer for detector control but directly acquire the data using the S100

system. The AIM computer had to be used to generate convert pulses because it was singularly capable of detecting the presence of valid analog data. The S100 computer was configured as the host machine with respect to the ADC system. During the data acquisition period the S100 simply waits for the end of conversion status from the ADC before reading in data. This configuration enables the acquisition of an entire spectrum and storage on disk in a matter of seconds. Hardcopy plots can also be generated much more quickly. This is an important advantage when real-time observation of a spectrum is impossible.

When data acquisition is to be carried out by the AIM computer alone a 25-wire ribbon cable is used to connect the ADC module to an I/O connector on the expansion board. The AIM computer is connected to the S100 system for network transmission using a similar ribbon cable. The System 1 software family can then be used to operate the entire detection system.

The alternate mode of operation involves connecting the ADC module to the S100 system via a 25-wire ribbon cable that terminates with two 25-pin D-type connectors at one end. These connectors plug into the rear of the S100 mainframe. A coaxial cable connects a control line and ground from the AIM to the channel 4 BNC connector on the front of the ADC module. Both the BUS and EXT switches must be enabled to allow the AIM to generate conversions and the S100 to acquire the data. The System 2 family of software routines can then be used to operate the detection system.

In either case, the convert pulse and analog channel select

line are asserted virtually simultaneously. The analog signal is passed through a unity gain amplifier so that the impedance of the multiplexer (MUX) does not degrade the voltage. The voltage appearing at the analog input of the ADC chip is converted to a 12-bit number in 25 to 30 microseconds. At the beginning of a conversion the ADC sets the Status line (STS) high indicating that a conversion is in progress. During the conversion the data lines are disconnected (tristated) from the rest of the circuit by the ADC internally. When the conversion is completed the ADC sends the Status line low and presents the converted value on the data lines. This signals the host computer that data is ready and can be read via the I/O system.

2.4 System Software

The design and implementation of software was integrally linked to the hardware configuration. In the beginning it was decided to dedicate small single-board microcomputers to the spectrometer and detection system. A more powerful disk based microcomputer could then be used to store programs and data, and perform more complex manipulations of the data. The advantages of such an arrangement is that the small computers are inexpensive yet more than powerful enough to fulfill their dedicated function. In addition, the small machines are modular and can easily be replaced if a failure occurs. Finally, by distributing the rather complex control tasks to "slave" computers the main system is freed to perform other functions.

The development of software for each machine followed a straightforward path once the hardware configuration was specified. In general the interaction hierarchy was as illustrated in Fig. 2.13.

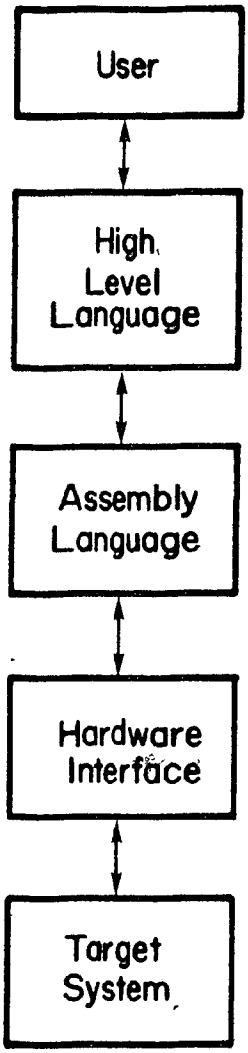

Figure 2.13: Hierarchy of system interfaces.

In all cases the user interacted with the detection system or scanning system via a high level language routine. This language was interpreter BASIC for the AIM computers and Pascal

for the S100 system. The high level language was responsible for invoking the assembly language routine required to perform the specified operation. For the spectrometer drive system and for some detection system operations the high level language routines communicated with the associated hardware interface directly. The hardware interfaces, which have already been discussed, were then responsible for the final translation of the original operation into concrete function. Documented listings of System 1 and System 2 software are presented in Appendix J.

2.4.1 Network

The laboratory network was used to transfer programs from the S100 computer to either of the AIM computers and sometimes to transfer data from AIM2 back to the S100 machine. Programs were developed on the S100 machine because of the availability of a powerful text editor (Wordstar) and because of the disk storage facility. The hardware for the network consists of a simple RS-232 link connecting either of the AIMs to the auxiliary port of the S100 terminal. Software residing in read only memory (ROM) of the AIM computers is capable of information transfer to or from the S100 computer using standard CP/M operating system calls. The network hardware and software resides in an expansion box for AIM1 and on one of the expansion boards for AIM2. Access to the network is made via specialized instructions from within programs or from the operating system of either computer system.

2.4.2 Spectrometer Wavelength Drive System

The software responsible for driving the spectrometer scanning system resides in ROM memory on AIM1. This software was placed in ROM so that it would not have to be down loaded from disk every time the spectrometer system was turned on. Except for a very short timing routine written in 6502 assembly language, the entire program was written in AIM BASIC. A fully documented version of the program is listed in Appendix J.

Throughout the following discussion commands to be typed by the user are enclosed in single quotes (') while computer responses are enclosed in double quotes ("). The system is initialized by the user as follows:

'N','ESC','N'

The computer responds with:

"COUNT UP OR DOWN"

The user replies with:

'UP' - to scan towards higher wavelengths

'DOWN' - to scan towards lower wavelengths.

The system responds with:

"COMMAND?"

to which the user may respond in one of the following ways.

'RESET': This command causes the spectrometer to scan toward lower wavelengths until the sine bar reaches the end of travel. The wavelength display is set to 000.000 and the stepping motor interface is primed to begin scanning in the positive direction. With the grating in this position the m=0 line is roughly centered on the photodiode array.

'U': If the motor is not running the Up command causes the motor to start scanning the spectrometer at a rate of about 0.05 nm/s. Each successive invocation of the Up command causes the speed to be increased by roughly a factor of 2. Table 2.1 lists the scanning rates as a function of the number of times the 'U' command is used from the stopped position.

N	Scanning Rate (nm/s)
1	0.0473
2	0.0939
3	0.185
4	0.359
5	0.678
6	1.22
7	2.03
8	3.05
9	6.09

Table 2.1: Scan rate vs. usage of 'U' command.

Any attempt to increase the speed beyond 6.09 nm/s will result in the message "AT MAX SLEW".

'D': The Down command decreases the motor scanning rate by the same factor employed for the 'U' command. If the motor is scanning at the slow speed it is stopped. Attempts to invoke the 'D' command when the motor is stopped results in the message

"MOTOR IS STOPPED".

'RU': The Ramp Up command causes the system to ramp the scanning rate from the current speed to the maximum rate of 6.09 nm/s.

'RD': The Ramp Down command slows the scanning rate from the current speed to zero.

'C': The direction of wavelength scanning is changed from positive to negative or vice versa using the Change command. If the motor is running, the Ramp Down routine is executed first to avoid jamming the motor. In such a case the motor is not restarted until the user provides the appropriate command.

'SCAN': When the Scan option is selected the computer prompts with "SCAN RATE (NM/S)?". The user may enter any value between 0.0239 (minimum rate) and 6.086 (maximum rate). The system will respond by ramping up or down to the desired scanning speed automatically.

'S': This command is used in emergencies to stop the motor immediately. Alternatively, the reset button on the AIM can be activated; however, this will cause the program to be exited.

'L': The Load command is used to enter a new wavelength value into the display. The user supplies the appropriate value in response to the prompt "WAVELENGTH (NNN.NNN)?".

'R': This command instructs the system to read the current wavelength from the display and print the value on the computer display and printer. This routine is also invoked by other routines to acquire positional information.

'P': The Pulse instruction provides a method of moving the grating by stepping the motor a discreet number of steps. This is especially useful for rotating the grating very small distances to center lines on the exit slit or on a particular photodiode.

'SLEW': This routine causes the system to slew from the current wavelength to any other wavelength automatically. After prompting the user for the new wavelength the routine determines the current wavelength and hence, which direction to scan. Then, if the new wavelength is far enough away the system ramps up then down to a point just prior to the new wavelength. The Pulse routine is then used to achieve the final position. If the new wavelength is very close to the current value then the Pulse routine is used to perform the entire task. This is not an absolute wavelength positioning routine, but rather, an efficient method of rapidly scanning from one point to another with the minimum amount of user interaction and attention.

'Q': The Quit command is used to exit from the program and return to the BASIC environment.

2.4.3 System 1 Interface Software

System 1 consists of a user interface written in AIM BASIC and a series of assembly language routines that interact directly with hardware. The object code for the assembler routines is concatenated into a single file called PDASYS1.HEX and is stored on the S100 computer. This permits all of the assembler routines to be down loaded from the S100 computer in one block. The following discussion will maintain the convention of enclosing user responses in single quotes and computer responses in double quotes.

The user interface is called PDASYS1.BAS and, like the assembler routines, is down loaded from the S100 computer. Upon invocation, PDASYS1.BAS prompts the user for general information. The first question

"DATA DISK ?"

requires that the user type 'A' or 'B' to indicate the disk drive spectra are to be stored on. The next prompt

"DATE (MONDD) ?"

requires a date code normally consisting of a three letter date and two digit day (ie. APR07). This string may be up to 8 characters in length but must start with a letter. The date code forms the first part of the filename. The question

"DATA ACQ (Y/N) ?"

requires a response of 'Y' if data acquisition is required and 'N' if not. The 'N' option is only used for system debugging and development. It causes the generation of an infinite loop when the PDA is scanned using the stopped clock integration method.

The response to the question

"# OF PIXELS ?"

should be an integer indicating the number of photodiodes to acquire from the beginning of the array. Normally the value 1024 is used, to acquire a full spectrum. If a direct sample insertion device (DSID) experiment is to be monitored then 'Y' should be input in response to

"DSID WAIT REQ'D ?".

If a steady state signal is expected then 'N' will signify that no wait is required. Following this response the system is initialized by the assembler routine PDAINIT1.ASM.

PDAINIT1.ASM: The initialization routine is responsible for setting up the versatile interface adapters (VIA). These are extremely powerful I/O chips with two 8-bit bit-programmable ports, two 16-bit timer/counters and 4 programmable control lines [132]. Three separate VIAs are used by the software interface. The VIA resident on the main computer board is designated VIA0. This chip is reserved to run the stepping motor if AIM1 malfunctions. Four more VIAs are located on the PIO expansion board and are designated VIA1 to VIA4 from top to bottom. Each VIA is accessed via a 50-pin header.

VIA1 is programmed to act as a timing device. Timer 1 is programmed to generate a 1 KHz square wave on the eighth bit of port B (PB7). Timer 2 is programmed to count pulses on the seventh bit of port B (PB6). PB7 and PB6 are connected externally. This arrangement is used to determine periods from

1 to 65536 ms by simply loading timer 2 with the appropriate value and waiting for it to count to zero. The integration periods are determined with a precision of 1 ms in this manner.

VIA2 is used to interface to the ADC system. All 8 bits of port A and the low order 4 bits of port B are programmed as inputs to accept the 12-bit digitized data. Port B bits 4 and 5 are used as outputs to select one of the four multiplexer channels as the analog input to the ADC chip. Channel 1 is always used for this purpose. Control line CB2 is programmed to generate the Convert pulse and CB1 is used to detect the end of conversion status signal. Automatic data latching is enabled so that when the end of conversion signal is detected, the data is automatically read into the VIA. The program can then read the data at leisure.

VIA3 is responsible for interacting with the PDA interface hardware. All 8 bits of port A and PB0 and PB1 are programmed as outputs. These 10 bits are used by the Blurt software to load the blurt counters. Port B bits 2, 3 and 4 are programmed as outputs to provide a three digit clock code to the clock control hardware. The three digit code selects one of eight possible clock sources (including ground) to drive the PDA. Port B bit 5 is used to select the readout clock source or the Blurt clock source. If PB5 is low, then the clock code supplied by PB2-4 is interpreted as the readout clock selector. If PB5 is high then PB2-4 is interpreted as the Blurt clock selector.

Timer 1 of VIA3 is programmed to generate a square wave on PB7. The clock so produced is invariably used as the readout clock. The frequency output on PB7, and hence the readout rate,

is set using another routine called CSELECT. Timer 2 is programmed to count pulses on PB6. Sampling pulses are input to PB6, therefore timer 2 is capable of counting pixels automatically (without a software loop) as they are read out by the PDA. Control line CB1 is used to detect sample pulses so that the ADC can be instructed to initiate a conversion. Control line CA1 is responsible for detecting the Start pulse from the PDA board. Control line CA2 functions as a "load enable" signal for the Blurt counters while CB2 is used to enable the rapid clock switching for Blurt operation.

After the execution of the initialization routine, control is passed back to PDASYS1.BAS. The user is subsequently prompted with

"COMMAND ?"

for which several options exist.

'CSELECT': This response invokes a subroutine that prompts the user for the desired readout frequency in kHz:

"READOUT FREQ (KHZ) ?"

The system is initialized for a readout rate of 9.615 kHz. Slower operation results in a less stable PDA signal. the available readout rates are listed in Table 2.2.

Readout Rate (kHz)	Application
9.615	System 1 readout clock
10.417	Not used
11.364	"
12.500	"
13.889	"
15.625	"
17.857	System 2 readout clock
20.833	Not used
25.000	"
31.250	"
41.667	"
62.500	"
125.000	Blurt clock
250.000	"
500.000	"
1000.000	"

Table 2.2: Readout rates available above 9.615 kHz.

The maximum readout rate for data acquisition under System 1 is 9.615 kHz. This relatively slow rate is due to the amount of software overhead required by the AIM to control the detector and ADC system. If a readout rate is selected that is not listed in Table 2.2, but less than 62.5 kHz, the system selects the next slowest rate and displays the value. If an intermediate rate in the Blurt range is selected the system

prints the warning

"FREQ NOT AVAILABLE".

When a satisfactory selection is made the subroutine invokes CSELECT.ASM, an assembler program that performs the clock selection.

'SCAN': The scan option is used to acquire a spectrum. The desired integration time is input in response to the message

"INT. TIME(SEC)?".

Any value from 0 to 65.535 seconds is valid. The minimum integration time is defined as

$$TMIN = 1038/(F*1000)$$

where F is the readout frequency in kHz. The number 1038 is the sum of 1024 pixels and the 14 extraneous sample pulses produced between readouts. Table 2.3 shows the minimum integration times for various readout rates.

The main program is always aware of the current readout rate and minimum integration time. If the user enters a value below the minimum, the system assumes the minimum, prints the value, and prompts with

"CONTINUE?".

A 'N' response results in another request for the integration time.

Readout Rate (kHz)	Minimum Integration Time (ms)
9.615	108.0
10.417	99.64
11.364	91.34
12.500	83.04
13.889	74.74
15.625	66.43
17.857	58.13
20.833	49.82
25.000	41.52
31.250	33.22
41.667	24.91
62.500	16.61
125.000	8.304
250.000	4.152
500.000	2.076
1000.000	1.038

Table 2.3: Minimum integration times vs. readout rate.

If a DSID wait period was requested at the beginning of the program, the prompt

"DSID WAIT PERIOD (S)?"

appears. The wait period was designed to allow the DSID probe time to enter the ICP discharge and come up to temperature before allowing the detection system to record a spectrum. Details of this will be discussed in the section outlining

System 2 software because System 2 employs a more sophisticated DSID interface.

In response to the message

"RUN LETTER (A,B,...)?"

a single character must be entered. The run letter is used along with the date code to create a filename for the acquired data. The prompt

"SCAN TYPE?"

instructs the user to enter a string of up to 20 characters describing the nature of the data or experiment. This is not a functional parameter, but rather, a short description that will be placed in the data file for future reference. Strings such as 'DARK', 'BLANK', 'SAMPLE', etc. are normally used.

The next input parameter is requested as

"# OF PRESCANS?".

Any integer between 0 and 255 may be entered. When the PDA is not being used to acquire data it is continuously clocked out at the current readout rate with the minimum integration time. This allows the user to monitor the spectrum in real-time on an oscilloscope. The prescan option forces the PDA to be read out up to 254 times successively, using the proposed integration time, before actually acquiring the data. This feature was installed as a testing procedure to see if better results could be obtained by allowing the system to "stabilize" at the proposed integration time before taking data. The results of this test are presented later in the System Performance section.

The final system request is

"PIXELS FOR XFER?"

which requires two values to be entered. The values entered correspond to the pixel data that the user wants transmitted to the S100 computer. The number of pixels actually acquired is determined at the beginning of the program and is usually the maximum of 1024. If the above prompt is answered with '15,970', for example, then data for diode 15 through 970 will be transferred to the S100 machine and stored on disk.

Most of the responses to the above system requests are stored in the upper portion of page zero memory (locations 224 to 255). This memory is reserved for system parameters to allow other routines to acquire status information and access parameters needed to fulfil their function. A list of reserved memory locations used by System 1 and System 2 software is located in Appendix K. When the parameter entry segment is completed, the SCAN subroutine passes control to PDASCAN1.ASM.

PDASCAN1.ASM is an assembler routine responsible for acquiring a spectrum under the conditions specified by the user. All of the pertinent parameters are accessed from their reserved locations in page zero memory. The detailed operation of this routine is sufficiently documented in the program listing. The operation can be summarized as follows.

First, the routine synchronizes with the free-running PDA by waiting for a Start pulse. Then, Timer 2 (VIA3) is primed to count pixels as they are read out. At the end of the readout the clock source is switched from PB7 to the grounded input. Within 20 microseconds timer 2 (VIA1) is loaded with the

integration count. When the integration period is over, the clock source is switched back to PB7. This causes the PDA to start reading out again. When the next Start pulse is detected, the routine monitors the Sample line. At every sample pulse the ADC is triggered producing a digitized pixel value. This value is stored in a data array starting at hexadecimal location 3000. When the appropriate number of pixels have been acquired control is returned to the SCAN subroutine of PDASYS1.BAS

The user is then prompted with

"CONTINUE?".

If the answer is 'Y', another spectrum is acquired. The same parameters specified for the first scan are used, except the new spectrum is stored at a new array location. This process can be repeated up to 99 times and is a very efficient method of obtaining multiple spectra for signal averaging purposes. However, the 24 kByte memory of the AIM limits the number of 1024-point spectra that can be simultaneously stored in memory to 6. If the user wishes to take a seventh spectrum the system automatically transfers the existing 6 spectra to the S100 computer.

When 'N' is finally entered as a response, any remaining spectra are transferred and the subroutine terminates. Control is passed back to the main program and the prompt

"COMMAND?"

is issued.

The filenames created by the data transfer routine have the format

D:MONDD.Rnn

where - D is the data disk (A or B),

- MONDD is the date code,

- R is the run letter,

- nn is a two digit number from 00 to 99 indicating the spectrum number. The user does not have to keep track of the number of spectra acquired; the system does this automatically. The format of the resulting data file is as follows:

```
DATE RL EXT
F
SCAN
W1
IT
D(m)   I(m)
D(m+1) I(m+1)
D(m+2) I(m+2)
   .
   .
   .
D(m+n) I(m+n)
```

where - DATE is the date code,

- RL is the run letter,

- EXT is the extension (spectrum number),

- F is the readout frequency used to acquire the spectrum,
- SCAN is the descriptive string input by the user,
- IT is the integration time,
- D(m) to D(m+n) are the diode numbers,
- I(m) to I(m+n) are the corresponding intensities detected by those diodes.

2.4.4 System 1 Support Software

(i) Graphics

Data files produced by System 1 are text files and can be plotted on a video screen or printer using the program PDAPLOT.ASC. This is a BASIC program that runs in the PBASIC environment. PBASIC is a modified version of the standard MBASIC interpreter that can make use of the Microangelo graphics system. PDAPLOT.ASC is a menu oriented program. A documented listing is included in Appendix J including a flow chart describing the various menus.

The main menu consists of the following selections:

"CHANGE PLOTTING PARAMETERS"

"VIDEO PLOT"

"PRINTER PLOT"

"SAVE SPECTRA"

"SUBTRACT SPECTRA (1-2)"

"AVERAGE SPECTRA"

When the program is initiated the terminal screen is cleared, the menu is presented and a blinking cursor is positioned to the

right of the first option. A menu option is selected by typing the Down or Up arrow until the cursor is beside the desired item, followed by 'RETURN'.

The first option selected should be "Change Plotting Parameters" because, upon initialization, no data has been read into memory from disk. The menu describing the plotting parameters is organized as follows:

```
"PLOTTING PARAMETERS"
"TITLE OF PLOT       :"
"DISPLAY (S OR D)    :"
"X-SCALE (DMIN,DMAX) :"
"Y-SCALE (YMIN,YMAX) :"
"POINT PLOT (ON/OFF) :"
"BAR GRAPH (ON/OFF)  :"
"DATA FILE NAME 1    :"
"DATA FILE NAME 2    :"
```

The cursor is positioned to the right of the first option. To change or modify any option the same selection process used for the main menu is employed. If data entry is required by the user, the appropriate prompt appears at the lower left hand corner of the screen.

Title of Plot: This option may be ignored, otherwise, the string input by the user is centered at the top of the plot.

Display: The plotting package was designed to allow either one or two plots to be displayed. Dual plotting is very useful for comparing spectra. The 'S' (single) option causes the system to use the entire screen to plot the data file while the 'D' (dual) option splits the vertical dimension in half and plots two data files. This is a "toggle" option; if one mode is current, then typing 'RETURN' when the cursor is properly positioned automatically switches to the other mode. The currently active display mode is indicated on the menu. The default mode is the single plot option.

X-Scale: The user can select the spectral segment to be plotted by entering the appropriate values as the X-scale. This entry consists of the first and last pixel to be plotted. The default scale is 1 to 1024.

Y-Scale: This parameter defines the full scale intensity range to be plotted. If the dual display mode is selected the Y-scale is applied to both halves of the plot, resulting in a factor of 2 loss in vertical resolution.

Point Plot: If this toggle option is turned on then the spectrum is plotted using small dots.

Bar Graph: If this toggle is turned on, the spectrum is plotted as a series of vertical lines extending from the minimum intensity value to the measured intensity value for each pixel.

Data File Name: Data files to be plotted are read into memory when a file name is associated with file name 1 or 2. If the single plot mode is selected, file 1 is plotted. If the dual plot mode is selected, file 1 is plotted on the top half of the screen and file 2 is plotted on the bottom half. The filenames entered remain unchanged until modified by the user or by the SUBTRACT or AVERAGE options available from the main menu.

When the plotting parameters have been set, control may be passed back to the main menu by typing the 'ESC' key. The data may be displayed, modified or stored by selecting one of the following options.

Video Plot: The video plot subroutine utilizes the plotting parameter information to furnish a plot on the screen. After viewing the plot it is often worthwhile to return to the plotting parameters menu and modify some of the values. For example, it may be desirable to "zoom in" on a spectral region or modify the intensity scale to get a better representation of the data. Each data file contains information pertaining to the scan type, readout frequency, integration time, etc. (see section 2.4.3). This information is reproduced at the top right of the video plot.

Printer Plot: At any time an exact copy of the information on the video screen can be sent to the printer. The resulting dot matrix plot is useful for spectrum comparisons and for future reference.

Subtract Spectra: This routine gives the user the option of using two currently available spectra or two spectra resident on disk. If the current spectra are used, the second file is subtracted from the first. The resulting spectrum is stored as data file 1, effectively erasing the original data file 1. This is necessary because the PBASIC system and the plotting routine consume a large portion of the available 64 kBytes of RAM.

If disk resident spectra are chosen the first action is to read in the data and then proceed with the subtraction. The corrected spectrum is automatically plotted on the video screen. The intensity axis is adjusted so that it bounds the smallest and largest values produced as a result of the subtraction. The name assigned to the corrected spectrum has the form:

D:MONDDab.COR

where - D is the data disk,

- MONDD is the date code common to both spectra,
- a is the run letter of the first spectrum,
- b is the run letter of the second spectrum,
- "COR" indicates that the file is corrected.

For example, if the blank file B:NOV26.B01 is subtracted from the analyte file B:NOV26.A01, the resulting spectrum would be named B:NOV26AB.COR. This data is not saved on disk until the SAVE option is selected from the main menu.

Average Spectra: When a number of similar spectra have been collected for signal averaging purposes, an average spectrum can be produced by selecting this option. The user is asked whether to place the averaged spectrum in data array 1 or 2, as

well as the data disk, date code, run letter and the number of replicate spectra. Following these entries, the program reads in the multiple files producing an average spectrum. The resulting file is named using the convention

D:MONDDa.AVG

where - a indicates the common run letter of the files used to produce the averaged spectrum,

- "AVG" indicates that the file is an averaged spectrum.

The subtract option can be used on AVG files. The program is capable of converting from one filename type to another. For example, if an averaged dark file called JUN24N.AVG is subtracted from a spectrum called JUN24C.AVG, the resulting data would be labelled JUN24CN.COR.

Save Spectra: After modifying spectra using the averaging or subtracting options the save option can be used to store the data on disk. The user is given the choice of retaining the currently assigned names or providing new ones. In addition, it is possible to store spectrum 1, 2 or both.

Only the points bounded by the X-scale values set in the plotting parameters section are saved under the specified filename. It is therefore possible to use the system to find peaks and save only those pixels of interest. This simplifies the software necessary to perform peak height, peak area and noise calculations.

The plotting program is terminated by typing the 'ESC' key from the main menu.

(ii) Peak Quantitation

The fixed pattern spectra produced using the SUBTRACT option of the plotting package are amenable to quantitation using a relatively simple algorithm. This algorithm was incorporated into a program called PDACALC.ASC. The documented listing is in Appendix J.

PDACALC.ASC is a BASIC program that runs in the MBASIC or PBASIC environment on the S100 computer. The program prompts the user for the data disk and filename and then reads the entire file. The header information included at the beginning of the data file is listed on the printer. This program will only quantitate the largest peak in the spectrum. If multiple peaks require analysis, the plotting package must be used to extract the individual spectral regions and save them as individual files.

When the program finds the peak pixel it lists the 10 pixels either side of the peak. The user is then asked whether to use one or two sided background correction. If one sided correction is specified a prompt will be issued to determine which side. The background regions encompass five pixels where the closest pixel is at least six diodes away from the peak.

The quantitation algorithm finds the sum and the sum of squares of the background diodes. The average background and the sample standard deviation is then calculated. A threshold value equal to the average background plus five standard deviations is used to identify those pixels to be used to find the peak area. A typical report might appear as follows:

FILE: B:SEP26AB.COR

READOUT FREQ. = 9.615

SCAN TYPE: COR A - B

INT. TIME = .059

2 SIDED CORRECTION

BACKGROUND = 1.3

BACKGROUND NOISE = 2.869

PEAK DIODE = 33

PEAK HEIGHT = 249.7

3 DIODES IN PEAK (32 - 34)

PEAK AREA = 355.1

SBR = 193.077

2.4.5 System 2 Interface and Support Software

System 2 evolved because of the lengthy transmission times dictated by the serial network. System 1 was, and still is, very useful for the acquisition of up to about 200 pixels, however; the need for a much more rapid acquisition method was evident when the full spectral range of the PDA was exploited. One way to improve the transmission rate would be to dedicate a high speed parallel link between AIM2 and the S100 computer. However, a simpler approach involved modifying the configuration slightly so that the S100 computer acquired the data directly.

Software had already been written by Robert Sing to interface completely with the ADC system for the acquisition of PMT data. The conversion trigger portion of this software was removed and the capability of acquiring a 1024 point data set was introduced. The acquisition routine was written in Z-80

assembly language and the user interface was written in Pascal. Further additions to the System 2 family were coded as overlays in the Pascal language.

The modifications to System 1 software were also relatively minor. The data acquisition portion of the PDA control program PDASCAN1.ASM was simply deleted. However, because the S100 computer would be connected as the host to the ADC system, an alternate electrical path was required for AIM2 to transmit the Convert pulse. This was provided by the CB2 control line of VIA1. A coaxial cable was used to connect CB2 to the fourth channel input of the ADC module. This input was internally rewired so that it could be recognized as a Convert pulse.

It is important to note that this modification does not affect the operation of System 1. System 1 is enabled by raising the toggle switch labelled EXT. System 2 is enabled by raising the switches labelled EXT, BUS, A0, A1 and A2. The network is still used to transfer software between computers.

Two user interfaces were required to implement System 2; one to operate each computer. The S100 program is called PDASYS2.COM. This is the load module produced from the source Pascal program PDASYS2.SRC located in Appendix J. A unique feature of the Pascal system is the possibility of using overlays. An overlay is a program segment that can be loaded from disk automatically when it is needed. The need for overlays results from the limited memory provided by a 64 kByte system. The advantage of overlays is that all routines envisioned to provide a desired function can be accessed from a

single program.

(i) PDASYS2.COM

Before initializing System 2, a program disk containing PDASYS2.COM, PDASYS2.001, PDASYS2.002 and PDASYS2.003 should be inserted in drive A and a disk to receive data should be placed in drive B. The system is invoked by typing

'PDASYS2'

from the S100 console in response to the CP/M prompt "A>". The first prompt from the program is

"Enter date code :"

requiring a response of 1 to 8 characters to define the filename. As with all CP/M files, the filename must begin with a letter, a typical example being 'JAN29/85' or 'FEB14A84'. A list of all of the available options is then issued:

"Enter function (Acquire,Load,Save,Plot,Calibrate,Display,
Restart,Quit) :"

A selection is made by typing the first letter of the desired function followed by 'RETURN'.

Acquire: Selection of this option results in the prompt

"Dark or Analyte :"

A single letter is input to define the data type. A "dark" spectrum is any spectrum to be subsequently subtracted from another spectrum. For example, a simple dark subtraction results in a fixed pattern, dark signal corrected spectrum. On

the other hand, a blank subtraction may be used to eliminate the fixed pattern signal, the blank level, and any other features furnished by the spectral source while running the blank. The program transfers control to the assembly language data acquisition routine GETPDA.MAC, the software interface to the ADC system. If the 'A' option is selected, the program simply transfers control to GETPDA.MAC.

When the data has been collected and if the 'D' option was selected, the spectrum is automatically stored using the ".DRK" extension. Therefore if the date code was MAY19/82, the "dark" spectrum would be stored on disk B as MAY19/82.DRK. If the spectrum is "analyte" data, it is simply left in a data array to be accessed by other routines. The "dark" data is also left in a data array for rapid access.

Save: This option is used to save "analyte" spectra on disk. The message

"Extension :"

requires a response of three characters. Normally a series of numbers such as 001, 002, 003 etc. are used to depict a series of spectra. The data residing in the data buffer are stored on disk using the date code and extension.

Load: If the data to be manipulated are already stored on disk the Load option can be used to copy files into the data buffer.

The prompt

"Dark or Analyte :"

asks whether a dark file or analyte file is to be loaded. If the user types 'D', the program loads the ".DRK" file corresponding to the current date code. If 'A' is selected the prompt

"Extension :"

is given and the user is expected to supply the 3 character extension indicating the desired file.

Plot: The original plotting routine was written by Robert Sing to plot multiple spectra, in a three dimensional perspective, on a Hewlett Packard 7074A plotter. The three dimensional plotting package was used to view the temporally resolved spectra produced from DSID experiments and will be described in Chapter 6.

The plotting package included in PDASYS2 is a simplified version of the three dimensional program. This routine was coded as an overlay. When the 'P' option is selected from the main menu, the overlay is automatically brought in from disk and executed. The plotter must be connected to the serial auxiliary port of the terminal. This will require temporarily disconnecting AIM2 from the S100 machine, however, at this point all software should have been down loaded to the AIM's.

The number of points to be plotted is entered in response to the prompts

"Enter first point to be plotted :"

"Enter last point to be plotted :"

This permits the generation of a plot of the whole spectrum or any segment thereof. The routine automatically subtracts the dark spectrum from the analyte spectrum. Before sending data to the plotter, the routine asks the user to enable the auxiliary port:

"Turn on aux port and hit return"

The plotting time for a 1024 point spectrum is about one minute. This is an adequate rate considering the excellent quality of the graphical information produced. The video graphics system was not considered to be necessary. When the plotting is finished, the user must turn off the auxiliary port and type 'RETURN' to return to the main program.

Calibrate: The wavelength calibration overlay is described in the Chapter 5 discussion of calibration and high resolution characteristics.

Display: The display overlay provides the capability of viewing the data in numerical form on the terminal screen. When invoked the routine prompts with

"Display Wavelength or Diode region ?"

If the character 'D' is typed, the system responds with

"Enter peak diode :"

The value entered in response to this question is treated as the center diode. The value entered in response to

"Enter number of diodes to display :"

instructs the program how many pixels to display in the vicinity

of the "peak" diode. The output from this routine consists of the diode number, the dark value, the uncorrected analyte value and the corrected value. The values are printed on the terminal screen 19 rows at a time. The user controls the scrolling process by typing 'RETURN' after a full screen is presented. The output sent to the screen can be routed to the printer by answering 'Y' to the question

"Print results (Y/N) ?"

The user can add a title to this printout by entering a string in response to

"Title for listing ?"

If the calibration routine has been used to determine the spectral window corresponding to the data, the 'W' option may be selected.
In this case the program asks

"Enter wavelength of line :"

If a wavelength value is entered that is not within the window boundaries, the error message

"Wavelength not in current window"

is presented. After the program determines which diode most closely corresponds to the wavelength of interest, the user is asked for the width of the wavelength region to be displayed.

Restart: This function allows the user to change the active date code so that another series of spectra can be examined or processed.

Quit: Entering 'Q' from the main program exits PDASYS2 and returns to the CP/M operating system environment.

(ii) PDASYS2.BAS

The user interface for the AIM computer is almost identical to the user interface for System 1. The System 2 program does not prompt for the data disk or date code because this responsibility is taken up by the S100 computer. The readout frequency is set to 17.857 kHz by PDAINIT2.ASM. Therefore the default minimum integration time under System 2 is 58.13 ms. In addition to changing the default readout rate, PDAINIT2.ASM sets up VIA1 so that CB2 can be used to initiate the data acquisition process.

In response to

"COMMAND ?"

the user may respond with one of

'SCAN'

'BLURT'

'CSELECT'

as in System 1. These routines are similar to those implemented by System 1 and only relevant changes will be documented below. However, all of the System 2 software is included intact in Appendix J for completeness.

'SCAN': There are essentially two differences between the SCAN routine, and the associated assembler routine PDASCAN2.ASM, and their predecessors. The System 2 software provides for integration times of up to 5.46 minutes while the previous

routine is only capable of 1.09 minute integrations. Secondly, the implementation of the DSID interface is slightly more sophisticated. PDASCAN1.ASM is capable of detecting the trigger of the DSID so that a delay can be inserted before acquiring the data. However, there is no guarantee that the DSID will be triggered by the user such that the delay period ends at the moment a readout is about to begin. Therefore, the delay period can be exactly as specified or longer than specified by one full integration period, TMIN. Accurate synchronization between the computer and the DSID is imperative when the low mass wire loop is employed as the sample substrate because signal evolution occurs in the millisecond time frame. Synchronization was achieved by having the computer trigger a solenoid that releases the sample holder so that it can be driven up into the ICP discharge. PDASCAN2.ASM waits for the end of a readout, triggers the DSID and then waits for the user specified delay period. In this way, a resolution of a few milliseconds is achieved, providing a reproducible method for the multiwavelength characterization of a transient signal. The solenoid is controlled by the CA2 interface line of VIA1.

'Blurt', 'CSELECT': The Blurt software will be discussed in the section devoted to dynamic range extension. The clock select routine is the same as the version implemented for System 1.

2.5 System Performance

The performance characteristics of the RL 1024S linear photodiode array have been well documented [31,79,80,85,93]. It is the purpose of this discussion to briefly outline the characteristics of the detection system used in this work so that its performance can be contrasted with other systems.

2.5.1 Dark Current

The maximum integration time that can be employed is dependent on the magnitude of the dark current. The dark current is dependent on the temperature of the device. The temperature of the PDA was measured using a copper-constantan (Type T) thermocouple referenced to 0 C. The lowest temperature obtainable when the PDA was running was approximately -20 C. To achieve this temperature, the voltage across the series connected stage 2 and stage 3 Peltier elements was set to 7 V and the voltage applied to the series connected miniature elements comprising stage 4 was 1.0 V. These voltages are only about half of the specified maximum values. Evidently, increasing the voltage beyond these values results in the generation of heat within the thermoelectric elements.

The measurement of the dark current produced by the cooled PDA was complicated by a characteristic of the system when longer integration times were employed. When the PDA is integrated for longer than about 0.2 seconds, the baseline video signal drops below the nominal value of 0 V. This drop-off is linear with respect to integration time. For an integration time of about 120 seconds at -21 C, the average dark signal is

about −10 V after amplification. Fortunately, the full scale saturation signal drops off at the same rate. This anomaly has been observed by others [133]. The cause of the problem has not been identified; however, the PDA chip itself is not thought to be at fault [134].

The 0 to 3 V signal range produced by the PDA board is amplified by 3.3 to produce a full scale range of 0 to 10 V. At the minimum integration time (0.058 seconds at 18 kHz) the readout range is 0 to 10 V but at 120 seconds the range is approximately −10 V to 0 V. Fortunately, the reciprocity of integration time vs. light level is maintained providing a linear dynamic range.

This characteristic poses several problems. The first one is that the analog input range of the ADC must be set to +/− 10V to accommodate the signal range at all integration times. However, since the full scale range is only 10 V within a readout, only half of the ADC range is exploited. Therefore, the effective precision of the ADC is 11−bits. The readout noise is sufficient to randomize the least significant bit so the system is not readout limited.

Secondly, the maximum integration time was limited to about 100 seconds. This is not a severe limitation for most applications. Finally, a measurement of the dark current could not be made by simply integrating for a long period and back calculating to determine the result. The rate of baseline drop−off must be known to do this. This drop−off cannot be determined using a plot of dark signal vs. integration time

because both the drop-off rate and the dark current contribute to the signal, albeit in different directions. However, the saturation signal should parallel the drop-off rate because it is determined by the fixed pixel saturation charge of 14 pCoul.

The measurement of the dark current was made by plotting the saturation signal for 3 pixels and the dark signal for the same pixels vs. integration time. The result is shown in Fig. 2.14. The upper curve corresponds to the average signal of diodes 547-549 when completely saturated by the m=0 line of an Fe hollow cathode lamp. The lower solid line corresponds to the average dark signal of diodes 547-549. The slopes of these two lines is linear from about 10 seconds onward.

The slope of the dark line is less severe than the slope of the saturation line because the dark signal increases with time. The dashed line was extended from the dark point at 10 seconds with a slope equal to that of the saturation line. This is the proposed baseline video drop-off rate. The shaded region corresponds to the dark signal which will increase linearly with time. At 120 seconds the extrapolated baseline value is -538 counts. The dark signal is 141 counts and the saturated signal is 1340 counts. Therefore the full scale saturation charge is:

$$Q_s = 1340 + 538 = 1878 \text{ counts}$$

The dark charge is:

$$Q_d = 538 + 141 = 679 \text{ counts}$$

If 14 pCoul is used for the saturation charge per pixel, then the dark charge at 120 seconds is 5.1 pCoul or 36% of full

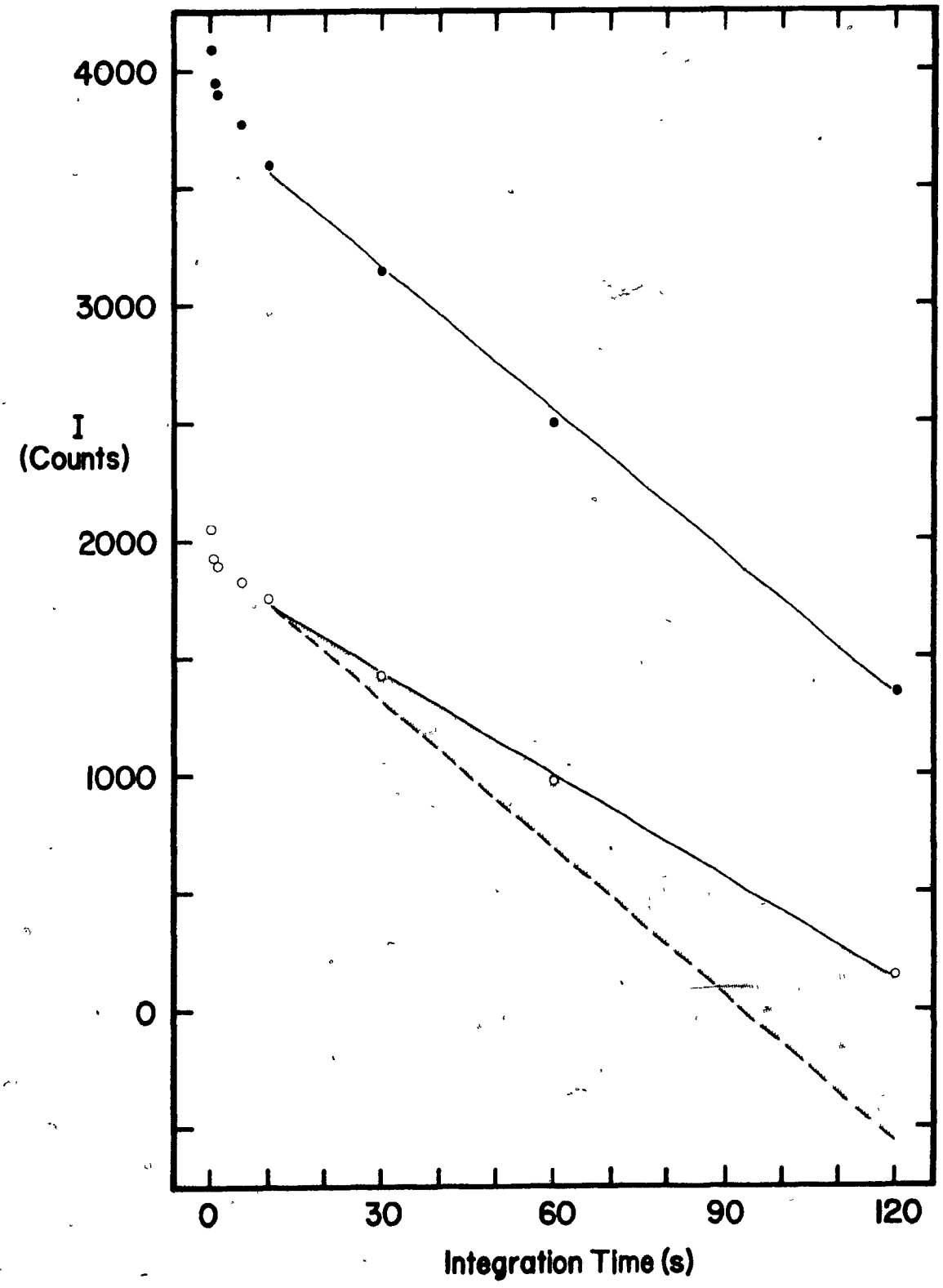

Figure 2.14: Saturation signal (●) and dark signal (○) as a function of integration time.

scale. This corresponds to a dark current of 0.0425 pA.

The temperature of the PDA can be determined from the following equation:

$$I_d = \frac{I_{d(25C)}}{2^{(\Delta T/6.7)}},$$

where - I_d is the dark current;

- $I_{d(25C)}$ is the specified dark current at 25 C;
- ΔT is the temperature differential.

This equation can be rearranged to yield

$$\Delta T = \frac{\left(\ln[I_{d(25C)}] - \ln[I_d]\right) \times 6.7}{\ln(2)}$$

Using the manufacturers dark value of 5 pA at 25 C and the experimentally determined value of 0.0425 pA the temperature differential was found to be 46 C. This corresponds to a temperature of -21 C which is very close to the value determined using the thermocouple of -20 C.

2.5.2 Detector Noise

The ideal detector does not have to be noiseless; it merely has to contribute significantly less noise than the experiment. One of the common methods of signal measurement using single channel detectors involves taking multiple readings of the blank signal followed by multiple readings of the analyte (total) signal. The net analyte signal is simply the average total signal minus the average blank signal. Multiple readings

provide a measurement of the statistical significance of the averaged values. Also, if the noise "seen" by the readout device has a large random component, multiple readings will improve the measurement precision by a factor of the square root of the number of measurements. Another method involves integrating the signals over time instead of collecting discreet measurements. Single readings of integrated intensities do not furnish statistical information but do provide true signal averaging.

When a multichannel detector is used, background and analyte information is present in a single measurement, or readout. An integrating multichannel detector like the PDA provides on-chip signal averaging.

The total analyte signal can be chosen as the value provided by the peak diode (peak height) or the sum of diodes that collect radiation of the analysis line (peak area). The diodes on either side of the peak diode(s) provide a measure of the background that has to be subtracted from the total signal to obtain the net analytical signal. Assuming that the background is comprised of uniform continuum radiation in the region of the analyte line, the background diodes should all report the same intensity if the detector is totally noiseless. Of course this is not the case; the diode values fluctuate and therefore provide a measure of the detector noise.

There are essentially three contributors to these diode to diode fluctuations. Dark current shot-noise can be reduced to negligible proportions by cooling the detector. Readout noise

produced by signal crosstalk between the digital clocking circuitry and the analog circuitry [85] is inherent to the device and cannot be eliminated. The major contributor to the diode to diode variations within a given readout is the fixed pattern signal. This results because the PDA is organized into odd and even pixels, with separate readout circuits. Fortunately, the fixed pattern signal is highly reproducible and can be virtually eliminated by subtracting two spectra, pixel by pixel.

The simplest method of removing the fixed pattern involves acquiring a dark spectrum, or averaging a series of dark spectra. The dark data can be stored as a special file, as is done with System 2, and automatically subtracted from all subsequent spectra. This is not a background correction procedure, although the dark contribution will be removed as a consequence.

Two methods were used to evaluate the readout noise. The first method involved acquiring a dark spectrum to be subtracted from subsequent dark spectra. A total of 16 dark spectra were then acquired. The first dark spectrum was subtracted from each of the 16 spectra yielding 16 fixed pattern corrected spectra. Since cooling the array effectively eliminates the dark current shot noise at short integration times, the diode to diode variations of each of the fixed pattern corrected spectra should indicate the magnitude of the readout noise. A simple computer program was written to calculate the population standard deviation of all 1024 pixels for each of the 16 fixed pattern corrected spectra. The average standard deviation of these 16

measurements is termed "average intraspectral noise". To eliminate the possibility that the subtrahend spectra was not representative, the whole process was repeated 5 times using randomly selected spectra from the group of 16 as the subtrahend. The results for these determinations are presented in Table 2.4 for integrations times of 0.058 seconds and 1.0 seconds.

Trial	Average Intraspectral Readout Noise	
	IT = 0.058 s	IT = 1.0 s
1	1.61	1.16
2	1.40	1.15
3	1.57	1.17
4	1.46	1.21
5	1.38	1.09
6	1.47	1.13
Average	1.48	1.16
Std. Dev.	0.09	0.04

Table 2.4: Intraspectral readout noise in digital counts for integration periods of 0.058 and 1.0 seconds.

The second method was to utilize the same 16 spectra for the two integration times and find the variation of each pixel from spectrum to spectrum. This is a more valid representation of the readout noise because it eliminates the necessity of performing the fixed pattern correction; a procedure that will

of itself add some noise. For each set of 16 spectra the variance of each of the 1024 diodes was determined. The resulting 1024 variance values were then averaged to produce an estimation of the average pixel readout noise, called the average interspectral readout noise. The results are presented in Table 2.5.

Integration Time (s)	Average Interspectral Noise
0.058	1.31
1.0	1.03

Table 2.5: Average interspectral readout noise in digital counts for integration periods of 0.058 and 1.0 seconds.

The interspectral (spectrum to spectrum) noise is slightly less than the intraspectral (within a spectrum) noise because the fixed pattern correction procedure adds a small amount of variance. The readout noise at the longer integration time of 1 second appears to be slightly lower than the noise at an integration time of 0.058 seconds. Data for other integration times was not taken to establish whether or not this was part of a trend.

The readout noise was converted to electrons using the fact that the full scale saturation signal of 14 pCoul, or 8.7×10^7 electrons, corresponds to a digital value of approximately 2048 using the bipolar analog range. Therefore a digital readout noise of 1.2 counts corresponds to about 51,000 electrons. This

is a factor of 5.7 higher than the specified readout noise of the RC1024SA evaluation board of 9000 electrons. The reason for the discrepancy is unknown, however, it may be a result of the modifications to the circuit board.

2.5.3 Linearity

The RL1024S PDA provides a linear response over approximately 4 orders of magnitude for a given integration time [31]. This range extends to upwards of 6 orders of magnitude if variable integration periods are employed [93]. For the system used in this work the fixed integration time (FIT) linearity and the variable integration time (VIT) linearity was verified under conventional experimental conditions.

The ICP was used as the spectral source. Sample introduction was carried out using a MAK fixed cross-flow nebulizer coupled to a MAK low flow torch. The conditions specified in Appendix B were employed vis a vis the MAK system in addition to the following:

Slit width: 25 microns

Viewing height: 11 - 14 mm above the load coil

Readout: System 2

The 324.754 nm Cu line was monitored for all measurements. Solutions were prepared from a 1000 ppm stock solution originally prepared by dissolving an appropriate quantity of Cu wire in 0.5 N reagent grade nitric acid.

the Cu 324.754 nm emission line for concentrations ranging from 1 to 40 ppm for an integration time of 5.0 seconds. Five replicate measurements were made at each concentration. The quality of the linear fit is illustrated by Fig. 2.15. The correlation coefficients are 0.9996 and 0.9998 for the peak height and peak area data respectively.

VIT Linearity: The VIT linearity of the detection system was measured for integration periods spanning 3 orders of magnitude. Plots of peak height and peak area, normalized to concentration, vs. integration time are shown in log-log format in Fig 2.16. The log-log slopes for the peak height and peak area data are 1.02 and 0.994 respectively.

2.5.4 Detection Limits

The detection limits for 4 elements with analysis lines from 200 to 400 nm were determined and contrasted with those obtained with a PMT under identical experimental conditions. For the PDA, integration times of 10 and 100 seconds were used: the 10 second data serves as a direct comparison to the PMT results while the 100 second data illustrates the best results obtainable with the PDA system as it is presently configured. Standard operating conditions were employed for the MAK sample introduction system. The slit width was 25 µm and the PDA viewed the region of the plasma 11 to 14 mm above the load coil. For the 100 second data, a blank spectrum was used to subtract both the fixed pattern signal, the dark signal and spectral

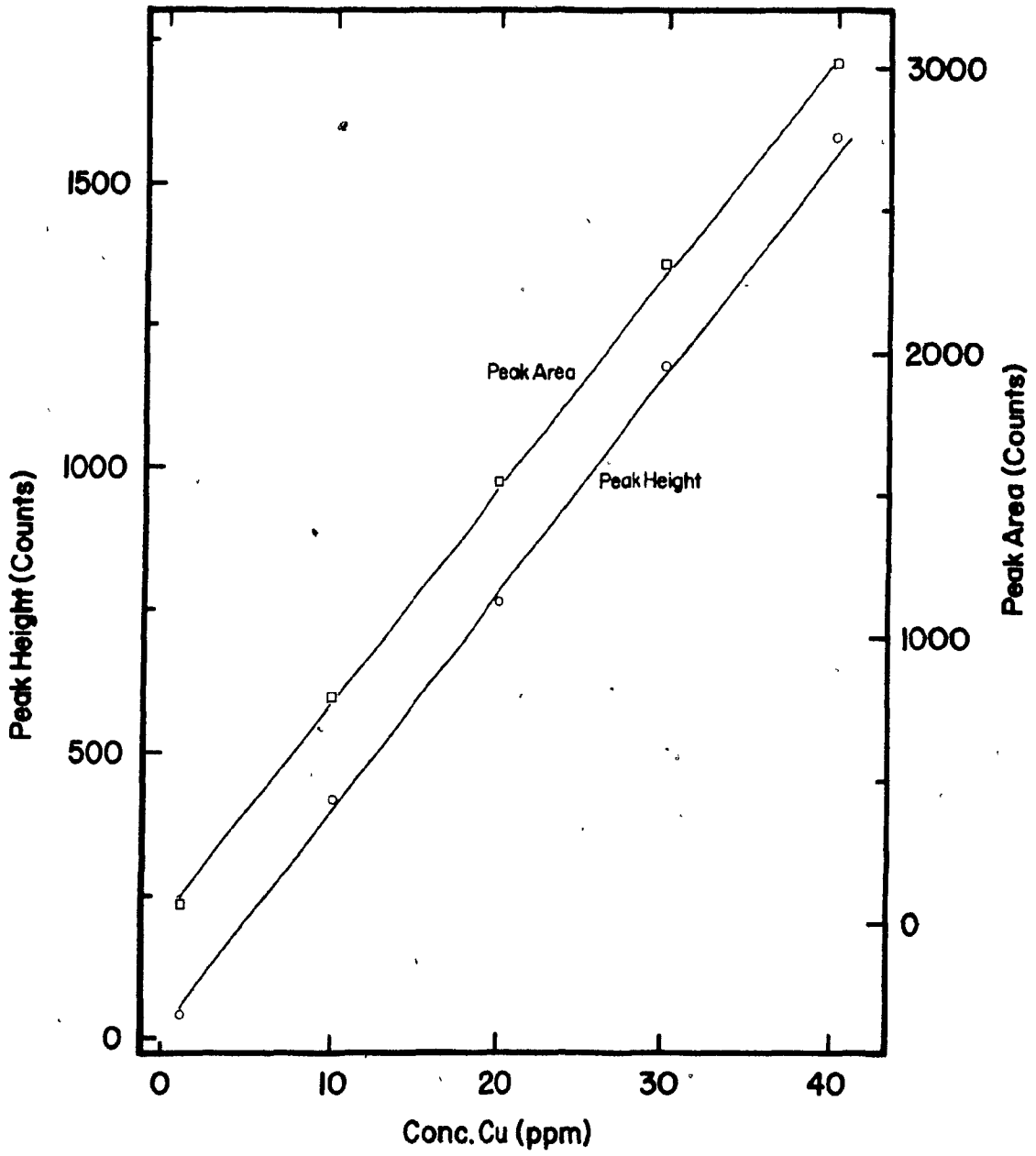

Figure 2.15: Fixed integration time linearity for integration periods of 5 seconds.

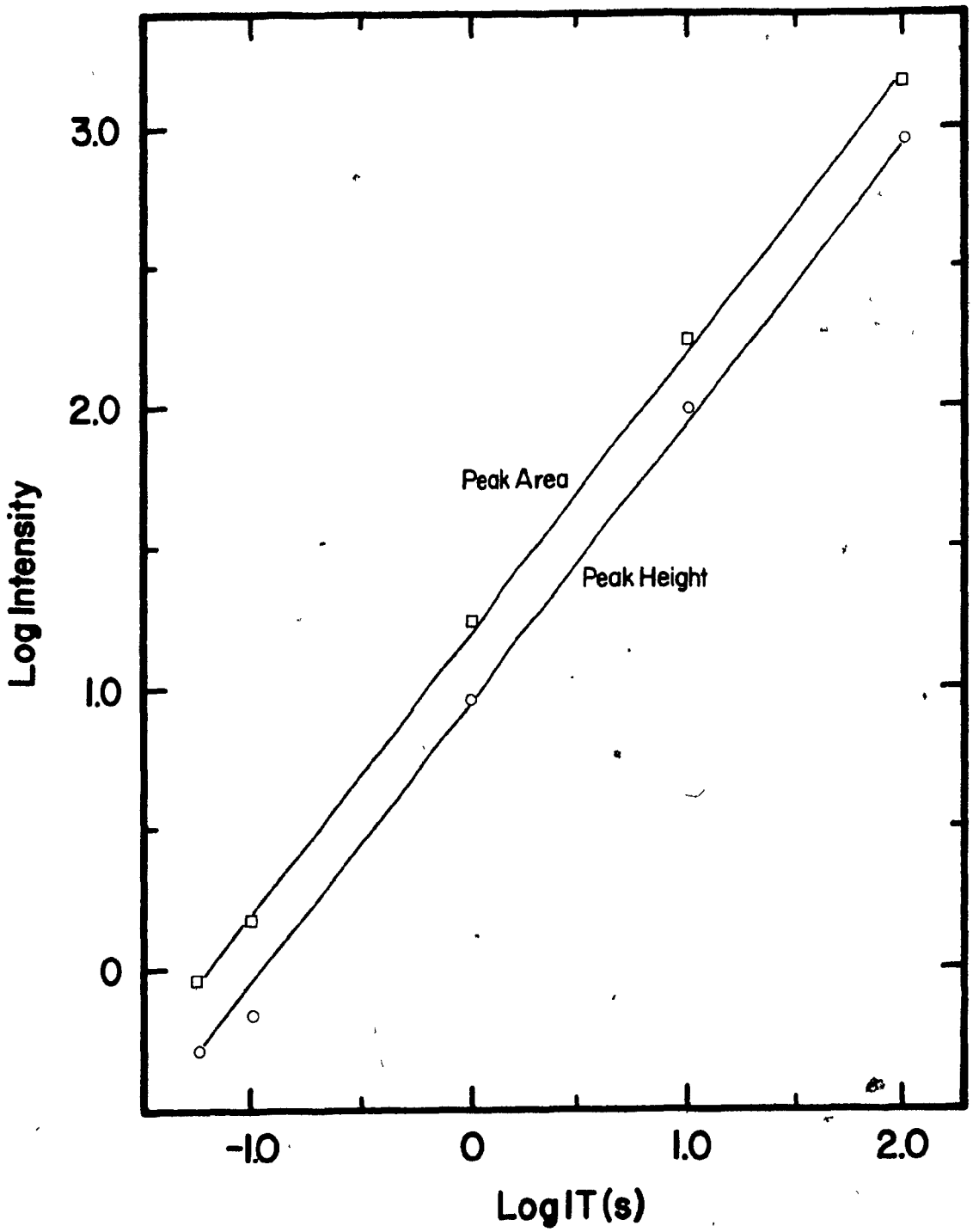

Figure 2.16: Variable integration time linearity. Intensity has units of Counts/ppm.

analysis lines. The detection limits shown in Table 2.6 were calculated as the analyte concentration that would produce a single pixel signal equal to 3 standard deviations above the background level.

Analysis Line (nm)	Int. Time = 10 s		Int. Time = 100 s
	PDA	PMT	PDA
Zn 202.551	4.0	0.004	0.8
Fe 259.940	0.5	0.02	0.1
Cu 324.754	0.02	0.01	0.004
Ca 393.367	0.001	0.001	

Table 2.6: Detection limit data in µg/ml.

This data illustrates that at wavelengths greater than 325 nm the PDA is capable of matching the detection limits provided by a PMT.

3. Some Theoretical and Practical Considerations for the Application of Linear Photodiode Arrays for Inductively Coupled Plasma Emission Spectrometry

Detailed evaluations of PDA sensors as detectors for spectrochemical measurements have been made previously [31,79,83,84,88-90,93,135]. However, the true potential of these sensors has not been evaluated from a fundamental standpoint. There is sufficient technical information available to theoretically predict the best performance obtainable with the RL1024S PDA if the characteristics of the spectral source are known.

The first part of this chapter deals with two of the most important characteristics of a detector for ICP atomic emission spectrometry: detection limits and signal to noise ratios. In this discussion the nomenclature and methodology of Ingle [136,137] and Bower [138] will be followed. The second portion is concerned with data acquisition considerations for the application of the RL1024S sensor to wide dynamic range spectral sources like the ICP. Most of the content of this chapter will be published as two separate manuscripts [119,139].

3.1 Signal to Noise Ratio Theory Applied to Linear Self-Scanning Photodiode Arrays

The electrical noise characteristics of the RL1024S PDA have been determined by Simpson [85] and the noise characteristics of ICP systems employing a variety of sample introduction systems have been evaluated by various groups [13,140-145]. The only additional information required to theoretically determine detection limits for any element is the ICP background flux seen by the detector at the wavelength of interest and the intensity of the analytical line as a function of concentration.

The PMT is a relatively "noiseless" detector because the noise generated by the photocathode and dynode chain is usually well below the level of the noise intrinsic to the experiment. As the ensuing discussion shows, using the PMT as a "benchmark" detector, the relative performance of the PDA can be evaluated knowing only the blank flux as a function of wavelength. The absolute spectral radiance of the background emission of an ICP has been measured by Tracy and Myers [146] from 200 to 600 nm. However, to determine the relative detection limit performance of the PDA detector the blank flux seen by the detector is required.

3.1.1 Experimental

Photon fluxes were determined using a subset of the equipment described in Appendix A and the conditions specified in Appendix B with the following exceptions.

The plasma and auxiliary gas flows were 12 and 0.2 L/min. A Meinhard TR-20-B1 concentric nebulizer, a standard Scott spray chamber and a standard Fassel type torch were used to aspirate distilled, deionized water into the ICP. The nebulizer was operated at 20 psi providing a nebulizer gas flow of 0.55 L/min.

The image of the ICP was focussed onto the entrance slit with 1:1 imaging using a quartz lens with a 12.8 cm focal length. The entrance and exit slit widths were 100 µm. The height of the entrance slit was 2 mm. The region of the discharge from 14 to 16 mm above the load coil was viewed for all measurements.

These conditions were chosen to comply with those used by Tracy and Myers so that the results could be compared. The only major difference between this work and that reported by Tracy and Myers is that this study was performed to measure the photon flux reaching the detector when a blank solution was being aspirated while the other measurements were made using calibrated light sources and a dry plasma (ie. no analyte channel).

A 4-1/2 digit multimeter connected to the 0 - 1 V output of the picoammeter was used as the readout device.

3.1.2 Calculation of Photon Flux

The photon flux reaching the photocathode of the PMT can be determined by back-calculation using the measured photoanodic current as a starting point. The picoammeter furnishes a voltage proportional to the current supplied by the PMT,

therefore the magnitude of the anodic current was easily determined knowing the gain setting of the picoammeter. The photocathodic current was determined using

$$i_c = \frac{i_B - i_D}{G}, \qquad (3.1)$$

where i_B is the photoanodic current produced by the blank flux; i_D is the dark current; and G is the gain of the PMT dynode chain. The gain was determined to be 1 X 10^5 using the method of Bower and Ingle [147]. The photon flux was calculated from

$$\Phi = \frac{i_c}{K_\lambda e}, \qquad (3.2)$$

where K_λ is the wavelength dependent quantum efficiency of the photocathode from the manufacturers literature; and e is the fundamental unit of charge equal to 1.602 X 10^{-19} Coulombs.

This flux is the number of photons striking the photocathode per unit time. The area of a pixel is much less than the area of the photocathode so the flux per unit area was determined using

$$\Phi_A = \frac{\Phi}{WH}, \qquad (3.3)$$

where W is the slit width; and H is the slit height. The flux emanating from the ICP can be estimated by

$$\Phi' = \left[\frac{\Phi_A}{S\Psi T}\right], \qquad (3.4)$$

where S is the spectral bandpass; Ψ is the solid angle collected by the optics; and T is an estimate of the spectrometer transfer function. The bandpass was 0.08 nm, Ψ was about 1×10^{-2} steradians and the transfer function was estimated to be 20%. The factors used to estimate the transfer function were the grating efficiency at 350 nm, and the reflectance losses due to the lens and the mirror surfaces. The results are shown in Table 3.1.

λ(nm)	K_λ	$\Phi(10^6/s)$	$\Phi_A(10^6/s\cdot mm^2)$	$\Phi'(10^9/s\cdot mm^2\cdot sr\cdot nm)$	$\Phi^\ddagger/\Phi'$
200	.04	1.6	0.8	5.0	5.0
225	.06	6.8	3.4	21	3.2
250	.10	14	7.0	44	4.2
275	.12	33	16	100	3.2
300	.14	56	28	170	2.8
325	.15	84	42	260	2.5
350	.15	120	60	370	2.3
375	.15	130	64	400	2.6
400	.14	200	100	640	1.9
425	.12	300	150	920	1.5
450	.10	380	190	1200	1.3

Table 3.1: Background flux from an ICP aspirating blank solution.

The flux per unit area, denoted by Φ_A, will be of use later in the discussion when the flux per diode is needed to determine the magnitude of various spectral noise sources. The last column of Table 3.1 illustrates the ratio of the data presented by Tracy and Myers ($\Phi^{\ddagger}$) to the estimated absolute flux determined for this work. The major reason why the absolute flux estimates for this work are universally low is that the ICP was operated with a central aerosol channel punched through the discharge. The reason for the divergence of the two data sets at shorter wavelengths could be due to the fact that the ICP image was focussed using the focal length of the lens stated for the visible region. Recent experiments indicate that the loss of radiation in the 200 nm region due to defocussing is as much as a factor of 5. In any event, the agreement of the data is sufficient for the purposes of the following discussion.

3.1.3 General Emission Expressions

The general simplified expression for emission spectroscopy assumes that a direct linear relationship between the analytical signal and the analyte concentration, C, exists. Expressed in a very general format where the signal, S, could be a voltage, current or a number of integrated electrons, the analytical signal, S_A, is

$$S_A = k\,[C], \qquad (3.5)$$

where k is a constant. Two measurements are usually required for a single point on an emission spectroscopic calibration

curve: a total analytical signal (sample or standard), S_T, and a total blank signal, S_B. Then a more complete working expression would be

$$S_A = S_T - S_B. \tag{3.6}$$

This can be further broken down to indicate the two major components of the total blank signal, the blank emission signal, S_b, and the dark signal, S_d, which is the noise from the detection system:

$$S_B = S_b + S_d. \tag{3.7}$$

Then the total analytical signal can be expressed as

$$S_T = S_A + S_b + S_d. \tag{3.8}$$

3.1.4 Photodiode Expressions

There are also several expressions which are applicable to photodiodes. The rate of electron-hole pair generation, r_e, [148] is described by:

$$r_e = \Phi K_\lambda, \tag{3.9}$$

where Φ is the photon arrival rate (flux) and and K_λ is the quantum efficiency. For photodiodes operated in the charge storage mode the total number of electron hole pairs generated, n_e, is

$$n_e = r_e t, \tag{3.10}$$

where t is the integration time.

3.1.5 General Noise Expressions

If no correlation exists between noise sources, then propagation of error techniques permit the addition of variances in the following manner. Since two measurements must be made to extract an analytically useful value, S_A, then

$$\sigma_A^2 = \sigma_T^2 + \sigma_B^2 \qquad (3.11)$$

where σ is the general term for rms (root mean square) noise expressed in the units of S. These noise sources can be further broken down. The total blank noise signal σ_B can be partitioned into its major components; shot noise, $(\sigma_B)_s$, flicker noise, $(\sigma_B)_f$ and dark noise, σ_d. The blank noise can be calculated from

$$\sigma_B^2 = (\sigma_B)_s^2 + (\sigma_B)_f^2 + \sigma_d^2. \qquad (3.12)$$

The total signal noise, σ_T^2, is comprised of the following components:

$$\sigma_T^2 = (\sigma_A)_s^2 + (\sigma_A)_f^2 + \sigma_B^2 \qquad (3.13)$$

where $(\sigma_A)_s$ and $(\sigma_A)_f$ are the shot and flicker noise components of the analyte emission signal.

In a shot noise situation, whether it be from the quantum nature of light or any other shot noise sources, Poisson statistics apply. Then the shot noise related variance $(n_D)_s^2$ for any source D (i.e. blank, analyte), producing a discrete number of events n_D during the measurement interval, can be shown to be

$$(n_D)_s^2 = n_D, \qquad (3.14)$$

where n_D is the average number of photons, electrons or electron-hole pairs produced in a given time interval [149]. Flicker noise evolves from non-fundamental sources and is sometimes called 1/f noise because it often has a frequency distribution displaying this character. It has a fixed direct relationship to the signal and must be determined empirically. It is expressed in the general format by

$$(\sigma_D)_f = XS_D, \qquad (3.15)$$

where S_D is the signal from any source D. X is called a flicker factor and is dimensionless. Specifically X_B and X_A are the blank and analyte flicker factors. It is expected that $X_B = X_A$ in the case of ICP spectrometry if the noise source or sources (e.g. nebulizer, gas flows) are the same. If the signal, S_D, is measured as a number of events, n_D, then the more specific flicker noise expression is

$$(\sigma_D)_f = Xn_D. \qquad (3.16)$$

3.1.6 Photodiode Noise Expressions

In the case of photodiode detection, the detector noise sources can be specifically related to a semiconductor detector operated in the charge storage mode and the total dark noise variance is

$$\sigma_d^2 = \sigma_{ar}^2 + (\sigma_d)_s^2 + \sigma_R^2, \qquad (3.17)$$

where σ_{ar} is the analytical measurement readout noise or precision; $(\sigma_d)_s$ is the dark current shot noise; and σ_R is the detector readout noise. The analytical readout noise, σ_{ar}, is the uncertainty introduced by the resolution of the final readout device, whether it be a digital display, analog display or analog to digital converter. It is significant only if noise from other sources is not observed in the final readout. Now that digital high resolution readout is available, it is not the problem that it has been with older instruments using analog needle type readouts usually only good to about 1% resolution. For the purposes of this discussion it is presumed that the system is not analytical readout limited.

A certain amount of noise will be present whenever the photodiode array is read out. The noise per readout, n_R, can be used with the number of readouts, m, to calculate the total readout noise contribution, σ_R, as follows:

$$(\sigma_R)^2 = m(n_R)^2. \qquad (3.18)$$

For an emission measurement with one analytical and one blank or dark measurement, m would minimally be 2 and might easily be as high as 100. The diode-to-diode fixed pattern variation is not a noise source, because no fluctuation is evidenced by a given diode in successive readouts other than those sources already mentioned. The dark current leakage noise is a shot noise and so will be symbolized by $(\sigma_d)_s$ for convenient grouping with other shot noises. Vogt [79] and Talmi [31] have presented excellent discussions of

the characterization and control of PDA dark current and Horlick [84] has discussed dark current with respect to atomic spectrochemical measurement systems.

Using the manufacturers specified dark current of 5 pA at 25 C it can be shown that a cooling temperature of -25 C will reduce the dark current to about 3×10^{-2} pA, or 2×10^{5} and 2×10^{6} electrons for 1 and 10 second integration times using a factor of 6.7 degrees for each factor of 2 change in dark current. The predicted dark current shot noise, $(\sigma_d)_s$, will then be the square roots of these numbers, 400 and 1000 electrons.

Using the minimum readout noise of 1000 electrons reported by Simpson for an RL1024S PDA and the dark current shot noise at -25 C, the combined noise will be 1100 and 1400 electrons for 1 second and 10 second integrations respectively. The analytical measurement readout uncertainty, σ_{ar}, can be eliminated by the proper choice of analog to digital conversion system. For the discussion pertaining to predicted performance, the total minimum readout noise, n_R, will be set to 1500 electrons for all integration times. This is a somewhat conservative value, however; the noise values reported above were obtained under ideal conditions, or using ideal parameters. Therefore,

$$(\sigma_d)^2 = m(n_R)^2, \qquad (3.19)$$

where 1500 electrons will be used for n_R.

3.1.7 Combined Signal and Noise Expressions

The general simplified form of an emission SNR expression is derived from equations 3.6 and 3.11:

$$\frac{S}{N} = \frac{S_A}{\sigma_A} = \frac{S_A}{\left[\sigma_T^2 + \sigma_B^2\right]^{1/2}}. \qquad (3.20)$$

Using equations 3.12 and 3.13 the SNR expression becomes:

$$\frac{S}{N} = \frac{S_A}{\left[(\sigma_A)_s^2 + (\sigma_A)_f^2 + 2(\sigma_B)_s^2 + 2(\sigma_B)_f^2 + 2\sigma_d^2\right]^{1/2}}. \qquad (3.21)$$

The first two noise terms in the denominator are the analyte emission terms and appear only once because the analyte emission is only measured once. The blank noise terms appear twice because the source of these terms is measured twice.

Substituting numbers of integrated electrons for a PDA operated in the charge storage mode in this general expression and using equations 3.14, 3.16 and 3.19 the SNR expression becomes:

$$\frac{S}{N} = \frac{n_A}{\left[(n_A+2n_B) + (X_A n_A)^2 + 2(X_B n_B)^2 + m(n_R)^2\right]^{1/2}}, \qquad (3.22)$$

where $n_A = n_T - n_B$. The components have been grouped from left to right as shot noise, analyte flicker, blank flicker and readout noise.

3.1.8 Application of Expressions

An instrument designer would prefer that the limiting noise in an experiment be a noise intrinsic to the phenomenon being measured and not from the measurement instrumentation. If this is not true then the experiment may be "instrument noise limited". The PMT has obtained a high degree of popularity, because it allows the measurement of light intensities which vary over many orders of magnitude without the introduction of instrumental noise in the form of "detector noise".

In the following section the use of the photodiode array with the relatively high intensity ICP source will be discussed. ICP spectrometry is an emission technique, therefore the lowest light levels measured will be those of the blank. If the detector is not a major source of noise at blank level intensities, then it will not be a major source of noise at higher levels if operated optimally. Salin and Horlick [13] have already demonstrated good diode array performance at higher intensities. The most serious question is whether the unintensified photodiode array can provide performance comparable to a PMT over the wavelength range used for ICP measurements at the lowest intensities likely to be encountered.

The PDA will not be limiting under any circumstances if the sum of the detector related variances is much less than the variances from the experiment. In the general format this is expressed as

$$m\sigma_R^2 \ll (\sigma_A)_s^2 + 2(\sigma_B)_s^2 + (X_A S_A)^2 + 2(X_B S_B)^2, \qquad (3.23)$$

and in an electron format

$$m(n_R)^2 \ll (n_A + 2n_B) + (X_A n_A)^2 + 2(X_B n_B)^2. \qquad (3.24)$$

At the detection limit S_A will be small compared to S_B, and the SNR expression illustrated by eq. 3.22 will simplify to

$$\frac{S}{N} = \frac{S_A}{\left[(2\sigma_B)_s^2 + 2(X_B S_B)^2 + m\sigma_R^2\right]^{1/2}}, \qquad (3.25)$$

or in electron format

$$\frac{S}{N} = \frac{n_A}{\left[(2n_B) + 2(X_B n_B)^2 + m(n_R)^2\right]^{1/2}}. \qquad (3.26)$$

This will simplify the evaluation of eq. 3.24 so that the PDA will not be limiting at the detection limit or under any other circumstances in emission spectrometry if

$$m\sigma_R^2 \ll 2(\sigma_B)_s^2 + 2(X_B S_B)^2. \qquad (3.27)$$

or in electron format

$$m(n_R)^2 \ll 2n_B + 2(X_B n_B)^2. \qquad (3.28)$$

3.1.9 Detection Limit Performance

The performance of the PDA at the detection limit can be estimated by comparing the predicted experimental noise

of an ICP and the added noise using a PDA. The predicted noise using a PDA is the denominator in equation 3.26, and the experimental noise is that same term with the readout noise removed. The data is presented as a degradation factor, DF. This is the ratio of the blank noise calculated with a PDA based system to one assuming a noiseless (PMT) based system.

$$DF = \frac{\left[(2n_B) + 2(X_B n_B)^2 + m(n_R)^2\right]^{1/2}}{\left[(2n_B) + 2(X_B n_B)^2\right]^{1/2}}. \qquad (3.29)$$

m is set equal to 1 in these calculations because many detection limit formulas use only the noise of the blank and include a $2^{1/2}$ or other term to account for the fact that the blank is measured twice. No degradation in detection limit is represented by a DF of 1.0, and a degradation by a factor of two produces a DF of 2.0.

Table 3.2 lists the ICP background flux per diode, the quantum efficiency and the number of electron hole pairs generated, as a function of wavelength.

λ(nm)	$\Phi_P(10^6/S)$	K_λ	$n_B(10^6/s)$
200	.05	.54	.027
225	.21	.54	.12
250	.44	.42	.18
275	1.0	.38	.38
300	1.8	.43	.75
325	2.6	.47	1.2
350	3.8	.50	1.9
375	4.0	.58	2.3
400	6.4	.62	4.0
425	9.2	.64	5.9
450	12	.65	7.7

Table 3.2: ICP blank photon flux per diode (Φ_P), PDA quantum efficiency (K_λ), and rate of electron-hole pair production (n_B) as a function of wavelength.

A comparison of several types of nebulizers [150] for ICP spectrometry has yielded percent relative standard deviations (%RSD) of 2 to 0.1 corresponding to flicker factors of 0.02 to 0.001 respectively. It should be noted that the best of these precisions was obtained using an internal standard, a technique for which the PDA is well suited [13]. It appears that the best unratioed precision was approximately 0.2 %RSD. We have observed %RSDs as high as 3 with certain nebulizers, particularly ultrasonic nebulizers. Consequently for this work we will consider %RSDs

to range from 3 to 0.2. Table 3.3 lists the degradation factors calculated from eq. 3.29 for flicker factors of 3% and 0.2% and integration periods of 1 and 10 seconds. The readout noise was fixed at 1500 electrons.

Flicker Factor (X) →	.03	.002	.03	.002	.03	.002
Integration (s) →	1.0	1.0	10	10	100	100
λ(nm)						
200	1.6	6.2	1	1.7	1	1
225	1	2.7	1	1.1	1	1
250	1	2.1	1	1	1	1
275	1	1.5	1	1	1	1
300	1	1.2	1	1	1	1
325	1	1.1	1	1	1	1
350	1	1	1	1	1	1
375	1	1	1	1	1	1
400	1	1	1	1	1	1
425	1	1	1	1	1	1
450	1	1	1	1	1	1

Table 3.3: Degradation factors for flicker factors of 3% and .02% and integrations periods of 1, 10 and 100 seconds. Readout noise (n_R) is 1500 electrons.

It is apparent that the detection limits will be degraded at shorter wavelengths for integration periods of 1 second or less only for an ICP system providing exceptional precision.

These results can be contrasted with those expected for the PDA system that is the subject of this thesis. Table 3.4 lists the degradation factors for a PDA detector contributing 50,000 electrons as the readout noise.

Flicker Factor (X) →	.03	.002	.03	.002	.03	.002
Integration (s) →	1.0	1.0	10	10	100	100
λ(nm)						
200	43	200	4.5	47	1.1	6.3
225	9.8	84	1.4	13	1	1.8
250	6.6	64	1.2	9.3	1	1.4
275	3.3	36	1.1	4.6	1	1.1
300	1.9	20	1	2.5	1	1
325	1.4	13	1	1.8	1	1
350	1.2	8.8	1	1.4	1	1
375	1.1	7.4	1	1.3	1	1
400	1	4.4	1	1.1	1	1
425	1	3.1	1	1	1	1
450	1	2.5	1	1	1	1

Table 3.4: Degradation factors for flicker factors of 3% and 0.02% and integration periods of 1, 10 an 100 seconds. Readout noise (n_R) is 50,000 electrons.

Integration periods of 100 seconds or more must be used if the detection limits at low wavelengths are to comparable to those of a PMT. This is corroborated in part by the detection

limit data shown at the end of Chapter 2. However, at an integration time of 100 seconds the flicker noise at 300 nm will be about 2×10^6 electrons and 2×10^5 electrons for flicker factors of 0.03 and 0.002 respectively while the shot noise will be about 1×10^4 electrons. This corresponds to a flicker noise limited situation where no advantage is gained by integrating for a longer period of time.

It should be noted that increases in intensity provide exactly the same effect as an equivalent increase in integration time, if all other factors remain unchanged. An increase of intensity of a factor of 5 or even 10 is not at all unreasonable. Ultrasonic nebulizer systems obtain superior detection limits by placing more analyte into the plasma. The resulting increase in analyte signal level is of the order of a factor of 10. Both Faires [151] and Demers [152] have discussed top down viewing of the plasma and their work indicates that there are advantages to this mode of operation. Faires reports an increase in intensity ranging from 3 to 8 for different elements in the ICP operated under normal conditions. Vogt [79] used a cylindrical lens immediately before the PDA to increase light collection efficiency by a factor of 4.5. Finally, the flux measurements reported above were made with an F 8.7, 1 meter focal length spectrometer using a 1200 g/mm grating and a reciprocal dispersion of 0.8 nm/mm. An F 3.9 system with similar characteristics is quite possible, and the collection efficiency change would produce an increase in intensity of a factor of 5. It appears quite likely that it

is possible to obtain an increase of an order of magnitude in intensity beyond that measured for this work.

3.1.10 Performance Above the Detection Limit

In order to make an evaluation of the effect of the PDA at signal levels greater than those found at the detection limit, equation 3.30 has been used to prepare the information in Tables 3.5 to 3.9. These tables describe the expected degradation in performance, as measured by signal to noise ratio, under a wide variety of circumstances. The ratio, DF, is determined by calculating the SNR that would be obtained with a "noise free" detection system and ratioing this with the SNR obtained with a PDA array system. The resulting expression is

$$DF = \frac{\left[(n_A+2n_B) + (X_A n_A)^2 + 2(X_B n_B)^2 + m(n_R)^2\right]^{\frac{1}{2}}}{\left[(n_A+2n_B) + (X_A n_A)^2 + 2(X_B n_B)^2\right]^{\frac{1}{2}}}. \quad (3.30)$$

For these calculations m = 2 because two diode measurements must be made. These two measurements may be made by acquiring two separate scans, one of the analyte and one of the blank, and using the same diode for the calculation of analyte and blank intensity. Alternatively, a single analyte scan may be used. The peak diode represents the analyte intensity while a diode to the side of the peak represents the blank level. This procedure assumes a flat continuum level.

Using the data of Table 3.2 for a flicker factor of 3%, an SBR of 0.1 and an integration period of 1 second, the SNR

degradation at 200 nm for a PDA detector having a readout noise of 1500 electrons would be:

$$DF = 2.1$$

where n_A = 2700 electrons; n_B = 27,000 electrons; X = .03; and n_R = 1500 electrons.

Signal to background ratios (SBR) have been used as intensity indicators, because this measurement is commonly used to report relative analyte signals. Tables 3.5 and 3.6 illustrate degradation factors for a low noise PDA system exhibiting 1500 electrons readout noise. SBR values of 0.1, 1 and 10 indicate the relative intensity of the analyte signal with respect to the background. Integration periods of 1 and 10 seconds have been used and the same flicker factors used for the detection limit evaluation were employed.

Flicker Factor (X) →	.03	.002	.03	.002	.03	.002
Signal to Background →	0.1	0.1	1.0	1.0	10	10
Integration (s) →	1.0	1.0	1.0	1.0	1.0	1.0
λ(nm)						
200	2.1	8.5	1.8	7.2	1	2.9
225	1.1	3.6	1.1	3.1	1	1
250	1	2.8	1	2.4	1	1
275	1	1.8	1	1.6	1	1
300	1	1.3	1	1.2	1	1
325	1	1.1	1	1.1	1	1
350	1	1.1	1	1	1	1
375	1	1	1	1	1	1
400	1	1	1	1	1	1
425	1	1	1	1	1	1
450	1	1	1	1	1	1

Table 3.5: Signal to noise ratio degradation for flicker factors of 0.03 and 0.002; SBR values of 0.1, 1.0 and 10; and integration periods of 1 second. Readout noise set to 1500 electrons.

Flicker Factor (X) →	.03	.002	.03	.002	.03	.002
Signal to Background →	0.1	0.1	1.0	1.0	10	10
Integration (s) →	10	10	10	10	10	10
λ (nm)						
200	1	2.2	1	1.9	1	1.1
225	1	1.1	1	1.1	1	1
250	1	1.1	1	1.1	1	1
275	1	1	1	1	1	1
300	1	1	1	1	1	1
325	1	1	1	1	1	1
350	1	1	1	1	1	1
375	1	1	1	1	1	1
400	1	1	1	1	1	1
425	1	1	1	1	1	1
450	1	1	1	1	1	1

Table 3.6: Signal to noise ratio degradation for flicker factors of 0.03 and 0.002; SBR values of 0.1, 1.0 and 10; and integration periods of 10 seconds. Readout noise set to 1500 electrons.

For integration periods of 1 second the readout noise of the PDA will degrade the SNR significantly for low light levels at wavelengths below 250 nm when observing the signal from a high precision ICP source. For an ICP exhibiting an RSD of 3% the SNR is not affected by an appreciable amount. If the

integration period is extended to 10 seconds, the PDA noise will degrade the SNR only by a small amount at 200 nm for low light level signals and an RSD of 0.2%.

Tables 3.7 to 3.9 illustrate the SNR degradation for a PDA system contributing a readout noise of 50,000 electrons. The extra integration time of 100 seconds is included to indicate the conditions required to match the SNR of a relatively noiseless detection system.

Flicker Factor (X) →	.03	.002	.03	.002	.03	.002
Signal to Background →	0.1	0.1	1.0	1.0	10	10
Integration (s) →	1.0	1.0	1.0	1.0	1.0	1.0
λ (nm)						
200	60	280	49	240	8.7	90
225	14	120	11	97	2.2	26
250	9.3	89	7.6	73	1.6	18
275	4.5	51	3.7	42	1.2	8.9
300	2.4	29	2.1	24	1	4.7
325	1.7	19	1.5	16	1	3.1
350	1.3	12	1.2	10	1	2.1
375	1.2	10	1.2	8.5	1	1.8
400	1.1	6.1	1.1	5.1	1	1.3
425	1	4.3	1	3.5	1	1.2
450	1	3.3	1	2.8	1	1.1

Table 3.7: Signal to noise ratio degradation for flicker factors of 0.03 and 0.002; SBR values of 0.1, 1.0 and 10; and integration periods of 1 second. Readout noise set to 50,000 electrons.

Flicker Factor (X) →	.03	.002	.03	.002	.03	.002
Signal to Background →	0.1	0.1	1.0	1.0	10	10
Integration (s) →	10	10	10	10	10	10
λ (nm)						
200	6.2	66	5.1	55	1.3	12
225	1.7	19	1.5	16	1	3.1
250	1.4	13	1.3	11	1	2.2
275	1.1	6.4	1.1	5.3	1	1.4
300	1	3.4	1	2.9	1	1.1
325	1	2.3	1	2.0	1	1
350	1	1.6	1	1.5	1	1
375	1	1.5	1	1.3	1	1
400	1	1.2	1	1.1	1	1
425	1	1.1	1	1.1	1	1
450	1	1.1	1	1	1	1

Table 3.8: Signal to noise ratio degradation for flicker factors of 0.03 and 0.002; SBR values of 0.1, 1.0 and 10; and integration periods of 10 seconds. Readout noise set to 50,000 electrons.

Flicker Factor (X) →	.03	.002	.03	.002	.03	.002
Signal to Background →	0.1	0.1	1.0	1.0	10	10
Integration (s) →	100	100	100	100	100	100
λ(nm)						
200	1.2	8.9	1.1	7.3	1	1.6
225	1	2.3	1	2.0	1	1
250	1	1.7	1	1.5	1	1
275	1	1.2	1	1.1	1	1
300	1	1.1	1	1	1	1
325	1	1	1	1	1	1
350	1	1	1	1	1	1
375	1	1	1	1	1	1
400	1	1	1	1	1	1
425	1	1	1	1	1	1
450	1	1	1	1	1	1

Table 3.9: Signal to noise ratio degradation for flicker factors of 0.03 and 0.002; SBR values of 0.1, 1.0 and 10; and integration periods of 100 seconds. Readout noise set to 50,000 electrons.

3.1.11 Summary and Conclusions

Given the intensity of the ICP, it appears that the linear PDA should be capable of performance comparable to that provided by PMT detection systems for wavelengths longer than 225 nm using systems with collection efficiencies and integration times

systems. For wavelengths less than 225 nm, the ICP/PDA performance at the detection limit may be degraded; however, the performance well above the detection limit will be comparable to that obtainable with a PMT based system. Performance of the PDA can approach that of PMT based systems for wavelengths down to 200 nm if the incident flux on the PDA is increased by approximately one order of magnitude.

For a well optimized ICP and 1 second integration periods the detection limit will be degraded by a factor of 6.2 at 200 nm. If the integration period is extended to 10 seconds then the degradation is only a factor of 1.7. Integration periods longer than 10 seconds may introduce long term drift and should not necessarily be used to enhance performance. At concentrations above the detection limit the degradation of SNR is 8.5 at 200 nm for an optimized ICP if the SBR is 0.1 and the integration period is 1 second. If the SBR is increased to 10, the degradation is only a factor of 2.9.

3.2 Data Acquisition Considerations

Optimal use of a detection system normally requires that the system be operated in a manner such that the noise from the detector system is small compared to the total noise observed at the detector during an experiment. If this is the case then measurements are not detector noise limited and essentially all the noise measured is from the experiment rather than the transducer monitoring the experiment. In many experiments it is possible to vary the noise contribution of the detector by operating it in a specific manner. In the previous discussion the applicability of a linear PDA as a detector for atomic emission spectrometry with an inductively coupled plasma was discussed. This section will introduce some of the more general aspects of data acquisition with a PDA. Many of the results have applicability to other experiments which employ integration in either the experimental transducer or its electronics.

If an experiment always produces a signal of approximately the same intensity, then configuration of the detector and data acquisition system is straightforward; however, many spectroscopic experiments produce signals that change over many orders of magnitude. The optimal conditions for a large signal may be completely inadequate for a small signal and vice versa. The optimization procedures discussed herein are based on straightforward calculations using experimentally measurable parameters. These parameters can be acquired in real time or pre-programmed into a data acquisition system.

In this discussion it is assumed that the experiment is

flicker noise dominated to simplify the expressions, however the basic philosophy is completely unchanged if a more complicated noise expression including shot noise terms must be substituted. ICP spectrometry is often flicker noise dominated over a wide wavelength range [140]. If this is the situation the noise from the experiment can be expressed as

$$\sigma_E = X_E S_E, \tag{3.31}$$

where σ_E is the noise from a flicker noise dominated experiment E; S_E is the signal from the experiment for a given integration period or electronic bandpass; and X_E is the flicker factor. The units will be electrons in this discussion but could be voltage or current.

3.2.1 Minimum Signal Calculations

The first required value is the minimum signal, S_{E-min}, that can be measured with "minimal" degradation by the detection system. A detection system will always have some noise, σ_d, associated with its readout. In this context it will include the noise generated by the detector and supporting analog electronics and is assumed to be independent of the signal level produced by the experiment. This noise is the minimum noise which must appear in every reading of the detection system. In PDA systems this noise remains fixed and equal to the readout noise if sufficient cooling is provided so that the dark current noise contribution is minimized. The dark noise can be easily measured by blocking all incoming radiation and making

repetitive measurements under the experimental conditions. Using standard propagation of error mathematics, the total noise measured at any readout of the detection system will be

$$\sigma_T^2 = \sigma_d^2 + \sigma_E^2, \qquad (3.32)$$

where σ_T is the total measured noise and σ_E is the noise introduced by the experiment.

If the detection system is to affect the measurement of the experiment "minimally", then the criteria for minimal must be established. This can be done by specifying a factor f which must assume a value between 1.0 and 0.0. If f = 0.15 then σ_d would be allowed to contribute a maximum of 15% to the total measured noise, σ_T. The experimental noise, σ_E, will then constitute a minimum of a (1-f) fraction of the total measured noise. If the experimental noise, σ_E, is proportional to the experimental signal, S_E of equation 3.1, and σ_d is fixed in magnitude, then σ_d will be a more significant contributor to the total measured noise, σ_T, at low signal levels. To solve for the minimum signal, S_{E-min}, a special case of equation 3.32 can be used to solve for σ_{T-min}, the minimum total noise, and σ_{E-min}, the minimum noise from the experiment at low signal levels. It is most convenient to use $(1-f)\sigma_{T-min} = \sigma_{E-min}$. Then equation 3.32 can be rearranged as

$$\sigma_{T-min}^2 = \sigma_d^2 + [(1-f)\sigma_{T-min}]^2. \qquad (3.33)$$

Since σ_d can be measured experimentally or obtained from the literature, σ_{T-min} can be calculated. Substitution of σ_{T-min} into eq. 3.32 will produce σ_{E-min}. Equation 3.31 can then be

used to calculate the minimum signal, S_{E-min}, that can be recorded with only an f factor of degradation.

Using 1500 electrons for σ_d and equation 3.33 σ_{E-min} is 2400 electrons. A 3% RSD for atomic spectroscopy would be considered relatively poor while a 0.3 %RSD would be considered very good. Using a compromise value of 1% (X_E = 0.01) as an example and equation 3.31, S_{E-min} would be 2.4×10^5 electrons. Therefore, 2.4×10^5 electrons is the signal that would generate a noise of 2400 electrons if the flicker factor were 0.01. Using the manufacturers specified saturation charge of 14 pCoulit is straightforward to calculate that the saturation charge of the PDA is 9×10^7 electrons. This is the maximum signal that can be recorded, S_{E-max}.

3.2.2 Dynamic and Usable Range Calculations

Dynamic range is normally defined as the largest signal that can be measured, before a degradation (or saturation) occurs, divided by the smallest signal that can be measured before the signal becomes buried in detector noise. The usable range, U, is the largest signal that can be measured without significant degradation introduced by the detector system (ie. saturation) divided by the smallest signal that can be measured without significant degradation by the detection system as quantified by the factor f. The upper limits of the dynamic range and U definitions are identical, however the lower limits and consequently the meanings of the two definitions are quite different. Expressed mathematically the

intrascenic usable range, U_I, is

$$U_I = \frac{S_{E-max}}{(\sigma_{E-min}/\chi_E)} = \frac{S_{E-max}}{S_{E-min}} = \frac{9\ E\ 7}{2.4\ E\ 5} = 380, \qquad (3.34)$$

where intrascenic refers to the smallest and largest spectral features that can be measured within a single readout without degradation.

Using the saturation data and substituting into eq. 3.34 U_I is found to be 380. It is important to note that the more precise (smaller RSD) the experiment is, the smaller the usable range. This should be contrasted with the intrascenic dynamic range, D_I, which can be 10^5 and does not vary with the experiment.

3.2.3. Time Dynamic Range

An integrating detector system like the PDA has its own "time" dynamic range. The smallest integration time may be imposed by the data acquisition system, while the largest time interval will be imposed by the experiment if long integration periods are possible without adding significant dark noise. The experiment imposes a limit when longer integration periods result in a degradation or plateau of the SNR of the experiment. This occurs when low frequency noise components from the experiment dominate. In any case, two limits will usually exist with any real system, a minimum acquisition time, t_{min}, and a maximum time, t_{max}. The time dynamic range is

$$D_T = \frac{t_{max}}{t_{min}}, \qquad (3.35)$$

and describes the range of signals that can be acquired by varying integration times. The maximum usable range for a detector system becomes

$$U_{max} = U_I D_T, \qquad (3.36)$$

where U_{max} is the maximum range of signals which can be monitored before significant degradation occurs.

To provide a basis for comparison it is appropriate to apply these equations to a potential system to evaluate their utility. The dynamic range of a single diode of an S series PDA is stated by the manufacturer [124] to be 10^5, however it is critical that this not be confused with usable range. In section 3.1 integration periods of 10 seconds were demonstrated to be adequate for performance at or near the detection limit for a large portion of the spectrum. Ten second integration periods are common for both plasma and flame spectroscopy and therefore provide the upper limit, t_{max}. Talmi has employed integration periods of up to 180 seconds [93] for analysis lines below 250 nm; however, Belchamber and Horlick [143] and McGeorge and Salin [153] have demonstrated that large low frequency components may exist in ICP spectral outputs and consequently long integration times may result in performance degradation. This is especially true if multiple spectra and/or samples are to be analyzed.

Data acquisition rates of 20 kHz are easily obtained using microprocessor based systems [154]. This will provide a minimum integration time of about 50 ms for a 1024 element PDA. There are techniques to produce shorter integration times including computer direct memory access (DMA)[155] or a technique called the "Blurt" method [120] which rapidly clocks through the PDA without taking data until the diodes of interest are reached. Both methods have their advantages, and either can produce a minimum integration time of approximately 5 ms. Therefore the time dynamic range, D_T, is 10/0.005 = 2000. Using eq. 3.36 and a U_I of 380, U_{max} is 6×10^5 if DMA type techniques are used or 6×10^4 using conventional computer readout techniques. This illustrates that the experiment and its requirements must be kept in mind when specifying the detector and its method of operation.

It is possible to have widely varying intensities fall on the PDA. Obviously, if the intensity differences exceed U_I, several integration times must be used. The following relationship can be used to determine the number of integration periods required to accommodate the full time dynamic range, D_T:

$$T_{ADD} = \frac{\ln D_T}{\ln U_I}. \qquad (3.37)$$

If T_{ADD} is a non-integer value, it must be rounded up to the next largest integer.

A graphical explanation of eq. 3.37 is illustrated in Fig. 3.1. In this example $U_I = 10$ and $D_T = 10^5$. It is assumed that

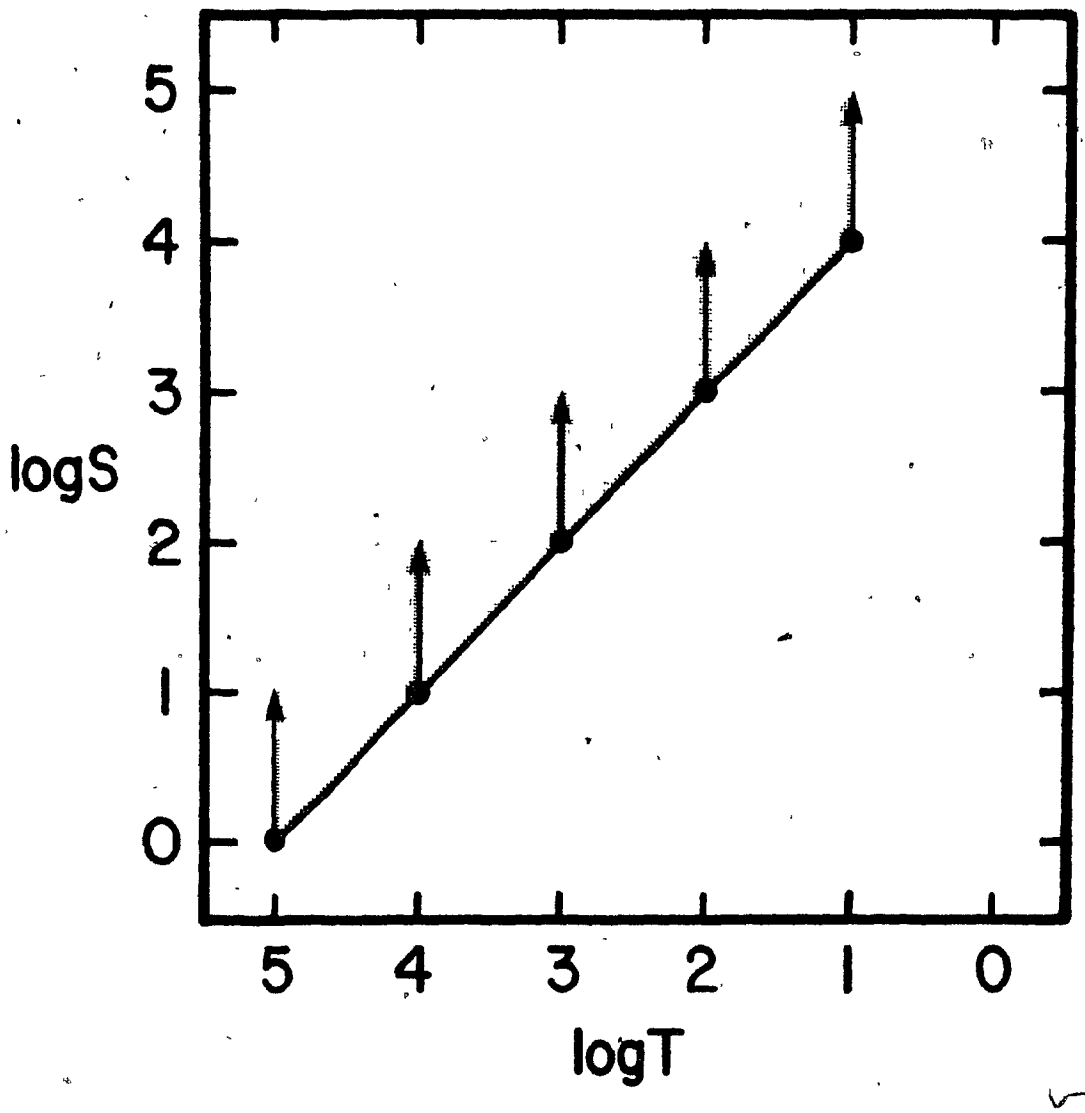

Figure 3.1: Demonstration of T_{ADD} calculation.

the integrated signal must be at least 10^5 electrons to achieve the minimum allowable SNR. Since the integrated signal is the product of the flux and time, the solid line of Fig. 3.1 can be constructed such that it passes through the minimum light flux level for the range of integration times. The shaded area above each integration time on the line corresponds to the usable range U_I. The vectors originate from the optimal integration

time choices for a minimum number of integration times given the U_I of 10. Each integration time choice covers a unique flux range. Then

$$T_{ADD} = \ln(10^5)/\ln(10) = 4.$$

In this example the result is an integer, however this will not always be the case. Non-integer values should be rounded up to the next largest integer. The total number of integrations will be T_{ADD} + 1 which is 5 in this example.

3.2.4 Acquisition Hardware Dynamic Range

The selection of an electronic signal acquisition device is integrally linked to the rate of acquisition and the required measurement precision. Data acquisition rates of the magnitude of 20-200 kHz clearly indicate the use of a rapid sampling ADC rather than an integrating device. Fast and relatively inexpensive ADCs with up to 14 bits of resolution and other suitable specifications are presently available. The minimum resolution required of an acquisition must be of the order of the experimental noise to avoid quantizing error. The usable range provided by an ADC system, U_{ADC}, must match or exceed that of the PDA detector to take advantage of the full PDA usable intrascenic range, U_I. The usable range of an ADC, U_{ADC}, when used in conjunction with an experiment which requires a minimum resolution of R_{MIN} is

$$U_{ADC} = \frac{R_{ADC}}{R_{MIN}}, \qquad (3.38)$$

where R_{ADC} is the resolution of the ADC expressed as the number of resolvable elements. A 12 bit ADC has a resolution of 2^{12} or 4096. The required minimum resolution of a system limited by a flicker factor of 0.01 will be the inverse of that flicker factor, 100. Since the smallest resolvable element is 1 the corresponding signal must be 100. With a 12 bit converter

$$U_{ADC} = \frac{2^n}{1/X_E} = \frac{4096}{100} = 41.$$

In this case U_{ADC} is less than U_I, requiring that additional circuitry, perhaps in the form of an autoranging circuit, is required to utilize the full U_I. If one does not take advantage of the U_I, then additional integration times may be necessary if signals of differing intensity are falling on the PDA. The number of total ADC ranges, R_T required of such a system can be calculated from the expression

$$R_T = \frac{\ln U_I}{\ln U_{ADC}}, \qquad (3.39)$$

where R_T must be rounded up to the next largest integer.

For example, if the maximum signal to be measured is 1000 (arbitrary units), the flicker factor is 0.2 and the ADC can resolve one part in 32 then

$$U_I = 1000/(1/0.2) = 200$$

and

$$U_{ADC} = 32/(1/0.2) = 6.4.$$

If the electronic gain is adjusted so that the minimum noise of the experiment is approximately equal to the smallest resolution element, 1, then the experiment is optimized, and the last bit or digit will be randomized by this noise. If the noise is 1, then the signal that produces this noise is 1/0.2 = 5 and the largest signal that can be recorded, based on R_{ADC}, is 32. Then the ADC can measure correctly (including the noise) all signals ranging in value from 5 to 32. If a signal greater than 32 must be recorded another ADC range is needed. A signal of magnitude slightly greater than 32 would have a noise of approximately 0.2 X 32 = 6.4. The electronic gain must be adjusted for the next range to bring a signal of magnitude 6.4 to be magnitude 1 on the ADC. Using the original units, the new range will be 32 to 6.4 X 32 = 204.8. Similarly the last range will be roughly 204 to 1306. The number 1305 exceeds 1000, so the design requirements have been satisfied with 3 ranges with gains of 1, 6.4 and 204. This is illustrated in the application of equation 3.39 producing a real number which must be rounded up to the next largest integer value:

$$R_{ADD} = \ln 200/\ln 6.4 = 2.8 \rightarrow 3.$$

3.2.5 Conclusions

Care must be taken when designing the software and hardware for a data acquisition system for any detection system. It is especially important in the case of the linear photodiode array and similar devices which provide a significant amount of detector noise. It is also quite clear that the choice or operation of data acquisition hardware and software must be integrally linked to the the experiment itself. This linkage must include a knowledge of the range of magnitude of the experimental signals as well as the noise of these signals. In situations where the noise characteristics of the signal are not known prior to the experiment, it may be possible to determine them by short preliminary measurements, and then have the software optimize the acquisition process using the expressions above.

For an S-series array with a usable range of 380, based on a 1% experiment RSD and a 15% noise contribution by the detector, a 16-bit ADC will be required to provide adequate digitization of all signals with only one range setting.

4. Control and Dynamic Range Extension of Linear Photodiode Arrays

It is often the case with atomic spectra that only a very limited portion of the spectrum contains analytically useful information. This fact has been used to advantage by researchers using vidicon and image dissector photomultiplier tubes [54] which have the capability of directly addressing the portion of the detector surface containing the spectral information of interest. The self-scanning PDA does not have this capability and is normally used to record the entire spectrum falling on the detector surface. This chapter demonstrates a technique of data collection using an inexpensive single board computer to collect atomic line spectral information of interest without the inclusion of unnecessary data. In addition, the collection technique provides a dynamic range extension which is very important for the application of photodiode array detectors to atomic emission spectrometry. The substance of this chapter has been published previously [120].

4.1 Experimental

The equipment used in these experiments is a subset of that listed in Appendix A. This work was carried out prior to the completion of the present PDA detection system. The detector was mounted in the focal plane of the 1 meter spectrometer using the apparatus described in section 2.2.3. The PDA interface is shown in Fig. 4.1 and a full schematic is included in Appendix G. This circuit is a simplified version of the present

interface and has served as an important development step.

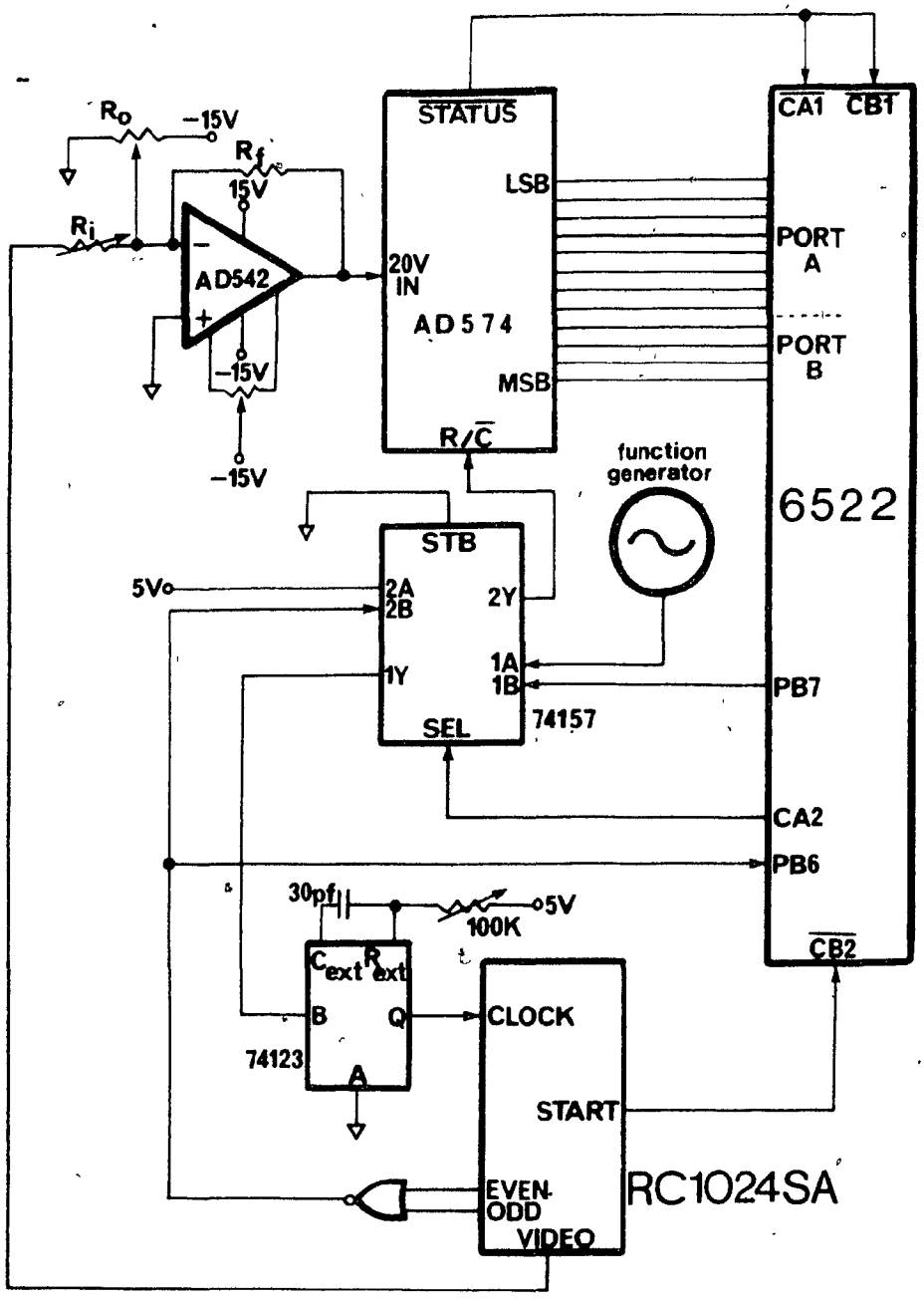

Figure 4.1: Simplified schematic diagram of hardware configuration used for Blurt mode study.

The RC1024SA module corresponds to the PDA detector and evaluation board combination. The 6522 is a Versatile Interface Adapter (VIA) which was located on a standard AIM-65 single board computer. Only one VIA was required for this interface while 3 are utilized in the present implementation. The remaining components: 74123 monostable, 74157 data selector, AD574 analog to digital converter (ADC), and AD542 precision operational amplifier; were mounted and wired on a breadboard.

The software used to operate the system was stored on cassette tape. In keeping with the hierarchical design philosophy discussed in Chapter 2, user commands were submitted to a BASIC program which invoked an assembly language routine. The assembly language routine provided similar functions to those supplied by the present software: clock frequency selection, clock source selection and data acquisition. The 4 kByte read-write memory of the AIM computer was just large enough to accommodate the software and one complete 1024 pixel spectrum. However, using the Blurt mode described below several spectra could be acquired because only the pixels furnishing data were collected. To provide spectral line images on the photodiode array, various light sources were used including a He-Ne laser, tungsten filament lamp, hollow cathode lamps and an ICP. The laser did not provide the stability required for quantitative work and the ICP was used for all high intensity quantitative measurements. Intensities were varied using neutral density filters. The neutral density filters were recalibrated at the wavelength of use.

4.1.1 Circuit Description

The VIA is a very powerful I/O device [156] and is used to provide the interface to the external electronics. As Fig. 4.1 indicates, very little supporting electronics are needed when operating with the RC1024SA evaluation board. The minimal hardware requirements result from software exploitation of the 6522 VIA. In fact, the 74157 can be eliminated if one is willing to be limited to conventional operation of the RC1024SA. During conventional operation of an RC1024SA system an onboard clock is adjusted to provide an output clock rate (readout rate) within the range of the computer acquisition system. The integration time can be varied by manually changing a value preset on several counters on the evaluation board.

The system illustrated in Fig. 4.1 uses the power of the VIA extensively to eliminate manual control requirements and simplify hardware and software. The onboard clock generation circuitry is bypassed allowing an external clock signal to be input called the input clock. The input clock can be selected to be either an external signal such as a function generator (or the 1.0 MHz computer system clock) or the output clock (T1) from PB7 of the 6522 VIA. The selection is under software control and is made by the CA2 control line. The 74157 quadruple 2-line-to-1-line data selector is used to select which clock signal will appear as the input clock to the evaluation board. A secondary function of the 74157 is that it connects and disconnects the evaluation board output clock from the ADC. This eliminates the possibility of any undesirable effects that might result from sending in an acquisition frequency rate

higher than that for which the device is specified. The video signal from the RC1024SA is fed to the AD574 12-bit ADC. The Status signal from the ADC is an end of conversion signal and is used to latch the converted data into both I/O ports of the 6522 VIA. The latching process also alerts the computer by setting an interrupt bit in the 6522 VIA. The output clock from the RC1024SA is available at PB6 which is the counter input of the 6522 VIA. This allows the 6522 VIA to count the number of diodes which have been read out after the Start signal from the evaluation board has been received.

The T1 VIA clock output can be used to provide a stable signal which is derived from the computer crystal controlled clock. A very important feature of this configuration is that it allows the user to either select variable clock rates or to simply stop the clock entirely. This gives the user effective software control over the integration time without the use of external switches and counters. The clock stopping technique was suggested by Horlick [129] and provides a significant improvement over manual or computer controlled counter adjustment. This arrangement allows the user to vary clock rates, and consequently integration times, by simple software as required by the experiment. There are two ways in which this capability can be used. If the readout rate of the diode array is lowered, then the time between readouts and the total integration time will be increased proportionally. This may be inconvenient in that the pulse shape from the electronics and capacitive readout noise [85] are readout frequency dependent.

To provide a more reproducible dark signal, it is more convenient to always read out at the same rate and to vary the integration time by changing the interval between readouts. If this timing is entirely under the control of the computer hardware, then the process is vastly simplified and completely under software control. The time required for a computer to carry out a given function is often referred to as the "software overhead". Software overhead can be a significant factor in the control of imaging devices. The software overhead in this application can be reduced significantly by using the timer-counter (TC2) of the 6522 VIA as a counter to count the number of clock pulses, and consequently the number of photodiodes, which have been read out. This enables the user to conveniently collect data only from those diodes which contain the spectral information of interest.

4.2 Dynamic Range Extension

The use of the 6522 VIA as a clocking, control, timing and counting device has enabled the development of software which, with a small amount of supplemental hardware, can provide an order of magnitude improvement in the ability of the PDA to monitor high intensity signals. Strong emitters such as Ca, Mg and Sr saturate the PDA for integration periods longer than about 50 ms, the minimum integration time at the nominal readout rate, at concentrations ranging from 10 to 100 ppm. Since the useable (but not necessarily linear) concentration range extends well beyond this level, some method of data acquisition is necessary which will provide the dynamic range extension

required. An order of magnitude increase in the dynamic range can be achieved by using the configuration described above in an unconventional mode. With this configuration the clock rate can be altered to much higher rates than the maximum acquisition frequency that would be allowed by either the computer software or the ADC. This mode of operation requires that the pixels of the array be clocked at a high rate until the spectral region of interest is reached as determined by the count set in the 6522 VIA TC1 counter. The array is then clocked at a normal rate and the data is collected and stored in the computer. The clock is then returned to the original high rate for the rest of the diode readout and integration period. This mode of operation is called the "Blurt" mode, because a major portion of the data is "divulged without thinking", i.e. not recorded.

Figure 4.2 illustrates the dynamic range extension that can be obtained using the Blurt Mode. The Blurt input clock was set to 1.0 MHz with a resulting pixel output rate of 250 kHz due to the divide by 4 operation of the internal circuitry. The desired diode data was obtained at 17.86 kHz. The PDA would be saturated by the spectral line at a relative intensity of approximately 0.1 if conventional acquisition procedures were used. It can be seen that an order of magnitue improvement in dynamic range is obtained. The slopes of the Ca II 393.4 and 396.8 lines of the log-log plot were 0.995 and 0.994 with respective r-squared coefficents of 0.9989 and 0.9992. This level of improvement could probably be obtained on computer systems using DMA (Direct Memory Access) techniques; however,

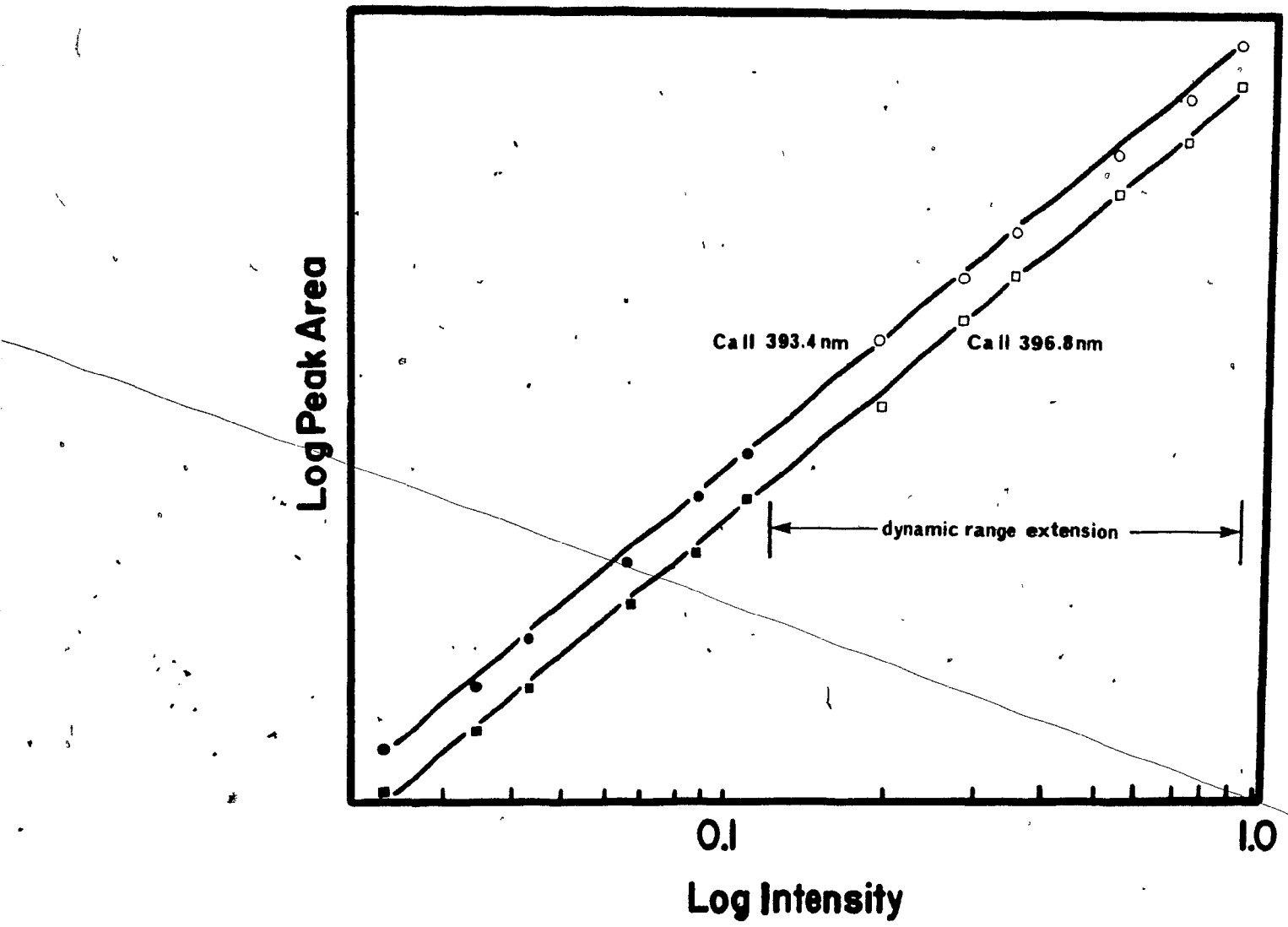

Figure 4.2: Dynamic range extension. Open symbols indicate signal intensities that would cause detector saturation with 18 kHz readout rate.

the present AIM-65 implementation is entirely in software without the addition of any further significant hardware, and the storage space necessary for the data is limited to the actual information desired. With conventional DMA acquisition a complete PDA spectrum would be stored.

The present PDA interface is capable of producing the maximum clock rate tolerated by the RC1024SA circuit of 4.0 MHz with a resulting readout rate of 1 MHz. This is a factor of 4 improvement over the previous system and was made possible by reducing the software overhead to an absolute minimum by implementing the pixel counting and clock switching in hardware. Table 4.1 presents data calculated using an acquisition time of 17.86 kHz and assuming that 10 diodes would be acquired for a spectral peak while the rest of the diode array would be Blurted out.

Blurt Rate (kHz)	Blurt Time (ms)	Acquisition Time (ms)	Integration Time (ms)	Range Extension
125	8.2	0.6	8.8	6.6
250	4.1	0.6	4.7	12
500	2.1	0.6	2.7	21
1000	1.0	0.6	1.6	36

Table 4.1: Readout times for various Blurt frequencies with corresponding dynamic range extension factor.

It is interesting to note that the more hardware intensive DMA approach, running at 200 kHz, would have a minimum integration time of 5.2 ms. No significant improvement can be gained by combining Blurt readout with DMA acquisition.

4.3 Conclusions

For many applications modern photodiode arrays do not require elaborate electronic or computer support. Simple techniques of the type described can be used to optimize performance using low cost equipment. Selective acquisition of data will minimize the memory required and may eliminate the need for computer acquisition systems with mass storage devices in certain applications. The integrated circuits used for interfacing during these experiments are particular to one family of microprocessors, however most microprocessor families offer components which can be used in combination to provide the same functionality. Therefore, it is reasonable to expect that the performance gains produced by these experiments can be achieved with many microprocessor based systems.

Further increases of photodiode array dynamic range are theoretically technically feasible and will be necessary for the utilization of these devices in applications requiring the monitoring of light fluxes which vary over many orders of magnitude. Extension of the dynamic range by electronic means is preferable to the use of optical methods such as neutral density filters because of the speed, reliability and simplicity of electronic arrangements.

5. Enhancement of Wavelength Prediction Accuracy and Image Positioning

Accurate wavelength calibration and a high degree of spatial resolution is required of a multichannel detector for ICP spectroscopy. The energetic nature of the ICP produces complex spectra for many samples and it is imperative that an unknown line be correctly identified. It is equally important that lines to be used for quantitative determination be spatially resolved from other spectral features. The first section of this Chapter describes a wavelength calibration technique based on sub-diode interpolations. Only one known peak wavelength is required to predict an unknown line with an accuracy ranging from $\pm$ 0.003 to $\pm$ 0.009 nm. The second section describes the theory, and offers experimental support, for the enhancement of spatial resolution using an image translation technique.

5.1 Wavelength Calibration

The identification of unknown lines in an ICP-PDA spectrum can be a difficult task if the spectrum consists of lines from elements like iron, chromium and other species which are capable of an extremely large number of different spectroscopic transitions. It is often the case that lines are observed that are not listed in common ICP wavelength tables [157,158] and a comprehensive listing like the MIT Wavelength Tables [159] must be consulted. The MIT Tables list virtually all of the known

atomic lines of significant intensity in the UV-visible region, however the relative intensity data for each line was obtained from arc and spark experiments and is therefore not necessarily the same as the relative intensity observed for the ICP. Given that there is a general similarity between the relative intensities produced by the arc, spark and ICP sources (ie. a strong line for one source is a strong line for the other sources) an unknown line can usually be unambiguously identified if the wavelength prediction is accurate to ± 0.01 nm. The MIT Tables often list 10 or more lines within a 0.02 nm range, but the intensity data is usually sufficient to deduce the identity of the unknown.

A prediction accuracy of ± 0.005 nm at 200 nm and ± 0.01 nm at 400 nm has been achieved [54] using an image dissector PMT (IDPMT) and an echelle spectrometer. Using the same spectrometer configuration, the prediction accuracy was ± 0.003 nm at 200 nm and ± 0.006 nm at 400 nm when a vidicon was used as the detector. Both of these performances can be attributed to the high degree of dispersion achieved using the echelle spectrometer. The wavelength calibration accuracy of a vidicon detector can be quite poor [51,93] compared to that of a PDA [93] when used with a conventional linear dispersion spectrometer. This is due to the fact that the spatial resolution of the vidicon is limited to the precision and accuracy of the electron beam scanning and positioning electronics. The spatial precision of the PDA is dependent only on the geometry of the photodiodes and, since the PDA is

fabricated using precise microelectronic techniques, the registration of the photodiodes is excellent [31].

A wavelength prediction accuracy of ± 0.02 nm has been reported [93] for an RL1024S PDA monitoring a 21 nm spectral window. This is based on a technique which employs any two known spectral lines to determine the reciprocal dispersion of the spectral window. The prediction accuracy results from multiplying the reciprocal dispersion of 0.825 nm/mm by the pitch of the pixels of 0.025 mm [93]. It is clear that a prediction accuracy of ± 0.01 nm or better can only be achieved if sub-diode image positioning can be established with a 20 nm window. It would also be advantageous if only one known line was required for calibration of the spectral window.

5.1.1 Experimental

The ICP was used as a source for calibration data. The MAK sample introduction system was used and the conditions specified in Appendix B were employed. A series of eight 20 nm windows, each containing several uniformly dispersed lines, were collected ranging from 200 to 400 nm. Elements were carefully selected such that as few elements as possible were used to provide prominent lines across a given window. This minimized the possibilty of spectral overlap. The concentrations of analyte solutions were adjusted such that all calibration lines were sufficiently intense for the integration period employed. Solutions were prepared from reagent grade salts in deionized/distilled water. The slit width was set to 25 µm.

5.1.2 Preliminary Calibration Results

The reciprocal dispersion for a conventional grating spectrometer is wavelength dependent as indicated by the relationship [160]

$$R_d = \frac{d\cos\beta}{|m|F}, \qquad (5.1)$$

where R_d is the reciprocal dispersion; d is the groove spacing of the grating; β is the angle of diffraction with respect to the grating normal (a function of wavelength); m is the order; and F is the focal length of the optical system. Since the calibration must be accurate to at least 0.01 nm and the parameters of the above equation were not known to this degree of precision, an empirical approach was used to determine R_d as a function of wavelength.

A series of 8 calibration windows (wavelength regions) were used to determine the average R_d for each 20 nm region. Each calibration line excited 5 diodes with the 25 µm slit width. A second order polynomial fit was performed on the 3 most intense pixels of each peak [161]. A typical result is shown in Fig. 5.1. This curve fit was coded in the Pascal overlay CALMOD.SRC (see Appendix J) where it could be accessed by the control program PDASYS2.SRC. The reciprocal dispersion given by a known line pair in nm/diode was calculated using

$$R_d = \frac{\lambda_2 - \lambda_1}{D_2 - D_1}, \qquad (5.2)$$

where λ represents the wavelength of the lines; and D represents

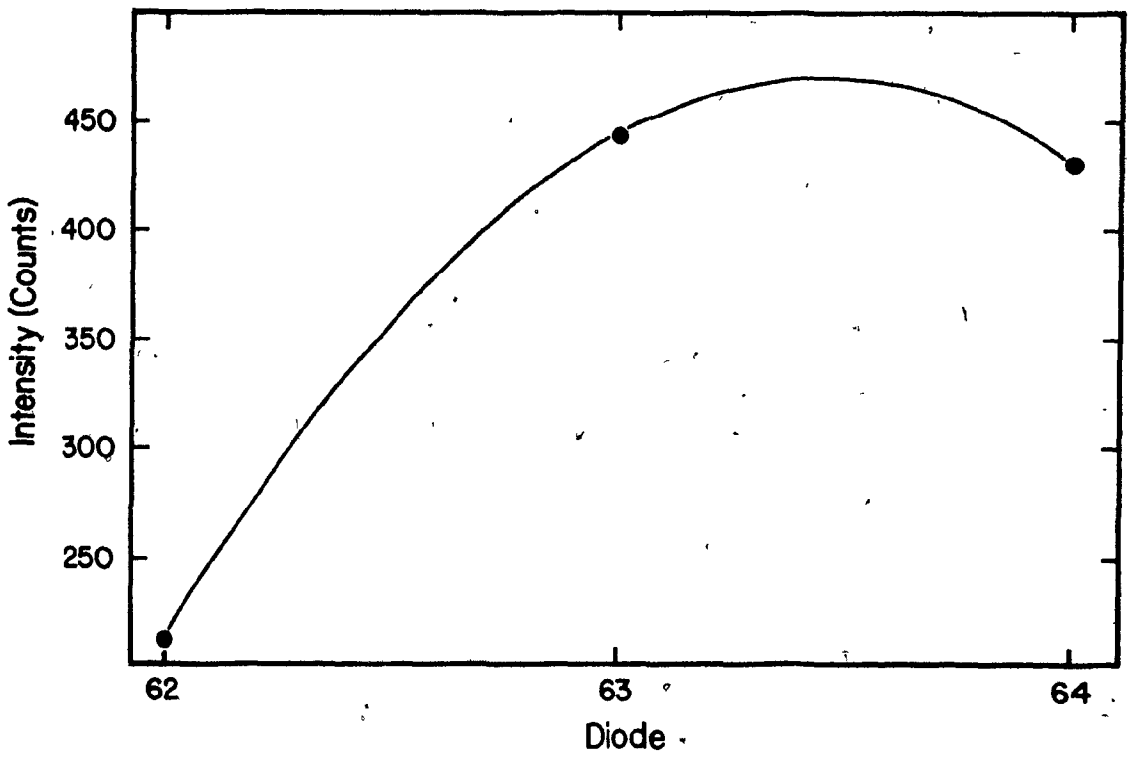

Figure 5.1: Demonstration of second order fit to 3 peak diodes.

the sub-diode position of the lines obtained from the polynomial fit. Table 5.1 lists the calibration lines and the average R_d values obtained from reference 159.

Window Range (nm)	Calibration Lines (nm)	Average R_d (10^2 nm/diode)
200-220	Zn 202.551	2.02785
	Zn 206.191	
	Zn 213.856	
	Pb 216.999	
	Pb 220.351	

220-240	Ag 224.641	2.02301
	Cu 224.700	
	Ag 241.319	
	Ag 243.779	
240-260	Ag 241.319	2.02184
	Ag 243.779	
	Pb 247.638	
	Zr 257.139	
	Pb 261.418	
260-280	Mn 260.569	2.01066
	Mg 279.553	
	Mg 280.270	
280-300	Mg 279.553	2.00708
	Mg 280.270	
	Mg 285.213	
	V 290.882	
	V 292.402	
	V 292.464	
	Hg 296.728	
310-330	V 309.311	1.99727
	V 310.230	
	V 311.071	
	Ca 315.887	
	Ca 317.933	
	Ag 328.068	

330-350	Na 330.232	1.98880
	Zr 339.198	
	Zr 343.823	
	Zr 349.621	
390-410	Ca 393.367	1.96321
	Ca 396.847	
	Sr 407.786	

Table 5.1: Calibration windows, elements for calibration and calculated reciprocal dispersion data.

Figure 5.2 illustrates the change in reciprocal dispersion as a function of wavelength.

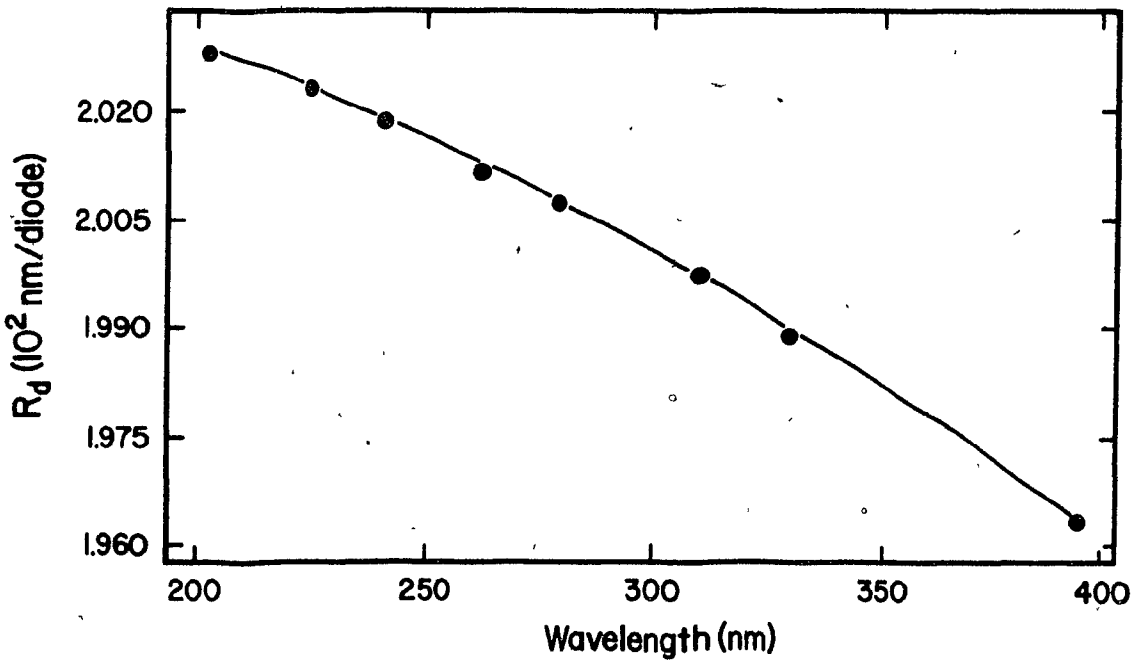

Figure 5.2: R_d vs. wavelength for average of 20 nm windows.

The data of Fig. 5.2 were fit using another second order polynomial resulting in the equation

$$R_d = 2.0503 \times 10^{-2} + \lambda(9.4204 \times 10^{-8}) - \lambda^2(5.8753 \times 10^{-9}), \quad (5.3)$$

where λ is the wavelength of the known line within a given window. This equation was inserted in the Pascal program PDASYS2.SRC. Using the sub-diode positioning information provided by the overlay CALMOD.SRC, unknown lines could be determined using only one known line for any window in the 200-400 nm range. Table 5.2 illustrates the results obtained using this method.

Many of the calibrations of Table 5.2 are within the 0.01 nm criterion established previously. However, a trend can be seen if this data is carefully inspected. In several cases an error of more than 0.01 nm is observed if the "unknown" line is more than 15 nm away from the calibration line. Possible sources for this type of error include the calibration method itself, noise giving rise to apparent peak shifting, the position of the PDA in the focal plane, inaccurate photodiode geometry or incorrectly reported wavelengths in the literature. The latter factor was not considered to be the probable cause.

Window Range (nm)	"Known Line"	"Unknown Lines"		Error (nm)
		Actual Line	Calculated line	
200-220	Zn 202.551	Zn 206.191	206.198	.007
		Zn 213.856	213.857	.001
		Pb 216.999	216.990	-.009
		Pb 220.3505	220.348	-.003
220-240	Ag 224.641	Cu 224.6995	224.697	-.003
		Ag 241.3188	241.311	-.008
		Ag 243.7791	243.777	-.002
260-280	Mn 260.5688	Mg 279.553	279.570	.017
		Mg 280.2695	280.291	.022
280-300	Mg 279.553	Mg 280.2695	280.267	-.003
		Mg 285.2129	285.208	-.005
		V 290.882	290.881	-.001
		V 292.402	292.404	.002
		V 292.464	292.463	-.001
		Hg 296.728	296.738	.010
310-330	V 309.311	V 310.2299	310.229	-.001
		V 311.0706	311.069	-.002
		Ca 315.8869	315.884	-.003
		Ca 317.9332	317.935	.002
		Ag 328.0683	328.093	.025
330-350	Na 330.2323	Zr 339.1975	339.191	-.007
		Zr 343.823	343.826	.003
		Zr 349.621	349.645	.024
390-410	Ca 393.3666	Ca 396.8468	396.843	-.004
		Sr 407.786	407.785	-.001

Table 5.2: Prediction accuracy for preliminary calibration.

5.1.3 Calibration Error Analysis

The data of Table 5.2 indicate that unacceptable calibration errors occur only when the unknown line is a long distance away from the calibration line. Two possibilities were weighed as causes of this phenomenon. If the PDA was situated at an angle with respect to the focal plane, then this type of error could occur. Secondly, if the R_d changes significantly within a window (ie. over 20 nm), then the further the unknown line is from the calibration line, the larger the error would be. Both of these causes would give rise to a monotonic error propagation along the PDA; a fact illustrated by some of the windows in Table 5.2.

The magnitude of the error induced by assuming a constant R_d within a window can easily be calculated. Using eq. 5.3 the R_d is 0.02029 nm/diode at 200 nm and 0.02024 nm/diode at 220 nm. At 300 nm the R_d is 0.02000 nm/diode and at 320 nm it 0.01993 nm/diode. These are relatively small differences corresponding to 0.25% and 0.35% respectively. To determine the effect on the calibration accuracy the 310 nm to 330 nm window was used as an example. The R_d at the V 309.311 nm calibration line is 0.01997 and changes to 0.01990 nm/diode at the Ag 328.0683 nm line. The peak sub-diodes were 54.00 for the V line and 994.55 for the Ag line. The calculated wavelength for the Ag line is therefore 328.093 nm as reported in Table 5.2. Using an average R_d of 0.01994 nm/diode instead, the calculated Ag wavelength is 328.066 nm. The error has been reduced by an order of magnitude from 0.025 nm to −0.002 nm.

Before proceeding with the development of an algorithm to

incorporate variable R_d calculations, two experiments were performed to ascertain the reproducibility of repeated calibrations within a window and the quality of the calibration if the spectrum is shifted along the window. The former experiment tests for the possibility of independent peak position variability due to readout noise while the latter tests for potential diode geometry variations.

The spectrum shown in Fig. 5.3 was used for these tests.

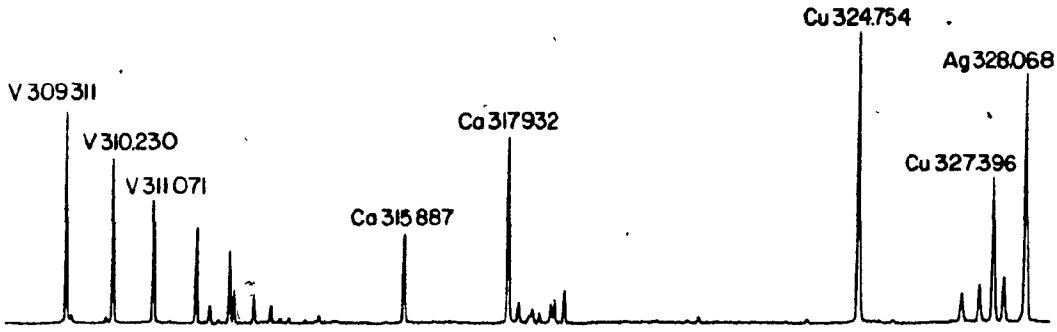

Figure 5.3: Spectrum of 310 to 330 nm window used for calibration error analysis.

For the first test 5 spectra were acquired without moving the grating. Each spectrum was calibrated using 3 "known" lines: one at the low wavelength end of the spectrum, one in the middle and one at the high wavelength end. The results are tabulated in Table 5.3.

Calibration Line (nm)	Unknown Lines (actual λ)	Errors for Replicates 1	2	3	4	5
V 309.3108	V 310.2299	-.001	-.001	-.001	-.001	-.001
	V 311.0706	-.002	-.002	-.002	-.001	-.002
	Ca 315.8869	0	.001	.001	.001	.001
	Ca 317.9322	.003	.003	.003	.003	.003
	Cu 324.754	.014	.014	.014	.014	.014
	Cu 327.3962	.024	.024	.024	.024	.024
Ca 317.9322	V 309.3108	.010	.010	.010	.010	.010
	V 310.2299	.008	.008	.008	.008	.008
	V 311.0706	.006	.006	.006	.006	.006
	Ca 315.8869	0	.001	.001	.001	.001
	Cu 324.754	0	0	0	.001	.001
	Cu 327.3962	.007	.006	.006	.007	.007
	Ag 328.0683	.009	.009	.009	.009	.009
Ag 328.0683	V 309.3108	.036	.036	.036	.036	.036
	V 310.2299	.032	.032	.032	.032	.032
	V 311.0706	.029	.029	.029	.029	.029
	Ca 315.8869	.014	.015	.015	.015	.015
	Ca 317.9322	.010	.010	.010	.010	.010
	Cu 324.754	-.002	-.003	-.003	-.002	-.002
	Cu 327.0683	-.001	-.002	-.002	-.001	-.001

Table 5.3: Calibration errors for replicate spectra obtained with static positioning.

These data clearly indicate that the spectrum to spectrum reproducibility of the calibration, and associated errors, is very high. It is also apparent that the "end-to-end" errors are reduced by a factor of two if a line in the center of the PDA is used as the calibration wavelength. This follows from the previous discussion regarding R_d changes within a window.

The second test involved acquiring 5 spectra where each spectrum was shifted slightly so that a different group of photodiodes were excited by the spectral lines. Each spectrum was shifted by approximately 0.2 nm (10 diodes) from its previous position. The same calibration procedure used for the replicate test was used and the results are shown in Table 5.4.

The error for a given line is slightly worse as a result of the spectrum translation. The majority of the error appears to be associated with the change in R_d and/or the positioning of the PDA in the focal plane. It is expected that the precision of the calibration could be degraded if long integration periods are employed due to mechanical effects like thermal expansion and vibration. The data shown here was obtained using relatively short integration periods.

Calibration Line (nm)	Unknown Lines (actual λ)	Errors for Replicates 1	2	3	4	5
V 309.3108	V 310.2299	-.001	-.001	-.001	-.001	-.001
	V 311.0706	-.002	-.002	-.002	-.001	-.002
	Ca 315.8869	0	-.003	-.002	.002	-.004
	Ca 317.9322	.003	.003	.003	.002	.001
	Cu 324.754	.014	.014	.014	.014	.012
	Cu 327.3962	.024	.023	.024	.023	.020
Ca 317.9322	V 309.3108	.010	.010	.010	.011	.013
	V 310.2299	.008	.008	.008	.010	.011
	V 311.0706	.006	.005	.005	.008	.008
	Ca 315.8869	0	-.003	-.002	.003	-.001
	Cu 324.754	0	0	0	.001	.001
	Cu 327.3962	.007	.006	.006	.006	.004
	Ag 328.0683	.009	.008	.009	.010	.004
Ag 328.0683	V 309.3108	.036	.037	.037	.037	.044
	V 310.2299	.032	.034	.033	.034	.040
	V 311.0706	.029	.029	.029	.031	.036
	Ca 315.8869	.014	.012	.013	.017	.017
	Ca 317.9322	.010	.011	.011	.010	.015
	Cu 324.754	-.002	-.002	-.002	-.002	.003
	Cu 327.0683	-.001	-.001	-.001	-.002	.001

Table 5.4: Calibration errors for replicate spectra obtained with spectrum shifting.

5.1.4 Modified Calibration Procedure

The solution to the variable R_d problem was envisioned as an algorithm which would independently calculate the reciprocal dispersion between the calibration line and each unknown line. The change in R_d is nonlinear with respect to wavelength; however, over the relatively small range of 20 nm it approaches linearity. The spectral series used to determine the R_d vs. wavelength plot shown in Fig. 5.2 was employed for the modified procedure. However, instead of averaging the R_d values calculated for the lines in a given window, separate plots of R_d vs. diode position were constructed for each 20 nm window. Figure 5.4 illustrates a typical plot for the 350 to 370 nm region.

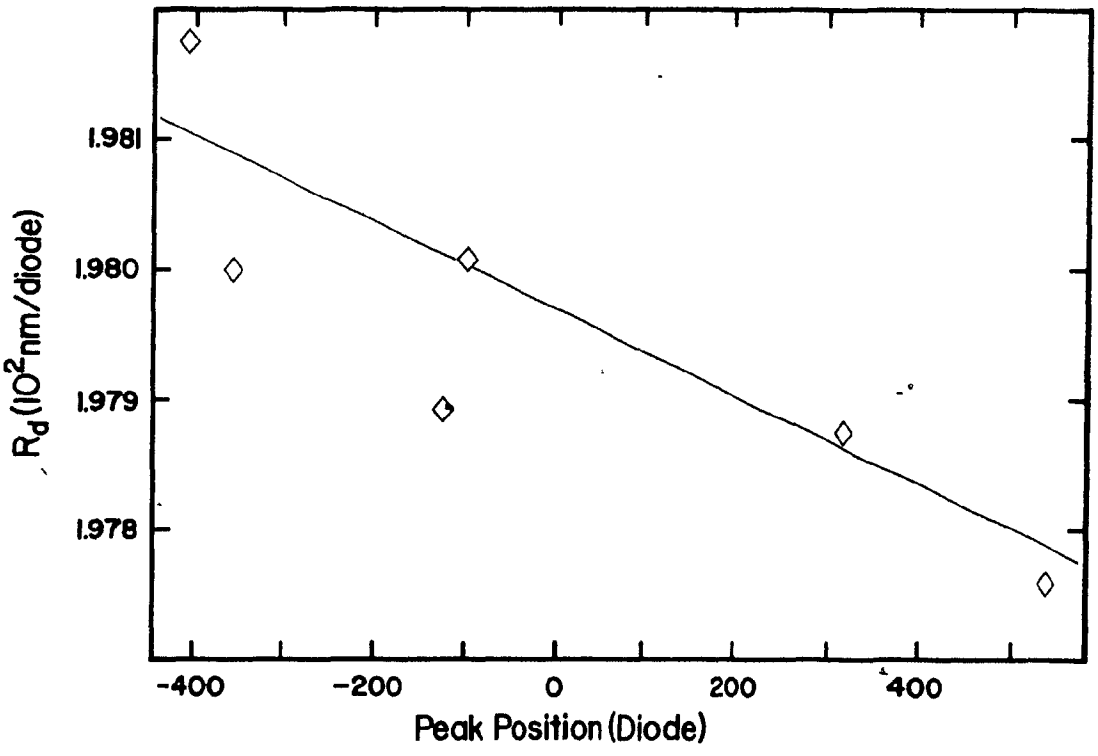

Figure 5.4: Plot of R_d vs. diode position within a window as a function of wavelength.

Because we are dealing with extremely small changes in R_d the data points begin to show the limit of the measurement technique as evidenced by erratic, non-monotonic behavior. Nonetheless, a linear regression provides a slope and intercept which does approximate the data over the window.

It is important to note that the abscissa axis is scaled in diode position from a central calibration diode. A line near the center of each window spectrum was chosen as the reference. The other line positions relative to the central line were then used to produce the R_d data. This means that the calibration technique is optimized for calibration lines which will appear near the center of the PDA. However, the technique still produces superior calibration results, compared to the preliminary method, if lines at either end of the PDA are used for calibration.

The preliminary calibration method involved plotting the average R_d within a window as a function of wavelength. For the modified procedure the linear functions pertaining to the R_d change within a window were described as a function of wavelength. This was done by plotting the slopes and intercepts for each R_d vs. diode position plot for each window as a function of wavelength. Figure 5.5 shows the intercept of the R_d vs. diode data for each window as a function of the reference wavelength. A second order polynomial fit was performed on this data giving rise to the indicated curve. The equation of the curve was found to be

$$y = 2.06515X10^{-2} - x(6.8546X10^{-7}) - x^2(4.7783X10^{-9}). \qquad (5.4)$$

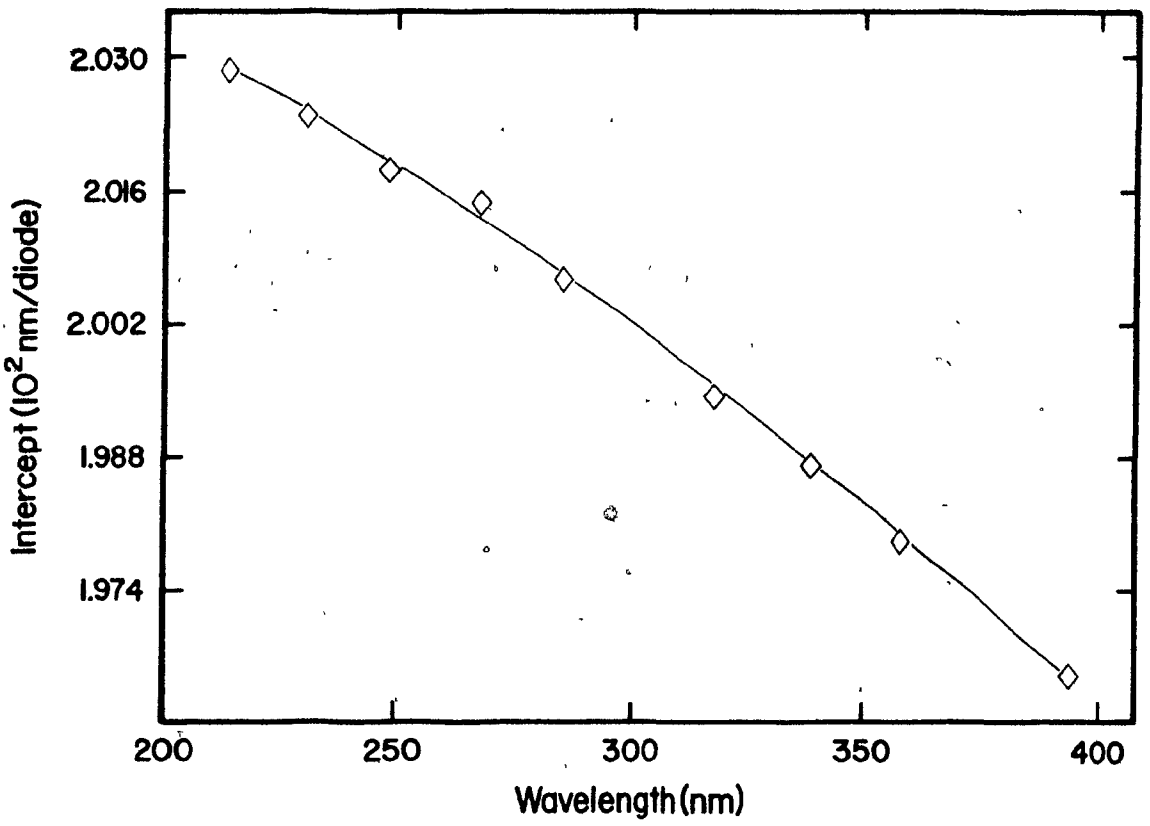

Figure 5.5: Plot of the intercept of each window calibration illustrated by Fig. 5.4 as a function of wavelength.

Figure 5.6 shows the slope of the R_d vs. diode position plots as a function of wavelength. An average value was used in the algorithm.

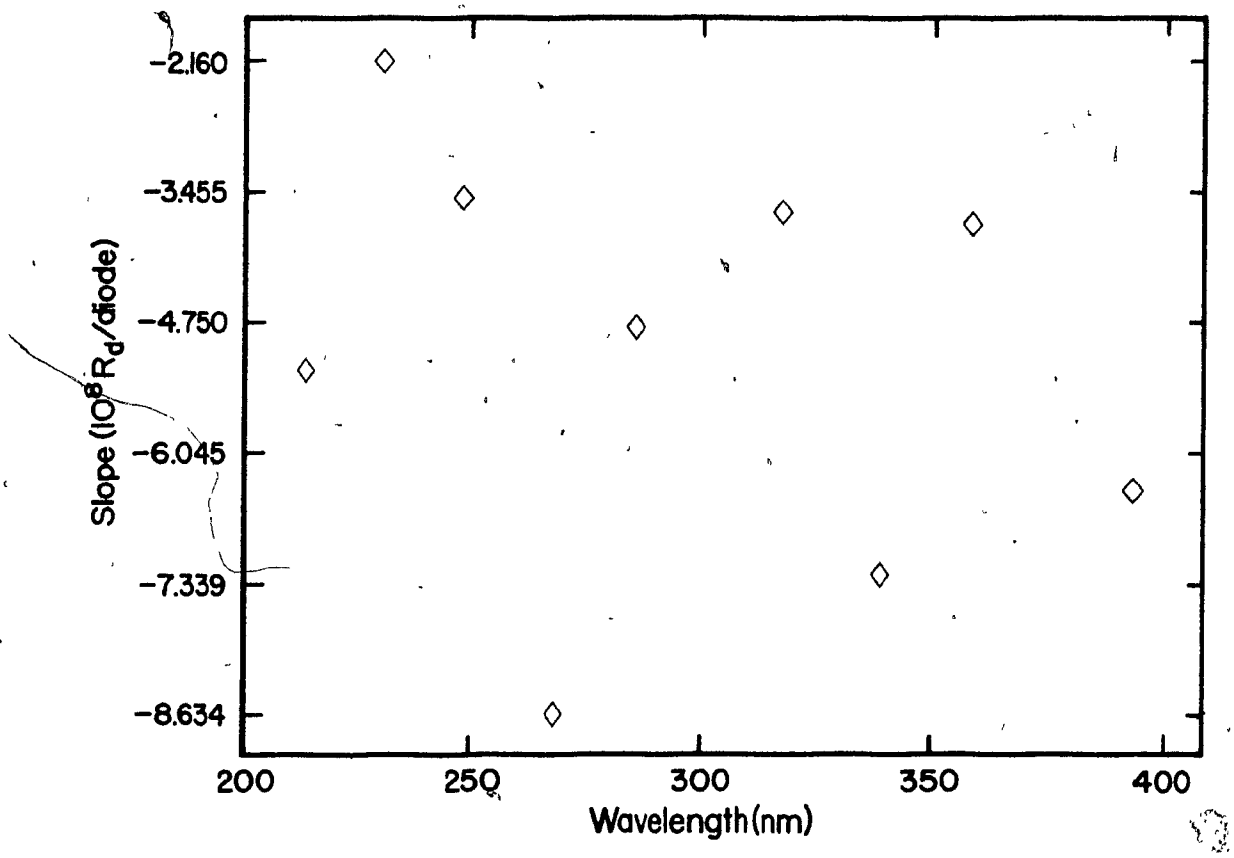

Figure 5.6: Plot of the slope of the window calibrations illustrated by Fig. 5.4 as a function of wavelength.

The implementation of the algorithm was coded in PDASYS2.SRC (Appendix J) within the Calibration routine. The operation of the algorithm is as follows.

1. A dark and analyte spectrum is loaded into memory from disk or acquired from the PDA.

2. The user invokes the 'C' command from the function list provided by the program.

3. The system prompts for the threshold value. This is a value in absolute ADC counts. To determine the baseline level,

and hence the threshold, the D(isplay) command may be used before invoking the calibration routine.

4. The main program loads the overlay CALMOD and performs a peak search for all pixels above the threshold value.

5. The 3 most intense diodes of each peak are fit using an optimized second order polynomial algorithm and the resulting sub-diode maximum is stored in an array to be passed back to the main program.

6. The peaks are listed on the terminal as sub-diode values and the user is prompted to select one of them as the reference, or calibration, line. This may be a simple matter if the user immediately recognizes a pattern or a prominent line. Alternatively, complex spectra may dictate that several attempts be made in conjunction with appropriate wavelength tables to identify a line.

7. The system calculates the intercept of the R_d vs. diode position plot using Eq. 5.4.

8. The sub-diode position of all peaks is now known as well as the wavelength of one peak. The R_d in nm/diode is calculated for each unknown line using

$$R_d = b + m(D_u - D_c), \qquad (5.5)$$

where b is the intercept from Eq. 5.4; D_u is the subdiode position of an unknown line; D_c is the subdiode position of the known line; and m is the average slope of the R_d vs. diode position data (a constant).

9. The unknown wavelength is determined using

$$\lambda_u = \lambda_c + R_d(D_u - D_c). \qquad (5.6)$$

The results using this modified algorithm are shown in Table 5.5. The number of lines tested was increased to provide a better indication of the effectiveness of the method. The lines denoted by 'C' indicate calibration wavelengths at different positions along the PDA. The error subscripts l, c and h correspond to the errors resulting from the use of a calibration line at the low, center and high wavelength region of the PDA.

Window Range	Line (nm)	$Error_l$	$Error_c$	$Error_h$
200-220	Zn 202.551	C	-.010	-.025
	Zn 206.191	.012	.007	-.005
	Zn 213.856	-.005	C	-.007
	Pb 216.999	-.010	-.001	-.006
	Pb 220.351	-.011	.003	C
220-240	Pb 220.351	C	-.005	-.021
	Pb 224.689	-.008	-.008	-.020
	Ba 230.424	-.006	C	-.007
	Ba 233.527	-.012	-.003	-.006
	Ba 234.758	-.012	-.001	-.003
	Pb 239.379	-.016	0	.002
	Pb 240.195	-.020	-.003	C

240-260	Fe 238.863	C	-.007	-.026
	Fe 239.563	.002	-.004	-.022
	Fe 239.933	-.006	-.011	-.030
	Fe 240.488	.002	-.004	-.021
	Fe 248.327	-.002	C	-.010
	Fe 248.815	-.003	-.001	-.010
	Fe 252.282	-.002	.003	-.003
	Fe 258.588	-.011	O	C
260-280	Mn 260.569	C	-.007	-.025
	Cr 266.342	.002	.003	-.013
	Cr 266.602	.001	.002	-.014
	Cr 267.716	-.002	C	-.015
	Cr 267.879	-.003	O	-.015
	Cr 276.259	-.006	.002	-.004
	Cr 276.654	-.004	.004	-.002
	Mn 279.482	-.007	.003	O
	Mn 279.827	-.008	.003	C
280-300	Mn 279.482	-.001	-.003	-.015
	Mn 279.827	C	-.001	-.013
	Mg 280.270	.003	.002	-.009
	Mn 285.213	-.001	C	-.007
	Mn 293.306	-.008	.003	-.003
	Mn 294.921	-.008	-.003	O
	Hg 296.728	-.010	-.004	C

310–330	V	309.311	C	−.004	−.015
	V	310.230	O	−.003	−.014
	V	311.071	−.001	−.004	−.014
	V	311.838	−.002	−.004	−.014
	V	312.528	−.001	−.003	−.012
	Ca	315.887	−.004	−.004	−.011
	Ca	317.933	−.002	C	−.006
	Cu	324.754	−.007	−.001	−.002
	Cu	327.396	−.007	.001	.001
	Ag	328.068	−.009	−.001	C
330–350	Zr	330.628	C	.003	−.008
	Zr	335.609	−.002	.004	−.004
	Zr	339.198	−.008	C	−.006
	Zr	343.053	−.006	.004	O
	Zr	343.823	−.008	.002	−.001
	Zr	347.939	−.008	.004	.003
	Zr	348.115	−.005	.003	.006
	Zr	349.621	−.007	.006	.007
	Zr	350.567	−.015	−.001	C
350–370	Zr	349.621	C	0	−.009
	Zr	350.567	−.007	−.007	−.016
	Zr	355.195	−.005	−.003	−.009
	Zr	355.660	−.004	.009	−.007
	Zr	357.685	−.004	C	−.005
	Pb	363.958	−.007	−.001	−.003
	Pb	368.347	−.008	0	C

380-400	Mg	383.231	C	.005	-.003
	Mg	383.826	.001	.006	-.002
	Ba	389.179	-.006	.001	-.005
	Ca	393.367	-.009	C	-.005
	Ca	396.847	-.012	-.001	-.005
	Mn	403.076	-.011	.002	C

Table 5.5: Calibration results for modified algorithm.

5.1.5 Conclusions

The average absolute error for the low, center and high calibration trials is .006, .003 and .009 nm respectively. In general the modified procedure yields errors about one half the magnitude of those produced by the preliminary method. When a line near the center of the PDA is used for calibration, all of the lines in the window can be predicted with an accuracy exceeding 0.01 nm. However, the previously observed end-to-end error is still apparent. This may be due to the positioning of the PDA in the focal plane. The end-to-end error is slightly worse if the calibration line is at the high rather than the low end of the PDA. This is understandable since the PDA was focussed with the aid of an oscilloscope using the Start pulse as a trigger and only the first 50 to 100 photodiodes could be viewed in real-time with sufficient resolution to achieve a focus. If the detector is situated at an angle with respect to the focal plane and the low end of the PDA is properly focussed then the high end is not. Choosing a calibration line in the center of the PDA simply results in a reduction of the error by

a factor of 2. It would be possible to compensate for these errors using further empirical techniques; however, the best solution would be to focus the system better. Focussing the detector so that the wavelength prediction accuracy is optimized will require a method which reports on the quality of the image at both ends of the PDA in real-time as the user manipulates the positioning adjustments.

5.2 Spatial Resolution Enhancement

One of the major limitations of linear multichannel sensors when used as detectors for atomic spectroscopy is that a wavelength coverage vs. resolution trade-off must be made. The majority of atomic lines lie in the 200 to 400 nm range for ICP emission spectroscopy. The maximum practical window width for a 1024 element sensor with a 25 μm pitch is limited to between 10 and 20 nm for medium resolution atomic work. It has been argued [93] that if the PDA is to achieve the same degree of spatial resolution as conventional entrance/exit slit systems using single channel detectors, the maximum spectral range covered by 1024 pixels should be 8 to 10 nm. This section presents the theory and some experimental support for a technique that can be used to accurately determine image positions, deduce image dimensions and aberrations, and potentially increase the resolution of the PDA by a significant amount.

The wavelength calibration technique presented in section 5.4 relies on a curve fitting approach to determine sub-diode image positions. The true capability of this technique is masked by the probability that the detector is not accurately positioned in the focal plane. If a wavelength calibration accuracy of 0.002 nm can be achieved, the corresponding sub-diode interpolation accuracy will be ± 0.1 diodes assuming a R_d of approximately 0.8 nm/mm. This is adequate for unknown identification purposes. The question that remains is whether this image positioning accuracy can be improved upon, and if so,

how can the information be used to advantage.

A key advantage photodiode arrays maintain over some charge-coupled device sensors is that the semiconductor region between diodes is light sensitive. The geometric response function (GRF) for an S-series photodiode is illustrated in Fig. 5.7.

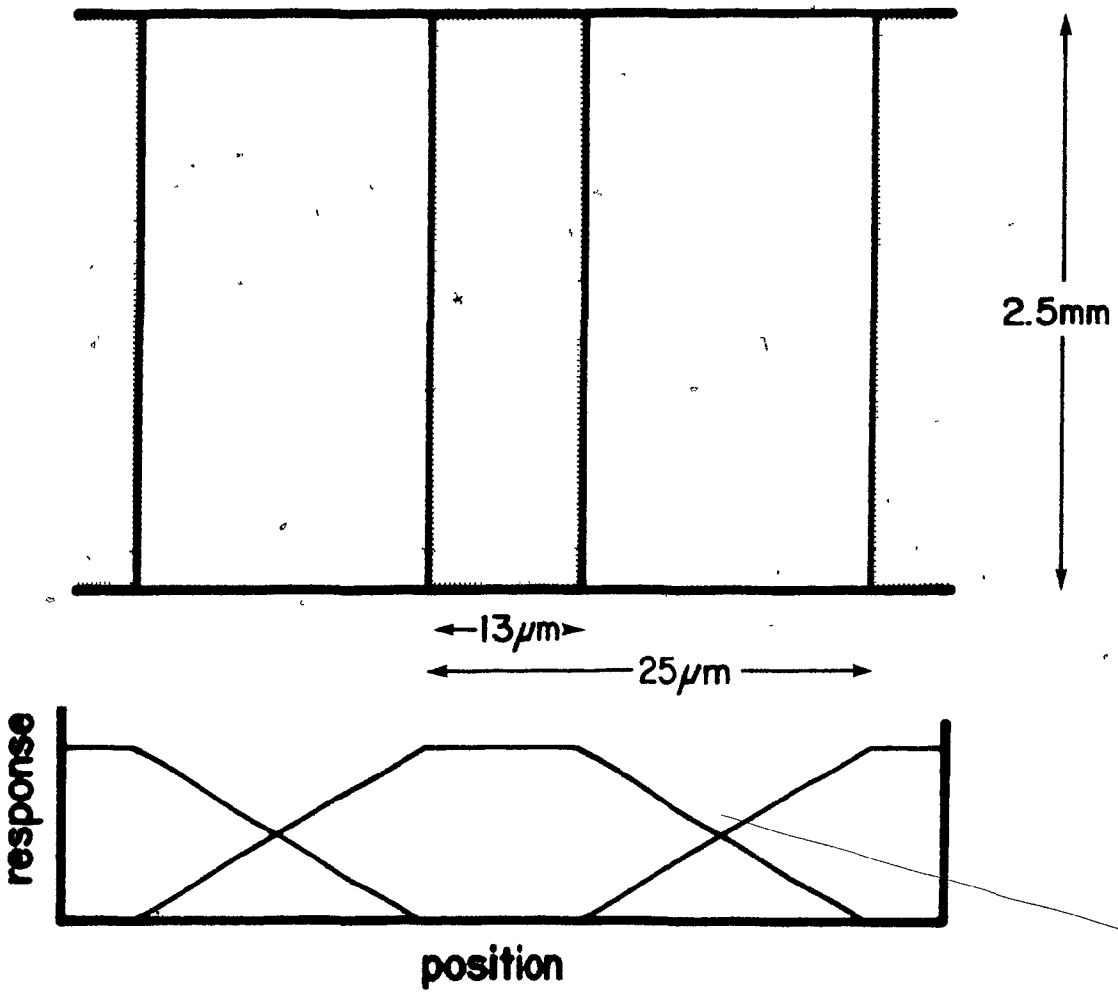

Figure 5.7: Segment of PDA shown with corresponding GRFs.

The GRF across the entire array is comprised of n overlapping trapezoids, where n is the total number of photodiodes. The response of a particular photodiode to a photon flux impinging directly on the 13 μm wide p-type island is constant as indicated by the flat top of the trapezoid. Electron-hole pairs generated in the region between photodiodes have a probability of migrating to a particular photodiode based on their proximity to that diode. This gives rise to the downward sloping edges of the GRFs which intersect at a point halfway between photodiodes.

Arrays exhibiting a rectangular GRF such as gate-side illuminated CCDs are subject to severe aliasing errors in the spatial domain because intensity information between pixels is lost [31]. With the PDA GRF all intensity information is retained, albeit distributed between pixels. If the spatial frequency (ie. image features per pixel) is high enough then the resolution is limited by the pitch (spacing) and width of the sensor elements. However, the fact that the GRF is a spatially defined function implies that it can be used to extract spatial (position) information. Since the geometric registration of the photodiodes is excellent, it should be possible to determine image positions with an accuracy far greater than that imposed by the pitch and width of the sensor elements.

5.2.1 Resolution Enhancement Theory

Figure 5.8 illustrates 3 photodiodes with their GRFs normalized to the position of the diodes. The shaded region corresponds to a spectral line image. For the purposes of the remaining discussion the GRF of a given pixel is defined as

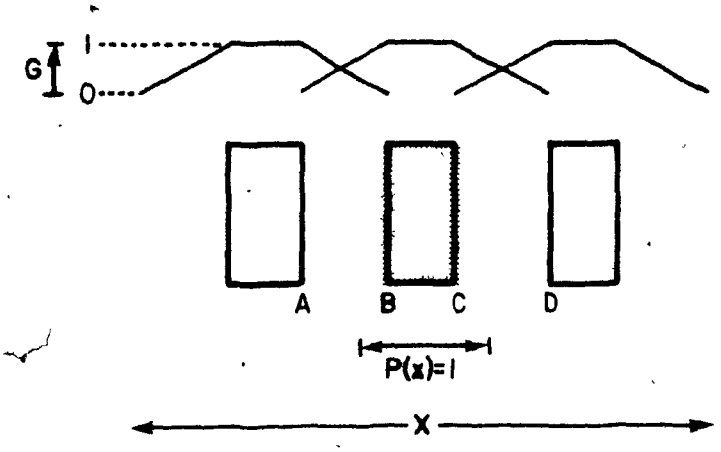

Figure 5.8: Segment of PDA shown with superposition of ideal image.

having a response of 1 within the boundary of a pixel and a linearly decreasing value on either side of the pixel terminating at zero at adjacent diode boundaries. A uniformly illuminated rectangular image is assumed giving rise to an image profile, P(x), that is equal to 1 within the image boundary and zero everywhere else. Since the image impinges on the n-type silicon on both sides of the central diode, all three diodes will integrate a portion of the electron-hole pairs produced.

The general equation for the calculation of the integrated response (IR) of a photodiode is

$$IR = \int_{LIB}^{RIB} G(x)P(x)dx, \qquad (5.7)$$

where LIB is the left image boundary; RIB is the right image boundary; G(x) is the GRF as a function of x (distance along

PDA); and P(x) is the image intensity profile as a function of x. The GRF is a discontinuous function comprised of the two sloping regions and the constant value region. The IRs for the three photodiodes of Fig. 5.8 are calculated using

$$IR_d = \int_A^B G_d^-(x)P(x)dx + \int_B^C G_d^0 P(x)dx + \int_C^D G_d^+(x)P(x)dx, \qquad (5.8)$$

where d defines a particular diode; $G_d^-(x)$ is the left-hand sloping portion of the GRF for diode d; $G_d^+(x)$ is the right-hand sloping portion of the GRF for diode d; and the letters A-D define the boundaries of the photodiodes. The constant region of the GRF, G_d^0, has been defined as equal to 1.

5.2.2 Generalized Determination of Geometric Response Functions

All of the information is available to represent GRFs as a function of position along the PDA. It is useful to define a frame of reference at the exact center of an arbitrary diode. The diodes on either side of the reference are identified by the subscript $\pm$ n where n is an integer and the positive sign represents diodes to the right of the central diode (ie. toward the high end of the array) and the negative sign refers to the opposite direction. A zero (0) subscript denotes the central diode.

Using Fig. 5.8 as a reference and defining the center of the middle diode as the positional reference point, equal to zero μm, Table 5.6 describes the distance from the reference

point to the boundaries of the GRFs for the central diode and two diodes either side of the central diode.

Diode	Boundary Displacements from Reference in μm			
	A	B	C	D
-2	-68.5	-56.5	-43.5	-31.5
-1	-43.5	-31.5	-18.5	-6.5
0	-18.5	-6.5	6.5	18.5
1	6.5	18.5	31.5	43.5
2	31.5	43.5	56.5	68.5

Table 5.6: Positions of GRF boundaries with respect to central diode.

The pattern displayed in Table 5.6 is a direct result of the equally spaced, overlapping trapezoidal GRFs. Since the abscissa coordinates for the GRF boundaries are established, and the ordinate values at the boundaries are defined (0 or 1) it is possible to calculate the GRFs for a central diode and the diodes on either side using a simple 2-point linear fit. The left-hand portion of the GRF is denoted by a "-" superscript while the right-hand portion is denoted by a "+" superscript. The subscript assignments are the same as previously defined.

$$G^{-}_{-2} = 0.0833x + 5.708$$

$$G^{+}_{-2} = -0.0833x - 2.625$$

$$G^{-}_{-1} = 0.0833x + 3.625$$

$$G_{-1}^{+} = -0.0833x - 0.542$$

$$G_{0}^{-} = 0.0833x + 1.542$$

$$G_{0}^{+} = -0.0833x + 1.542$$

$$G_{1}^{-} = 0.0833x - 0.0542$$

$$G_{1}^{+} = -0.0833x + 3.625$$

$$G_{2}^{-} = 0.0833x - 2.625$$

$$G_{2}^{+} = -0.0833x + 5.708$$

The G_{d}^{0} GRFs are all equal to 1. All of the slopes of the GRF functions are equal in magnitude and differ only in polarity. The slopes and intercepts can be understood with the aid of Fig. 5.9.

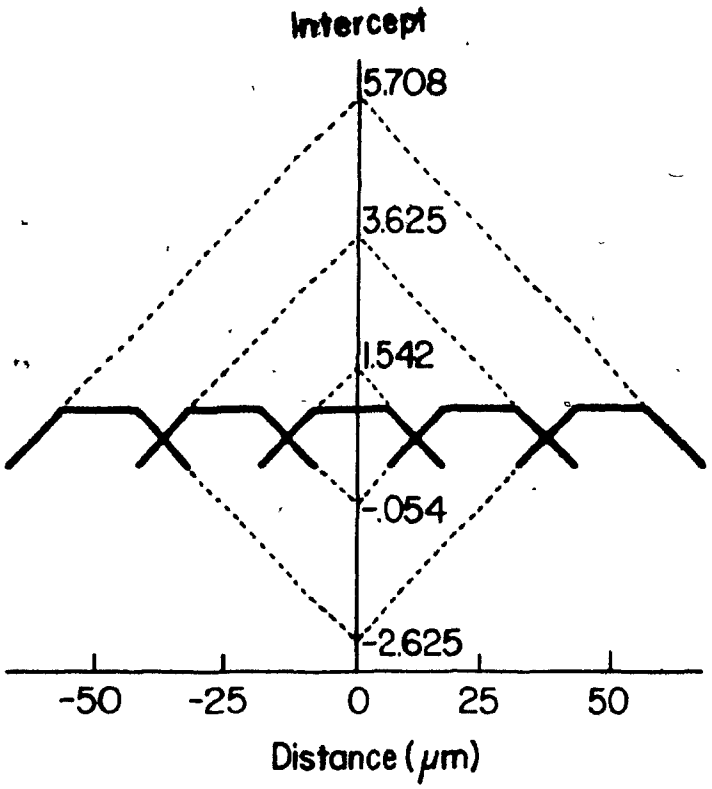

Figure 5.9: Extrapolation of GRFs to illustrate slopes and intercepts.

Figure 5.10 is a plot of the intercepts for the G_d^- and G_d^+ functions as a function of diode displacement from the central diode. The plots are linear and can be used to formulate generalized versions of the GRFs:

$$G_d^- = 0.0833x + (-2.083d + 1.542) \quad (5.9)$$

$$G_d^+ = -0.0833x + 2.083d + 1.542 \quad (5.10)$$

where x is the displacement in μm from the center of the central diode and d is the signed integer value describing a particular diode (d=-2,-1,...,1,2).

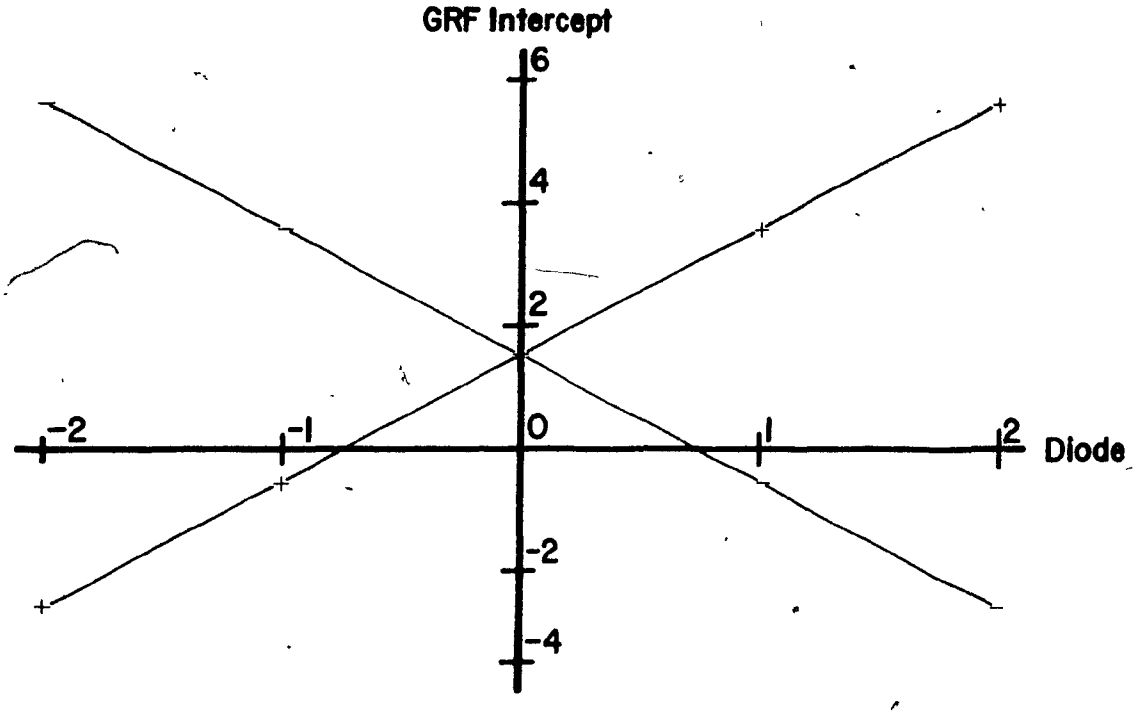

Figure 5.10: Plot of GRF intercepts as a function of diode number from central diode for left-hand and right-hand GRF regions.

5.2.3 Integrated Response Calculations for Single Images

The calculation of a diode's integrated response involves the evaluation of up to 6 different boundaries. To provide a notation which is more descriptive than that offered by Fig. 5.8 and to provide meaningful variable names for programmed solutions the following definitions will be adopted. These definitions are relative to the photodiode that is being evaluated (ie. d_0).

Left Diode Boundary (LDB): The boundary of the diode to the left of the diode being evaluated. (A of Fig. 5.8).

Diode Left Boundary (DLB): The left-hand boundary of the diode being evaluated. (B of Fig. 5.8).

Diode Right Boundary (DRB): The right-hand boundary of the diode being evaluated. (C of Fig. 5.8).

Right Diode Boundary (RDB): The boundary of the diode to the right of the diode being evaluated. (D of Fig. 5.8).

Image Left Boundary (ILB): The left-hand boundary of the image.

Image Right Boundary (IRB): The right-hand boundary of the image.

The following example assumes that the ideal image of Fig. 5.8 is 25 μm wide and is centered on the central diode. Therefore the ILB and IRB are −12.5 μm and 12.5 μm respectively.

Equation 5.8 can be used to evaluate the relative response of the central diode using the generalized GRF Eq.s 5.9 and 5.10.

$$IR_0 = \int_{ILB}^{DLB} G_0^-(x)P(x)dx + \int_{DLB}^{DRB} G_0^0 P(x)dx + \int_{DRB}^{IRB} G_0^+(x)P(x)dx$$

$$= \int_{ILB}^{DLB} (0.0833x+1.542)dx + \int_{DLB}^{DRB} dx + \int_{DRB}^{IRB} (-0.0833x+1.542)dx$$

Substituting values for the boundaries from Table 5.6,

$$IR_0 = \left[0.04165x^2+1.542x\right]_{-12.5}^{-6.5} + \left[x\right]_{-6.5}^{6.5} + \left[-0.04165x^2+1.542x\right]_{6.5}^{12.5}$$

$$IR_0 = 22.0$$

It is useful to normalize the IR to the image width so that 22.0/25 = 0.88. Similarly IR_{-1} and IR_1 evaluate to 0.06. The symmetry is expected considering that the image is centered on the central diode. Therefore, for a uniform 25 μm image centered on a particular photodiode, 88% of the signal should be collected by that photodiode. Each immediate neighbor should collect 6% of the signal. This result, of itself, is not very significant; however, if the image is shifted to the right by 1 μm the integrated responses are: IR_{-1} = 4.2%; IR_0 = 87.6%; and

IR_1 = 8.2%. A change in position of only 1 μm, or 0.004 diodes, effects a change in neighboring diodes of about 2%.

5.2.4 Integrated Response Ratios

The position of an image can be characterized by the ratio of a peak diode to one of its neighbors. For this work the integrated response ratio (IRR) was defined as

$$IRR = IR_O/IR_1 \qquad (5.11)$$

To study the effect of image translation on the IRR for a variety of image widths a Pascal program was written to perform a simulation. The code for PROFILE1.SRC is included in Appendix L. The program assumes that the image is initially centered on a diode and calculates the IRR for each translation of 1 μm to the right. Image widths ranging from 5 to 50 μm were simulated, in increments of 5 μm. These images were assumed to be ideal (ie. P(x) = 1 for ILB < x < IRB).

Figure 5.11 illustrates the results of the PROFILE1 simulation. The ordinate axis is scaled as Log(IRR). Two significant features of this family of sigmoid plots are that a very small change in spatial position yields a relatively large change in the IRR, and each curve uniquely defines a particular image width. The curves simultaneously cross the Log(IRR) = 0 point at a position 12.5 μm from the center of the central diode. This is the necessary condition for a photodiode pitch of 25 μm: when the image is in this position it is halfway between the two diodes and the IRR is equal to 1.

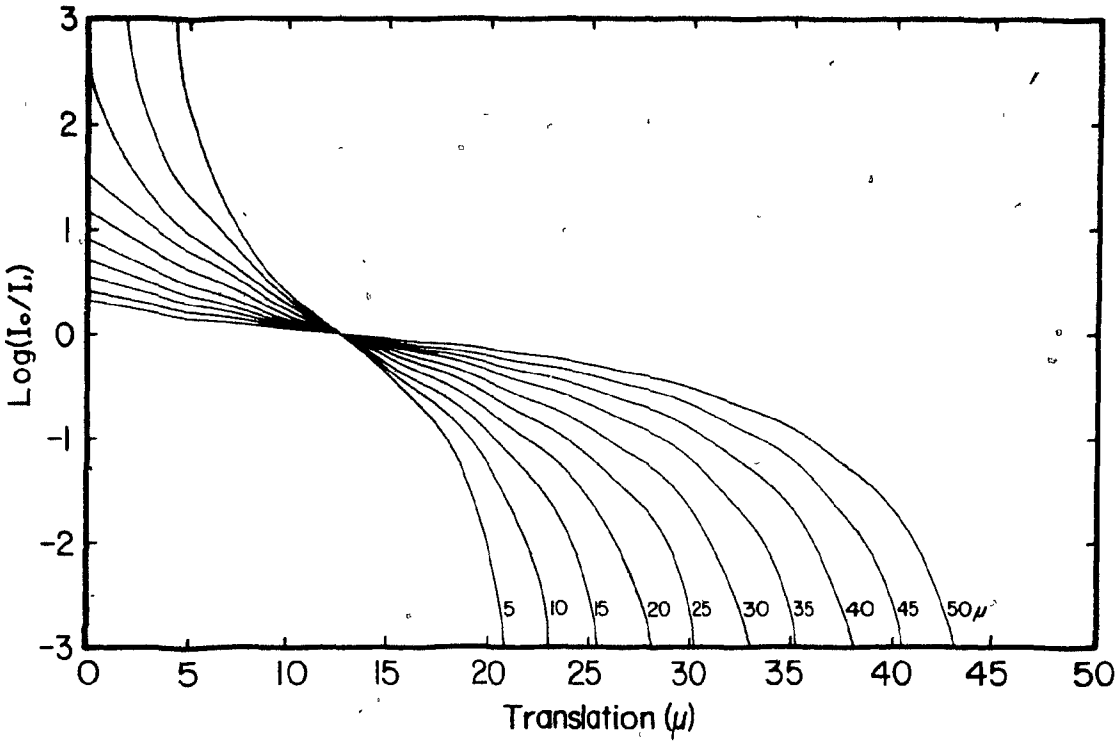

Figure 5.11: IRR plots for translation of images ranging from 5 to 50 μm in width.

It follows that if the profile, P(x), of an image is known including its width, then its position can be determined by simply measuring the intensity of the peak diode and its neighbor. This provides a more rapid, and potentially more accurate method of achieving sub-diode position information. Conversely, if the image profile is unknown it can be inferred by translating the image to produce a characteristic sigmoid curve which can be analyzed to extract P(x). Another possibility for this technique may include image fidelity analysis since an asymmetrical curve implies an asymmetrical image.

Methods already exist for precise spectrum shifting including refractor plates and moving entrance slits. These methods were not available for this work; however, the stepping motor based spectrometer drive system has a resolution of about

0.003 nm corresponding to a translation of 3.7 μm.

5.2.5 Experimental Verification

The procedure used for verification involved the translation of an image by repeatedly pulsing the stepping motor and alternately reading out a portion of the spectrum. This was accomplished using the expanded AIM (AIM2) to control both the spectrometer drive system and the detection system. Subsets of the System 1 user interface, PDASYS1.BAS, and the stepping motor control program, STEPPER.BAS, were combined into a single program called PDARES.BAS. This routine invoked the standard initialization routine, PDAINIT1.ASM, and readout routine, PDASCAN1.ASM, to perform initial image positioning. An additional assembler routine, PDARES.ASM, was used to alternately pulse the motor and perform readouts. PDARES.BAS and PDARES.ASM are included in Appendix L.

It was necessary to shift the image as quickly as possible because the belt connecting the stepping motor drive shaft to the sine bar gear exhibits an irreproducible relaxation if the motor is simply pulsed and the system allowed to settle. The maximum readout rate using System 1 is about 10 kHz permitting a stepping rate of 9.6 Hz. The light source for this experiment was the 632.8 nm line of a He-Ne laser. This source was chosen because it was intense enough to produce a large peak at the maximum readout rate and, more importantly, it would require that a relatively un-used portion of the sine bar drive screw was engaged. Nonetheless, it was expected that the drive screw

would introduce some error because the pitch of the threads is only accurate to between 5 and 10% [162].

An entrance slit width of 10 μm was used for all translations. The 632.8 nm line was roughly centered on diode 60. The motor was pulsed 32 times at 9.6 Hz and the 15 pixels surrounding the peak were collected for each pulse and stored in the AIM memory. The 32 sets of 15 pixels were subsequently sent to the S100 system via the network. The 32 steps produced an image translation of approximately 5 diodes, so after the first translation series the peak was roughly centered on diode 65. This process was repeated 9 more times eventually invoking diode 107 as the maximum.

The image was then returned to diode 60 and the entire process was repeated a second, and finally, a third time. This resulted in 3 replicates of 10 translation series where each group of 3 translations used the same portion of the sine bar drive screw. This minimized the propagation of error due to thread pitch changes. Since 320 steps corresponds to one complete revolution of the drive screw, the 10 translations of 32 steps effectively utilized the entire diameter of the screw.

Figures 5.12 through 5.21 illustrate the results. The scale of Fig.s 5.13 to 5.21 are the same as for Fig. 5.12. Generally the sigmoid shape exhibited by the theoretical curves is produced. For a given run (symbol), the data are usually monotonic and trace out a smooth curve. The three sets of curves per plot were normalized to produce the superposition because the three replicate passes were not initiated from exactly the same position with respect to diode 60.

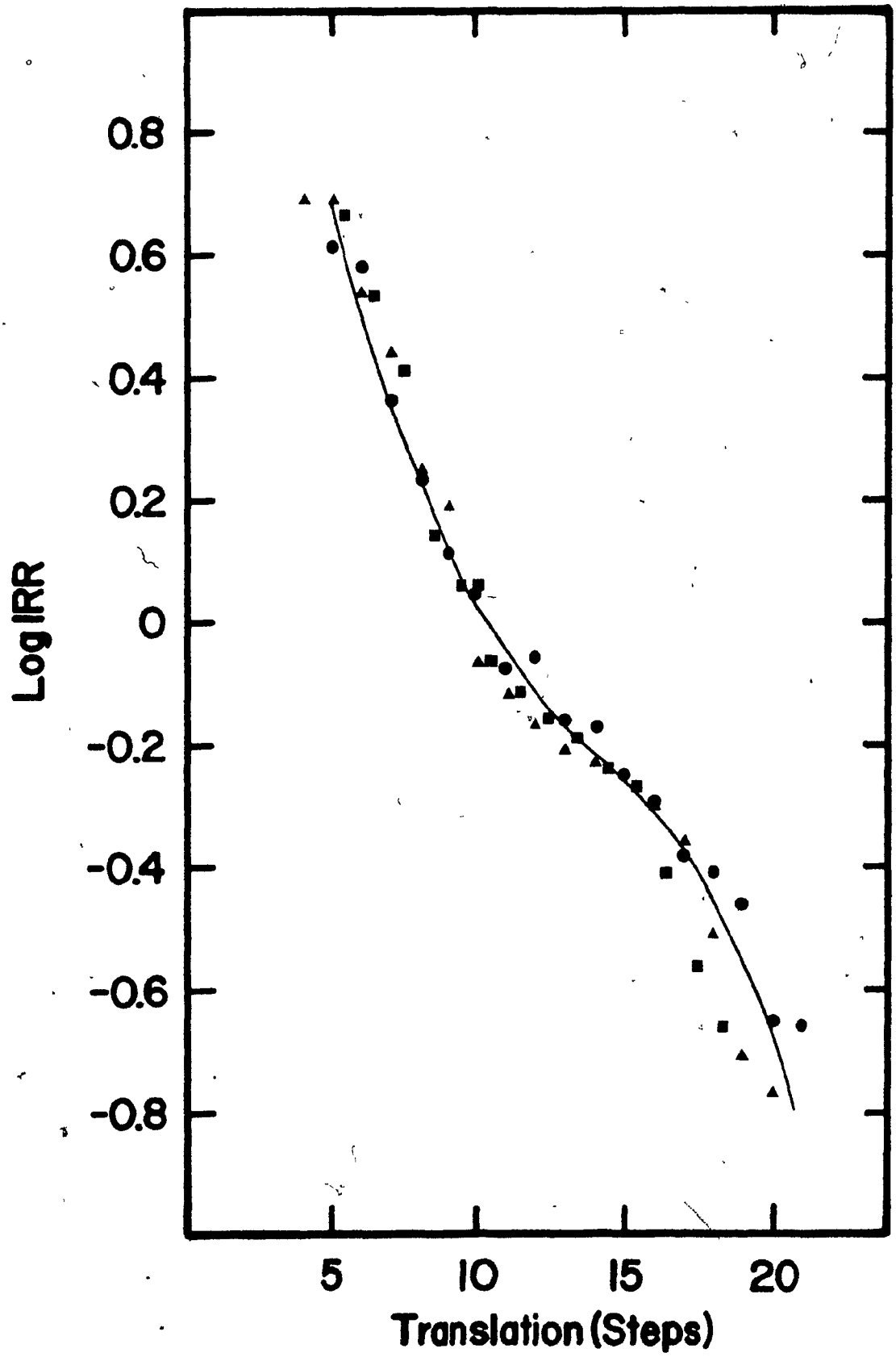

Figure 5.12

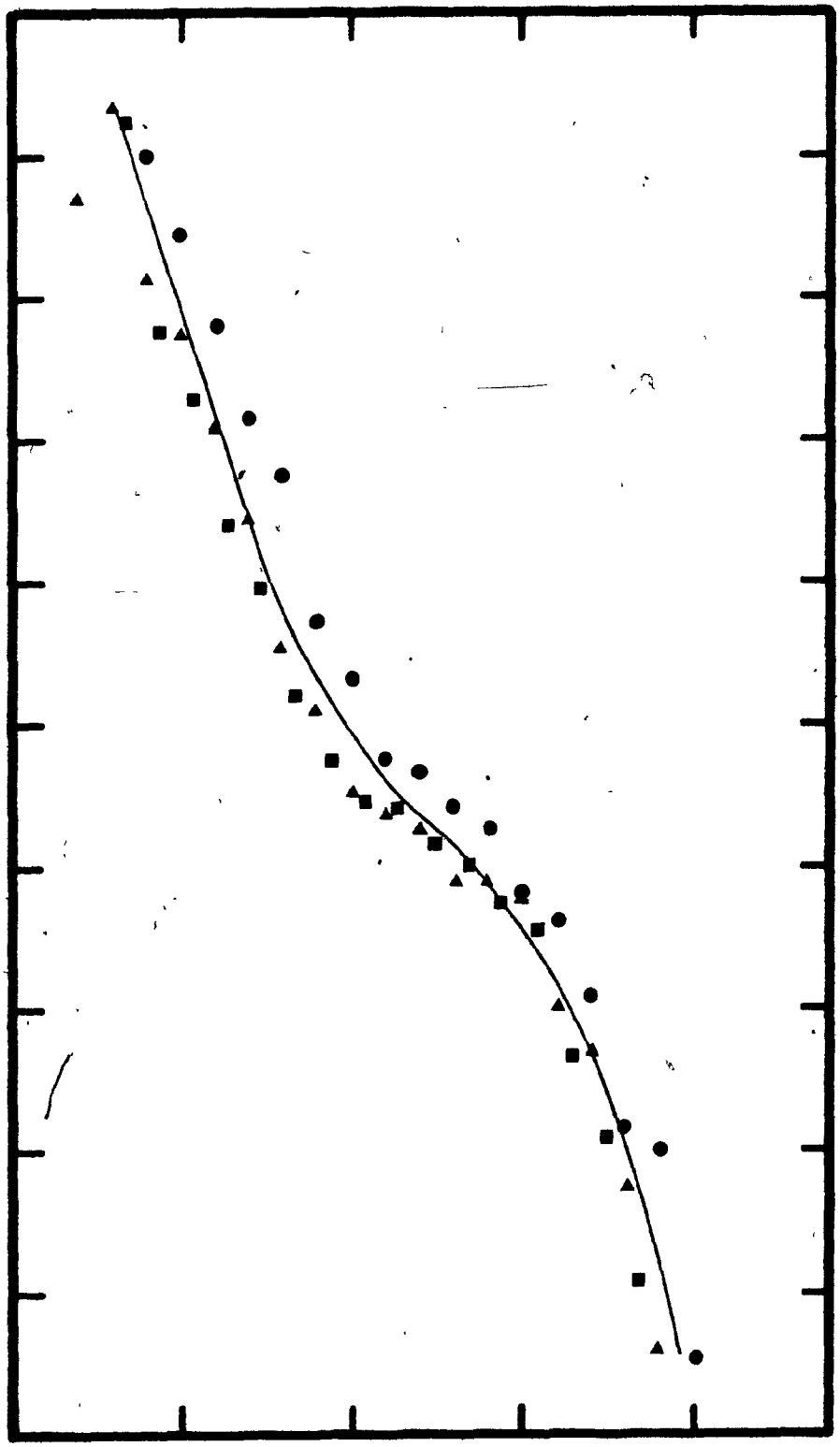

Fig. 5.13

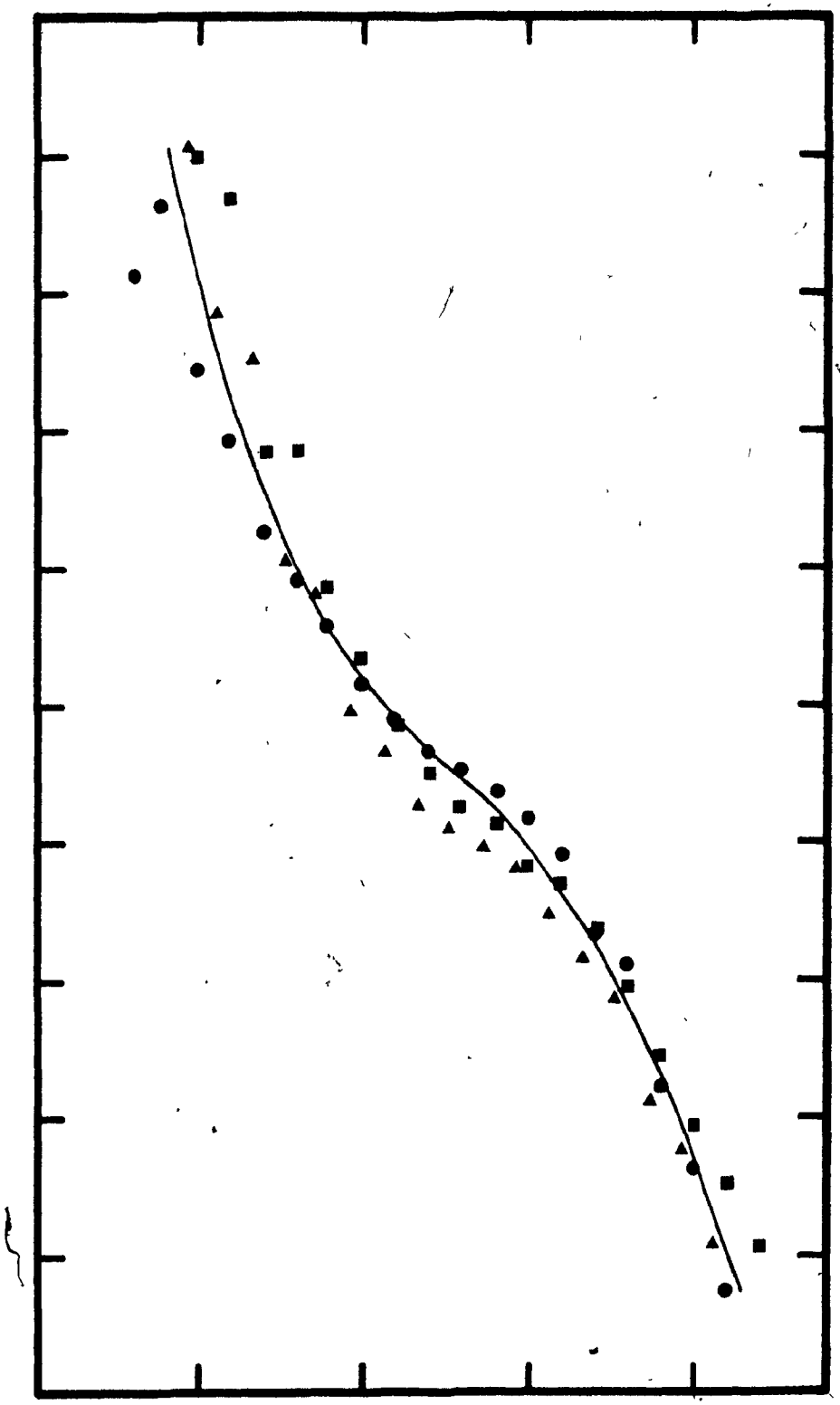

Fig. 5.14

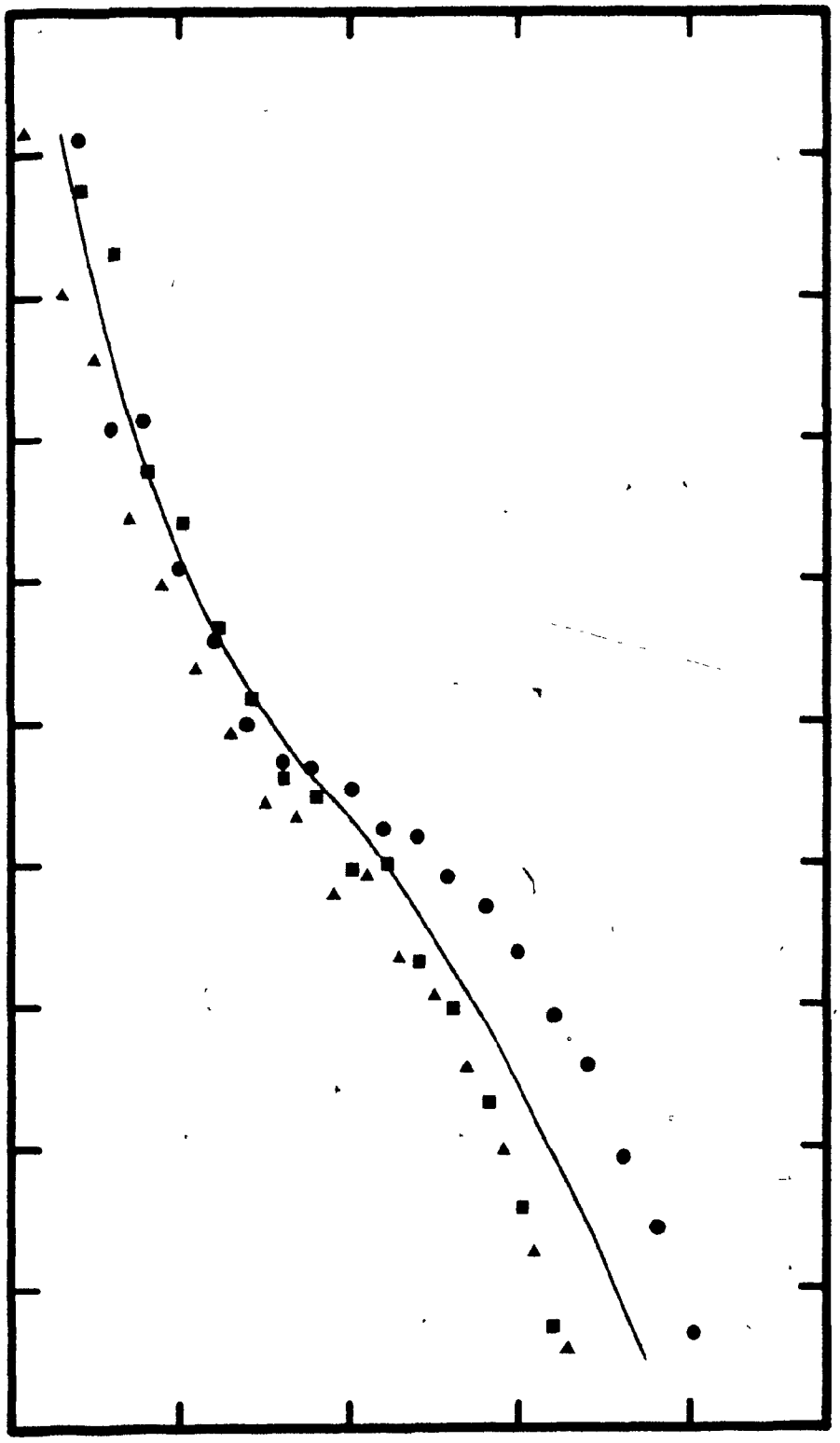

Fig. 5.15

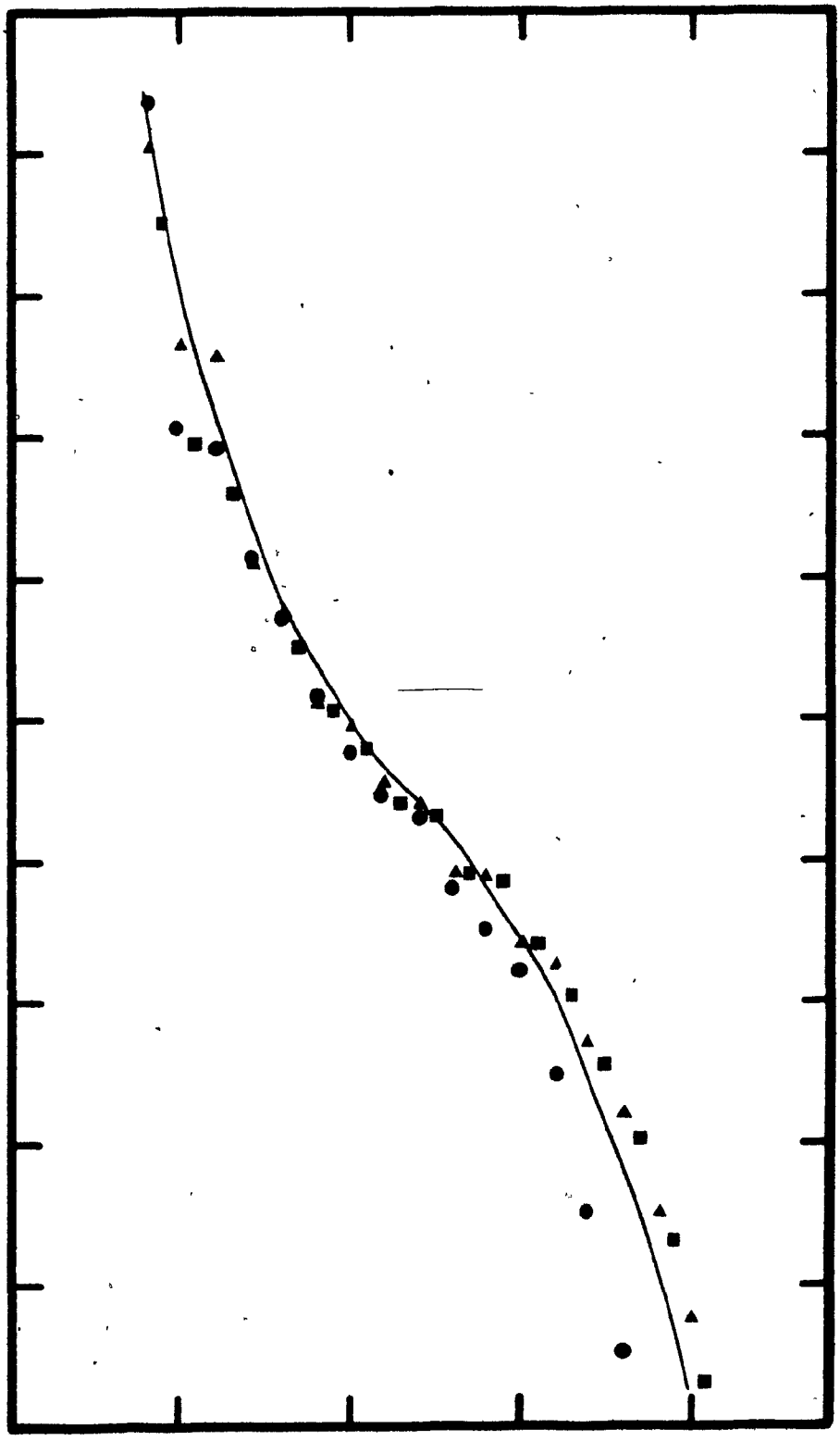

Fig 5.16

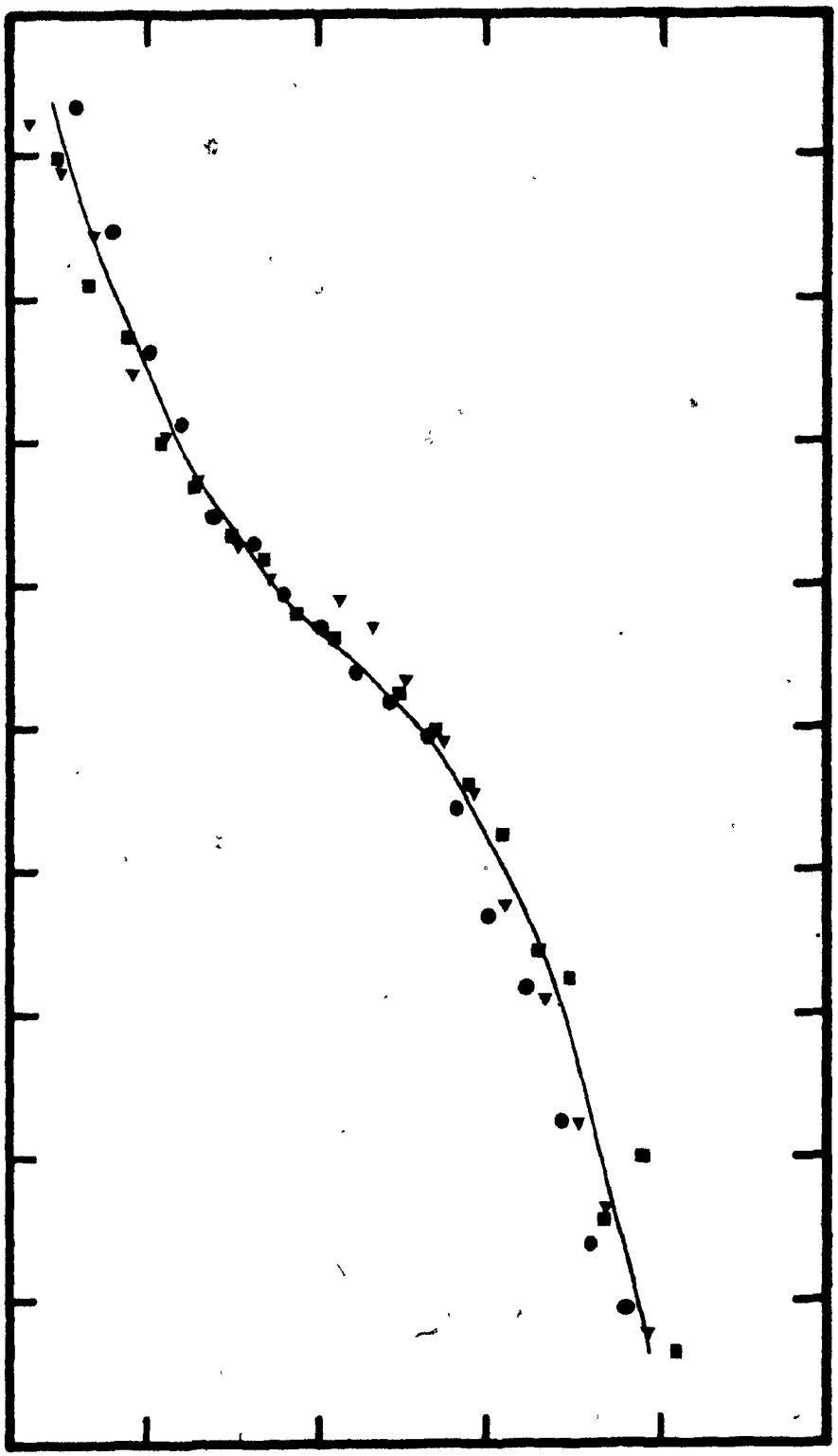

Fig. 5.17

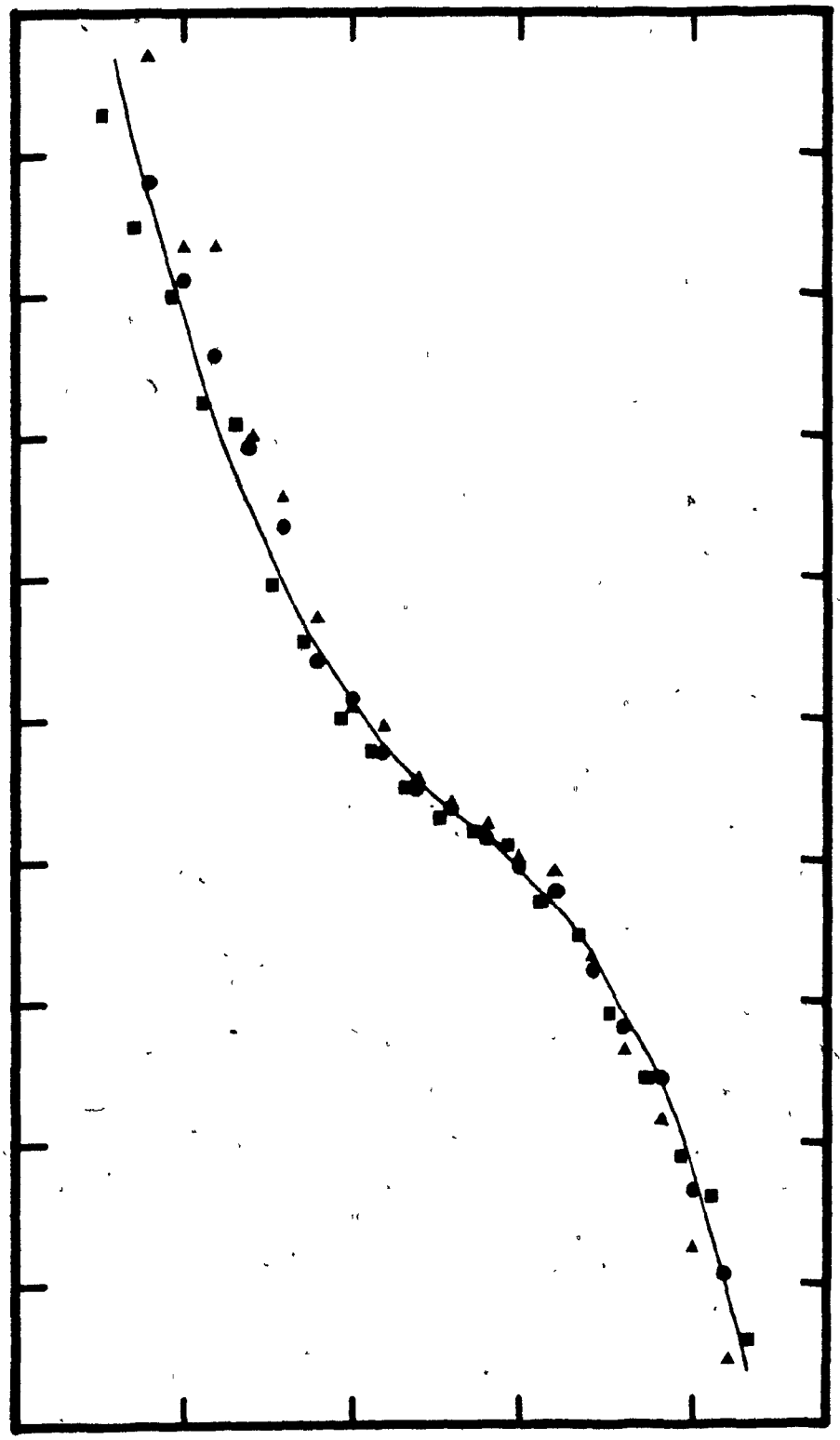

Fig. 5.18

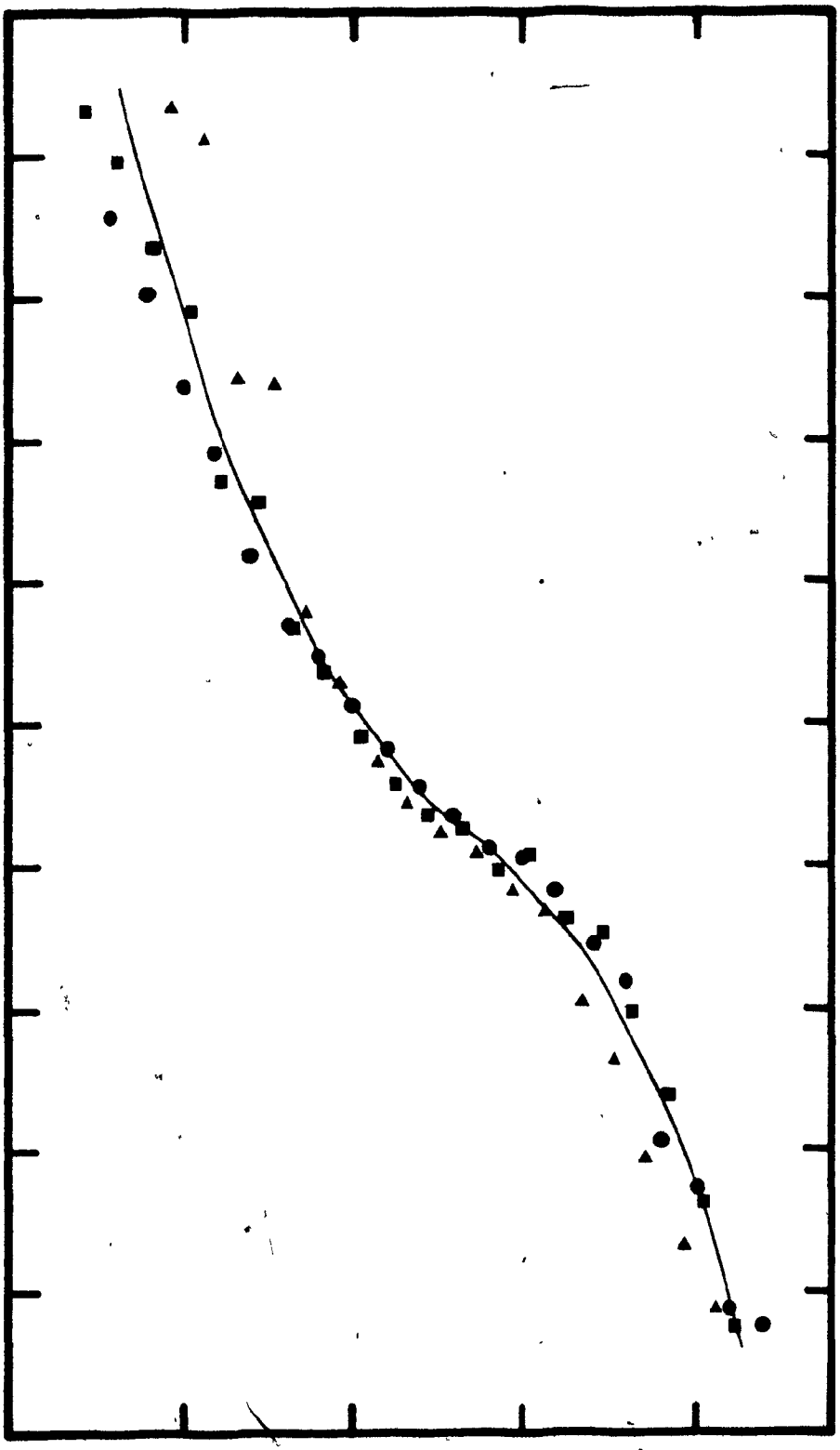

Fig. 5.19

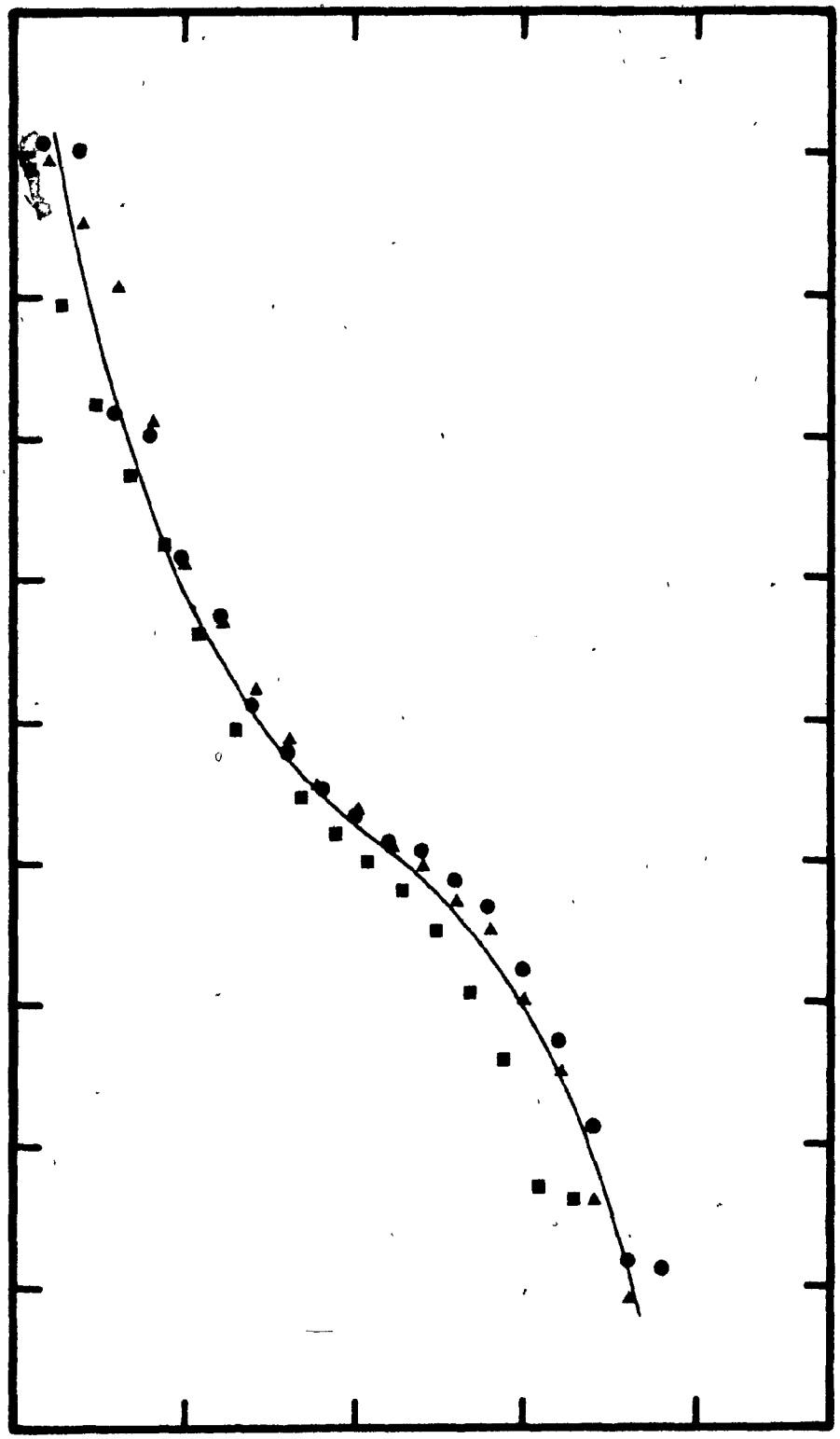

Fig. 5.20

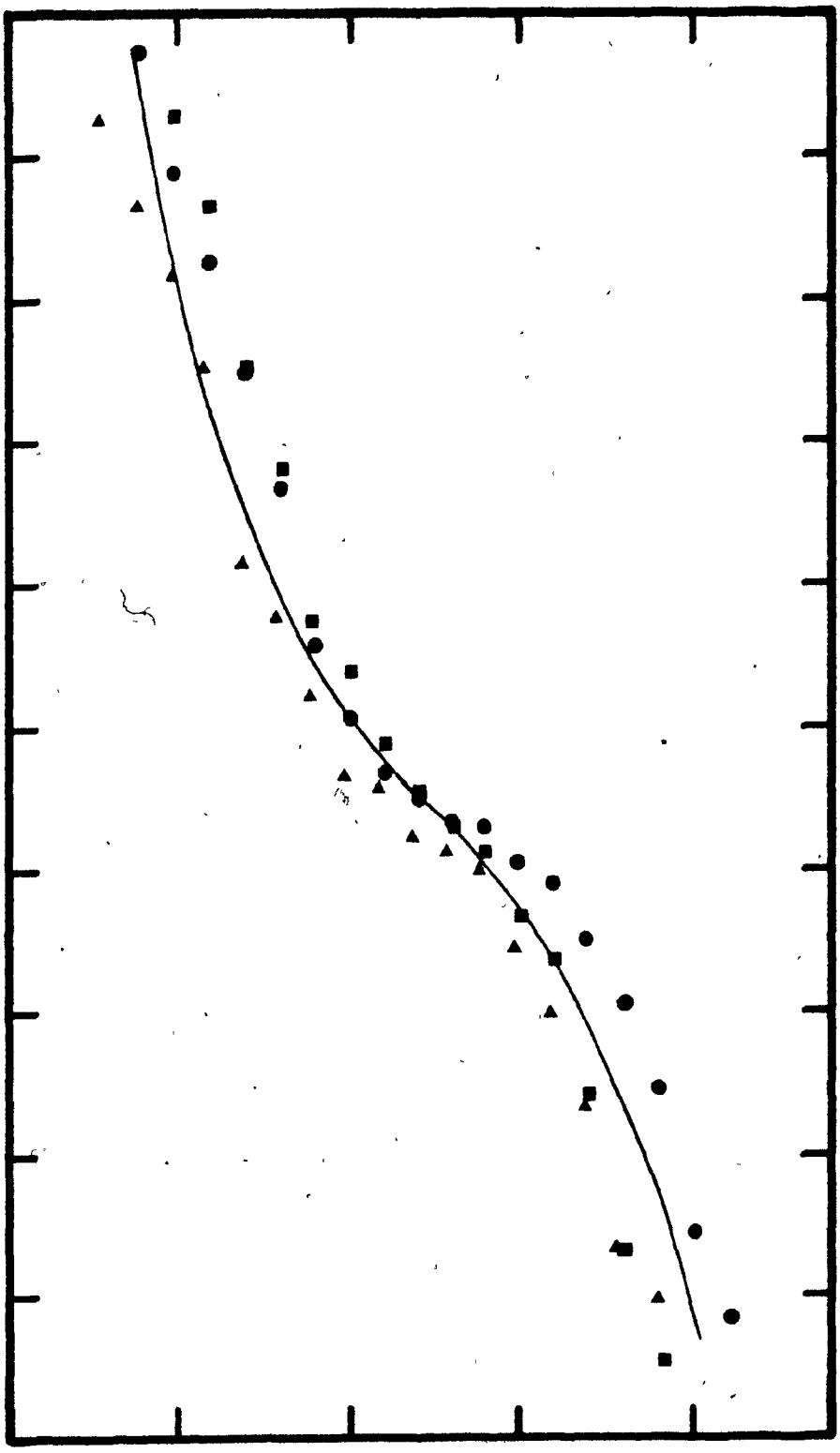

Fig. 5.21

To attempt to evaluate the actual image width and the quality of the image the data of Fig 5.16 (identified by the symbol ♦) were plotted on the same scale as the theoretical curves for a 45 and 50 μm image. The results are shown in Fig. 5.22 where the ■ symbols represent the experimental data. The IRR axis is scaled linearly to produce a slightly expanded vertical dimension compared with a Log scale.

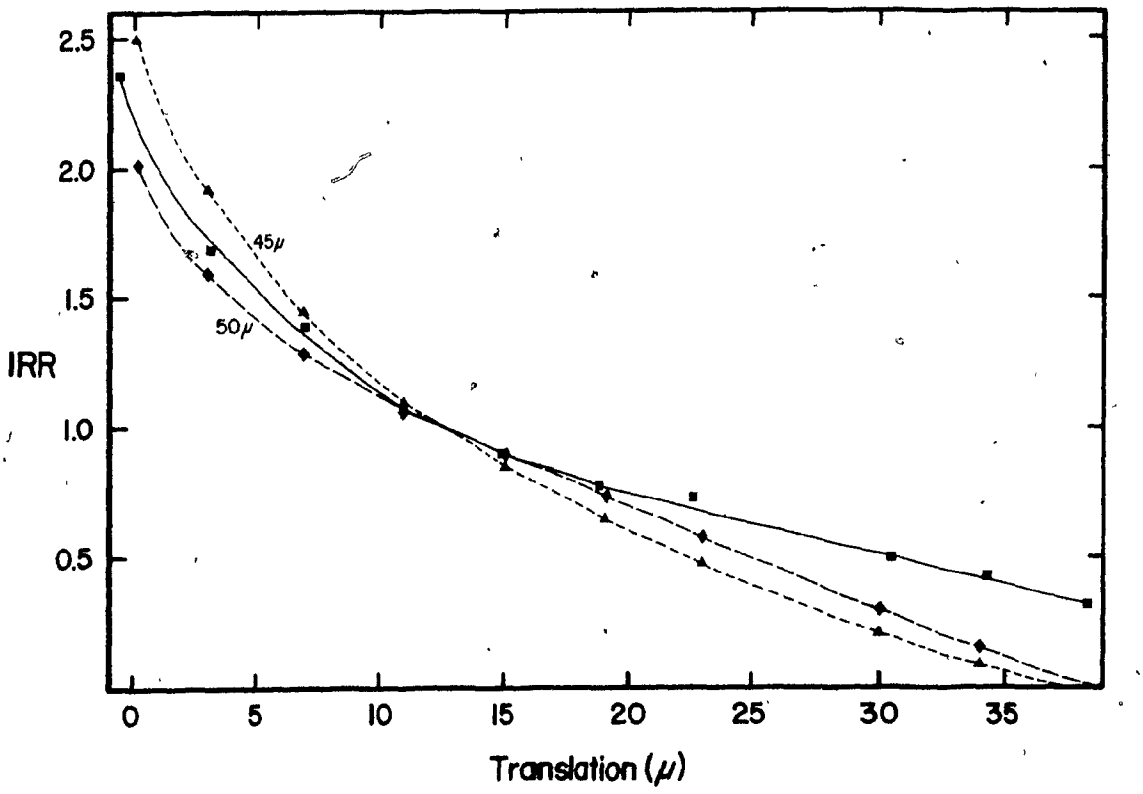

Figure 5.22: Data of Fig. 5.16 plotted with theoretical curves for 45 and 50 μm wide images.

The experimental data follows between the theoretical data up to the halfway mark at 12.5 μm at which point it diverges. This suggests two things. First, the 10 μm entrance slit did not result in a 10 μm image. This could be due to the

spectrometer and/or detector focus. It is also possible that the quartz faceplate of the PDA is responsible for some image degradation. Secondly, it appears that the image is slightly asymmetric based on the deviation from the theoretical plot. If the left-hand side of the image was broader than the right-hand side this deviation would be seen.

5.2.6 Integrated Response Calculations for Two Images

Some of the most difficult problems in ICP emission spectroscopy are those resulting from partial or direct spectral overlap. Spectral overlaps can be minimized by providing a high degree of dispersion; however, this reduces the width of the spectral window. Another approach is to successfully detect an overlap situation and then either choose an alternate analytical line or perform a spectral stripping procedure. The spatial resolution enhancement theory provides the potential for detecting spectral overlaps. At the present state of development the theory is not capable of deconvoluting spectral overlaps, but this will be addressed in the future.

Two-line IRR calculations are a simple extension of the single line general approach. The widths of both images will be the same if a single entrance slit is used. The image separation as well as the relative intensities will affect the IRR. A computer program called PROFILE2.SRC was written to simulate multi-image IRRs as a function of translation. Ideal images were again assumed and both images were defined to be of equal intensity. PROFILE2.SRC generates a series of IRR values

for 50, 1 μm translations. The user specifies the image width and the center to center image separation. Another version of this program, called PROFILE3.SRC, was used to provide IRR tables for image widths of 5 to 30 μm in increments of 5 μm. For each image width, image separations ranging from 2 to 50 μm were employed in increments of 2 μm. The output from this program consists of 150 pages of IRR tables and is far too extensive to be reproduced here. Some noteworthy excerpts are discussed below.

As an extreme example, using a relatively small image width of 5 μm, the IRR values for image separations (S) of 2 and 4 μm are listed in Table 5.7 as a function of image pair translation. It is important the note that these images are overlapping. The data indicate that small differences in image separation produce IRR patterns that are significantly different from one another. These image separations correspond to wavelength differences of .0016 and .0032 nm respectively with a reciprocal dispersion of 0.8 nm/mm. To distinguish these situations it is necessary to make at least 2 measurements. This can be contrasted with the single image case where one measurement yields positional information. In a real implementation it may be necessary to develop a significant portion of the sigmoid.

Translation (μm)	Integrated Response Ratios	
	S = 2 μm	S = 4 μm
4	236.6	58.7
5	58.7	25.6
6	22.9	14.0
7	11.0	8.2
8	6.0	5.1
9	3.7	3.4
10	2.4	2.4

Table 5.7: IRR values vs. image translation for 5 μm images.

The data of Table 5.8 illustrate IRR values for two 5 μm images separated by 48 and 50 μm. The patterns are compressed closer together, however, the difference between them should be measurable using a conventional readout system.

Translation (μm)	Integrated Response Ratio	
	S = 48 μm	S = 50 μm
4	.009	0
5	.034	.009
6	.076	.035
7	.139	.082
8	.226	.155
9	.337	.264
10	.474	.412
11	.647	.600
12	.866	.846

Table 5.8: IRR values vs. image translation for 5 μm images.

Tables 5.9 and 5.10 indicate IRR values for 30 μm images. Two IRR values were used to describe the data. IRR_0 is the ratio previously defined as the signal integrated by the central diode (d_0) divided by the signal integrated by the right-hand neighboring diode (d_1). IRR_1 is the ratio of d_1 to d_2 and, in the first example, amplifies the difference between the IRR patterns.

Translation (μm)	S = 2 μm		S = 4 μm	
	IRR_0	IRR_1	IRR_0	IRR_1
16	.622	3560	.624	394
17	.540	416	.542	149
18	.467	151	.470	79.4
19	.401	70.2	.404	49.4
20	.342	39.8	.344	32.2
21	.288	25.6	.292	22.2
22	.240	17.8	.246	16.1

Table 5.9: IRR values vs. image translation for 30 μm images.

Translation (μm)	S = 48 μm		S = 50 μm	
	IRR_0	IRR_1	IRR_0	IRR_1
16	1.56	.716	1.61	.623
17	1.76	.628	1.85	.540
18	1.97	.553	2.13	.471
19	2.19	.491	2.42	.413
20	2.42	.441	2.74	.365
21	2.65	.399	3.08	.325
22	2.86	.365	3.424	.292

Table 5.10: IRR values vs. image translation for 30 μm images.

5.2.7 Conclusions

The spatial resolution enhancement theory suggests that a simple measurement of diode ratios can be used to determine the position of an image with a high degree of accuracy. The experimental results demonstrate the trend described by theory. For a practical implementation it will be necessary to achieve a very fine focus or calibrate the image profile, P(x). Spectrum shifting can be implemented using a precisely controlled grating rotation mechanism, or preferably, a refractor plate in the optical path. If the profile of an image is known then its position can be determined with a single measurement. If the profile of the image is not known, then it may be deduced by translating the image to produce a characteristic sigmoid plot.

The image pair data indicates that overlapping or near overlapping lines can be detected using the translation method. The separation of the images has a significant effect on the integrated response ratios. It may be possible to deconvolute overlapped or closely spaced images, even though the PDA reports a single image, by spectrum shifting in conjunction with the application of the IRR theory.

6. Applications of a Linear Photodiode Array as a Detector for Transient Signal Experiments

Integrating multichannel detectors are capable of simultaneously capturing multiwavelength information produced by transient signal experiments. This cannot be done using single channel detector systems or sequential access imaging systems like the image dissector PMT. Salin and Horlick [163] and Sommer and Ohls [164] were the first to describe direct sample insertion devices (DSID) capable of introducing solids or liquids directly into the ICP discharge. This method of sample introduction has the advantage of requiring little or no sample preparation when compared to traditional nebulizer based systems. Other methods resulting in the production of transient signals include laser ablation [106,107,165], flow injection analysis [166] and electrothermal atomization [167].

There have been several reports published which discuss the application of imaging detectors to transient signal measurements. Fricke et al. [76] used a vidicon to monitor the signals produced by electrothermal atomization of 5 µL samples into a microwave induced plasma. Talmi et al. have investigated the use of a vidicon and a PDA as detectors for multielement laser-microprobe analysis [106]. Laser vaporization of metal disk samples with subsequent excitation by an ICP has been reported by Carr and Horlick [107].

This Chapter deals with some applications of the PDA system as a detector for microsample liquid analysis using a tungsten wire-loop DSID. This DSID was developed in the laboratory by R.

Sing and has been described previously [122]. The wire-loop support has a very low mass compared with other commonly employed supports like carbon electrodes. As a result the wire-loop rapidly achieves a high temperature and sample volatilization occurs in a relatively short period of time. The DSID is pneumatically driven by an independent argon gas cylinder. This is quite different from the stepping motor and drive screw system employed by Li-Xing et al. [168]. The pneumatic system provides the very fast insertion into the plasma which is essential for the wire-loop DSID technique to be successful. Detection limits for 10 µL samples using PMT detection are 50 to 100 times better than those reported in the literature [122] for furnace vaporization and conventional nebulizer sample introduction.

6.1 System Operation

The DSID experiments were performed using the PDA control software comprising System 2. This enabled the DSID to be triggered by the computer, as described in Chapter 2 section 2.4.5 (ii), and synchronized with the PDA readout. When the DSID is lowered, the wire-loop is well below the bottom of the torch enclosure enabling sample application while the ICP is running. For all experiments a 10 µL sample volume was used.

After application of the sample, the loop is manually raised to the first stop position and held in place by opening the gas valve controlling the DSID insertion pressure. In this

position the loop is approximately 15 mm below the bottom of the discharge where the heat from the plasma is sufficient to dry the sample in 10 to 15 seconds. During the drying time commands are issued to both computers to prepare for data acquisition. For the temporal resolution studies PDA3D.SRC was used in place of PDASYS2.SRC. The code for PDA3D.SRC is included in Appendix M. In either event, the S100 system is fully primed and waiting for data before the AIM2 computer is instructed to trigger the DSID.

The mechanical stop preventing the loop from entering the plasma is disengaged by a solenoid switch. When the final AIM2 prompt

"# OF SCANS"

is answered by typing the value followed by 'RETURN', AIM2 monitors the PDA for the end of a readout cycle. At this point the solenoid is triggered, allowing the wire-loop to be driven into the plasma by the pneumatic transport mechanism. If the used had specified a DSID delay period, data acquisition is postponed until the appropriate time. If the PDA3D software is invoked on the S100 computer, up to ten 1024-point spectra can be acquired where each spectrum must be recorded using the same integration time. This capability was used to monitor the temporal behavior of DSID signals.

For the acquisition of single spectra the standard PDASYS2 control program is used. The optimal time period for spectrum acquisition is determined first, by running several samples using the PDA3D control program to produce time resolved emission profiles. Figure 6.1 illustrates the Start and Video

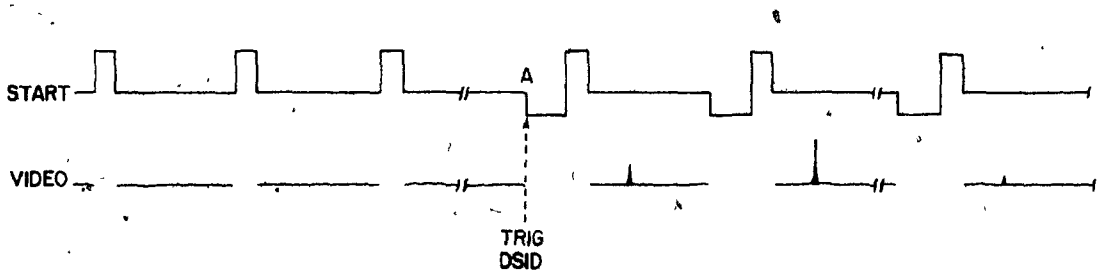

Figure 6.1: PDA signal sequence for multiple spectrum acquisition.

signals as a function of time as they might appear during one of these runs. Before the DSID is triggered at point A, the PDA is read out continually at its maximum rate. At any time during a readout the user may invoke the data acquisition software. When this happens the software waits for the end of a readout and then triggers the solenoid which allows the wire loop to be driven into the plasma. A series of 10 readouts are collected at the user specified integration time. The video trace of Fig. 6.1 illustrates the onset, peak and disappearance of a spectral line. The resulting 3 dimensional plot is then used to determine how long to wait before starting a PDA integration and how long to integrate the signal such that the peak is captured as a "snap-shot" in time.

When a single spectrum is to be acquired for analytical purposes the user specifies the DSID wait period and the integration period to be employed. Figure 6.2 illustrates the Start and Video signals for this mode of spectrum acquisition. The interval between points A and B is the DSID wait period. It is not possible to simply stop the PDA during this period

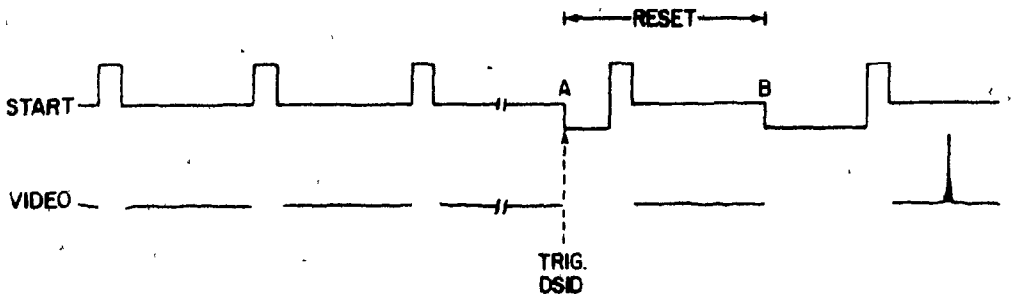

Figure 6.2: PDA signal sequence for transient signal acquisition.

because the photodiodes would still continue to integrate light flux. In addition, there is no guarantee that the DSID wait period will be an integral number of 58 ms readouts. Fortunately a simple solution exists. Starting at point A, when the DSID is triggered, the PDA is integrated for a period of time equal to the specified DSID delay minus one full 58 ms readout. When this integration period has elapsed the PDA is read out to reset all of the pixels in preparation for the acquisition of the spectrum. No data is acquired during the reset period. At point B the user specified integration period is invoked followed by a single readout of the analyte spectrum. The time resolution of the snapshot is ± 1 ms.

6.2 Temporal Volatilization Behavior of Some Species using a Tungsten Wire DSID

One of the most striking features of the tungsten wire DSID is that selective, highly reproducible volatilization occurs for analyte species. Using the DSID described in this work Sing and

Salin [122] have measured volatilization times of 270 ms for Zn and 310 ms for Cu. The standard deviations for the peak evolution times are between 3 and 4 ms. Selective volatilization can be used to advantage if spectral overlap is a problem. The tungsten wire is fairly resistant to corrosion in the Ar atmosphere of the plasma; however, a small amount of W does enter the plasma during each insertion. Tungsten provides an abundant number of spectral lines and consequently, spectral overlaps can result. One such overlap occurs between the Zn 213.856 nm line and the W 213.815 nm line. Fortunately the different evolution times of these elements results in baseline resolution in the time domain.

The PDA detection system was employed to demonstrate the ability to monitor the multiwavelength behavior of transient emission signals in the time domain. It had already been demonstrated [122] that many elements vaporize after a residence time of 200 ms or more in the plasma. In addition, trace quantities of several elements produced emission signals lasting in excess of 100 ms. These facts indicated that the 58 ms minimum integration time of the PDA detection system would be adequate to temporally characterize the multiwavelength emission profiles if several sequential scans could be acquired. The ability to acquire up to 10 spectra was provided by the PDA3D.SRC control program for the S100 system.

6.2.1 Experimental

The standard operating conditions for DSID experiments are listed in Appendix B. Solutions were prepared from reagent grade salts in deionized/distilled water. Some solutions were stabilized by the addition of small quantities of HNO_3, but this was avoided if possible to prevent oxidation of the W wire. Tungsten emission is greatly enhanced following air and/or chemically induced oxidation.

Temporal information was recorded by acquiring 10 sequential scans with integration periods set to multiples of 58 ms. This was done for experiment-to-experiment comparison purposes. The PDA scans were plotted with a 3-dimensional perspective using a routine written by R. Sing (see Appendix M). This routine was embedded in the PDA3D.SRC control program.

6.2.2 Results and Discussion

Carr and Horlick used a 1024-element PDA to monitor the temporal behavior of multielement signals produced by laser ablation of metal samples into an ICP [107]. Their temporal resolution was limited to 100 ms per scan; however, this was adequate to demonstrate that emission signals for several elements in the sample matrix reached a maximum intensity in the same time frame.

The situation is quite different for the W wire DSID. Figure 6.3 illustrates a 3-D plot of the temporal behavior of Cu and Ag. A 10 µL aliquot of a 5 ppm solution was deposited on the loop. Each scan frame corresponds to an integration time of 58 ms. This data illustrates that Ag is vaporized from the wire

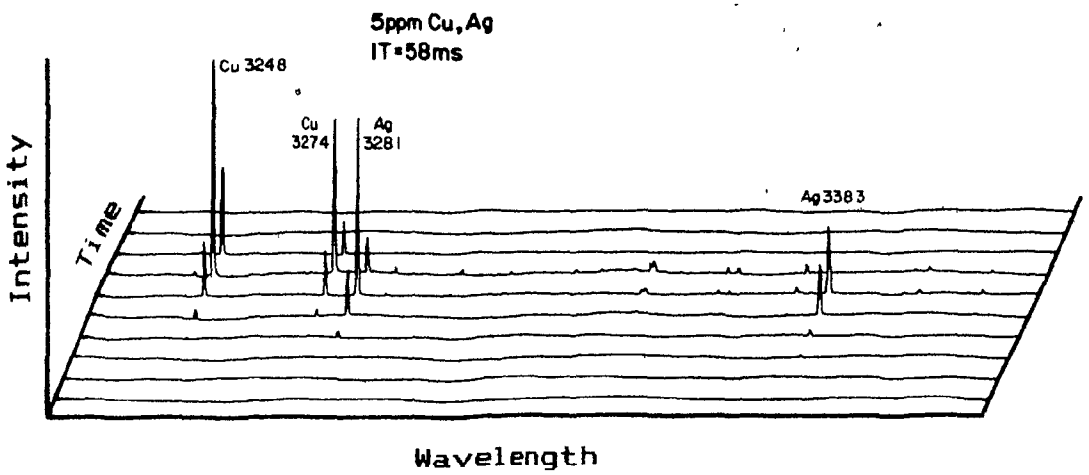

Figure 6.3: 3-D spectrum of 5 ppm Cu and Ag using 58 ms readout periods.

one scan frame before Cu is vaporized. For both elements the peak duration is approximately 200 ms.

The spectral window of Fig. 6.3 covers the region from about 323 nm to 343 nm. Other elements with prominent lines in this window are V and Sr. When an attempt was made to record a spectrum of all 4 elements using 58 ms scan frames, an identical spectrum to that shown in Fig. 6.3 was obtained. After increasing the integration time to 174 ms, exactly 3 times the minimum of 58 ms, the spectrum of Fig 6.4 was recorded. This plot clearly shows that the Sr emission occurs well after the Cu and Ag emission.

Figure 6.5 shows an expanded view of the region where the V emission occurs. The stipple pattern identifies the Cu 327.4 nm line while the diagonal pattern identifies the Ag 328.1 nm line. The V triplet peaks at about the same time as the Sr signal, and well after the Cu and Ag signals. Furthermore, the V emission

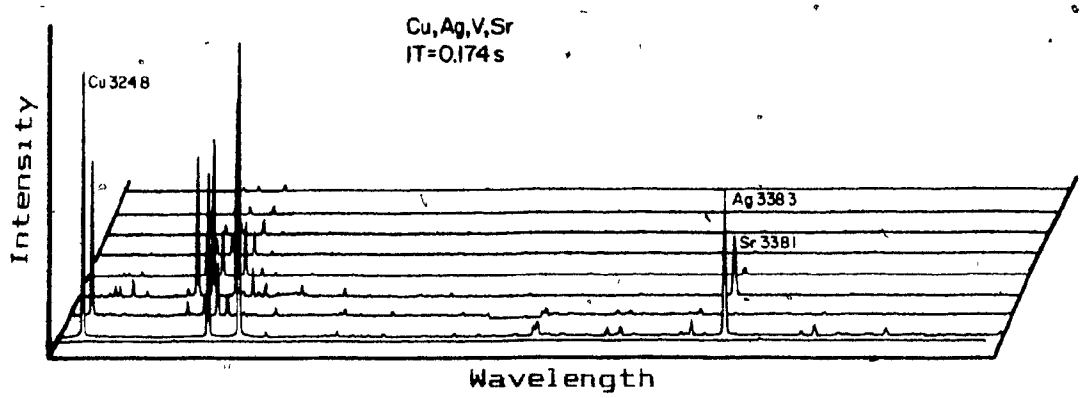

Figure 6.4: 3-D spectrum of Cu, Ag, V and Sr using 174 ms readout periods.

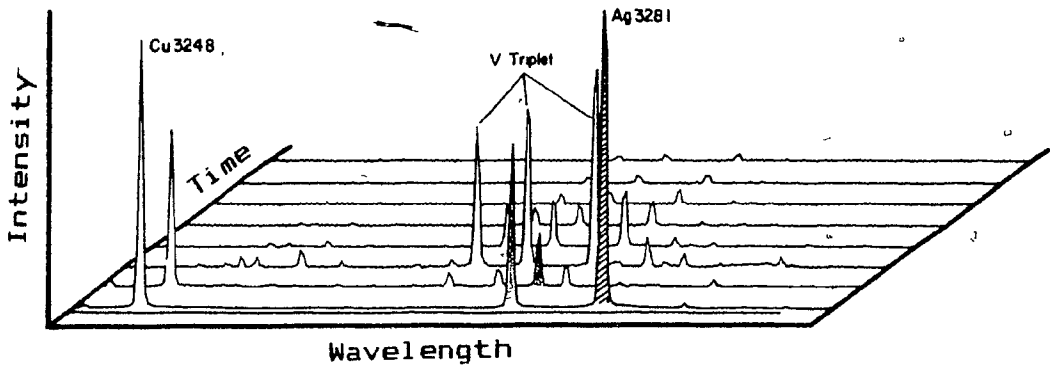

Figure 6.5: Enlarged segment of Fig. 6.4 showing V lines appearing after Cu and Ag lines.

is prolonged with respect to the other elements. The V triplet is still visible 700 ms after the Sr signal has disappeared. The temporal behavior illustrated by these plots is highly reproducible.

Temporal information is useful for two reasons. First, it permits the time dependent evaluation of multielement samples using a transient sample introduction technique. Secondly, it informs the analyst of the optimum time period for spectrum integration. If the spectrum is integrated during the time period before and/or after the evolution of the signal, the SBR will be lower and excess noise will be introduced. If spectral overlap is not a major problem it would be advantageous if all species peaked at the same time enabling the shortest possible integration time to be used. Unfortunately, some elements exhibit significantly different volatilization times. Therefore an attempt was made to force all elements to enter the plasma at the same time.

The procedure involved coating the wire with tungsten oxide. This technique had been used routinely by R. Sing to induce intense W emission for several of his experiments. This is done by lowering the wire from within the ICP discharge into an air atmosphere. The oxide layer produced was clearly visible as the bright metallic-blue coating characteristic of W_2O_5 or W_4O_{11}. The small peaks seen throughout the spectra of Figs. 6.3 and 6.4 are due to W emission following the vaporization of the oxide. This emission occurs in the same time frame as the Cu and Ag emission and well before the V and Sr signals. It was hoped that by coating the wire with a uniform layer of oxide first, the sample components would be simultaneously vaporized into the ICP.

This hypothesis was tested by depositing 10 µL of a Sr

solution on an oxidized wire loop. The time dependent spectra of Fig. 6.6 indicate that the Sr emission occurred 2 full 174 ms scan frames after the evolution of the tungsten oxide. This is the same volatilization time observed using a "clean" wire. This experiment was repeated several times with Sr and then with V with the same result.

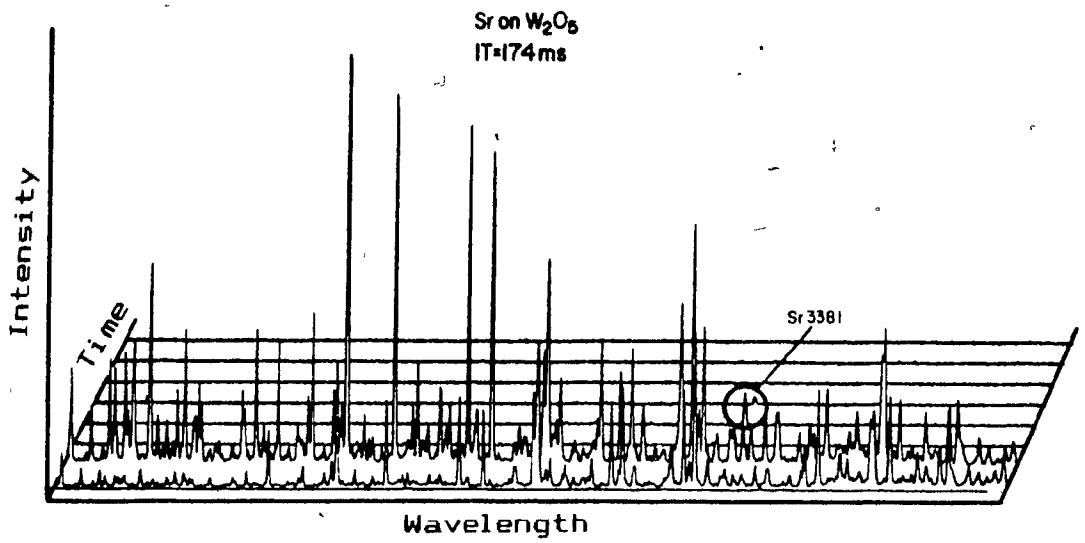

Figure 6.6: 3-D spectrum of Sr after first coating W wire with an oxide layer.

Several other interesting phenomena were observed using the PDA detection system for time-resolved studies. Figure 6.7 shows the behavior of Fe and Co using scan frames of 116 ms. The emission from these elements is observed as two distinct events separated by about 100 ms. Figure 6.8 illustrates the behavior of Mn. The vaporization occurs in about one half of the time but the same double peak is observed. The high

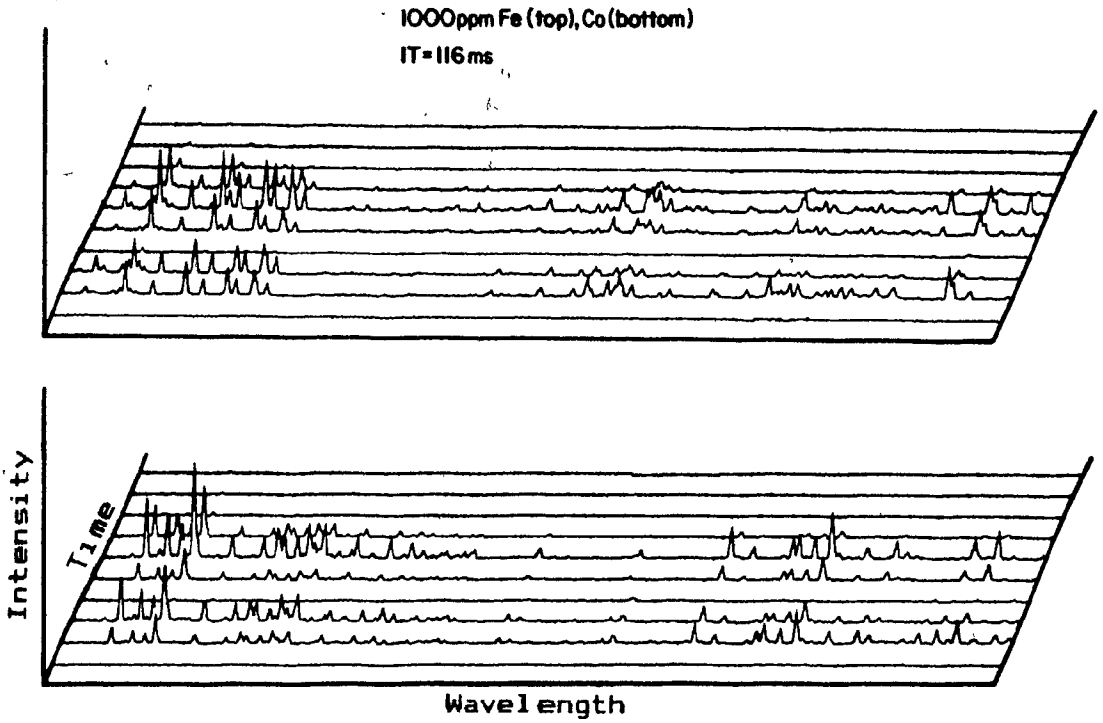

Figure 6.7: 3-D spectra of Fe (top) and Co (bottom) showing double peak phenomenon in the time domain.

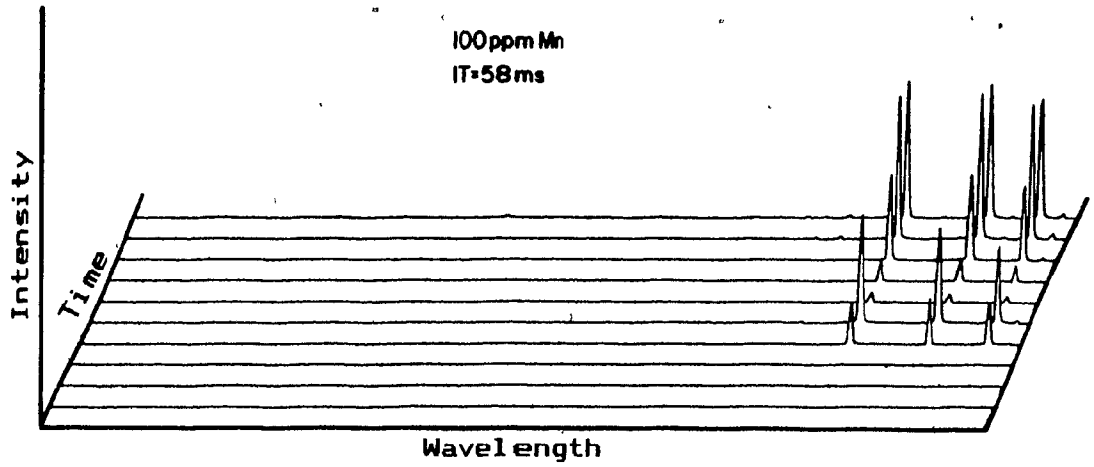

Figure 6.8: 3-D spectrum of Mn showing similar double peak phenomenon as for Fe and Co.

temperature, electron rich atmosphere of the ICP suggests that complex surface interactions are possible between analyte species and the tungsten wire. One possibility for the behavior of these species is the temporary formation of compounds of different oxidation states with different vaporization temperatures. These phenomena were not pursued and no explanation for these events is currently available.

The last series of 3-D spectra were obtained while trying to determine detection limits for Ca. The procedure was to decrease the concentration of the analyte to the point where the background noise was prominent. Single readouts were employed for these measurements. In the course of running the standard solutions severe memory effects were observed. Figure 6.9 illustrates a 3-D series for a 10 µL injection of 0.1 ppm Ca.

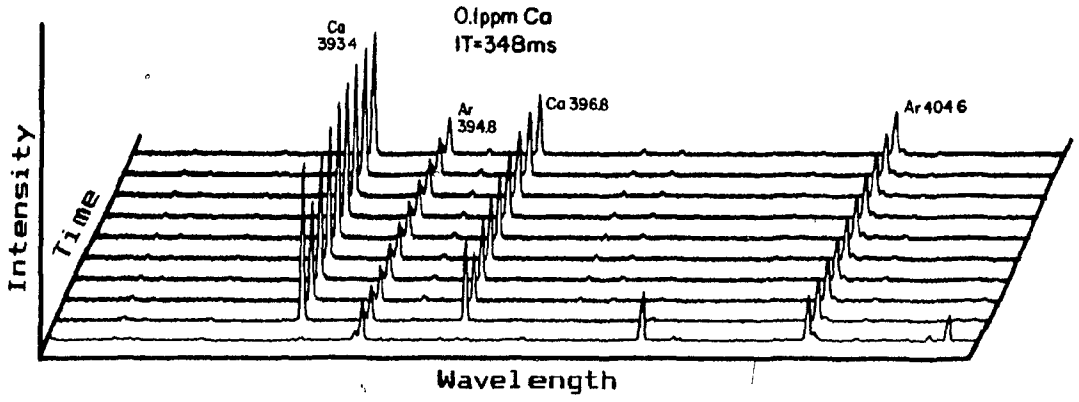

Figure 6.9: 3-D spectrum of Ca illustrating memory effect.

The entire series spans 3.5 seconds and indicates that after an initial Ca evolution in the second scan frame, the Ca emission

stabilizes at a constant and relatively intense level. A series of water blanks were then run, resulting in the series of Fig. 6.10. Again, an initial Ca signal is observed followed by a constant emission signal.

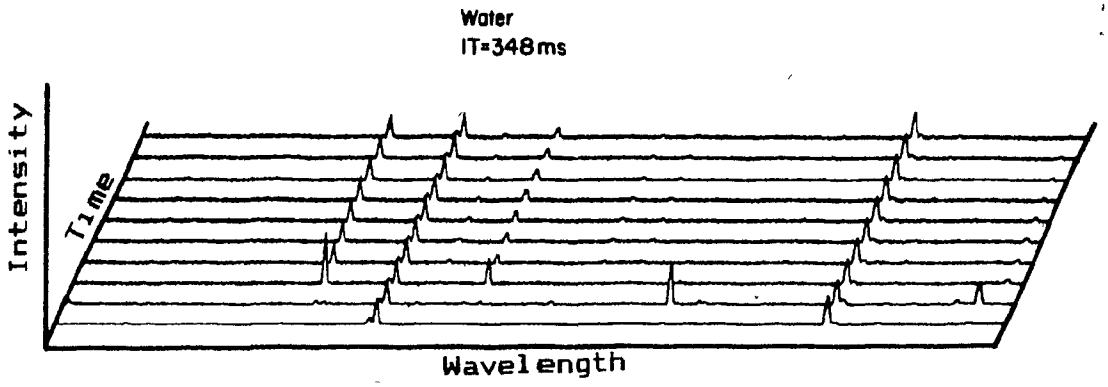

Figure 6.10: 3-D spectrum of blank showing Ca retention.

These data indicated that Ca was being strongly attached to the surface of the W wire. The Ca solutions were prepared from $CaCl_2$. The boiling point of $CaCl_2$ is listed [168] as greater than 1600 C. To try to deduce whether the Ca retention was due to the high boiling point of $CaCl_2$ or some other influence a 1 ppm solution of $SrCl_2$ was run immediately following the water blank series. The result is shown in Fig. 6.11. The boiling point of $SrCl_2$ is only 1250 C [169] and is well below the boiling point of W_2O_5 of approximately 1530 C. However, the same retention phenomenon observed for $CaCl_2$ was observed. In addition, the initial spike of the Sr signal in the third frame

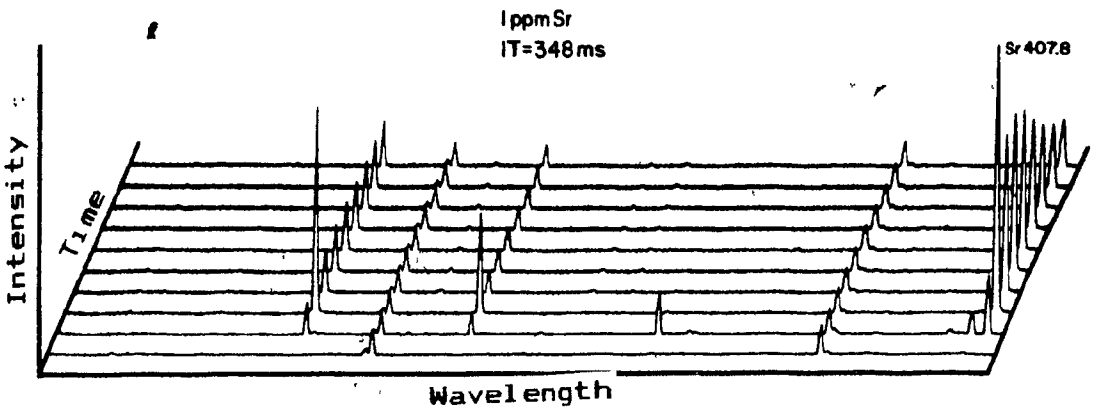

Figure 6.11: 3-D spectrum of 1 ppm Sr acquired immediately after the water blank spectrum of Fig. 6.10.

appears to have induced a similar spike of the Ca signals. The magnitude of the Ca signal cannot reasonably be attributed to the 1 to 2 % Ca impurity in the $SrCl_2$ used to prepare the Sr solutions. The cause of these puzzling results has not been discovered.

6.2.3 Conclusions

The PDA has been demonstrated as a useful diagnostic tool for the evaluation of analyte temporal behavior for fast transient signals. Some potential problems in using tungsten as a sample support material were discovered which prompted the selection of the more chemically inert tantalum as a future support material. The detection of these problems would have been delayed if a single channel detector like the PMT had been used.

6.3 Precision Enhancement using the Method of Internal Standardization

The method of internal standards has been a popular technique in spectroscopy since its introduction in 1925 [30]. This technique is particularly valuable for transient signal analysis because periodic changes in the experimental parameters resulting in a large fluctuation of the signal cannot be compensated for by the traditional method of signal averaging. The effect of internal standardization on measurement precision was determined using the wire-loop DSID as the sample introduction system.

6.3.1 Experimental

The analysis lines used for the precision study were the Cu 324.8 nm and 327.4 nm lines and the Ag 328.1 nm and 338.3 nm lines. A solution of 1 µg/ml Cu and Ag was prepared from their reagent grade nitrate salts in 1 % HNO_3. The DSID conditions described in Appendix B were employed. A DSID wait period of 174 ms seconds followed by an integration period of 290 ms was used for all acquisitions.

6.3.2 Results and Discussion

Figure 6.12 shows both Cu lines and the Ag 328.1 nm line for 3 out of 10 replicate measurements. The amount of sample deposited on the loop was varied intentionally to produce the unequal peak intensities from sample to sample. Table 6.1 lists the sample precision of the unratioed Cu lines and the precision

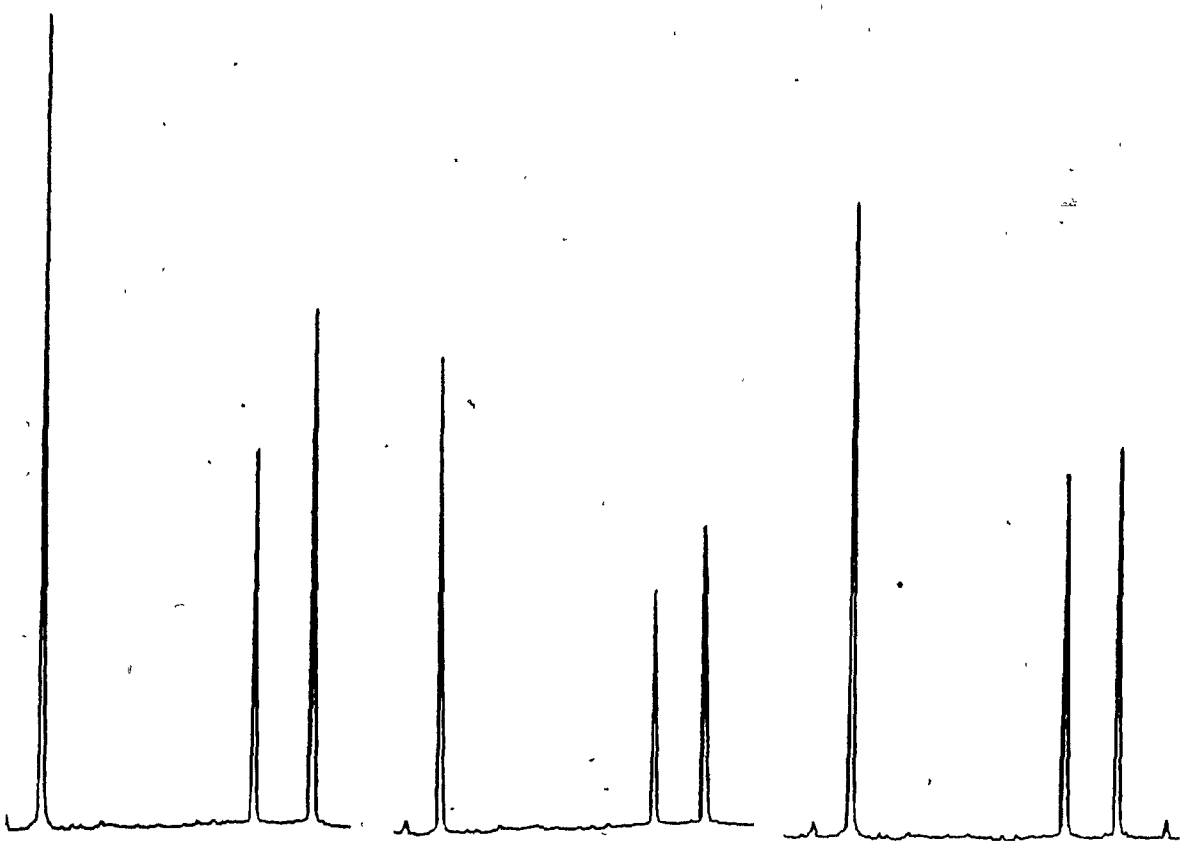

Figure 6.12: Spectrum segments showing Cu 324.8, Cu 327.4 and Ag 328.1 nm lines for 3 of 10 insertions.

enhancement when both Ag lines were used as internal standards. Poor precision values are calculated for the unratioed Cu intensities. This is the result of intentionally varying the sample volume. Combining both Cu intensities improves the % RSD markedly, but a dramatic improvement is realized by ratioing the Cu intensities with those of the Ag lines. A precision of 2 % or better is achieved using peak areas as opposed to peak heights. The ratio of the Cu 327.4 nm peak height to either of the Ag peak heights is relatively imprecise. This may have been

the result of the fact that the line was roughly centered between diodes, and a reduced SNR was produced. The error was compensated for by utilizing the peak areas. The ratio of the sum of Cu and Ag intensities did not produce a significant improvement.

Line or Ratio	Peak Height	Peak Area
Cu 324.8	17	18
Cu 327.4	19	18
Sum of Cu	13	13
Cu 324.8/Ag 328.1	3.1	1.7
Cu 324.8/Ag 338.3	3.1	2.0
Cu 327.4/Ag 328.1	10.8	1.9
Cu 327.3/Ag 338.3	5.5	2.2
Sum Cu/Sum Ag	3.9	1.8

Table 6.1: % RSDs for unratioed and ratioed peak heights and peak areas.

Another experiment was carried out to see if the precision could be improved by eliminating contributions from the W emission. For these results the sample was applied to the loop using a precision 10 µL syringe. Figure 6.13 shows a spectrum of the 1 ppm Cu/Ag solution. This spectrum has had the fixed pattern signal removed by simple dark subtraction. A relatively large contribution from W is evident in the spectrum. Figure

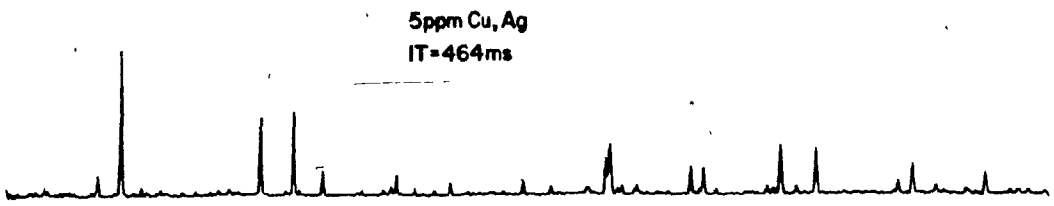

Figure 6.13: Spectrum of 5 ppm Cu and Ag after simple dark subtraction.

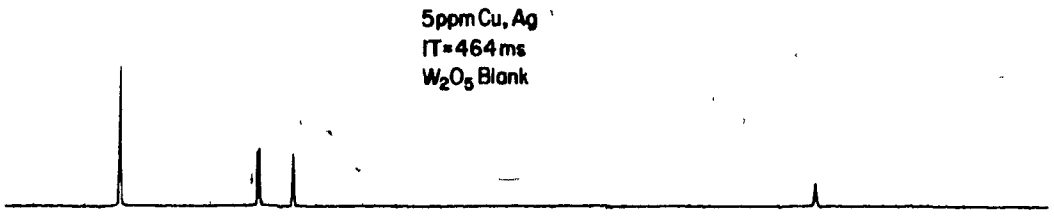

Figure 6.14: Spectrum of Fig. 6.13 with Tungsten background removed by spectral stripping.

6.14 shows the same spectrum when a tungsten blank was subtracted from the analyte spectrum. An apparent improvement in the quality of the spectrum results. Table 6.2 shows the unratioed precision of the Cu lines for 5 replicate measurements for uncorrected and corrected spectra.

Line	Peak Height		Peak Area	
	Uncorrected	Corrected	Uncorrected	Corrected
Cu 324.8	2.6	4.2	2.4	3.6
Cu 327.4	4.0	6.5	1.7	4.3
Sum of Cu	2.2	3.5	1.7	2.8
Ag 328.1	4.8	19.7	5.3	16.0
Ag 338.3	6.3	18.1	7.0	19.3
Sum of Ag	3.8	14.9	4.2	12.4

Table 6.2: RSDs for peak heights and peak areas. Uncorrected spectra (Fig. 6.13) and corrected spectra (Fig. 6.14 Tungsten emission removed by blank subtraction).

It is interesting to note that the precision is actually degraded by performing the tungsten correction. The effect is most pronounced on the Ag lines but no significant W overlap is listed for these lines [158]. No significant improvement was obtained by ratioing the results.

6.3.3 Conclusions

The multichannel nature of the PDA provides the advantage of internal standardization. Dramatic improvements in the sample to sample precision can be achieved by ratioing peak intensities. Care must be exercised if spectral stripping procedures are employed since removal of background features can degrade the precision.

6.4 Detection Limits

The PDA is several orders of magnitude less sensitive than a PMT and detection limits are worse as a result. One of the consequences of transient signal analysis is that extended integration periods cannot be used to lower the detection limits. However, since the wire-loop DSID introduces proportionately more analyte into the plasma [122] than conventional pneumatic nebulizer systems, the detection limits for many elements are improved to the point where they may be adequate for many analysis situations. The PDA detection limits for Cu and Ag are contrasted with those obtained using other methods in Table 6.3.

Method	Cu Detection Limit		Ag Detection Limit	
	ng/ml	pg	ng/ml	pg
Nebulizer [158]	10	--	7	--
PDA/DSID	6	60	52	520
PMT/DSID [122]	.2	2	.04	0.4

Table 6.3: Detection limits for several sample introduction techniques.

These data indicate that the detection limits for the PDA/DSID system are in the same region as those obtained using conventional nebulization but are a factor of 50 to 100 times poorer than those using the same DSID with a PMT.

References

1. G.M. Hieftje, Pittsburgh Conference and Exposition on Analytical Chemistry and Applied Spectroscopy, Atlantic City, NJ, USA, Paper 10 (1984).
2. R.F. Browner and A.W. Boorn, Anal. Chem. **56**, 786A (1984).
3. R.F. Browner and A.W. Boorn, Anal. Chem. **56**, 875A (1984).
4. S.W. McGeorge and E.D. Salin, Can. J. Spec. 27, 25 (1982).
5. R.M. Barnes and R.G. Schliecher, Spectrochim. Acta **36B**, 81 (1981).
6. G. Horlick, Ind. Res./Dev. **20**, 70 (1978).
7. G.F. Larson, V.A. Fassel, R.K. Winge and R.N. Kniseley, Appl. Spectrosc. 30, 4 (1976).
8. A.G. Marshall and M.B. Comisarow, Anal. Chem. **47**, 491A (1975).
9. P. Fellgett, Ph.D. thesis, Cambridge University, Cambridge (1951).
10. J.D. Winefordner, J.J. Fitzgerald and N. Omenetto, Appl. Spectrosc. **29**, 369 (1975).
11. M.A. Floyd, V.A. Fassel, R.K. Winge, J.M. Katzenberger and A.P. D'Silva, Anal. Chem. **52**, 431 (1980).
12. G. Kunselman, J. Bernier and K. Kaltenbach, Pittsburgh Conference and Exposition on Analytical Chemistry and Applied Spectroscopy, Atlantic City, NJ, USA, Paper 152 (1982).
13. E.D. Salin and G. Horlick, Anal. Chem. 52, 1578 (1980).
14. M. Margoshes, Spectrochim. Acta **25B**, 113 (1970).
15. P. Burke, Ind. Res./Dev. **April**, 24 (1973).
16. K.W. Busch and G.H. Morrison, Anal. Chem. **45**, 712A (1973).

17. R.E. Santini, M.J. Milano and H.L. Pardue, Anal. Chem. 45, 915A (1973).

18. Y. Talmi, Anal. Chem. 47, 699A (1975).

19. Y. Talmi, Anal. Chem. 47, 658A (1975).

20. Y. Talmi, American Laboratory March, 79 (1978).

21. Y. Talmi, D.C. Baker, J.R. Jadamec and W.A. Saner, Anal. Chem. 50, 936A (1978).

22. A.F. Fell, Anal. Proc. July, 266 (1980).

23. Y. Talmi, Ed., "Multichannel Image Detectors", Vol. 1, American Chemical Society, Washington, DC (1979).

24. Y. Talmi, Ed., "Multichannel Image Detectors", Vol. 2, American Chemical Society, Washington, DC (1983).

25. H.L. Pardue, "Topics in Automatic Chemical Analysis 1", Ed. J.K. Foreman and P.B Stockwell, Vol. 1, Chapt. 6, John Wiley and Sons, NY, (1981).

26. R.W. Engstrom, "Photomultiplier Handbook", RCA Corp., Lancaster, PA (1980).

27. R. Mavrodineanu and R.C. Hughes, Appl. Optics 7, 281 (1968).

28. J.D. Ingle, Jr. and S.R. Crouch, Anal. Chem. 43, 1331 (1971).

29. A.H. Sommer, "Photoemissive Materials", John Wiley and Sons (1968).

30. W. Gerlach, Z. Anorg. Allg. Chem. 142, 383 (1925).

31. Y. Talmi and R.W. Simpson, Appl. Optics 19, 1401 (1980).

32. G. Everson, "The Story of Television, The Life of Philo T. Farnsworth", W.W. Norton and Co. Inc., NY (1949).

33. R.A. Harber and G.E. Sonnek, Appl. Optics 5, 1039 (1966).

34. D.J. Baker and A.J. Steed, Appl. Optics 7, 2190 (1968).

35. A. Danielsson and P. Lindblom, Appl. Spectrosc. **30**, 151 (1976).

36. A. Gustavsson and F. Ingman, Spectrochim. Acta **34B**, 31 (1979).

37. H.L. Felkel, Jr. and H.L. Pardue, Clin. Chem. **24**, 602 (1978).

38. D.W. Golightly, R.N. Kniseley and V.A. Fassel, Spectrochim. Acta **25B**, 451 (1970).

39. J.T. Agnew, R.G. Franklin, R.E. Benn and A. Bazarian, J. Opt. Soc. Am. **39**, 409 (1949).

40. R.E. Benn, W.S. Foote and C.T. Chase, J. Opt. Soc. Am. **39**, 529 (1949).

41. J.E. Anderson, Rev. Sci. Instruments **37**, 1214 (1966).

42. S.A. Johnson, W.M. Fairbank, Jr. and A.L. Schawlow, Appl. Optics **10**, 2259 (1971).

43. U. Ascoli-Bartoli, A. De Angelis and M. Nardi, Appl. Optics **8**(1), 59 (1969).

44. P.K. Weimer, S.V. Forgue and R.R. Goodrich, RCA Rev. **12**, 306 (1951).

45. M.H. Crowell, T.M. Buck, E.E. Labunda, J.V. Dalton and E.J. Walsh, Bell Sys. Tech. **46**, 491 (1967).

46. P.H. Wendland, IEEE Trans. Electron Dev. **ED-14**, 285 (1967).

47. R.A. Anders, D.E. Callahan, W.F. List, D.H. McCann and M.A. Schuster, IEEE Trans. Electron Dev. **ED-15**, 191 (1968).

48. F.J. Morin and J.P. Maita, Phys. Rev. **96**, 28 (1954).

49. S.M. Blumenfield, G.W. Ellis, R.W. Redington and R.H. Wilson, Phys. Rev. **ED-18**, 1036 (1971).

50. R.M. Madden, D.A. Kiewit and C.R. Crowell, IEEE Trans. Electron Dev. **ED-18**, 1043 (1971).

51. T.A. Nieman and C.G. Enke, Anal. Chem. 48, 619 (1976).

52. H.L. Felkel, Jr. and H.L. Pardue, Anal. Chem. 49, 1112 (1977).

53. K.W. Jackson, K.M. Aldous and D.G. Mitchell, Spectrosc. Lett. 6, 315 (1973).

54. H.L. Felkel, Jr. and H.L. Pardue, Anal. Chem. 50, 602 (1978).

55. N.G. Howell and G.H. Morrison, Anal. Chem. 49, 106 (1977).

56. N. Furuta, C.W. McLeod, H. Haraguchi and K. Fuwa, Appl. Spectrosc. 34, 211 (1980).

57. K.W. Busch, N.G. Howell and G.H. Morrison, Anal. Chem. 46, 575 (1974).

58. D.G. Mitchell, K.W. Jackson and K.M. Aldous, Anal. Chem. 45, 1215A (1973).

59. R.E. Santini, M.J. Milano, H.L. Pardue and D.W. Margerum, Anal. Chem. 44, 826 (1972).

60. M.J. Milano, H.L. Pardue, T.E. Cook, R.E. Santini, D.W. Margerum and J.M.T. Raycheba, Anal. Chem. 46, 374 (1974).

61. D.O. Knapp, N. Omenetto, L.P. Hart, F.W. Plankey and J.D. Winefordner, Anal. Chim. Acta. 69, 455 (1974).

62. D.L. Wood, A.B. Dargis and D.L. Nash, Appl. Spectrosc. 29, 310 (1975).

63. J.D. Gangei, N.G. Howell, J.R. Roth and G.H. Morrison, Anal. Chem. 48, 505 (1976).

64. T.L. Chester, H. Haraguchi, D.O. Knapp, J.D. Messman and J.D. Winefordner, Appl. Spectrosc. 30, 410 (1976).

65. J.W. Olesik and J.P. Walters, "Multichannel Image Detectors", Ed. Y. Talmi, Vol. 2, Chapt. 2, p. 31, American Chemical Society, Washington, DC (1983).

66. K.W. Busch, N.G. Howell and G.H. Morrison, Anal. Chem. 46, 1231 (1974).

67. T.E. Cook, M.J. Milano and H.L. Pardue, Clin. Chem. 20, 1422 (1974).

68. K.W. Jackson, K.M. Aldous and D.G. Mitchell, Appl. Spectrosc. 28, 569 (1974).

69. K.M. Aldous, D.G. Mitchell and K.W. Jackson, Anal. Chem. 47, 1034 (1975).

70. K.W. Busch, N.G. Howell and G.H. Morrison, Anal. Chem. 46, 2074 (1974).

71. N.G. Howell, J.D. Gangei and G.H. Morrison, Anal. Chem. 48, 319 (1976).

72. R.M. Hoffman and H.L. Pardue, Anal. Chem. 50, 1458 (1978).

73. T.E. Cook, R.E. Santini and H.L. Pardue, Anal. Chem. 49, 871 (1977).

74. R.M. Hoffman and H.L. Pardue, Anal. Chem. 51, 1267 (1979).

75. K.W. Busch, B. Malloy and Y. Talmi, Anal. Chem. 51, 670 (1979).

76. F.L. Fricke, O. Rose, Jr. and J.A. Caruso, Anal. Chem. 47, 2018 (1975).

77. G.P. Weckler, Electronics May, 75 (1967).

78. P.W. Fry, J. Phys. E 8, 337 (1975).

79. S.S. Vogt, R.G. Tull and P. Kelton, Appl. Optics 17, 574 (1978).

80. Application Note 121, E.G. and G. Reticon, Sunnyvale, CA (1979).

81. P.W.J.M. Boumans and G. Brouwer, Spectrochim. Acta **27B**, 247 (1972).

82. P.W.J.M. Boumans, R.F. Rumphorst, L. Willemsen and F.J. de Boer, Spectrochim. Acta **28B**, 227 (1973).

83. G. Horlick and E.G. Codding, Anal. Chem. **45**, 1490 (1973).

84. G. Horlick, Appl. Spectrosc. **30**, 113 (1976).

85. R.W. Simpson, Rev. Sci. Instruments **50**, 730 (1979).

86. R.E. Blank and C.B. Johnson, preprint, Proceedings of SPIE Symposium, San Diego, CA (1980).

87. M. Kubota, Y. Fujishiro and R. Ishida, Spectrochim. Acta. **37B**, 849 (1982).

88. G. Horlick and E.G. Codding, Appl. Spectrosc. **29**, 167 (1975).

89. F.S. Chuang, D.F.S. Natusch and K.R. O'Keefe, Anal. Chem. **50**, 525 (1978).

90. E.G. Codding, J.D. Ingle, Jr. and A.J. Stratton, Anal. Chem. **52**, 2133 (1980).

91. E.G. Codding and G. Horlick, Spectrosc. Lett. **7**, 33 (1974).

92. S.K. Hughes, R.M. Brown, Jr. and R.C. Fry, Appl. Spectrosc. **35**, 396 (1981).

93. F. Grabau and Y. Talmi, "Multichannel Image Detectors", Ed. Y. Talmi, Vol. 2, Chapt. 4, American Chemical Society, Washington, DC (1983).

94. S.W. McGeorge and E.D. Salin, Pittsburgh Conference and Exposition on Analytical Chemistry and Applied Spectroscopy, Atlantic City, NJ, USA, Paper 155 (1982).

95. M. Franklin, C. Baber and S.R. Koirtyohann, Spectrochim. Acta 31B, 589 (1976).

96. T.E. Edmonds and G. Horlick, Appl. Spectrosc. 31, 536 (1977).

97. M.W. Blades and G. Horlick, Spectrochim. Acta 36B, 861 (1981).

98. G. Horlick and M.W. Blades, Appl. Spectrosc. 34, 229 (1980).

99. H. Kawaguchi, T. Ito, K. Ota and A. Mizuike, Spectrochim. Acta 35B, 199 (1980).

100. M.W. Blades and G. Horlick, Spectrochim. Acta 36B, 881 (1981).

101. M.W. Blades and G. Horlick, Appl. Spectrosc. 34, 696 (1980).

102. E.G. Codding and G. Horlick, Appl. Spectrosc. 27, 366 (1973).

103. G. Horlick and E.G. Codding, Anal. Chem. 45, 1749 (1973).

104. K.R. Betty and G. Horlick, Appl. Spectrosc. 32, 31 (1978).

105. G. Horlick, E.G. Codding and S.T. Leung, Appl. Spectrosc. 29, 48 (1975).

106. Y. Talmi, H.P. Sieper and L. Moenke-Bankenburg, Anal. Chim. Acta. 127, 71 (1981).

107. J.W. Carr and G. Horlick, Spectrochim. Acta 37B, 1 (1982).

108. W.S. Boyle and G.E. Smith, Bell Sys. Tech. J. 49, 587 (1970).

109. M.F. Tompsett, W.J. Bertram, D.A. Sealer and C.H. Sequin, Electronics January, 162 (1973).

110. R. Melen, Electronics May, 106 (1973).

111. J.E. Carnes and W.F. Kosonocky, RCA Review 33, 607 (1972).

112. G.F. Amelio, W.J. Betram, Jr. and M.F. Tompsett, IEEE Trans. Electron Dev. ED-18, 986 (1971).

113. K.L. Ratzlaff, Anal. Chem. 52, 916 (1980).

114. M.B. Denton, H.A. Lewis and G.R. Sims, "Multichannel Image Detectors", Ed. Y. Talmi, Vol. 2, Chapt. 6, p.133, American Chemical Society, Washington, DC (1983).

115. H.O. Pritchard, R.W. Nicholls and A. Lakshmi, Appl. Optics **18**, 2085 (1979).

116. G.R. Sims and M.B. Denton, "Multichannel Image Detectors", Ed. Y. Talmi, Vol. 2, Chapt. 5, p. 117, American Chemical Society, Washington, DC (1983).

117. Y. Talmi and K.W. Busch, "Multichannel Image Detectors", Ed. Y. Talmi, Vol. 2, Chapt. 1, p. 1, American Chemical Society, Washington, DC (1983).

118. G.W. Liesegang and P.D. Smith, Appl. Optics 21, 1437 (1982).

119. S.W. McGeorge and E.D. Salin, Spectrochim. Acta 40B, 435 (1985).

120. S.W. McGeorge and E.D. Salin, Spectrochim. Acta 38B, 633 (1983).

121. D.M. Coleman and J.P. Walters, Spectrochim. Acta. 33B, 127 (1978).

122. R.L. Sing and E.D. Salin, Anal. Chem. 56, 2596 (1984).

123. Instruction Manual, Jarrell Ash Co. of Allied Analytical, Waltham MA, Engineering Publication 78-460/1M (1967).

124. E.G.&G. Reticon, Product description for S-series solid state line scanners, Sunnyvale CA, Publication 97250 (1978).

125. Princeton Instruments Inc., Princeton NJ, Product description.

126. Tracor Northern Inc., Middleton WS, Product description.

127. Princeton Applied Research, Princeton NJ, Product description.

128. Operational Instructions for RC-1024SA Evaluation Board, E.G.&G. Reticon Corp., Sunnyvale CA, p. 3 (1978).

129. G. Horlick, personal communication, June 1981.

130. Application Notes for Thermoelectric Devices, Materials Electronic Products Corp., Trenton NJ, (1982).

131. R.L. Sing and E.D. Salin, Talanta 31, 565 (1984).

132. R6500 Microcomputer System Hardware Manual, Rockwell International, Anaheim CA, Chapt. 6 (1978).

133. J. Hubert, personal communication, February 1985.

134. Y. Talmi, personal communication, February 1985.

135. Y. Talmi, Appl. Spectrosc. 36, 1 (1982).

136. J.D. Ingle, Jr., Anal. Chem. 46, 2161 (1974).

137. J.D. Ingle, Jr. and S.R. Crouch, Anal. Chem. 44, 1375 (1972).

138. N.W. Bower and J.D. Ingle, Jr., Anal. Chem. 48 (1976).

139. S.W. McGeorge and E.D. Salin, Spectrochim. Acta, in press (1985).

140. P.W.J.M. Boumans, R.J. McKenna and M. Bosveld, Spectrochim. Acta 36B, 1031 (1981).

141. R.P.J. Duursma, H.C. Smit and F.J.M.J. Maessen, Anal. Chim. Acta Comp. Tech. 133, 393 (1981).

142. R.M. Belchamber and G. Horlick, Spectrochim. Acta 37B, 17 (1982).

143. R.M. Belchamber and G. Horlick, Spectrochim. Acta 37B, 71 (1982).

144. P. Benetti, A. Bonelli, M. Cambiaghi and P. Frigieri, Spectrochim. Acta 37B, 1047 (1982).

145. R.M. Belchamber and G. Horlick, Spectrochim. Acta 37B, 1075 (1982).

146. D.H. Tracy and S.A. Myers, Spectrochim. Acta 37B, 1055 (1982).

147. N.W. Bower and J.D. Ingle, Jr., Anal. Chem. 47, 2069 (1975).

148. H.V. Malmstadt, C.G. Enke and S.R. Crouch, "Electronics and Instrumentation for Scientists", Benjamin Cummings Inc., p. 382 (1981).

149. G. Friedlander, J.W. Kennedy and J.M. Miller, "Nuclear and Radiochemistry", 2nd. Ed., John Wiley and Sons Inc., pp. 174-178 (1964).

150. H. Anderson, H. Kaiser and B. Meddings, International Winter Conference on Developments in Atomic Plasma Spectrochemical Analysis, San Juan, Puerto Rico, paper 65 (1980).

151. L.M. Faires, C.T Apel, T.M. Bieniewski and M.F. López, Pittsburgh Conference and Exposition on Analytical Chemistry and Applied Spectroscopy, paper 150 (1982).

152. D.D. Demers, C.D. Allemand, Anal. Chem. 53, 1915 (1981).

153. S.W. McGeorge and E.D. Salin, Appl. Spectrosc., in press (1985).

154. R.L. Sing, S.W. McGeorge and E.D. Salin, Spectrochim. Acta 30, 805 (1983).

155. D.F. Marino and J.D. Ingle, Jr., Anal. Chem. 53, 645 (1981).

156. AIM 65 Users Guide, Rockwell International, Anaheim CA, Chapt. 8 (1979).

157. R.K. Winge, V.J. Peterson and V.A. Fassel, Appl. Spectrosc. **33**, 206 (1979).

158. M.L. Parsons, A. Forster and D. Anderson, "An Atlas of Spectral Interferences in ICP Spectroscopy", Plenum Press, NY (1980).

159. G.R. Harrison, "MIT Wavelength Tables", John Wiley and Sons, NY (1939).

160. R.M. Barnes and R.F. Jarrell, "Analytical Emission Spectroscopy", Ed. E.L. Grove, Vol. 1, Part 1, Chapt. 4, p. 225, Marcel Dekker Inc., New York, NY (1971).

161. D.E. Montgomery, "Design and Analysis of Experiments", John Wiley and Sons, Toronto, Chapt. 3, pp.55-58 (1976).

162. S. Muldari, Jarrell Ash Corp., Personal communication.

163. E.D. Salin and G. Horlick, Anal. Chem. 51, 2284 (1979).

164. D. Sommer and K. Ohls, Fresenius' Z. Anal. Chem. 97, 304 (1980).

165. M. Thompson, J.E. Goulter and F Sieper, Analyst 106, 32 (1981).

166. A. Aziz, J.A.C. Broeckaert and F. Leis, Spectrochim. Acta **36B**, 251 (1981).

167. H.M. Swaidan and G.D. Christian, Anal. Chem. 56, 120 (1984).

168. Z. Li-Xing, G.F. Kirkbright, M.J. Cope and J.M. Watson, Appl. Spectrosc. 37, 250 (1983).

169. "CRC Handbook of Chemistry and Physics", 53rd Ed., Ed. R.C. Weast, pp. B64-B156, The Cleveland Rubber Co., Cleveland OH (1972-73).

Appendix A - Equipment List

ICP System

ICP generator, model HFP2500D.	Plasma Therm Inc. Route 73 Kresson, NJ
Automatic impedance matching unit, model AMN2500E.	Plasma Therm Inc.
Torch enclosure, model PT2500.	Plasma Therm Inc.

Sample Introduction Systems

MAK nebulizer, spray chamber and torch combination, model 200.	Sherritt Research Analytical Services Fort Saskatchewan, Alta
Meinhard glass concentric nebulizer, model TR-30-C2 and Scott spray chamber.	J E Meinhard Assoc. Inc 1900-J East Warner Ave. Santa Ana, CA.
JA fixed cross-flow nebulizer.	Jarrell Ash Co. Division of Allied Ind. 590 Lincoln St. Waltham, MA.
Direct sample insertion device, laboratory constructed by R.L.A. Sing.	

Optical System

20 cm focal length quartz lens.	
One meter Czerny-Turner monochromator, model 78-462.	Jarrell Ash Co.
1200 groove/mm holographic grating.	American Holographic 8 Harris St. Acton, MA.
Spectrometer mirrors recoated by:	3B Optical 3806 Gibsonia Rd. Gibsonia, PA.
Stepping motor, model M062-FC04.	Superior Electric Co. 38 Torlake Cres. Toronto, Ont.
Drive belt, model 3DCF-130-E.	RPM Mechanical Products 9575 Cote de Liesse Rd. Dorval, Que.
Stepping motor drive unit and logic interface, laboratory constructed using commonly available digital and analog electronic components.	
Neutral density filters.	Melles Girot 1770 Kettering St. Irvine, CA.

Miscellaneous Light Sources

Helium-Neon laser,	Spectra Physics Inc. 1250 West Middlefield Rd Mountainview, CA.
Mercury pen lamp,	Fisher Scientific Ltd. 8505 Devonshire Rd. Montreal, PQ
Hollow cathode lamps,	Perkin Elmer Norwalk, CN.

Photodiode Array Detection System

Linear self-scanning photodiode array, model RL1024S.	E.G.&G. Reticon Corp. 345 Potrero Ave. Sunnyvale, CA.
Photodiode array evaluation board, model RC-1024SA-03, modified in laboratory.	E.G.&G. Reticon Corp.
Instrumentation amplifier, laboratory constructed using AD521KD.	Analog Devices Inc. One Technology Way Norwood, MA.
Temperature monitor, laboratory constructed using AD594CD.	Analog Devices Inc.

Photodiode array interface, laboratory constructed using commonly available Transistor-Transistor Logic (TTL) digital integrated circuits.	
Power supply for photodiode array system, model BAA-40W.	Condor Inc. 4880 Adohr Lane Camarillo, CA.

Photomultiplier Tube Detection System

Photomultiplier tube, model 1P28B	RCA Solid State Div. Lancaster, PA.
High voltage power supply, model 6525A.	Hewlett-Packard Co. Palo Alto, CA.

Miscellaneous Measurement Electronics

Picoammeter, model 410A	Keithly Instruments Inc Cleveland, OH.
Digital multimeter, model 179 TRMS	Keithly Instruments Inc
Oscilloscope, model DM63	Tektronics Canada Ltd. Montreal, PQ.

Computer Systems

AIM 65 single board microcomputer with laboratory built memory expansion and network interface.	Rockwell International 3310 Miraloma Ave. Anaheim, CA.
AIM 65 with: expansion motherboard, EPROM programmer, expansion memory board, expansion I/O board and laboratory built network interface.	Seawell Marketing Inc. P.O. Box 17170 Seattle, WA.
S100 20-slot mainframe with:	Cromemco Inc. 280 Bernardo Ave. Mountainview, CA.
Z80 central processing unit board, model SBC-200.	SD Systems P.O. Box 28810 Dallas, TX.
256 kByte memory board, model Expandoram III.	SD Systems
Disk controller board, model Versafloppy II.	SD Systems
I/O board, model TUART.	Cromemco Inc.
Microangelo graphics board.	Scion Corp. 12310 Pinecrest Rd. Reston, VA.

Dual 8 in. single sided, double density, model 801R.

Shugart
475 Oakmead Parkway
Sunnyvale, CA.

Appendix B - Standard Operating Conditions

Nebulizer Sample Introduction

	Nebulizer System		
	Meinhard	Jarrell-Ash	MAK
Plasma gas flow (L/min)	14	14	8
Auxiliary gas flow (L/min)	0.4	0.4	0.5
Nebulizer pressure (psi)	36	30	200
Liquid uptake rate (ml/min)	1.5	2.2	1.9
Forward power (kW)	1.25	1.25	0.75

Source imaging: 1:1

PMT bias: -600 V

PMT readout: PMT --> Picoammeter --> Instrumentation amplifier (gain of 10) --> Analog to digital converter.

PDA readout: Evaluation board video --> Instrumentation amplifier (gain of 2.3 to 3.7) --> Analog to digital converter.

DSID Sample Introduction

Plasma gas flow: 16 L/min

Auxiliary gas flow: 0.8 L/min

Central channel gas flow: 1.1 L/min

Forward power: 1.75 kW

Source imaging: 1:1

PDA readout: same as above.

Appendix C - Spectrometer Specifications

Focal length: 1.0 meter

Reciprocal linear dispersion at exit slit (first order):

1200 groove/mm - 0.8 nm/mm

Concave mirrors:

Collimating - 6.0 in., slabbed

Camera - 6.0 in., circular

Effective aperture ratio: f/8.7 using 10.2 X 10.2 cm grating.

Spectral range: Zero order to 1600 nm (1200 groove/mm grating).

Drive screw accuracy: 4 in. travel, 1/40 in. pitch error less than +/- 30 micrometers.

Slit assembly: Dual unilateral entrance and exit slits with single ganged micrometer control. Model 78-472.

Appendix D - Spectrometer Drive System

Stepping Motor Specifications

Model number: M062-FC04

Motor type: Slo-Syn dc with 1.8 degree stepping angle.

Accuracy: 3 %.

Time for single step: 2.8 ms with 24 Vdc drive.

Current rating per winding: 1.9 A.

Nominal Resistance per winding: 2.2 Ohms.

Nominal voltage drop per winding: 4.2 V.

Nominal inductance per phase: approximately 5.9 mH.

Torque: 65 ounce-inches.

Steps per revolution:

200 (4 step sequence),

400 (8 step sequence).

Stepping Motor Logic Interface

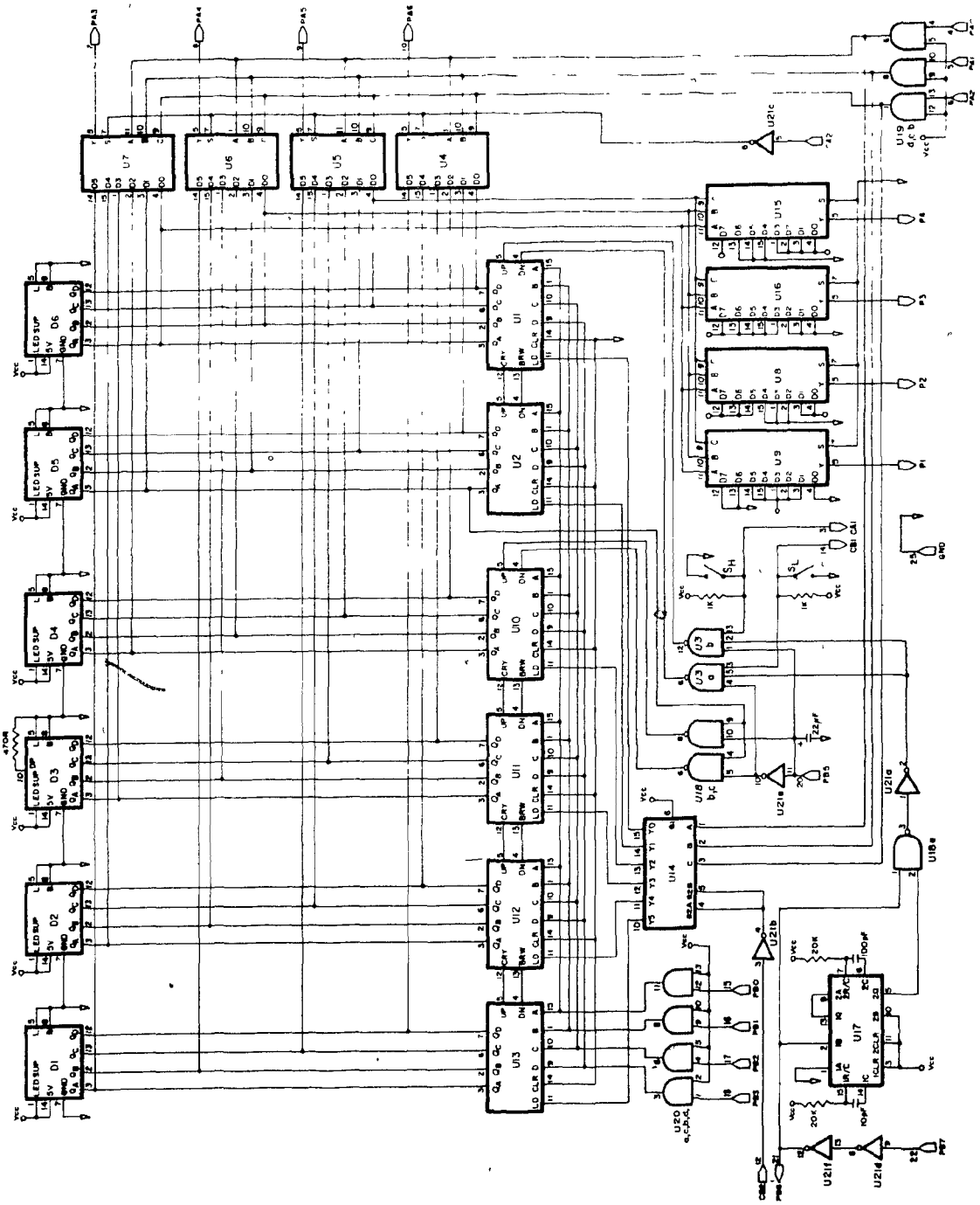

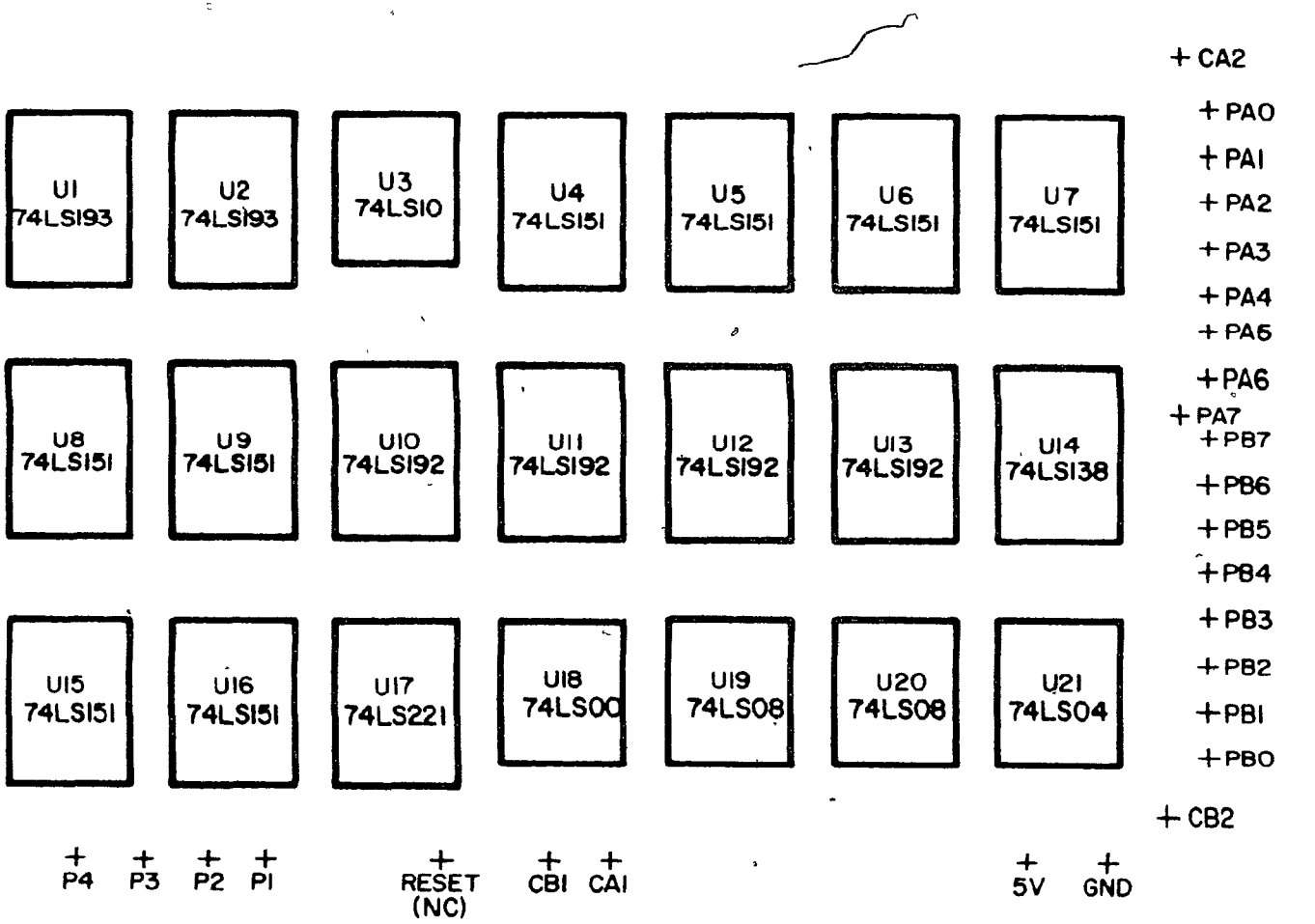

Note: Display (D1-D6)= TIL311

Stepping Motor Drive Unit

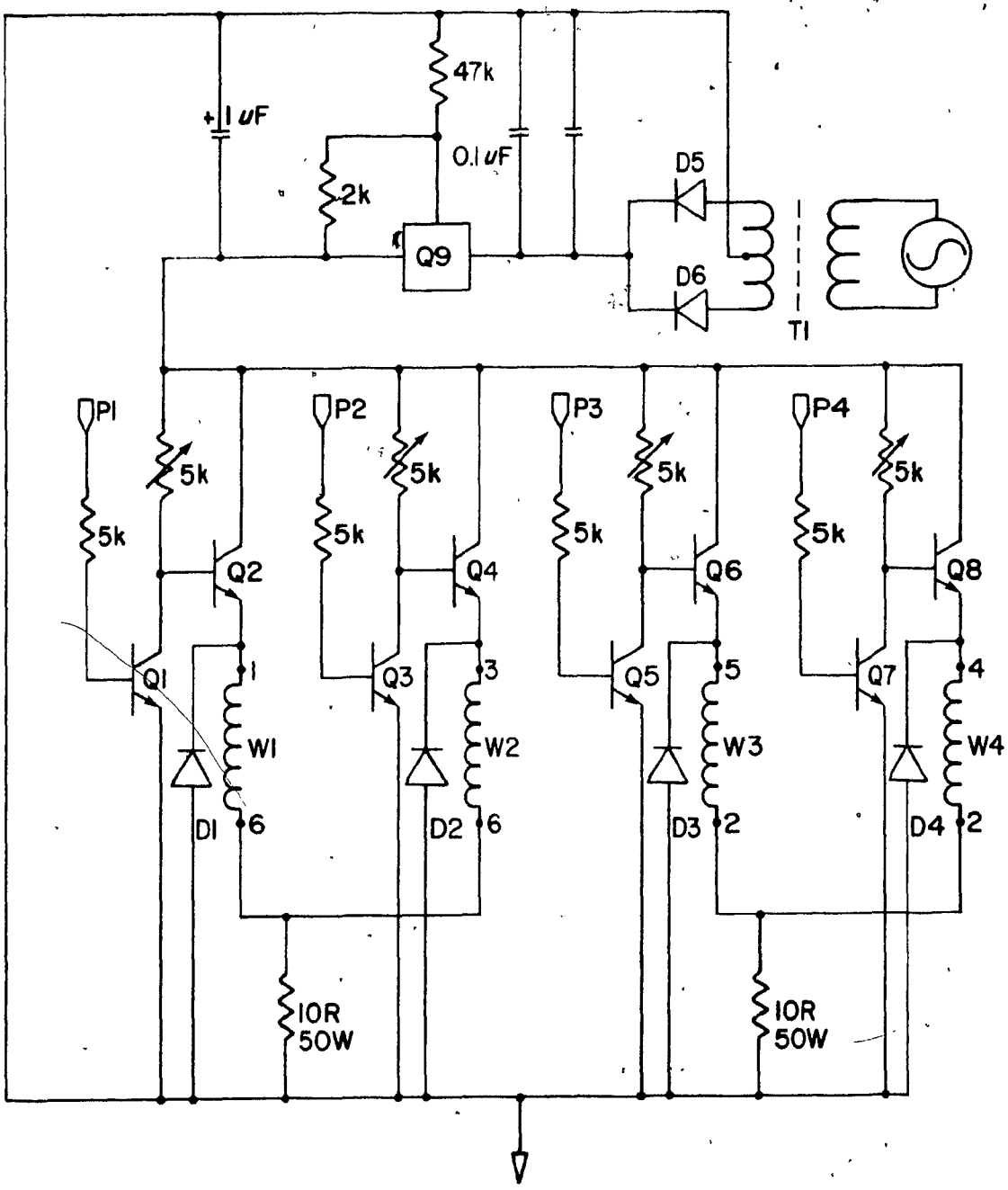

Transformer: Hammond 167P50

Q1, Q3, Q5, Q7: 2N3904

Q2, Q4, Q6, Q8: 2N6101

Q9: LM 350K

Power Transistor Replacement Procedure

From time to time one of the power transistors situated on the drive unit fails. When this happens, or is about to happen, the motor behaves eratically and may actually jam while scanning. The reason for the failure appears to be thermal breakdown, however, the transistors are rated for the current that they conduct during normal operation.

Refer to the drive unit schematic for the remaining discussion.

Troubleshooting:

1. Turn off the stepping motor power supply.
2. Disconnect the motor from the drive unit by unplugging the 9-pin D-type connector.
3. Short pins 1 and 6 using medium gauge wire. This effectively simulates the first motor winding (W1).
4. Connect an oscilloscope probe to the terminal of one of the 50W power transistors where a white wire terminates. The other terminal is ground denoted by the black wire.
5. Turn on the stepping motor power supply.
6. From the AIM keyboard invoke the U (Up) command a few times and view the signal across the power transistor with the oscilloscope. If no signal is present then connect the scope probe to the white terminal of the other power transistor. Adjust the time base and voltage axis of the scope so that a square wave is visible.

7. If a sharp square wave is present then the corresponding power transistor is working properly. If a distorted waveform is observed, then the corresponding power transistor has failed or is about to fail.

8. Repeat steps 3 to 7 shorting pins:

   3 and 6 for transistor 2

   5 and 2 for transistor 3

   4 and 2 for transistor 4.

Do not short more than two pins at a time.

Replacement Procedure

1. Disconnect the drive unit from the rest of the system.
2. Carefully separate the large heat sink from the component board by unscrewing the fastening screws. Note that the small guage wires running from the component board to the power transistors are easily broken.
3. Desolder the 3 wires from the faulty transistor(s). There is a sticker with a number 1 on it beside transistor number 1. The other 3 transistors follow in sequence.
4. Remove the faulty transistor(s) from the heat sink and replace with new components. Take care to replace the electrical insulator on the backside of the new component(s) and apply the minimum amount of thermal compound.
5. Resolder the wires previously removed taking care to observe the correct order.
6. Ensure that the heat sink is electrically insulated from all three transistor terminals. **This is extremely important.**
7. Assemble the drive unit, install, and test using the motor.

8. If the slightest problem is observed when activating the motor, turn off the stepping motor power supply immediately and check all connections.

Appendix E - Electro-Optical Characteristics of PDA

Center-to-center spacing: 25 micrometers

Aperture width: 2.5 mm

Responsivity: 2.8 X 10^{-4} Coul/Joule/cm^2

Non-uniformity of response: +/- 10 %

Saturation exposure: 50 nJoules/cm^2

Saturation charge: 14 pCoul

Average dark current: 5 pAmp

Quantum efficiency at 750 nm: 75 %

Peak spectral response: 750 nm

Spectral response range: 250 - 1000 nm

RC-10248A Evaluation Board Modifications

1. The "even sample" signal was extracted by connecting pin 6 of U7 (5610) to the Y contact on the edge connector.
2. The "odd sample" signal was extracted by connecting pin 5 of U7 to the X contact on the edge connector.
3. The internal clock was disabled by cutting the trace between pins 5 and 10 of U1 (9602). The clock signal from AIM2 was brought in on the W contact of the edge connector and connected to pin 5 of U1.

Appendix F - Technical Data for Peltier Cooling Modules

Stage	Catalog Number	Max. Current (A)	Max. Voltage (V)
2	CP-1.4-71-06L	6.0	8.6
3	CP-1.4-71-10L	3.6	8.6
4	FC-0.6- 8-06L	1.1	0.97

Stage 1 is the water cooled heat sink (see Fig. 2.5). Stage 4 is comprised of 2 elements. Stages 2 and 3 are operated in series as are the two elements of stage 4.

Appendix G – PDA Interface Schematic

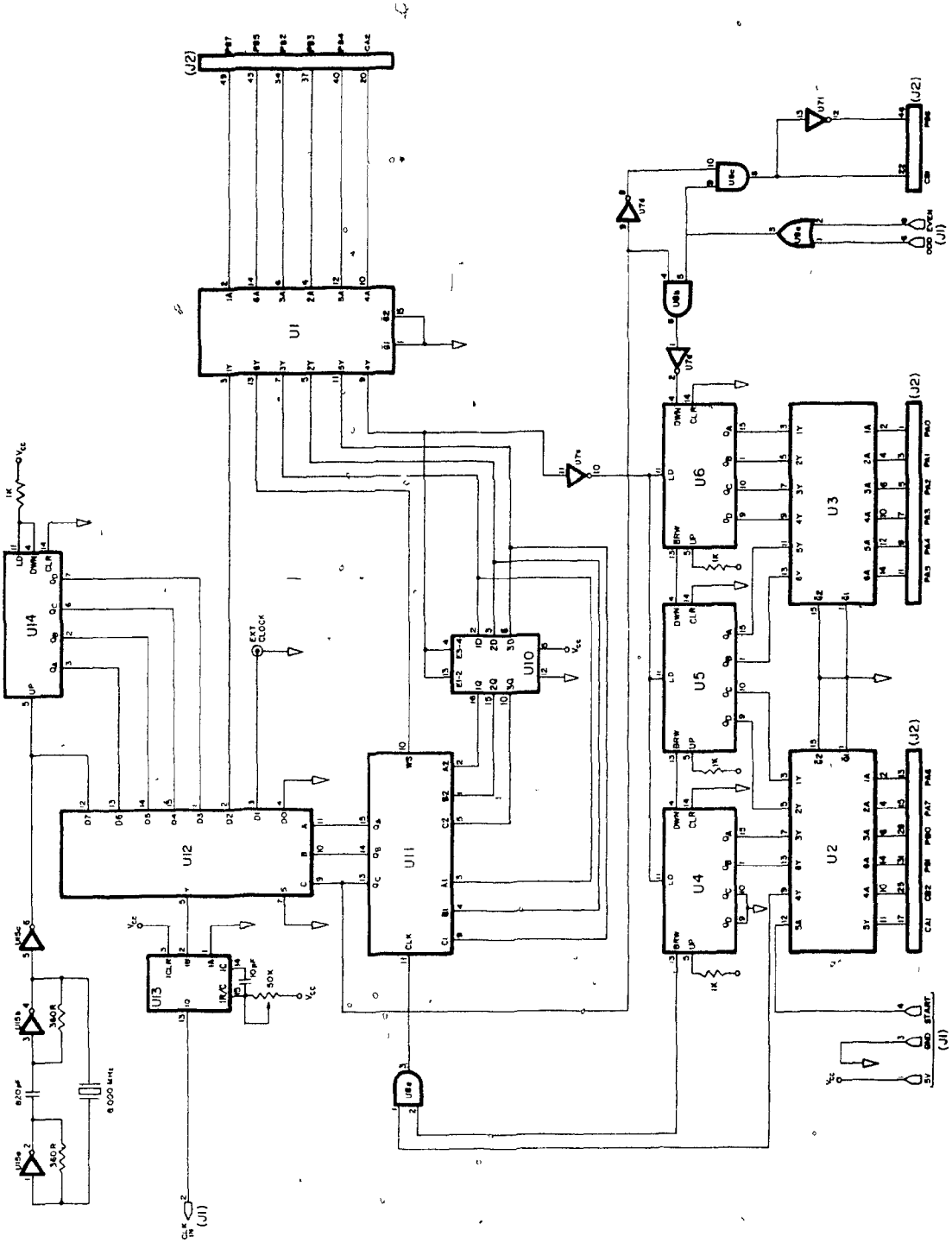

Integrated Circuit Layout - Top View

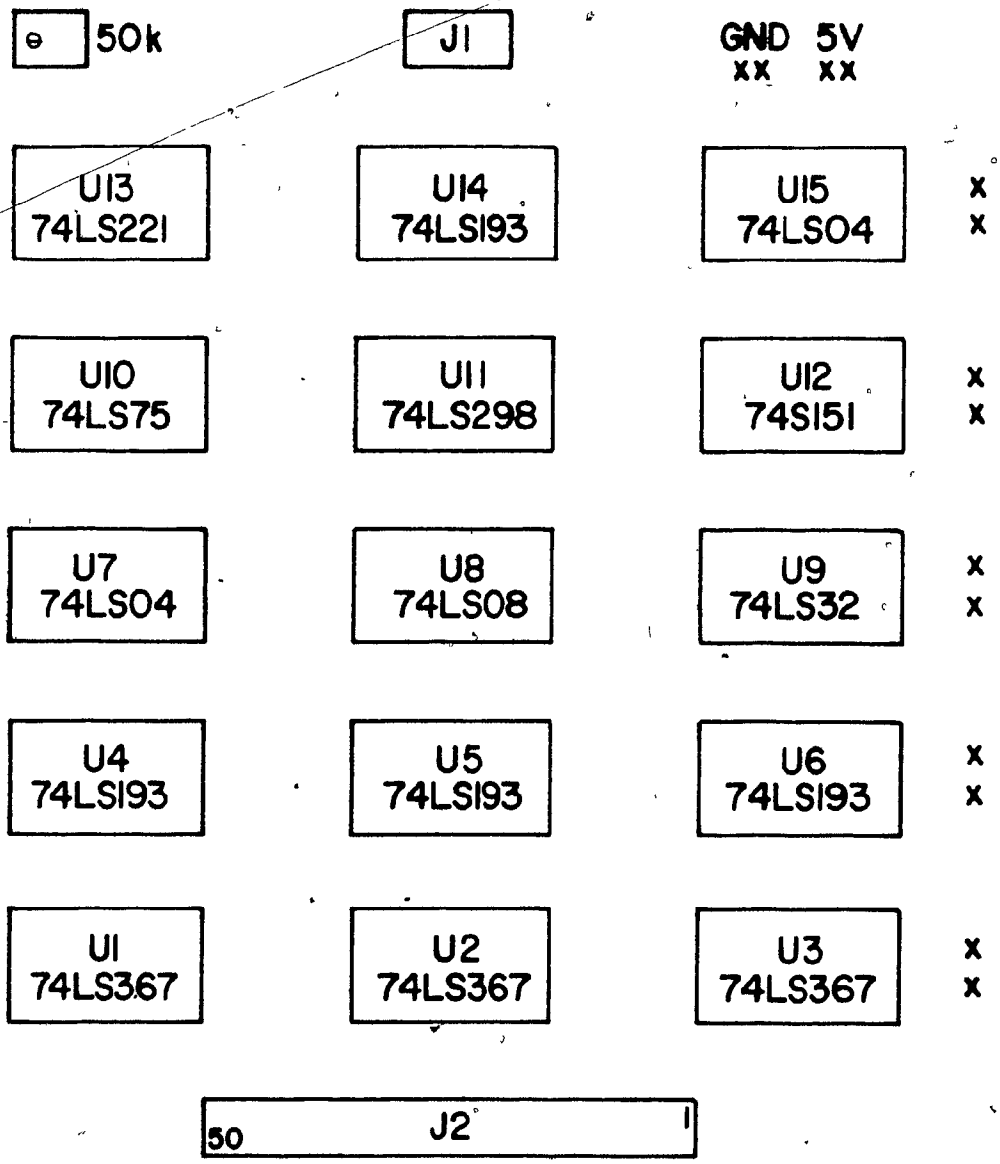

Appendix H - Power Supply Data

The PDA power supply is a commercially available triple output module make by Condor Inc. (see Appendix A). The specifications are listed below.

AC input: 115/230 vac ± 10% 47-440 Hz

DC output: + 5.0 V at 3.0 A

± 12 at 1.0 A or ± 15 at 0.8 A

Line regulation: ± 0.05 % for 10 % input change.

Load regulation: ± 0.05% for a 50% load change.

Output ripple: 3.0 mV Pk-Pk maximim, 0.4 mV RMS.

Overvoltage protection: Set to 6.4 V for 5 V supply.

Set to 33 V for tandem ± 15 V supply.

Schematic for Laboratory Built Cooler Power Supply

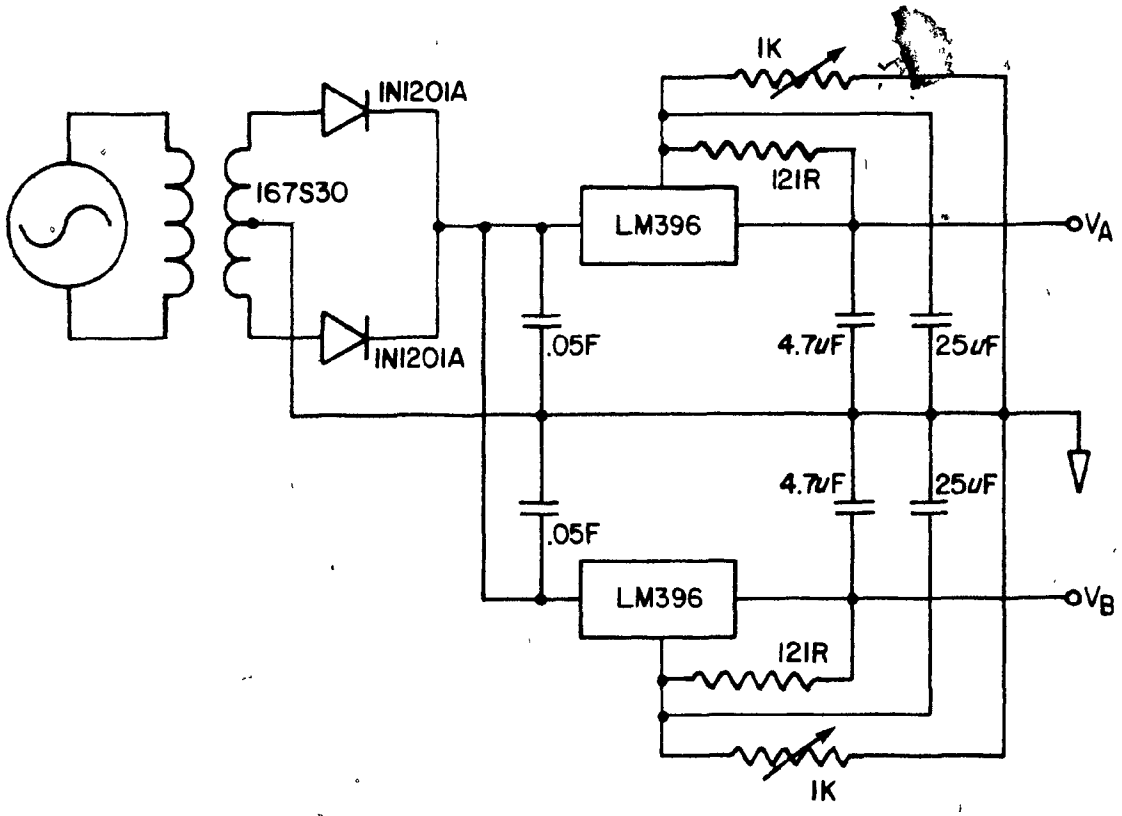

Note: V_A used to drive Stages 2 and 3, V_B used to drive stage 4.

Appendix I - Analog to Digital Converter System

ADC Specifications

Resolution: 12-bits

Nonlinearity error: ± 1/2 LSB

Analog input ranges: -5 to 5V

-10 to 10V

± 5V

± 10V

Power supplies: V_{logic} 4.5 to 5.5V

V_{cc} 13.5 to 16.5V

V_{dd} -13.5 to -16.5V

Power dissipation: 450 MW typ.

Conversion time: 25µSeconds typ.

Analog Multiplexer Specifications

R_{on}: 170 Ω typ.

t_{on}/t_{off}: 0.8 µseconds typ.

Power supplies: ± 17V maximum.

Power dissipation: 450 mW typ.

Analog to Digital Converter Schematic

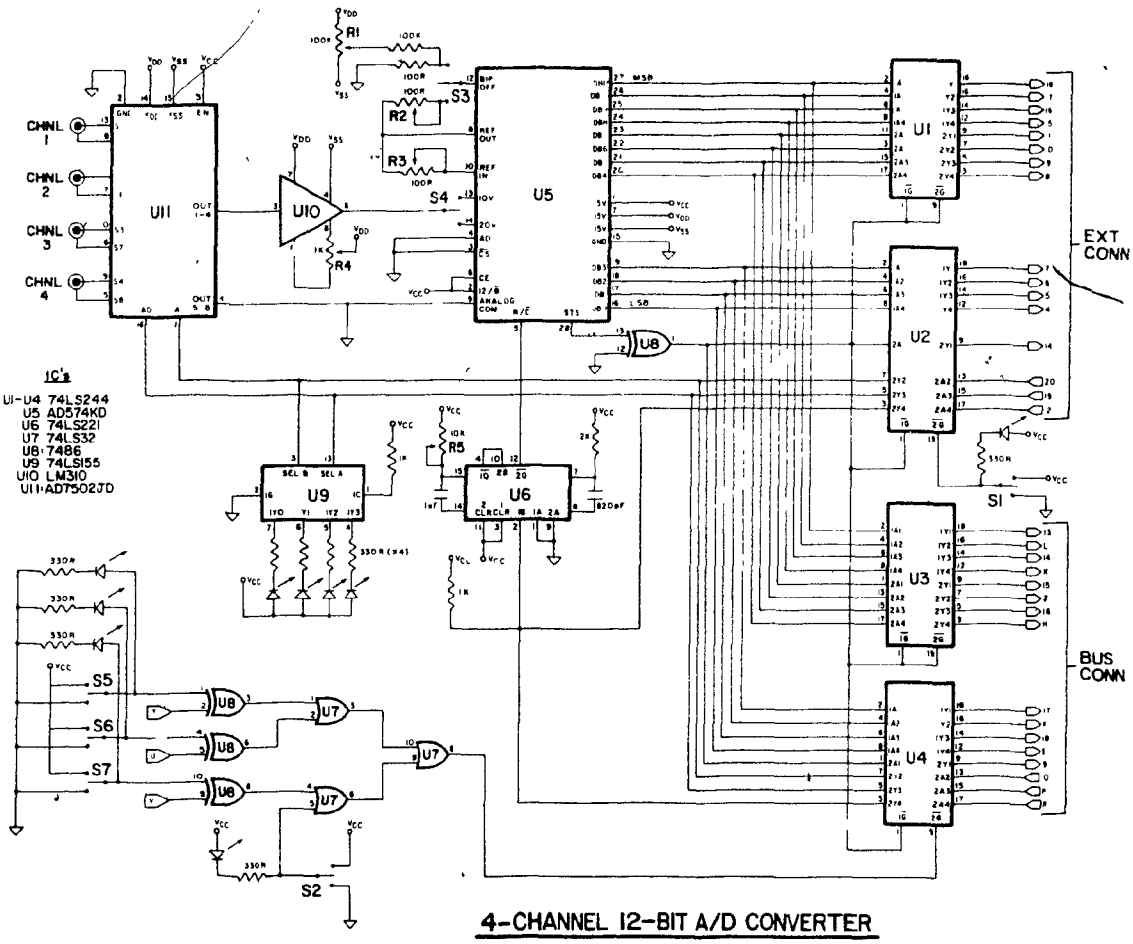

4-CHANNEL 12-BIT A/D CONVERTER

Appendix J - System Software

```
1 REM************************************************************
2 REM
3 REM          PROGRAM: STEPPER.BAS (NOT EXECUTIBLE IN THIS FORM)
4 REM               BY: S.W. MCGEORGE
5 REM             DATE: DEC 1982
6 REM         MODIFIED: AUGUST 1984
7 REM
8 REM     THIS PROGRAM FUNCTIONS AS THE USER INTERFACE TO THE
10 REM STEPPING MOTOR WAVELENGTH DRIVE SYSTEM.  A BRIEF ASSEMBLER
11 REM ROUTINE CALLED PCOUNT.HEX MUST ALSO BE LOADED IF THE "SLEW"
12 REM COMMAND IS TO BE USED.
13 REM
14 REM************************************************************
15 DIM C(6),HB(9),LB(6),DE(9)
16 F2=0                          :REM 0=MOTOR STOPPED 1=MOTOR RUNNING
17 PCR=40972                     :REM PERIPHERAL CONTROL REGISTER
19 TL=40964:TH=40965             :REM TIMER 1 ADDRESSES (LO,HI BYTE)
20 LL=40966:LH=40967             :REM TIMER 1 LATCH ADDRESSES
21 POKE 40962,191                :REM INITIALIZE DATA DIRECTION
                                      REGISTER FOR PORT B
22 POKE 40963,7                  :REM INITIALIZE DATA DIRECTION
                                      REGISTER FOR PORT A
23 POKE PCR,204                  :REM CA1,CB1 TRIGGERED BY NEG. TRANS.
                                      CA2,CB2 HELD LOW (LOAD AND READ
                                      OF COUNTERS DISABLED)

25 INPUT"COUNT UP OR DOWN";A$
30 IF A$="UP" GOTO 45
35 IF A$="DOWN" GOTO 60
40 GOTO 25
45 POKE 40960,32                 :REM POSITIVE SCAN
50 F1=1                               (F1 IS DIRECTION INDICATOR)
55 GOTO 70
60 POKE 40960,0
65 F1=0                          :REM NEGATIVE SCAN
66 S=0                           :REM S INDICATES MOTOR RATE.  EVERY
                                      TIME THE RATE INCREASES BY FACTOR
                                      OF 2, S IS INCREMENTED. S=0 IF
                                      STOPPED.
70 LB(1)=240                     :REM LB(N) ARRAY CONTAINS VALUES TO
71 LB(2)=220                          BE STORED IN LOW BYTE OF TIMER 1
72 LB(3)=200                          LATCH DURING RAMPING PROCESS.
73 LB(4)=180                          THE 16-BIT CONTENTS OF TIMER 1
74 LB(5)=160                          CONTROL THE FREQUENCY OUTPUT
75 LB(6)=140                          ON PB7 AND HENCE THE MOTOR SPEED.
                                      THE RATE DETERMINED BY THE LOW
                                      BYTE CONTENTS IS REFERRED TO AS
                                      THE "MINOR" RATE

80 HB(1)=128
81 HB(2)=64                           HB(N) ARRAY CONTAINS VALUES TO
82 HB(3)=32                           BE STORED IN HIGH BYTE OF TIMER 1
83 HB(4)=16                           LATCH DURING RAMPING PROCESS.
84 HB(5)=8                            THE RATE DETERMINED BY THE HIGH
```

```
85 HB(6)=4                          BYTE CONTENTS IS REFERRED TO AS
86 HB(7)=2                          THE "MAJOR" RATE.
87 HB(8)=1
88 HB(9)=0
90 DE(1)=128                  :REM DE(N) ARRAY CONTAINS THE DELAY
91 DE(2)=64                         VALUES PROVIDING THE PAUSE
92 DE(3)=32                         BETWEEN SPEED CHANGES.  OTHER-
93 DE(4)=16                         WISE RAMP WOULD BE TOO FAST AND
94 DE(5)=8                          PULSES COULD BE MISSED
95 DE(6)=4
96 DE(7)=2
97 DE(8)=1
98 DE(9)=0
100 INPUT"COMMAND";Q$
101 IF Q$="SLEW" THEN GOSUB 3000
102 IF Q$="U" THEN GOSUB 200
103 IF Q$="RESET" THEN GOSUB 4000
104 IF Q$="D" THEN GOSUB 300
105 IF Q$="P" THEN GOSUB 2000
106 IF Q$="S" THEN POKE 40971,32
108 IF Q$="RU" THEN GOSUB 400
110 IF Q$="RD" THEN GOSUB 700
112 IF Q$="C" THEN GOSUB 800
114 IF Q$="Q" THEN STOP
116 IF Q$="L" THEN GOSUB 500
118 IF Q$="R" THEN GOSUB 600
119 IF Q$="SCAN" THEN GOSUB 900
122 GOTO 100
123 REM*************************************************************
124 REM "UP" SUBROUTINE
125 REM
200 IF S<9 GOTO 215
205 PRINT"AT MAX SLEW"
210 GOTO 260
215 IF F2=1 GOTO 250
220 POKE TL,255               :REM IF MOTOR IS NOT RUNNING THEN
225 POKE 40971,224                  LOAD TIMER WITH VALUE
230 POKE TH,HB(1)                   CORRESPONDING TO LOWEST MAJOR
                                    RATE.
235 F2=1                      :REM SET FLAG INDICATING MOTOR ON
240 GOTO 255
250 POKE LH,HB(S+1)           :REM IF MOTOR RUNNING INCREASE SPEED
255 S=S+1                           BY APPROX. FACTOR OF 2 USING
260 RETURN                          MAJOR RATE VALUE.
270 REM*************************************************************
280 REM "DOWN" SUBROUTINE
290 REM
300 IF F2=1 GOTO 315
305 PRINT"MOTOR IS STOPPED"
310 GOTO 345
315 IF S>1 GOTO 335
317 POKE LL,255               :REM IF MOTOR RUNNING AT SLOWEST SPEED
320 POKE 40971,32                   STOP MOTOR (DISABLE FREQ. ON PB7)
325 F2=0                      :REM SET FLAG INDICATING MOTOR OFF
330 GOTO 340
```

```
335 POKE LL,255              :REM IF MOTOR RUNNING AT ANY OTHER
337 POKE LH,HB(S-1)              SPEED THEN DECREASE BY APPROX.
340 IF S>0 GOTO 344              FACTOR OF 2 USING MAJOR RATE
                                 VALUE.
342 S=0 : GOTO 345
344 S=S-1                    :REM SET SPEED INDICATOR FLAG
345 RETURN
350 REM*****************************************************
360 REM "RAMP UP" SUBROUTINE
370 REM
400 IF S<9 GOTO 415
405 PRINT"AT MAX SLEW"
410 GOTO 470
415 IF F2=1 GOTO 445
420 POKE TL,255              :REM IF MOTOR STOPPED, START AT
425 POKE 40971,224               SLOWEST RATE.
430 POKE TH,HB(1)
435 FOR J=1 TO DE(1) : NEXT J    :REM DELAY TO ALLOW A FEW PULSES.
440 F2=1
445 POKE LL,255
447 FOR I=S+1 TO 8           :REM RAMP SPEED TO MAJOR RATE 8.
450 POKE LH,HB(I)                ALLOW PULSES BETWEEN SPEED
455 FOR J=1 TO DE(I) : NEXT J    CHANGES.
460 NEXT I
465 S=8                      :REM SET SPEED INDICATOR FLAG
470 RETURN
480 REM*****************************************************
490 REM "LOAD DISPLAY" SUBROUTINE
495 REM
500 IF F2=0 GOTO 510
505 GOSUB 700                    :REM IF MOTOR RUNNING, RAMP DOWN
510 INPUT"WAVELENGTH(NNN.NNN)";W1
515 C(6)=INT(W1/100)             :REM CALCULATE VALUES TO LOAD
520 C(5)=INT((W1-C(6)*100)/10)       INTO DISPLAY COUNTERS
525 C(4)=INT(W1-C(6)*100-C(5)*10)
530 C(3)=INT((W1-C(6)*100-C(5)*10-C(4))*10)
535 X=INT((W1-C(6)*100-C(5)*10-C(4)-C(3)*0.1)/0.003125)
540 C(2)=INT(X/16)
545 C(1)=INT(X-C(2)*16+0.5)      :REM THE 2 LEAST SIG.FIG. IN HEX
550 FOR I=1 TO 6
555 POKE 40961,(I-1)             :REM LOAD PORT A WITH COUNTER #
560 TEMP=PEEK(40960) AND 32
561 POKE 40960,C(I) OR TEMP      :REM LOAD PORT B WITH VALUE
565 POKE PCR,236
570 POKE PCR,204                 :REM PULSE CB2 TO WRITE COUNTER
575 NEXT I
580 RETURN
590 REM*****************************************************
592 REM "READ DISPLAY" SUBROUTINE
594 REM
600 IF F2=0 GOTO 605
602 GOSUB 700                :REM IF MOTOR RUNNING, RAMP DOWN
605 FOR I=1 TO 6
610 POKE 40961,I-1           :REM LOAD PORT A WITH COUNTER #
612 POKE PCR,206             :REM ENABLE DISPLAY READING USING CA2
```

```
613 TEMP=PEEK(40961) AND 120    :REM READ COUNTER VALUE
614 POKE PCR,204                :REM DISABLE DISPLAY READING
615 C(I)=INT(TEMP/8)            :REM SHIFT BINARY VALUE 3 BITS
620 NEXT I
630 C=INT(C(2)/2)               :REM CALCULATE WAVELENGTH POSITION
635 C(2)=(C(2)-2*C)*16
640 W1=C(6)*100+C(5)*10+C(4)+C(3)*0.1+(C(2)+C(1))*0.003125
645 PRINT"WAVELENGTH=";W1;"NM"
650 RETURN
660 REM*************************************************************
670 REM "RAMP DOWN" SUBROUTINE
680 REM
700 IF F2=1 GOTO 715
705 PRINT"MOTOR STOPPED"
710 GOTO 760
715 IF S>1 GOTO 735
717 POKE LL,255                 :REM IF MOTOR AT SLOWEST SPEED
720 POKE 40971,32                   STOP BY DISABLING FREQ. ON PB7
725 S=0 : F2=0                  :REM SET SPEED AND MOTION FLAGS
730 GOTO 760
735 POKE LL,255
737 FOR I=S-1 TO 1 STEP -1
740 POKE LH,HB(I)               :REM IF MOTOR AT ANY OTHER SPEED THEN
745 FOR J=1 TO DE(I) : NEXT J       RAMP DOWN TO 0 USING APPROPRIATE
750 NEXT I                          DELAYS
755 GOTO 720
760 RETURN
770 REM*************************************************************
780 REM "CHANGE DIRECTION" SUBROUTINE
790 REM
800 IF F2=0 GOTO 811
810 GOSUB 700                   :REM IF MOTOR RUNNING RAMP DOWN
811 GOSUB 605                   :REM READ DISPLAY (CHANGING DIRECTION
                                    CAN CAUSE DISPLAY TO CHANGE)
815 IF F1=1 GOTO 835
820 TEMP=PEEK(40960) AND 255    :REM READ CONTENTS OF PORT A AND
822 TEMP=TEMP OR 32                 CHANGE PB5 FROM 0 TO 1 (NEG.
824 POKE 40960,TEMP                 TO POS. SCAN)
825 F1=1                        :REM SET DIRECTION FLAG
830 GOTO 842
835 TEMP=PEEK(40960) AND 223    :REM READ CONTENTS OF PORT A AND
837 POKE 40960,TEMP                 CHANGE PB5 FROM 1 TO 0
840 F1=0                        :REM SET DIRECTION FLAG
842 GOSUB 515                   :REM RELOAD COUNTERS TO ENSURE CORRECT
                                    DISPLAY READING
845 RETURN
850 REM*************************************************************
860 REM "SCAN" SUBROUTINE
870 REM
900 INPUT"SCAN RATE (NM/S)";R
902 IF R<6.086 GOTO 907
904 PRINT"MAX RATE=6.086"
906 GOTO 900
907 IF R>0.0239 GOTO 910
908 PRINT"MIN RATE=.0239"
```

```
909 GOTO 900
910 N=((3125/R)-3.5)/2          :REM CALCULATE 16-BIT VALUE REQUIRED
920 N=INT(N+0.5)                    TO PRODUCE DESIRED SCANNING RATE
930 NH=INT(N/256)               :REM NEW MAJOR RATE VALUE
940 NL=N-(NH*256)               :REM NEW MINOR RATE VALUE
942 T1=0:T2=0                   :REM T1=MAJOR, T2=MINOR RATE FLAG
950 IF NH=0 GOTO 982            :REM IF NEW RATE >= 9 ...
960 FOR I=1 TO 9
970 IF NH<HB(I) THEN NEXT I     :REM FIND NEW MAJOR RATE FROM HB ARRAY
980 T1=I-1 : GOTO 1020          :REM SET T1=RATE JUST BELOW DESIRED
                                    MAJOR RATE.
982 T1=9                        :REM ELSE SET T1=RATE 9
990 FOR I=1 TO 6                    AND FIND
1000 IF NL<LB(I) THEN NEXT I        NEW MINOR RATE FROM LB ARRAY.
1010 T2=I-1                     :REM SET T2=RATE JUST BELOW DESIRED
                                    MINOR RATE.
1020 T=T1+T2                    :REM T=SUM OF MAJOR AND MINOR RATE
                                    INDICATORS. T WILL BE USED TO
                                    RAMP FROM THE OLD RATE (CURRENT)
                                    TO A RATE NEAR THE NEW RATE. THE
                                    VALUES NH AND NL WILL BE STORED
                                    IN TIMER 1 TO PROVIDE THE NEW
                                    RATE.
1030 IF F2=1 GOTO 1225          :REM IF MOTOR RUNNING ...
1040 IF T>0 GOTO 1090           :REM IF MOTOR STOPPED AND NEW RATE >=
                                    0.0473 ...
1050 POKE TL,NL                 :REM IF MOTOR STOPPED AND NEW RATE IS
1060 POKE 40971,224                 LESS THAN 0.0473 THEN SET NEW
1070 POKE TH,NH                     RATE WITHOUT RAMPING.
1080 GOTO 1560
1090 POKE TL,255                :REM START MOTOR
1100 POKE 40971,224                 AT SLOWEST
1110 POKE TH,255                    SPEED.
1120 FOR I=1 TO T1              :REM RAMP UP
1130 POKE LH,HB(I)                  TO NEW
1140 FOR J=1 TO DE(I) : NEXT J      MAJOR RATE.
1145 NEXT I
1150 IF T2=0 GOTO 1540
1160 FOR I=1 TO T2              :REM FOR RATES > 9,
1170 POKE LL,LB(I)                  RAMP UP
1180 NEXT I                         USING MINOR RATE VALUES.
1200 GOTO 1550
1225 IF T=S GOTO 1380           :REM IF NEW/OLD RATE INDICATORS = ...
1230 IF T>S GOTO 1400           :REM IF NEW RATE > OLD RATE ...
1240 IF S<9 GOTO 1330           :REM IF NEW RATE < OLD RATE AND
                                    OLD RATE < 9 ...
1250 IF T<9 GOTO 1300           :REM IF NEW RATE < OLD RATE AND
                                    NEW RATE < 9 AND
                                    OLD RATE > 9 ...
1260 FOR I=S-9 TO T+1 STEP -1   :REM IF NEW RATE < OLD RATE AND
1270 POKE LL,LB(I)                  NEW RATE > 9 AND
1280 NEXT I                         OLD RATE > 9 RAMP UP USING
                                    MINOR RATE VALUES.
1290 GOTO 1550
1300 FOR I=S-9 TO 1 STEP -1     :REM RAMP DOWN
```

```
1310 POKE LL,LB(I)                    USING MINOR
1320 NEXT I                           RATE VALUES.
1325 S=9
1330 POKE LL,255                 :REM SET MINOR RATE TO MINIMUM
1340 FOR I=S-1 TO T+1 STEP -1    :REM RAMP DOWN TO
1350 POKE LH,HB(I)                    MAJOR RATE JUST
1360 FOR J=1 TO DE(I) : NEXT J        ABOVE NEW RATE.
1365 NEXT I
1370 GOTO 1540
1380 IF S>8 GOTO 1550            :REM IF OLD RATE>8 ADJUST MINOR
1390 GOTO 1540                        RATE ONLY.
1400 POKE LL,255                 :REM ELSE SET MINOR RATE TO MINIMUM,
1410 IF T<9 GOTO 1500                 AND
1420 FOR I=S+1 TO 9                   RAMP UP TO
1430 POKE LH,HB(I)                    RATE 9 USING
1440 FOR J=1 TO DE(I) : NEXT J        MAJOR RATE
1450 NEXT I                           VALUES,
1460 FOR I=1 TO T-9                   THEN RAMP UP
1470 POKE LL,LB(I)                    TO RATE JUST BELOW
1480 NEXT I                           NEW RATE USING MINOR VALUES.
1490 GOTO 1550
1500 FOR I=S+1 TO T              :REM RAMP UP FROM OLD RATE TO JUST
1510 POKE LH,HB(I)                    BELOW NEW RATE
1520 FOR J=1 TO DE(I) : NEXT J        USING MAJOR RATE
1530 NEXT I                           VALUES.
1540 POKE LH,NH                  :REM FINAL ADJUSTMENT OF MAJOR RATE
1550 POKE LL,NL                  :REM FINAL ADJUSTMENT OF MINOR RATE
1560 S=T                         :REM SET SPEED FLAG TO INDICATE NEW
1570 F2=1                             RATE AND SET RUNNING FLAG.
1580 RETURN
1590************************************************************
1592 REM "PULSE SUBROUTINE
1594 REM
2000 INPUT"# OF STEPS";NS
2005 NS=NS-1
2030 IF F2=1 THEN GOSUB 700      :REM IF MOTOR RUNNING, RAMP DOWN
2040 HB=INT(NS/256)              :REM CALCULATE 16-BIT VALUE TO STORE
2050 LB=NS-HB*256                     IN TIMER 2. TIMER 2 COUNTS
                                      PULSES AND WILL BE USED TO
                                      DETERMINE WHEN THE DESIRED # OF
                                      PULSES HAVE BEEN SENT TO MOTOR.
2060 POKE 40968,LB               :REM STORE COUNT
2062 POKE 40969,HB                    IN TIMER 2
2070 POKE TL,255                 :REM START MOTOR
2072 POKE 40971,224                   AT SLOWEST
2074 POKE TH,255                      SPEED.
2080 WAIT 40973,32               :REM WAIT FOR TIMER 2 TO COUNT DOWN
2085 POKE 40971,32               :REM STOP MOTOR
2110 RETURN
2115 REM***********************************************************
2120 REM "SLEW" SUBROUTINE
2130 REM
3000 GOSUB 600                   :REM READ DISPLAY
3010 INPUT"NEW W";W2
3020 DW=W2-W1                    :REM CALCULATE WAVELENGTH DIFFERENCE
```

```
3030 IF DW=0 GOTO 3200
3050 IF DW>0 AND F1=0 THEN GOSUB 800    :REM CHANGE SCAN DIRECTION
3060 IF DW<0 AND F1=1 THEN GOSUB 800        IF NECESSARY.
3070 IF ABS(DW)>0.3 GOTO 3076           :REM IF DIFFERENCE>0.3 NM
                                            THEN SLEW
3072 NS=INT(ABS(DW)*320+0.5)                OTHERWISE CALCULATE
3073 POKE 40971,0                           THE NUMBER OF STEPS
3074 GOSUB 2020: GOTO 3200                  AND USE THE PULSE ROUTINE
3076 IF DW>0 THEN DW=DW-0.3             :REM DECREASE DIFFERENCE BY
3078 IF DW<0 THEN DW=DW+0.3                 0.3 NM (AVOID OVERSHOOT)
3080 NS=INT(ABS(DW)*320+0.5)            :REM CALCULATE # OF STEPS
3100 LAPS=INT(NS/65536)                 :REM CALC. MULTIPLES OF 16-
                                            BITS (TIMER 2 IS 16-BIT
                                            COUNTER)
3110 COUNT=NS-LAPS*65536                :REM LEFTOVER COUNT
3120 HB=INT(COUNT/256)                  :REM BREAK LEFTOVER COUNT INTO
3130 LB=COUNT-HB*256                        LOW AND HIGH BYTE
3140 POKE 254,LAPS+1                    :REM STORE LAPS IN PAGE ZERO.
                                            PCOUNT SUBROUTINE WILL
                                            ACCESS THIS VALUE DURING
                                            SLEW.
3145 POKE 40971,224                     :REM ENABLE SCAN
3150 POKE 40968,LB: POKE 40969,HB       :REM LOAD TIMER 2 WITH
                                            LEFTOVER COUNT. (PROGRAM
                                            COUNTS LEFTOVER FIRST,
                                            THEN MULTIPLES OF 65536)
3170 POKE 4,0: POKE 5,31                :REM ADDRESS OF PCOUNT ROUTINE
3180 GOSUB 415                          :REM RAMP UP USING STD ROUTINE
3190 X=USR(0)                           :REM JUMP TO PCOUNT
3195 GOSUB 715                          :REM RAMP DOWN
3196 GOSUB 600                          :REM READ DISPLAY TO FIND OUT
                                            CURRENT WAVELENGTH
3197 NS=INT(ABS(W2-W1)*320+0.5)-1       :REM CALCULATE # OF STEPS
                                            REQUIRED TO ACHIEVE NEW
                                            POSITION.
3198 GOSUB 2040                         :REM JUMP TO PULSE ROUTINE
3199 W1=W2: GOSUB 515                   :REM ENSURE DISPLAY IS LOADED
                                            WITH CORRECT WAVELENGTH.
3200 RETURN
3990 REM*****************************************************
3992 REM "RESET" ROUTINE
3994 REM
4000 IF F2=1 THEN GOSUB 700     :REM IF MOTOR RUNNING, RAMP DOWN
4010 IF F1=1 THEN GOSUB 800     :REM IF SCAN DIRECTION POSITIVE
                                    CHANGE DIRECTION
4020 R=2.0: GOSUB 910           :REM RAMP TO SCAN RATE OF 2NM/S
4030 WAIT 40973,2               :REM WAIT FOR CB1 TO TRIGGER
                                    INDICATING END OF SINE BAR
                                    TRAVEL.
4040 GOSUB 800                  :REM CHANGE SCAN DIRECTION TO POS.
4045 W1=0: GOSUB 515            :REM LOAD DISPLAY WITH 000.000
4050 RETURN
```

```
;*************************************************************
;
;              PROGRAM: PCOUNT.ASM
;                   BY: S.W. MCGEORGE
;                 DATE: AUGUST 1984
;
;THIS PROGRAM IS USED IN CONJUNCTION WITH STEPPER.BAS ON THE AIM
;USED TO CONTROL THE STEPPER MOTOR.  THIS ROUTINE COUNTS PULSES
;GENERATED BY THE MOTOR WHEN THE "SLEW" FUNCTION IS SELECTED
;
     *=$1F00          ; STARTING ADDRESS
     LDX $FE          ; LOAD X-REG. WITH NUMBER OF LAPS
WAIT LDA $A009        ; WAIT FOR TIMER 2 TO
     ORA $A008        ;  COUNT DOWN LEFTOVER
     BNE WAIT         ;  VALUE LOADED FROM BASIC PGM.
     LDA #$FF         ; LOAD 65536 INTO ACCUMULATOR
     STA $A008        ; STORE 65536 INTO TIMER 2 LOW BYTE
     STA $A009        ; STORE 65536 INTO TIMER 2 HIGH BYTE
     DEX              ; DECREMENT X-REGISTER BY 1
     BNE WAIT         ; IF X-REGISTER <> 0 CONTINUE TO WAIT
     RTS              ; RETURN TO BASIC PROGRAM
     END
```

```
1 REM*************************************************************************
2 REM
3 REM          PROGRAM: PDASYS1B.DOC
4 REM              BY: S.W. MCGEORGE
5 REM            DATE: 1 FEBRUARY 1985 (DOCUMENTATION)
9 REM
10 REM      THIS DOCUMENTATION DESCRIBES THE USER INTERFACE FOR THE
15 REM AIM COMPUTER WHEN THE PDA DETECTOR IS OPERATED UNDER SYSTEM 1.
20 REM THE PROGRAM FILE IS CALLED PDASYS1.BAS.   ROUTINES CALLED BY
22 REM PDASYS1.BAS INCLUDE THE ASSEMBLER PROGRAMS PDAINIT1.ASM,
25 REM CSELECT1.ASM, PDASCAN1.ASM AND PDABLURT.ASM.
30 REM     THE DATA ACQUIRED VIA THE 12-BIT ADC SYSTEM IS TRANSFERRED
35 REM TO THE S100 COMPUTER VIA THE SERIAL NETWORK.  IN ADDITION,
40 REM THIS PROGRAM AND THE ASSEMBLER ROUTINES ARE DOWN LOADED FROM
45 REM THE S100 COMPUTER USING THE NETWORK.  THE ASSEMBLER ROUTINES
45 REM ARE CONCATENATED IN THE FILE PDASYS1.HEX.
46 REM     MOST OF THE PARAMETERS REQUESTED BY THIS PROGRAM ARE STORED IN
47 REM RESERVED PAGE ZERO LOCATIONS (224-255) TO BE ACCESSED BY THE
48 REM ASSEMBLER ROUTINES, SINCE THESE ROUTINES CARRY OUT THE ACTUAL
49 REM FUNCTIONS.
50 REM
55 REM*************************************************************************
60 REM
62 REM MAIN PROGRAM
64 REM
66 INPUT"DATA DISK";D$          :REM DISK TO RECEIVE DATA
68 INPUT"DATE(MONDD)";DATE$     :REM DATE CODE IE. JAN23
70 INPUT"DATA ACQ.(Y/N)";Q$     :REM "Y" FOR ACQUISITION
75 IF Q$="Y" GOTO 100
80 POKE 248,255                 :REM MEM LOCATION 248 IS ACQ. FLAG
90 GOTO 110                     :REM  255 CAUSES INFINITE LOOP WITH
100 POKE 248,0                  :REM  NO DATA TAKEN, 0 TAKES DATA
110 INPUT"# OF PIXELS";P        :REM NUMBER OF DIODES TO READ OUT
120 PH=INT(P/256):PL=P-256*PH   :REM 246,247 ARE HBYTE,LBYTE OF PAGE
130 POKE 246,PL:POKE 247,PH     :REM  ZERO LOCATIONS CONTAINING PIXEL COUNT
140 INPUT"DSID WAIT REQ'D";QD$
150 IF QD$="N" GOTO 190
160 POKE 224,255                :REM MEM LOCATION 224 IS DSID WAIT FLAG
170 GOTO 200                    :REM  255 MEANS WAIT IS REQUIRED, 0 MEANS
190 POKE 224,0                  :REM  NO WAIT REQUIRED
200 POKE4,0:POKE5,32:X=USR(0)   :REM JUMP TO INITIALIZATION ROUTINE (PDAINIT1.ASM)
204 POKE240,8                   :REM MEM LOCATION 240 IS CLOCK CODE !
205 REM                              CODE 8 SELECTS AIM GENERATED CLOCK
206 TMIN=0.108                  :REM MIN. INTEGRATION TIME=.108 SECONDS
208 F=9.615                     :REM  WHEN DEFAULT READOUT FREQ. = 9.615 KHZ
210 REM
530 INPUT"COMMAND";C$           :REM PROMPT FOR COMMAND
540 IF C$="SCAN" THEN GOSUB 600
550 IF C$="BLURT" THEN GOSUB 1410
560 IF C$="CSELECT" THEN GOSUB 2000
580 IF C$="QUIT" THEN STOP
590 GOTO 530
```

```
595 REM*************************************************************
596 REM "SCAN" SUBROUTINE ACQUIRES SPECTRUM AT GIVEN INTEGRATION
597 REM TIME.  INVOKES ROUTINE PDASCAN1.ASM.
598 REM
600 INPUT"INT. TIME(SEC)";IT    :REM ENTER DESIRED INTEGRATION TIME
630 IF IT>TMIN THEN T=(IT-TMIN)*1000:GOTO 680  :REM T=MS EXCEEDING TMIN
640 PRINT"TMIN=";TMIN/1000      :REM IF IT<TMIN ASK USER IF
650 INPUT"CONTINUE";Q$          :REM  TMIN SHOULD BE USED.
660 IF Q$="N" GOTO 600
670 T=0                         :REM T=0 IF TMIN USED
680 IH=INT(T/256)               :REM CONVERT T TO 16-BIT VALUE
690 IL=INT(T-IH*256+.5)         :REM  FOR TIMER2 OF VIA1
700 POKE244,IL:POKE245,IH       :REM MEM LOC. 244,255=LBYTE,HBYTE OF INT. COUNT
710 IF QD$="N" GOTO 760
720 INPUT"DSID WAIT PERIOD (S)";WP      :REM INPUT DSID WAIT IN SECONDS
730 WP=WP*1000                          :REM CONVERT TO MILLISECONDS
740 WH=INT(WP/256): WL=WP-WH*256        :REM STORE 16-BIT VALUE IN PAGE ZERO
750 POKE 225,WL: POKE 226,WH            :REM  LOCATIONS 225,226
760 INPUT"RUN LETTER(A,B,..)";R$
762 REM I COUNTS THE TOTAL NUMBER OF SEQUENTIAL SPECTRA SO THAT THEY MAY BE
764 REM ASSIGNED EXTENSIONS. J = 1 TO 6. WHEN J=6 AVAILABLE MEMORY IS FILLED
766 REM WITH DATA AND MUST BE TRANSMITTED TO S100 VIA NETWORK. BASE IS THE
768 REM FIRST LOCATION OF EACH OF THE 6 AVAILABLE DATA BUFFERS.
770 I=0:J=0:EXT=100:BASE=12288
780 INPUT"SCAN TYPE";SCAN$
790 INPUT"# OF PRESCANS";PS
800 POKE253,PS+1                        :REM STORE # OF PRESCANS IN 253
810 INPUT"PIXELS FOR XFER";PB,PF
820 PB=(PB-1)*2:PF=(PF-1)*2     :REM CONVERT PIXEL POINTERS TO INDEX 12-BIT DATA
830 DVEC=BASE+J*2048            :REM J CONTROLS CURRENT 2048 BYTE DATA BUFFER
840 DH=INT(DVEC/256):DL=DVEC-DH*256     :REM CONVERT BUFFER START ADDRESS TO
850 POKE254,DL:POKE255,DH       :REM 16-BIT VALUE USED BY PDASCAN1.ASM
860 POKE4,0:POKE5,34:X=USR(0)   :REM JUMP TO PDASCAN1.ASM
870 I=I+1:J=J+1
880 IF J>5 THEN GOSUB 960       :REM IF J=6 TRANSFER DATA BUFFERS
890 INPUT"CONTINUE";Q$          :REM ACQUIRE ANOTHER SPECTRUM?
900 IF Q$="Y" GOTO 830
910 IF J=0 GOTO 930
920 GOSUB 960                   :REM TRANSFER REMAINING SPECTRA TO S100
930 RETURN
940 REM*************************************************************************
950 REM SUBROUTINE TO TRANSFER SPECTRA TO S-100 SYSTEM
955 REM
960 FOR K=0 TO J-1              :REM K SELECTS DATA BUFFER
970 FD$=D$+":"+DATE$+"."+R$+RIGHT$(STR$(EXT+K+1),2)     :REM BUILD FILENAME
980 DVEC=BASE+K*2048            :REM SELECT KTH BUFFER
990 POKE4,0:POKE5,122           :REM NETWORK SOFTWARE ADDRESS
1000 Z=USR(0)                   :REM ACTIVATE NETWORK. PRINT CAUSES TRANMISSION
1010 PRINT DATE$;" ";R$;EXT+K-99        :REM SEND HEADER INFORMATION
1020 PRINT F
1030 PRINT SCAN$
1040 PRINT W1
1050 IF IT<TMIN THEN IT=TMIN
1060 PRINT IT
1070 FOR L=PB TO PF STEP 2
```

```
1080 PRINT L/2+1;PEEK(DVEC+L)+PEEK(DVEC+L+1)*256        :REM SEND PIXEL DATA
1090 NEXT L
1100 Z=USR(3):Z=USR(1)          :REM DEACTIVATE NETWORK
1110 NEXT K
1120 J=0                        :REM RESET J WHEN ALL SPECTRA TRANSMITTED
1130 EXT=EXT+I                  :REM INCREMENT EXTENSION NUMBER
1140 RETURN
1150 REM*************************************************************************
1160 REM BLURT SUBROUTINE
1170 REM
1410 INPUT"BLURT FREQ.(MHZ)";BF                 :REM SELECT BLURT FREQ. AND
1420 IF BF=1 THEN POKE 241,56: GOTO 1470        :REM  STORE CODE AT LOCATION
1430 IF BF=.5 THEN POKE241,52: GOTO 1470        :REM  241 OF PAGE ZERO
1440 IF BF=.25 THEN POKE 241,48: GOTO 1470
1450 PRINT BF;"IS NOT A BLURT FREQ."
1460 GOTO 1410
1470 INPUT"RUN LETTER";R$
1480 INPUT"SCAN TYPE";SCAN$
1490 INPUT"# OF BLURT REPS";BR          :REM # OF CONSECUTIVE BLURT READOUTS
1500 IF BR>48 GOTO 1490                 :REM  CANNOT EXCEED 48
1510 POKE 243,BR                        :REM STORE BLURT COUNT AT LOCATION 243
1520 INPUT"PEAK DIODE";PD
1530 INPUT"# OF DIODES TO ACQ.";ND      :REM 16 TO 128 DIODES SURROUNDING
1540 IF ND>128 GOTO 1530                :REM  PEAK CAN BE ACQUIRED.  NORMALLY
1550 IF ND<15 GOTO 1530                 :REM  16 CHOSEN FOR FASTEST READOUT
1560 NP=PD+INT(ND/2+.5)
1570 PH=INT(NP/256): PL=NP-PH*256       :REM CALCULATE LBYTE,HBYTE PIXEL COUNT
1580 POKE 246,PL: POKE 247,PH           :REM  AND STORE AT 246,247
1590 B=1035-ND                  :REM B IS NUMBER OF PIXELS TO BLURT OVER
1600 BH=INT(B/256): BL=B-BH*256 :REM CALCULATE LBYTE,HBYTE BLURT COUNT
1610 POKE 249,BL: POKE 250,BH   :REM  AND STORE AT 249,250
1620 POKE 251,0                 :REM 251 CONTAINS INDEX TO DATA BUFFER
1630 POKE 254,0: POKE 255,48    :REM 254,255=LBYTE,HBYTE ADDRESS OF DATA BUFFER
1640 POKE 252,ND                :REM ND IS NUMBER OF DIODES TO ACQUIRE
1650 POKE 4,0: POKE 5,35        :REM LBYTE,HBYTE ADDRESS OF PDABLURT.ASM
1660 X=USR(0)                   :REM JUMP TO PDABLURT.ASM
1670 DVEC=12288                 :REM DVEC POINTS TO BEGINNING OF DATA BUFFER
1680 EXT=100                    :REM INITIALIZE EXTENSION
1690 FOR I=1 TO BR              :REM I COUNTS THE # OF BLURT REPETITIONS
1700 FD$=D$+":"+DATE$+"."+R$+RIGHT$(STR$(EXT+I),2)      :REM BUILD FILENAME
1710 POKE 4,0: POKE 5,122       :REM LBYTE,HBYTE ADDRESS OF NETWORK SOFTWARE
1720 Z=USR(0)                   :REM ACTIVATE NETWORK
1730 SCAN$="BLURT"              :REM TRANSFER HEADER INFORMATION
1740 PRINT DATE$
1750 PRINT BF*1000
1760 PRINT SCAN$
1770 PRINT W1
1780 IT=0
1790 PRINT IT                   :REM SEND DUMMY INT. TIME (NOT USED)
1800 D=PD-INT(ND/2)
1810 FOR J=DVEC TO DVEC+(ND-1)*2 STEP 2
1820 PRINT D;PEEK(J)+PEEK(J+1)*256      :REM TRANSFER PIXEL DATA
1830 D=D+1
1840 NEXT J
1850 DVEC=DVEC+256              :REM EACH BLURT DATA BUFFER CONSISTS OF 256 LOC.
```

```
1860 Z=USR(3): Z=USR(1)          :REM DEACTIVATE NETWORK
1870 NEXT I
1880 INPUT"REPEAT";Q$            :REM BLURT AGAIN?
1890 IF Q$="Y" GOTO 1410
1900 RETURN
1910 REM*************************************************************************
1920 REM CSELECT SUBROUTINE TO CHANGE READOUT FREQUENCY
1930 REM
2000 INPUT"READOUT FREQ(KHZ)";F$         :REM INPUT FREQ AS STRING
2010 FLAG=0
2020 IF VAL(F$) < 125 GOTO 2100
2030 IF F$="1000" THEN POKE 240,24 : GOTO 2200  :REM COMPARE DESIRED FREQ.
2040 IF F$="500" THEN POKE 240,20 : GOTO 2200   :REM TO AVAILABLE XTAL
2050 IF F$="250" THEN POKE 240,16 : GOTO 2200   :REM  CONTROLLED VALUES
2060 IF F$="125" THEN POKE 240,12 : GOTO 2200
2070 IF F$="EXT" THEN POKE 240,4 : GOTO 2200    :REM NOT CONNECTED
2080 IF F$="GND" THEN POKE 240,0 : GOTO 2200    :REM FOR STOPPED CLOCK INT.
2090 GOTO 2000
2100 F=VAL(F$)           :REM CONVERT STRING TO NUMBER
2110 FLAG=1
2120 N=INT(125/F-1.5)    :REM IF FREQ IS WITHIN RANGE OF PB7 VALUES CALCULATE
2130 IF N>=0 GOTO 2160   :REM  NUMBER TO BE PLACED IN TIMER1 OF VIA3
2140 PRINT "FREQ NOT AVAILABLE"
2150 GOTO 2000
2160 IF N > 255 GOTO 2140
2170 POKE 242,N          :REM STORE NUMBER CORRESPONDING TO DESIRED FREQ. AT 242
2180 F=125/(N+2)         :REM DETERMINE ACTUAL FREQUENCY TO BE OUTPUT
2190 POKE 240,8          :REM CLOCK CODE 1 SELECTS PB7 AS PDA CLOCK SOURCE
2200 IF FLAG=1 GOTO 2220
2210 F=VAL(F$)
2220 PRINT "ACTUAL READOUT RATE = ";F;"KHZ"      :REM PRINT ACTUAL READOUT RATE
2230 IF F <= 10 GOTO 2290
2240 PRINT"READOUT RATE IS TOO" :REM READOUT RATES HIGHER THAN 10 KHZ CANNOT
2250 PRINT"FAST FOR DATA ACQ."  :REM  BE USED FOR DATA ACQUISITION
2260 INPUT"CONTINUE (Y/N)";Q$   :REM IF HIGHER RATE STILL DESIRED, ENTER "Y"
2270 IF Q$ = "Y" GOTO 2290      :REM  OTHERWISE INPUT ANOTHER READOUT FREQ.
2280 GOTO 2000
2290 POKE 4,0: POKE 5,33         :REM LBYTE,HBYTE ADDRESS OF CSELECT1.ASM
2300 X=USR(0)                    :REM JUMP TO CSELECT1.ASM
2310 TMIN=1038/(F*1000)          :REM CALCULATE TMIN FOR NEW READOUT RATE
2320 RETURN
2325 REM*************************************************************************
2330 END
```

```
;*************************************************************
;
;              PROGRAM: PDAINIT1.ASM
;                   BY: S.W. MCGEORGE
;                 DATE: 29 OCTOBER 1984 (MODIFIED)
;
;    THIS PROGRAM INITIALIZES THE PDA AT FOR A READOUT RATE OF
; 10 KHZ.
;
;*************************************************************
;
       * = $2000       ;PROGRAM START AT $2000
;
; VIA REGISTER LOCATIONS
;
       T1CL1 = $9004
       T1CH1 = $9005
       ACR1  = $900B
;
       DDRB2 = $9012
       DDRA2 = $9013
       ACR2  = $901B
       PCR2  = $901C
;
       DRB3  = $9020
       DDRB3 = $9022
       DDRA3 = $9023
       T1CL3 = $9024
       T1CH3 = $9025
       ACR3  = $902B
       PCR3  = $902C
;
; INITIALIZE VIA 2 FUNCTIONS
;
       LDA    #$B0
       STA    DDRB2  ;PB0-3 FOR INPUT, PB4,5 FOR OUTPUT.
       AND    #00
       STA    DDRA2  ;PORT A FOR INPUT.
       LDA    #$A0
       STA    PCR2   ;CB2 TO GENERATE CONVERT PULSE.
       LDA    #$03
       STA    ACR2   ;ENABLE AUTO LATCHING.
;
; INITIALIZE VIA 3 FUNCTIONS
;
       LDA    #$FF
       STA    DDRA3  ;PA0-7 FOR OUTPUT
       LDA    #$BF
       STA    DDRB3  ;PB0-5 FOR OUTPUT
       LDA    #$E0
       STA    ACR3   ;PB6 FOR PULSE COUNTING, PB7 CLOCK GEN.
       LDA    #$BC
       STA    PCR3   ;CA2 SET LOW,CB2 PULSE MODE
       LDA    #$0B
       STA    T1CL3
```

```
        LDA     #$00
        STA     TC1H3   ;START 9.615 KHZ CLOCK ON PB7
        LDA     #$08
        STA     DRB3    ;SELECT PB7 AS CLOCK SOURCE
;
; INITIATE VIA #1 FOR GENERATION AND COUNTING OF 1 MS INTERRUPTS
;
        LDA     #$E0
        STA     ACR1    ;PB7 TO GENERATE 1 MS INTERRUPTS
        LDA     #$F2    ;PB6 TO COUNT INTERRUPTS
        STA     TC1L1
        LDA     #$01
        STA     TC1H1   ;START PULSES
;
        RTS
        END
```

```
;*********************************************************
;
;              PROGRAM: PDASCAN1.ASM
;                  BY: S.W. MCGEORGE
;                DATE: 17 MAY 1984
;
;     THIS PROGRAM IS CALLED BY PDASYS1.BAS WHICH ACTS
; AS THE USER INTERFACE.  THE PROGRAM DETECTS A START PULSE,
; COUNTS OUT A USER SPECIFIED NUMBER OF DIODES, TURNS OFF THE
; READOUT CLOCK FOR A USER SPECIFIED INTEGRATION TIME, AND
; FINALLY READS OUT THE PDA PERFORMING 12-BIT A/D CONVERSION.
;
;*********************************************************
;
; VIA REGISTER LOCATIONS
;
       TC2L1 = $9008   ; T2 OF VIA1 COUNTS 1 MS INTEGRATION
       TC2H1 = $9009   ;  PULSES FOR STOPPED CLOCK MODE.
       ACR1  = $900B   ;
       IFR1  = $900D   ;
;
       DRB2  = $9010   ; PORT B CONN. TO 12-BIT ADC
       DRA2  = $9011   ; PORT A   "  "   "    "
       IFR2  = $901D   ;
;
       DRB3  = $9020   ; PORT B CONN. TO PDA LOGIC
       DRA3  = $9021   ; PORT A  "   "  "   "
       TC2L3 = $9028   ; T2 OF VIA3 COUNTS SAMPLE PULSES
       TC2H3 = $9029   ;  GENERATED BY PDA
       IFR3  = $902D   ;
;
; PAGE ZERO LOCATIONS
;
       CC1   = $F0     ; CLOCK CODE (PB2,3,4)
       INTL  = $F4     ; LOW BYTE OF INTEGRATION COUNT
       INTH  = $F5     ; HIGH  "  "      "       "
       PIXLO = $F6     ; LOW BYTE - NUMBER OF PIXELS TO READOUT
       PIXHI = $F7     ; HIGH BYTE    "   "            "
       RFLAG = $F8     ; REPEAT FLAG (=0 FOR ACQ, =$FF FOR LOOP)
       PSCAN = $FD     ; NUMBER OF PRESCANS BEFORE DATA ACQUISITION
       DATA  = $FE     ; LOW BYTE FOR INDIRECT INDEXED ADDRESSING
                       ;  TO DATA VECTOR ($FF CONTAINS HIGH BYTE)
       * = $2200
;
       LDY    #00      ; INITIALIZE Y INDEX REGISTER
       LDX    PSCAN    ; LOAD X REG. WITH # OF PRESCANS
;
       LDA    DRA3     ;CLEAR CA1 FLAG
STRT1  LDA    IFR3
       AND    #$02
       BEQ    STRT1    ;WAIT FOR FIRST START PULSE
       LDA    DRA3     ;CLEAR CA1 FLAG
;
       LDA    PIXLO
       STA    TC2L3
```

```
        LDA     PIXHI
        STA     TC2H3   ;LOAD TC2 VIA3 WITH PIXEL COUNT
;
SCAN1   LDA     IFR3
        AND     #$20
        BEQ     SCAN1   ;CHECK FOR END OF READOUT
;
        LDA     DRB3
        AND     #$E3    ;SELECT CLOCK CODE 000 (GND)
        STA     DRB3    ;STOP CLOCK
;
        LDA     INTL
        STA     TC2L1
        LDA     INTH
        STA     TC2H1   ;LOAD TIMER 2 VIA1 WITH INTEGRATION COUNT
;
INT     LDA     IFR1
        AND     #$20
        BEQ     INT     ;WAIT FOR END OF INTEGRATION PERIOD
;
        LDA     DRB3
        ORA     CC1
        STA     DRB3    ;RESTART CLOCK FOR READOUT PERIOD
;
        LDA     RFLAG
        AND     #$FF
        BNE     STRT1   ;IF RFLAG > 0, LOOP INDEFINITELY
;
        DEX
        BNE     STRT1   ;IF X>0 RE-SCAN
;
STRT2   LDA     IFR3
        AND     #$02
        BEQ     STRT2   ;WAIT FOR SECOND START PULSE
        LDA     DRA3    ;CLEAR CA1 FLAG
;
        LDA     PIXLO
        STA     TC2L3
        LDA     PIXHI
        STA     TC2H3   ;LOAD TC2 VIA3 WITH PIXEL COUNT
;
SAMPL   LDA     IFR3
        AND     #$10
        BEQ     SAMPL   ;WAIT FOR A SAMPLE PULSE (PIXEL READOUT)
        STA     IFR3    ;CLEAR CB1 FLAG
;
        AND     #00
        STA     DRB2    ;TRIGGER CONVERSION ON CHANNEL 1 OF ADC
CONV    LDA     IFR2
        AND     #$10
        BEQ     CONV    ;WAIT FOR END OF CONVERSION
;
        LDA     DRA2
        STA     (DATA),Y
        INY
```

```
        LDA     DRB2
        AND     #$0F
        STA     (DATA),Y ;STORE DIGITIZED PIXEL VALUE.
        INY
        BNE     CONT    ; CONTINUE IF WITHIN CURRENT PAGE-
        INC     DATA+1  ; OTHERWISE, TURN PAGE.
CONT    LDA     IFR3
        AND     #$20
        BEQ     SAMPL   ; CHECK FOR END OF SCAN
        RTS
        END
```

```
;*************************************************************
;
;      PROGRAM: CSELECT1.ASM
;           BY: S.W. MCGEORGE
;         DATE: 13 MARCH 1984
;     MODIFIED: 8 APRIL 1984
;
;    THIS ROUTINE IS CALLED BY PDASYS1.BAS THE USER INTERFACE
; FOR SYSTEM 1 OPERATION OF THE PDA.  THIS ROUTINE READS THE
; CLOCK CODE AND SELECTS THE CORRESPONDING CLOCK SOURCE FOR
; READING OUT THE PDA.
;
;*************************************************************
;
       * = $2100        ; PROGRAM START AT $2100
;
       DRB3   = $9020  ; PORT B (VIA 3) LOCATION
       TL1L3  = $9026  ; TIMER 1 LOW BYTE LATCH LOCATION
       CC1    = $F0    ; VARIABLE "CLOCK CODE 1"
       TC1VAL = $F2    ; LOCATION OF TIMER 1 LOW BYTE FREQ COUNT
;
; PERFORM CLOCK SELECT SEQUENCE
;
       LDA     TC1VAL
       STA     TL1L3   ; LOAD TIMER 1 LOW LATCH WITH FREQ COUNT
       LDA     CC1
       STA     DRB3    ; SELECT CLOCK USING CB2 AUTO PULSE MODE
;
       RTS             ; RETURN TO CALLING PROGRAM
;
       END
```

```
;*********************************************************
;
;              PROGRAM: PDABLURT.ASM
;                   BY: S.W. MCGEORGE
;                 DATE: 1 OCTOBER 1984
;
;    THIS ROUTINE IS CALLED FROM PDASYS1.BAS WHEN THE USER
; SELECTS THE BLURT MODE OF OPERATION.  THE USER SUPPLIES
; THE PEAK POSITION, THE NUMBER OF DIODES TO ACQUIRE, AND
; THE BLURT FREQUENCY.  WHEN THIS ROUTINE IS ACTIVATED IT
; SETS UP THE CLOCK MUX LATCH AND LOADS THE BLURT COUNTERS
; WITH THE BLURT COUNT.
;     THE PDA IS READ OUT AT NORMAL RATE UNTIL THE LAST
; DIODE IN THE PEAK SEQUENCE IS REACHED.  THE BLURT
; CLOCK IS SWITCHED IN AND UNWANTED INFORMATION IS BLURTED.
; WHEN SAMPLE PULSES ARE GENERATED ONCE MORE, BLURT IS
; FINISHED AND THE ROUTINE ACQUIRES THE DIODES OF INTEREST.
;
;*********************************************************
;
; VIA REGISTER LOCATIONS
;
       DRB2  = $9010   ; PORT B CONN. TO 12-BIT ADC
       DRA2  = $9011   ; PORT A   "   "    "    "
       IFR2  = $901D   ;
;
       DRB3  = $9020   ; PORT B CONN. TO PDA LOGIC
       DRA3  = $9021   ; PORT A   "   "   "   "
       TC2L3 = $9028   ; T2 OF VIA3 COUNTS SAMPLE PULSES
       TC2H3 = $9029   ;  GENERATED BY PDA
       PCR3  = $902C   ; PCR OF VIA3
       IFR3  = $902D   ;
;
; PAGE ZERO LOCATIONS
;
       CC1   = $F0     ; CLOCK CODE 1 (PB2,3,4 - NORMAL OPERATION)
       CC2   = $F1     ; CLOCK CODE 2 (PB2,3,4 - BLURT OPERATION)
       REPS  = $F3     ; # OF SEQUENTIAL BLURTS
       PIXLO = $F6     ; LOW BYTE - NUMBER OF PIXELS TO READOUT
       PIXHI = $F7     ; HIGH BYTE    "    "            "
       BCLO  = $F9     ; BLURT COUNT LOW BYTE
       BCHI  = $FA     ; BLURT COUNT HIGH ORDER 2 BITS (TOTAL=10)
       INDEX = $FB     ; INDEX INTO DATA VECTOR
       ACQU  = $FC     ; ACQUISITION DIODE COUNT
       DATA  = $FE     ; LOW BYTE FOR INDIRECT INDEXED ADDRESSING
                       ;  TO DATA VECTOR ($FF CONTAINS HIGH BYTE)
       * = $2300
;
       LDY     INDEX   ; INITIALIZE Y INDEX REGISTER
       LDA     #$FC
       STA     PCR3    ; CB2=1 (DISABLE CB2 PULSE MODE)
       LDA     BCLO
       STA     DRA3    ; LOAD BLURT COUNT LOW BYTE
       LDA     BCHI
       ORA     CC2
```

```
        STA     DRB3    ; LOAD BLURT COUNT HI BITS OR'D WITH CC2
;
        LDA     #$FE
        STA     PCR3    ; CA2=1
        LDA     #$FC
        STA     PCR3    ; CA2=0, LOAD MUX LATCH AND BLURT COUNTERS
;
        LDA     CC1
        TAX             ; SAVE CC1 IN CPU FOR FAST ACCESS LATER
;
        LDA     DRA3    ; CLEAR CA1 FLAG
STRT1   LDA     IFR3
        AND     #$02
        BEQ     STRT1   ; WAIT FOR FIRST START PULSE
        LDA     DRA3    ; CLEAR CA1 FLAG
;
        LDA     PIXLO
        STA     TC2L3
        LDA     PIXHI
        STA     TC2H3   ; LOAD TC2 VIA3 WITH PIXEL COUNT
;
SCAN1   LDA     IFR3
        AND     #$20
        BEQ     SCAN1   ; CHECK FOR END OF READOUT
;
BLURT   LDA     #$DC
        STA     PCR3    ; SWITCH TO BLURT CLOCK
        LDA     #$FC
        STA     PCR3    ; CB2=1 (RETURNED TO NORMALLY HIGH POSITION)
;
        TXA             ; RELOAD CC1 AND SET -
        STA     DRB3    ;  WORD SELECT=0 FOR RETURN TO READOUT FREQ.
        LDX     ACQU    ; X REGISTER COUNTS ACQUISITION DIODES
;
SAMPL   LDA     IFR3
        AND     #$10
        BEQ     SAMPL   ; WAIT FOR A SAMPLE PULSE (PIXEL READOUT) -
                        ;  FIRST PULSE IS END OF BLURT
        STA     IFR3    ; CLEAR CB1 FLAG
        AND     #00
        STA     DRB2    ; TRIGGER CONVERSION ON CHANNEL 1 OF ADC
CONV    LDA     IFR2
        AND     #$10
        BEQ     CONV    ; WAIT FOR END OF CONVERSION
;
        LDA     DRA2
        STA     (DATA),Y
        INY
        LDA     DRB2
        AND     #$0F
        STA     (DATA),Y ; STORE DIGITIZED PIXEL VALUE.
        INY
CONT    DEX
        BNE     SAMPL   ; CHECK FOR END OF ACQUISITION
        DEC     REPS
```

```
        BEQ     DONE    ; IF REPS=0 BLURT FINISHED
        LDA     CC1
        TAX
        LDA     BCHI    ;  ELSE, LOAD COUNTERS AGAIN
        ORA     CC2
        STA     DRB3
        LDA     #$FE
        STA     PCR3
        LDA     #$FC
        STA     PCR3    ; LOAD MUX LATCH AND BLURT COUNTERS
        INC     DATA+1
        LDY     INDEX
        JMP     BLURT   ; RE-BLURT
;
DONE    RTS
        END
```

```
10 REM          PROGRAM: PDAPLOT.ASC
20 REM               BY: S.W. MCGEORGE
30 REM             DATE: 15 AUGUST 1984
35 REM           REV 2: 13 SEPTEMBER 1984
36 REM           REV 3: 24 SEPTEMBER 1984
40 REM
50 REM     THIS PLOTTING PACKAGE IS USED TO PLOT PDA SPECTRA USING
60 REM THE MICROANGELO HARDWARE ON THE VIDEO SCREEN AND THE PRINTER.
70 REM REFER TO THE MENU'S PRODUCED AT RUN TIME FOR FURTHER INFO.
80 REM
100 REM DECLARE PLOT ROUTINE ADDRESSES
110 MOVE=&HA031:   DRAW=MOVE+3:   IMOVE=DRAW+3:   IDRAW=IMOVE+3
120 PLOT=IDRAW+3:  XAXIS=PLOT+3:  YAXIS=XAXIS+3: LABEL=YAXIS+3
130 CPLOT=LABEL+3: CDRAW=CPLOT+3: GCLEAR=CDRAW+3:DEFAULT=GCLEAR+3
140 ERAS=DEFAULT+3:SCALE=ERAS+3:  XHAIR=SCALE+3:  XMOVE=XHAIR+3
150 HAIROF=XMOVE+3:PIXON=HAIROF+3:CDES=PIXON+3:   INIT=CDES+3
160 HAPO=INIT+3:   MX80=HAPO+3
170 DEFINT Z
172 DIM ZSPEC1(1024),ZSPEC2(1024)
175 WIDTH 255
180 REM ASSIGN DEFAULT PLOTTING VALUES
190 TITLE$="": DFN1$="": DFN2$="": DIS$="S": PP$="ON": BG$="OFF"
200 XMIN=1: XMAX=1024: YMIN=0: YMAX=4095
210 REM ASSIGN ASCII DECIMAL CODES
220 VT=11: FF=12: CR=13: DC1=17: DC2=18: ESC=27: FS=28: TILDE=126
230 REM DEFINE MAIN MENU MESSAGES
240 DIM MSG1$(6)
250 MSG1$(1)="CHANGE PLOTTING PARAMETERS"
260 MSG1$(2)="VIDEO PLOT"
270 MSG1$(3)="PRINTER PLOT"
280 MSG1$(4)="SAVE SPECTRA"
290 MSG1$(5)="SUBTRACT SPECTRA (1-2)"
300 MSG1$(6)="AVERAGE SPECTRA"
310 GOSUB 1000  :REM OUTPUT MAIN MENU
315 VCX=0: VCY=23: GOSUB 2000
320 END
998 REM*****************************
999 REM SUBROUTINE TO OUTPUT MAIN MENU
1000 PRINT CHR$(TILDE);CHR$(FS);CHR$(TILDE);CHR$(DC2);:REM CLEAR,HOME
1002 VCX=0: VCY=0: GOSUB 2000
1004 PRINT"TYPE 'ESC' TO RETURN TO SUPERVISOR PROGRAM";
1010 VCX=36: VCY=5: YTEMP=0
1020 GOSUB 2000 :REM POSITION CURSOR
1040 PRINT"MAIN MENU";
1050 VCX=28: VCY=7
1060 FOR I=1 TO 6
1070 GOSUB 2000: PRINT MSG1$(I);: REM PRINT MAIN MENU
1080 VCY=VCY+1
1090 NEXT I
1100 VCX=27: VCY=7: GOSUB 2000: REM CURSOR TO START OF MAIN MENU
1110 C$=INPUT$(1)
1120 IF C$="" GOTO 1110 ELSE IF ASC(C$)=TILDE THEN C$=INPUT$(1)
1125 C=ASC(C$)
1126 IF C=ESC THEN RETURN
1130 IF C=CR GOTO 1200: REM CHECK FOR CR
```

```
1160 IF C<>FF GOTO 1170
1161 IF VCY=7 THEN VCY=12 ELSE VCY=VCY-1
1162 GOSUB 2000: GOTO 1110: REM SCROLL UP OR WRAP
1170 IF C<>VT GOTO 1110
1171 IF VCY=12 THEN VCY=7 ELSE VCY=VCY+1
1172 GOSUB 2000: GOTO 1110: REM SCROLL DOWN OR WRAP
1200 IF VCY=7 THEN GOSUB 3000: GOTO 1000: REM CHANGE PLOT PARMS
1210 IF VCY=8 THEN GOSUB 4000: GOTO 1000: REM VIDEO PLOT
1220 IF VCY=9 THEN CALL MX80: GOTO 1000: REM PRINTER PLOT
1225 IF VCY=10 THEN GOSUB 5000: GOTO 1000: REM SAVE SPECTRA
1230 IF VCY=11 THEN GOSUB 6000: GOTO 1000: REM SUBTRACT SPECTRA
1240 IF VCY=12 THEN GOSUB 7000: GOTO 1000: REM AVERAGE SPECTRA
1260 VCX=0: VCY=0: GOSUB 2000
1270 PRINT"MENU SELECT ERROR"
1280 GOTO 1000
1998 REM**********************
1999 REM CURSOR POSITIONING SUBROUTINE
2000 IF VCX>=0 OR VCX<=79 GOTO 2030
2010 GOSUB 8018: GOSUB 2000
2020 PRINT"VCX ERROR": GOTO 2055
2030 IF VCY>=0 OR VCY<=23 GOTO 2060
2040 GOSUB 8018: GOSUB 2000
2050 PRINT"VCY ERROR"
2055 FOR I=1 TO 71: PRINT" ": NEXT I: STOP
2060 IF VCX>31 GOTO 2080
2070 XPOS=VCX+96: GOTO 2090
2080 XPOS=VCX
2090 YPOS=VCY+96
2100 PRINT CHR$(TILDE);CHR$(DC1);CHR$(XPOS);CHR$(YPOS);
2110 RETURN
2998 REM**********************
2999 REM SUBROUTINE TO CHANGE PLOT PARMS
3000 PRINT CHR$(TILDE);CHR$(FS);CHR$(TILDE);CHR$(DC2);
3002 VCX=0: VCY=0: GOSUB 2000
3004 PRINT"TYPE 'ESC' TO RETURN TO MAIN MENU";
3010 VCX=30: VCY=5: GOSUB 2000
3020 PRINT"PLOTTING PARAMETERS";
3030 VCY=7: GOSUB 2000
3040 PRINT"TITLE OF PLOT      : ";TITLE$;
3050 FOR I=1 TO 27-LEN(TITLE$): PRINT" ";: NEXT I
3060 VCY=VCY+1: GOSUB 2000
3070 PRINT"DISPLAY (S OR D)   : ";DIS$;
3080 VCY=VCY+1: GOSUB 2000
3090 PRINT"X-SCALE (DMIN,DMAX): ";
3091 PRINT RIGHT$(STR$(XMIN),LEN(STR$(XMIN))-1);",";STR$(XMAX);
3100 VCY=VCY+1: GOSUB 2000
3102 PRINT"Y-SCALE (YMIN,YMAX): ";
3104 TEMP=LEN(STR$(YMIN))
3106 IF YMIN>=0 THEN TEMP=TEMP-1
3111 PRINT RIGHT$(STR$(YMIN),TEMP);",";STR$(YMAX);
3112 VCY=VCY+1: GOSUB 2000
3113 PRINT "POINT PLOT (ON/OFF): ";PP$;" ";
3114 VCY=VCY+1: GOSUB 2000
3116 PRINT"BAR GRAPH (ON/OFF) : ";BG$;" ";
3118 VCY=VCY+1: GOSUB 2000
```

```
3120 PRINT"DATA FILE NAME 1   : ";DFN1$;"                ";
3130 VCY=VCY+1: GOSUB 2000
3140 PRINT"DATA FILE NAME 2   : ";DFN2$;"                ";
3150 VCX=50: IF YTEMP=0 THEN VCY=7 ELSE VCY=YTEMP
3155 GOSUB 2000
3160 C$=INPUT$(1)
3165 IF C$="" THEN GOTO 3160 ELSE IF ASC(C$)=TILDE THEN C$=INPUT$(1)
3170 C=ASC(C$)
3180 IF C=CR GOTO 3260
3190 IF C<>FF GOTO 3220
3200 IF VCY=7 THEN VCY=14 ELSE VCY=VCY-1
3210 GOSUB 2000: GOTO 3160
3220 IF C<>VT GOTO 3250
3230 IF VCY=14 THEN VCY=7 ELSE VCY=VCY+1
3240 GOSUB 2000: GOTO 3160
3250 IF C=ESC THEN RETURN
3260 IF VCY>7 GOTO 3300
3270 GOSUB 8018
3280 INPUT"TITLE OF PLOT: ",TITLE$
3290 GOTO 3000
3300 IF VCY>8 GOTO 3340
3310 IF DIS$="S" THEN DIS$="D" ELSE DIS$="S"
3320 YTEMP=8
3330 GOTO 3000
3340 IF VCY>9 GOTO 3380
3350 GOSUB 8018
3360 INPUT"X-SCALE (DMIN,DMAX): ",XMIN,XMAX
3370 GOTO 3000
3380 IF VCY>10 GOTO 3420
3390 GOSUB 8018
3400 INPUT"Y-SCALE (YMIN,YMAX): ",YMIN,YMAX
3410 GOTO 3000
3420 IF VCY>11 GOTO 3460
3430 IF PP$="ON" THEN PP$="OFF" ELSE PP$="ON"
3440 YTEMP=11
3450 GOTO 3000
3460 IF VCY>12 GOTO 3500
3470 IF BG$="ON" THEN BG$="OFF" ELSE BG$="ON"
3480 YTEMP=12
3490 GOTO 3000
3500 IF VCY>13 GOTO 3540
3510 GOSUB 8018
3512 INPUT"DATA FILE NAME 1: ",DFN1$
3514 CLOSE#1
3515 FOR I=1 TO 1024: ZSPEC1(I)=0: NEXT I
3516 OPEN "I",1,DFN1$
3518 INPUT#1,DATE1$,F1,SCAN1$,N1,IT1
3520 INPUT#1,D,TEMP
3521 I=0: ISTART=0: ZSPEC1(I)=TEMP
3522 WHILE NOT EOF(1)
3524 I=I+1
3526 INPUT#1,D,ZSPEC1(I)
3528 WEND
3529 CLOSE#1
3530 NP1=I
```

```
3532 VCX=0: VCY=23: GOSUB 2000
3534 PRINT NP1;" POINTS FOUND IN FILE ";DFN1$;
3535 FOR I=1 TO 500: NEXT I
3536 IF SKIP=1 GOTO 3542
3538 GOTO 3000
3540 GOSUB 8018
3542 INPUT"DATA FILE NAME 2: ",DFN2$
3544 CLOSE#2
3545 FOR I=1 TO 1024: ZSPEC2(I)=0: NEXT I
3546 OPEN "I",2,DFN2$
3548 INPUT#2,DATE2$,F2,SCAN2$,W2,IT2
3550 INPUT#2,D,TEMP
3551 I=D: ZSPEC2(I)=TEMP
3552 WHILE NOT EOF(2)
3554 I=I+1
3556 INPUT#2,D,ZSPEC2(I)
3558 WEND
3559 CLOSE#2
3560 NP2=I
3562 VCX=0: VCY=23: GOSUB 2000
3564 PRINT NP2;" POINTS FOUND IN FILE ";DFN2$;
3565 FOR I=1 TO 500: NEXT I
3566 IF SKIP=1 THEN SKIP=0: RETURN: REM RETURN TO SUBTRACT ROUTINE
3568 GOTO 3000
3998 REM*******************************
3999 REM VIDEO PLOT SUBROUTINE
4000 CALL GCLEAR
4010 XDIFF=XMAX-XMIN
4020 XTICK=XDIFF/10
4030 LEFT=XMIN-.07*XDIFF
4040 RIGHT=XMAX+.05*XDIFF
4050 IF DIS$="D" THEN YMAX=YMAX*2-YMIN
4060 YDIFF=YMAX-YMIN
4070 IF DIS$="D" THEN YTICK=YDIFF/20 ELSE YTICK=YDIFF/10
4080 TOP=YMAX+.05*YDIFF
4090 BOTTOM=YMIN-.05*YDIFF
4100 CALL SCALE(LEFT,RIGHT,BOTTOM,TOP)
4110 CALL XAXIS(YMIN,XTICK,XMIN,XMAX)
4120 X=XMIN: Y=BOTTOM
4130 FOR I=1 TO 11
4140 CALL MOVE(X,Y)
4150 X$=STR$(X)
4160 A=INSTR(X$,"."): IF A>0 THEN X$=MID$(X$,2,A-2)
4170 CX=LEN(X$)/-2: CY=0
4180 CALL CPLOT(CX,CY): CALL LABEL(X$)
4190 X=X+XTICK
4200 NEXT I
4210 CALL YAXIS(XMIN,YTICK,YMIN,YMAX)
4220 YMID=YMIN+YDIFF/2
4230 IF DIS$="D" THEN CALL XAXIS(YMID,XTICK,XMIN,XMAX)
4240 X=XMIN: Y=YMIN
4250 CY=-.5: F=1
4260 FOR I=1 TO 11-F
4270 CALL MOVE(X,Y)
4280 IF F=1 THEN Y$=STR$(Y) ELSE Y$=STR$(Y-YDIFF/2)
```

```
4290 A=INSTR(Y$,"."): IF A>0 THEN Y$=MID$(Y$,2,A-2)
4300 CX=-LEN(Y$): CALL CPLOT(CX,CY)
4310 CALL LABEL(Y$)
4320 Y=Y+YTICK
4330 NEXT I
4340 IF F=0 GOTO 4355
4350 IF DIS$="D" THEN F=0: Y=YMID: GOTO 4260
4355 IF TITLE$="" GOTO 4400
4360 X=LEFT+(RIGHT-LEFT)/2: Y=TOP
4370 CALL MOVE(X,Y)
4380 CX=-LEN(TITLE$)/2: CY=-1
4390 CALL CPLOT(CX,CY): CALL LABEL(TITLE$)
4400 X=RIGHT: Y=YMAX: CX=-25: CY=-1
4410 GOSUB 4880
4420 S$="FILE: "
4430 CALL LABEL(S$): CALL LABEL(DFN1$)
4440 CY=CY-1: GOSUB 4880
4450 S$="DATE: ": CALL LABEL(S$): CALL LABEL(DATE1$)
4460 CY=CY-1: GOSUB 4880
4470 S$="FREQ.: ": CALL LABEL(S$)
4480 S$=STR$(F1): CALL LABEL(S$)
4490 CY=CY-1: GOSUB 4880
4500 S$="SCAN TYPE: ": CALL LABEL(S$): CALL LABEL(SCAN1$)
4510 CY=CY-1: GOSUB 4880
4520 S$="STARTING W.L.: ": CALL LABEL(S$)
4530 S$=STR$(W1): CALL LABEL(S$)
4535 CY=CY-1: GOSUB 4880
4540 S$="INT. TIME: ": CALL LABEL(S$)
4550 S$=STR$(IT1): CALL LABEL(S$)
4560 IF DIS$="S" GOTO 4730
4570 Y=YMID: CY=-1
4580 GOSUB 4880
4590 S$="FILE: ": CALL LABEL(S$): CALL LABEL(DFN2$)
4600 CY=CY-1: GOSUB 4880
4610 S$="DATE: ": CALL LABEL(S$): CALL LABEL(DATE2$)
4620 CY=CY-1: GOSUB 4880
4630 S$="FREQ.: ": CALL LABEL(S$)
4640 S$=STR$(F2): CALL LABEL(S$)
4650 CY=CY-1: GOSUB 4880
4660 S$="SCAN TYPE: ": CALL LABEL(S$): CALL LABEL(SCAN2$)
4670 CY=CY-1: GOSUB 4880
4680 S$="STARTING W.L.: ": CALL LABEL(S$)
4690 S$=STR$(W2): CALL LABEL(S$)
4700 CY=CY-1: GOSUB 4880
4710 S$="INT. TIME: ": CALL LABEL(S$)
4720 S$=STR$(IT2): CALL LABEL(S$)
4730 FOR I=XMIN TO XMAX
4740 IF DIS$="D" GOTO 4790
4750 Y=ZSPEC1(I)
4760 IF PP$="ON" THEN CALL PIXON(I,Y)
4770 IF BG$="ON" THEN CALL MOVE(I,YMIN): CALL DRAW(I,Y)
4780 GOTO 4850
4790 IF PP$="OFF" GOTO 4820
4800 Y1=YMID-YMIN+ZSPEC1(I): Y2=ZSPEC2(I)
4810 CALL PIXON(I,Y1): CALL PIXON(I,Y2)
```

```
4820 IF B6$="OFF" GOTO 4850
4830 CALL MOVE(I,YMID): CALL DRAW(I,Y1)
4840 CALL MOVE(I,YMIN): CALL DRAW(I,Y2)
4850 NEXT I
4860 IF DIS$="D" THEN YMAX=(YMAX+YMIN)/2
4861 IF SFLAG=0 GOTO 4870
4862 X=XMIN: Y=0
4864 CALL MOVE(X,Y)
4866 X=XMAX
4868 CALL DRAW(X,Y)
4869 SFLAG=0
4870 RETURN
4880 CALL MOVE(X,Y)
4890 CALL CPLOT(CX,CY)
4900 RETURN
4998 REM*******************************
4999 REM SUBROUTINE TO SAVE SPECTRA
5000 VCX=0: VCY=14: GOSUB 2000
5010 INPUT"SAVE 1,2 OR BOTH";Q$
5020 IF Q$="1" GOSUB 5100: GOTO 5060
5030 IF Q$="2" GOSUB 5200: GOTO 5060
5040 IF Q$="BOTH" GOSUB 5100: GOSUB 5200: GOTO 5060
5050 GOTO 5000
5060 RETURN
5100 INPUT"USE CURRENT FNAME";Q$
5102 IF Q$="Y" THEN FO$=DFN1$: GOTO 5106
5104 INPUT"OUTPUT FNAME (D:FN.EXT)";FO$
5106 OPEN"O",3,FO$
5110 PRINT#3,DATE1$
5120 PRINT#3,F1
5130 PRINT#3,SCAN1$
5140 PRINT#3,W1
5150 PRINT#3,IT1
5160 FOR I=XMIN TO XMAX
5170 PRINT#3,XMIN+I-1,ZSPEC1(I)
5180 NEXT I
5190 CLOSE#3
5195 RETURN
5200 INPUT"USE CURRENT FNAME";Q$
5202 IF Q$="Y" THEN FO$=DFN2$: GOTO 5206
5204 INPUT"OUTPUT FNAME (D:FN.EXT)";FO$
5206 OPEN"O",3,FO$
5210 PRINT#3,DATE2$
5220 PRINT#3,F2
5230 PRINT#3,SCAN2$
5240 PRINT#3,W2
5250 PRINT#3,IT2
5260 FOR I=XMIN TO XMAX
5270 PRINT#3,XMIN+I-1,ZSPEC2(I)
5280 NEXT I
5290 CLOSE#3
5295 RETURN
5998 REM*******************************
5999 REM SUBROUTINE TO SUBTRACT SPECTRA
6000 VCX=0: VCY=14: GOSUB 2000
```

```
6010 INPUT"USE CURRENT SPECTRA";Q$
6020 IF Q$="Y" GOTO 6040
6030 SKIP=1: GOSUB 3512
6080 VCX=0:VCY=0
6090 IF F1=F2 GOTO 6140
6095 GOSUB 2000
6100 PRINT"READOUT FREQ. MISMATCH          "
6110 PRINT"F1=";F1;" AND ";"F2=";F2
6120 INPUT"CONTINUE";Q$
6130 IF Q$="N" GOTO 6410
6140 IF SCAN1$=SCAN2$ GOTO 6190
6145 GOSUB 2000
6150 PRINT"SCAN TYPE MISMATCH              "
6160 PRINT"SCAN1 = ";SCAN1$;" AND SCAN2 = ";SCAN2$
6170 INPUT"CONTINUE";Q$
6180 IF Q$="N" GOTO 6410
6190 IF W1=W2 GOTO 6240
6195 GOSUB 2000
6200 PRINT"WAVELENGTH MISMATCH             "
6210 PRINT"SPEC1 W1 =";W1;"AND SPEC2 W1 =";W2;"          "
6220 INPUT"CONTINUE";Q$
6230 IF Q$="N" GOTO 6410
6240 IF IT1=IT2 GOTO 6290
6245 GOSUB 2000
6250 PRINT"INTEGRATION TIME MISMATCH        "
6255 GOSUB 2000
6260 PRINT"SPEC1 IT =";IT1;" AND SPEC2 IT =";IT2;"        "
6270 INPUT"CONTINUE";Q$
6280 IF Q$="N" GOTO 6410
6290 FOR I=ISTART TO NP1+ISTART-1
6292 ZSPEC1(I)=ZSPEC1(I)-ZSPEC2(I)
6294 NEXT I
6300 TITLE$=DFN1$+"-"+DFN2$
6310 IF RIGHT$(DFN2$,3)="AVG" THEN INDEX=8 ELSE INDEX=9
6320 RL2$=MID$(DFN2$,INDEX,1)
6330 IF RIGHT$(DFN1$,3)="AVG" THEN INDEX=8 ELSE INDEX=9
6340 RL1$=MID$(DFN1$,INDEX,1)
6350 DFN1$=LEFT$(DFN1$,7)+RL1$+RL2$+"."+"COR"
6360 DATE1$=LEFT$(DFN1$,7)
6370 SCAN1$="CORRECTED"+" "+RL1$+" - "+RL2$
6380 DIS$="S"
6385 YMIN=ZSPEC1(ISTART): YMAX=ZSPEC1(ISTART)
6386 FOR I=ISTART+1 TO NP1+ISTART-1
6387 IF ZSPEC1(I)<YMIN THEN YMIN=ZSPEC1(I)
6388 IF ZSPEC1(I)>YMAX THEN YMAX=ZSPEC1(I)
6389 NEXT I
6390 SFLAG=1
6392 GOSUB 4000
6410 RETURN
6998 REM*******************************
6999 REM SUBROUTINE TO AVERAGE SPECTRA
7000 VCX=0: VCY=14: GOSUB 2000
7005 INPUT"USE ARRAY 1 OR 2";AN
7010 INPUT"DATA DISK";D$
7020 INPUT"GFC";GFC$
```

```
7030 INPUT"RUN LETTER";RL$
7040 INPUT"# OF REPLICATES";NR
7050 FOR I=1 TO 1024
7060 IF AN=1 THEN ZSPEC1(I)=0 ELSE IF AN=2 THEN ZSPEC2(I)=0
7070 NEXT I
7080 EXT=100
7090 FOR I=1 TO NR
7100 F$=D$+":"+GFC$+"."+RL$+RIGHT$(STR$(EXT+I))
7110 OPEN"I",1,F$
7120 IF AN=1 THEN INPUT#1,DATE1$,F1,SCAN1$,W1,IT1
7125 IF AN=2 THEN INPUT#1,DATE2$,F2,SCAN2$,W2,IT2
7130 J=1
7140 WHILE NOT EOF(1)
7150 INPUT#1,D,S
7160 IF AN=1 THEN ZSPEC1(J)=ZSPEC1(J)+S
7165 IF AN=2 THEN ZSPEC2(J)=ZSPEC2(J)+S
7170 J=J+1
7180 WEND
7190 CLOSE#1
7200 IF AN=1 THEN NP1=J-1 ELSE IF AN=2 THEN NP2=J-1
7210 VCX=0: VCY=23: GOSUB 2000
7215 IF AN=1 THEN NP=NP1 ELSE IF AN=2 THEN NP=NP2
7220 PRINT NP;" POINTS FOUND IN ";F$;"          ";
7230 NEXT I
7240 FOR I=1 TO NP
7250 IF AN=1 THEN ZSPEC1(I)=INT(ZSPEC1(I)/NR+0.5)
7255 IF AN=2 THEN ZSPEC2(I)=INT(ZSPEC2(I)/NR+0.5)
7260 NEXT I
7270 IF AN=1 THEN DFN1$=D$+":"+GFC$+RL$+"."+"AVG"
7280 IF AN=1 THEN DATE1$=GFC$+" "+RL$: SCAN1$="AVERAGE"
7282 IF AN=2 THEN DFN2$=D$+":"+GFC$+RL$+"."+"AVG"
7284 IF AN=2 THEN DATE2$=GFC$+" "+RL$: SCAN2$="AVERAGE"
7290 RETURN
7998 REM*********************************
8008 REM SUBROUTINE TO POSITION CURSOR AT LOWER LEFT
8018 XTEMP=VCX: YTEMP=VCY
8028 VCX=0: VCY=22: GOSUB 2000
8038 RETURN
```

```
1 REM*************************************************************
5 REM          PROGRAM: PDACALC.ASC
10 REM         BY: S.W. MCGEORGE
15 REM         DATE: 26 SEPTEMBER 1984
20 REM
25 REM     THIS PROGRAM IS USED TO CALCULATE PEAK HEIGHTS, PEAK
30 REM AREAS, AND PEAK HEIGHT TO BACKGROUND RATIOS.  DATA FILES
35 REM CREATED BY THE PDASYS1 FAMILY THAT ARE FIXED PATTERN CORRECTED
40 REM ARE EXPECTED AS INPUT.
50 REM     THIS ROUTINE WILL FIND THE LARGEST PEAK IN THE DATA SET
55 REM FOR CALCULATIONS.  IF MORE THAN ONE LINE IS REQUIRED TO BE
60 REM ANALYZED, THE PDAPLOT.ASC PACKAGE SHOULD BE USED TO CREATE
65 REM TWO SEPARATE FILES.  ONE OR TWO SIDED BACKGROUND CORRECTION
70 REM IS PERFORMED.  THE BACKGROUND IS CALCULATED USING 5 OR 10
75 REM POINTS.  THE DIODES USED FOR BACKGROUND CORRECTION ARE AT
80 REM LEAST 6 DIODES AWAY FROM THE PEAK DIODE.  THE PROGRAM
85 REM INCLUDES ANY DIODES IN THE PEAK AREA WHICH ARE 5 STANDARD
90 REM DEVIATIONS HIGHER THAN THE BACKGROUND NOISE.
98 REM
99 REM*************************************************************
110 DIM Z1(1024),Z2(1024)       :REM Z1 FOR DIODES, Z2 FOR INTENSITY
120 INPUT"DATA DISK";D$
130 INPUT"FILENAME";FI$
210 FI$=D$+":"+FI$
220 OPEN"I",1,FI$
230 INPUT#1,DATE$,F,SCAN$,W,IT  :REM READ HEADER INFORMATION
240 LPRINT"FILE: ";FI$          :REM AND PRINT ON PRINTER
250 LPRINT"READOUT FREQ.=";F
260 LPRINT"SCAN TYPE: ";SCAN$
280 LPRINT"INT. TIME =";IT
290 LPRINT
300 J=1
305 WHILE NOT EOF(1)
310 INPUT#1,Z1(J),Z2(J)         :REM READ IN DATA
315 J=J+1
320 WEND
322 CLOSE#1
325 NP=J-1
330 YMAX=0                      :REM FIND PEAK DIODE
335 FOR J=1 TO NP
340 IF Z2(J)>YMAX THEN YMAX=Z2(J): DMAX=Z1(J): INDEX=J
345 NEXT J
352 FOR I=INDEX-10 TO INDEX+10
354 PRINT Z1(I),Z2(I)           :REM OUTPUT +/- 10 DIODES EITHER
356 NEXT I                      :REM  SIDE OF PEAK DIODE
358 INPUT"1 OR 2 SIDED CORRECTION";S
360 IF S=1 THEN INPUT"L OR R SIDE";S$
362 B1=INDEX-10
364 B2=INDEX+6
366 SUM#=0: SSQ#=0
368 IF S=1 AND S$="R" GOTO 382
370 FOR I=B1 TO B1+4
372 SUM#=SUM#+Z2(I)             :REM SUM BACKGROUND ON LEFT SIDE
374 SSQ#=SSQ#+Z2(I)^2           :REM SUM SQUARES ON LEFT SIDE
378 NEXT I
```

```
380 IF S=1 GOTO 390
382 FOR I=B2 TO B2+4
384 SUM#=SUM#+Z2(I)            :REM SUM BACKGROUND ON RIGHT SIDE
386 SSQ#=SSQ#+Z2(I)^2          :REM SUM SQUARES ON RIGHT SIDE
388 NEXT I
390 IF S=1 THEN NB=5 ELSE NB=10
392 BAVG=SUM#/NB               :REM CALCULATE AVERAGE BACKGROUND
394 SD=SQR((SSQ#-SUM#^2/NB)/(NB-1))  :REM CALCULATE BACKGROUND NOISE
398 TH=5*SD                    :REM THRESHOLD IS 5 STD. DEV'S
400 J=INDEX-10
410 WHILE Z2(J)<BAVG+TH
420   J=J+1                    :REM SEARCH FOR FIRST DIODE IN PEAK
430 WEND
435 P1=Z1(J)                   :REM P1 INDICATES FIRST DIODE IN PEAK
440 PA=0
450 WHILE Z2(J)>BAVG+TH
460   PA=PA+Z2(J)-BAVG         :REM CALCULATE PEAK AREA
470   J=J+1
480 WEND
490 P2=Z1(J-1)                 :REM P2 IS LAST DIODE IN PEAK
492 REM
494 REM OUTPUT RESULTS TO PRINTER
496 REM
500 IF S=2 THEN LPRINT "2 SIDED CORRECTION" : GOTO 590
510 IF S$="L" THEN LPRINT"LEFT SIDED CORRECTION" : GOTO 590
520 LPRINT"RIGHT SIDED CORRECTION"
590 LPRINT
600 LPRINT"BACKGROUND =";BAVG
605 LPRINT"BACKGROUND NOISE =";SD
610 LPRINT
615 LPRINT"PEAK DIODE =";DMAX
620 LPRINT"PEAK HEIGHT =";YMAX-BAVG
630 LPRINT P2-P1+1;"DIODES IN PEAK (";P1;"-";P2;")"
632 LPRINT
640 LPRINT"PEAK AREA =";PA
650 LPRINT
652 LPRINT"SBR =";YMAX/BAVG
660 LPRINT
670 LPRINT"************************"
730 END
```

```
program PDASYS2;

(*****************************************************************************

                PROGRAM: PDASYS2.SRC
                  DATE: AUGUST 1984
                    BY: S.W. MCGEORGE AND R.L. SING

    This program acts as the user interface when the PDA detection system is
operated under System 2.  This routine and the BASIC program PDASYS2.BAS run
concurrently, the latter on the extended AIM computer.  All of the relevant
System 2 routines for analysis and display on the S100 system can be invoked
from this program because they exist as overlays that are automatically brought
into memory from disk when they are needed.  The syntax for linking the separately
compiled modules is as follows:

Link syntax for PDASYS2: LINKMT B:PDASYS2,B:GETPDA,FPREALS/S,PASLIB/S/D:9000/V1:8000
Link syntax for modules: LINKMT B:PDASYS2=B:PDASYS2/O:n,B:'MODn',PASLIB/S/P:8000

where n refers to the module number that determines the resulting overlay
number and MODn is the filename of the module.

*****************************************************************************)

const

   SLOPE = -5.05E-8;     (* Slope of the reciprocal dispersion vs. wavelength
                            function. *)

type

  DATA_ARRAY = array[1..1024] of integer;

var

  I,          (* General counting variable *)
  IO_RES,     (* Reports status of I/O operations *)
  PEAK_NUM,   (* Identifies the peak to be used for calibration *)
  POINT,      (* Used to index dark or data array *)
  PEAK_COUNT : integer; (* Provides a count of the number of peaks above the
                           specified threshold that were found. *)

  THE_DATA  : DATA_ARRAY;                (* Array to hold "analyte" spectrum *)
  TEMP_DATA : array[1..1024] of integer; (* Temporary array used by Calibrate routine *)
  DARK      : array[1..1024] of integer; (* Array to hold "dark" spectrum *)
  TEMP_LIST : array[1..5] of integer;    (* Temporary list of peak diodes used
                                            by Calibrate routine *)

  RD,               (* Reciprocal dispersion - changes with wavelength *)
  INTERCEPT,        (* Intercept of recip. disp. vs. wavelength plot *)
  CAL_DIODE,        (* Interpolated fractional diode corresponding to calibration wavelength *)
  MIN_WAVELEN,      (* Wavelength falling on diode 1 *)
  MAX_WAVELEN,      (* Wavelength falling on diode 1024 *)
  CAL_WAVELEN : real; (* Wavelength used for calibration of spectrum *)
```

```
  PEAK_LIST      : array[1..5] of real;  (* Fractional diodes corresponding to peaks above threshold *)
  INTENSITY_LIST : array[1..5] of real;  (* List of interpolated peak intensities *)

  DATA_FILE  : file;  (* Filename assigned to analyte spectrum *)
  DARK_FILE  : file;  (* Filename assigned to dark spectrum *)

  QUERY : char;       (* Variable for single letter responses *)
  DATE  : string[8];  (* Date code used to create filename *)
  EXT   : string[3];  (* File extension *)



external procedure GET_PDA(THE_DATA:integer;NUM_PTS:integer); (* ZBO routine to acquire data from PDA *)

external [1] procedure HP_PLOT;   (* Procedure to plot spectra on plotter *)

external [2] procedure CALIBRATE; (* Procedure to calibrate spectrum *)

external [3] procedure DISPLAY;   (* Procedure to display spectra numerically
                                     by diode number or wavelength *)



begin

  write('Enter date code : ');
  readln(DATE);
  INTERCEPT := 0;  (* Important to set INTERCEPT to zero so that Display routine knows that the
                      Calibrate routine has not been run. Therefore, wavelength display is impossible *)
  repeat

    write('Enter function (Acquire, Load, Save, Plot, Calibrate, Display, Restart, Quit) : ');
    readln(QUERY);

case QUERY of

'A','a' : begin  (* Acquire dark or analyte spectrum *)

          write('Dark or Analyte : ');
          readln(QUERY);

          if (QUERY = 'D') or (QUERY = 'd') then
            begin
              GET_PDA(addr(DARK),1024);  (* Acquire 1024 point spectrum *)

              assign(DARK_FILE,concat('B:',DATE,'.DRK'));
              rewrite(DARK_FILE);
              blockwrite(DARK_FILE,DARK,IO_RES,2048,-1);  (* Write spectrum to disk using
                                                             ".DRK" extension *)
              close(DARK_FILE,IO_RES);
            end

          else
            GETPDA(addr(THE_DATA),1024);  (* Acquire 1024 point spectrum *)
        end;
```

```
'P','p' : HP_PLOT;  (* Plot data residing in data arrays *)


'S','s' : begin  (* Save analyte spectrum under user defined extension *)

          write('Extension : ');
          readln(EXT);

          assign(DATA_FILE,concat('B:',DATE,'.',EXT));
          rewrite(DATA_FILE);
          blockwrite(DATA_FILE,THE_DATA,IO_RES,2048,-1);

          close(DATA_FILE,IO_RES);
        end;


'L','l' : begin  (* Load dark or analyte spectrum from disk into memory *)

          write('Dark or Analyte : ');
          readln(QUERY);

          if (QUERY = 'D') or (QUERY = 'd') then
            begin
              assign(DARK_FILE,concat('B:',DATE,'.DRK'));
              reset(DARK_FILE);
              blockread(DARK_FILE,DARK,IO_RES,2048,-1);

              close(DARK_FILE,IO_RES);
            end
          else
            begin
              write('Extension : ');
              readln(EXT);

              assign(DATA_FILE,concat('B:',DATE,'.',EXT));
              reset(DATA_FILE);
              blockread(DATA_FILE,THE_DATA,IO_RES,2048,-1);

              close(DATA_FILE,IO_RES);
            end

        end;

'C','c' : begin  (* Calibration routine *)

          CALIBRATE;  (* Transfer to Calibrate routine for peak finding and interpolation of
                         fractional diodes *)
          if PEAK_COUNT > 0 then
            begin
              writeln('Peak Number  Subdiode');
              for I := 1 to PEAK_COUNT do       (* Type peak numbers and fractional diodes
                writeln(I:6,PEAK_LIST[I]:14:2);   corresponding to significant peaks *)
```

```
                write('Peak to calibrate : ');
                readln(PEAK_NUM);              (* Identify peak to calibrate *)
                write('Wavelength : ');
                readln(CAL_WAVELEN);           (* Enter known wavelength *)

                CAL_DIODE := PEAK_LIST[PEAK_NUM];  (* CAL_DIODE is fractional diode corresponding
                                                      to CAL_WAVELEN *)

              (* Calculate intercept of recip. disp. vs. wavelength plot using experimentally
                 determined second order polynomial fit *)
                INTERCEPT := 2.0651515E-2 - CAL_WAVELEN*6.854592E-7 - sqr(CAL_WAVELEN)*4.776324E-9;

                RD := INTERCEPT + (1.0 - CAL_DIODE)*SLOPE;            (* Recip. disp. at diode 1 *)
                MIN_WAVELEN := CAL_WAVELEN + RD*(1.0 - CAL_DIODE);    (* Wavelength at diode 1 *)
                RD := INTERCEPT + (1024-CAL_DIODE)*SLOPE;             (* Recip. disp. at diode 1024 *)
                MAX_WAVELEN := CAL_WAVELEN + RD*(1024.0 - CAL_DIODE); (* Wavelength at diode 1024 *)

                writeln('Peak Number  Wavelength');
                for I := 1 to PEAK_COUNT do         (* Print peak numbers and corresponding wavelengths
                                                       on screen *)
                    if I = PEAK_NUM then
                      writeln(I:6,CAL_WAVELEN:16:3)
                    else
                      begin
                        RD := INTERCEPT + (PEAK_LIST[I] - CAL_DIODE)*SLOPE;
                        writeln(I:6,CAL_WAVELEN + RD*(PEAK_LIST[I] - CAL_DIODE):16:3)
                      end
              end

          end;

'D','d' : DISPLAY;  (* Display diode or wavelength regions *)

'R','r' : begin     (* Restart by redefining date code *)

            write('Enter date code : ');
            readln(DATE);
            INTERCEPT := 0

          end;

'Q','q' : exit  (* Return to CP/M environment *)

end;

until (QUERY = 'Q') or (QUERY = 'q')

end.
```

```
; File: GETPDA.MAC
; By: R.L. Sing

; This routine will acquire any number of 12 bit data from the
; 12 bit analogue to digital converter, store them at the user
; specified location. The acquisition is externally triggered.
; The program acquires data when the EOC is detected.
;
; This routine is designed to be used as a Pascal subroutine with
; the following declaration:

; external procedure GET_SET( DESTINATION : ^DATA_BUF;
;                             NUM_PTS     : integer);

; Where DATA_BUF is an array[1:NUM_PTS] of integer.

; The TUART parallel ports are used in the hardware interface.

; Equates

PORTA   EQU     014H            ; Parallel port A
PORTB   EQU     024H            ; Parallel port B
INTREGA EQU     013H            ; Port A interrupt register
TIMER1  EQU     015H            ; Port A timer 1
SENS    EQU     0D7H            ; SENS mask for interrupt register
TIMEMSK EQU     0C7H            ; Timer 1 mask for interrupt register


        NAME    ('GETDAT')
        PUBLIC  GETPDA

        .Z80

GETPDA:
        POP     DE              ; Pop return address
        POP     BC              ; BC holds number of points
        POP     HL              ; HL has address for storage
        PUSH    DE              ; Restore return address



INIT:   LD      A,04            ; This will enable SENS
        OUT     (INTREGA),A     ; to show in interrupt register
        IN      A,(INTREGA)     ; To clear any previous interrupts

        LD      A,00
        OUT     (PORTA),A       ; Use channel 0;

        LD      D,SENS          ; Get SENS mask into D
WTEOC:  IN      A,(INTREG)      ; Get interrupt register
        CP      D               ; Check with mask
        JR      NZ,WTEOC        ; Wait till same

        IN      A,(PORTA)       ; Get low bits
```

```
        LD      (HL),A          ; Store them
        INC     HL              ; Advance pointer
        IN      A,(PORTB)       ; Get high bits
        AND     0FH             ; Strip high 4 bits
        LD      (HL),A          ; Store them
        INC     HL              ; Advance pointer


        DEC     BC              ; Decrement count
        LD      A,B
        OR      C               ; Check if BC = 0
        JR      NZ,WTEOC        ; Continue if not done
        RET                     ; Return if done


        END                     ; End of it.
```

```
module PLOT;

(*****************************************************************************************

                Module: PLOTMOD.SRC
                    By: S.W. McGeorge (Adapted from PDA3D.SRC by R.L. Sing)
                  Date: August 1984

    This module is an overlay which is invoked when the option 'P' (Plot) is
selected from the menu of PDASYS2.  This procedure plots a dark corrected
spectrum on a Hewlett-Packard plotter attached to the auxilliary port of the
S100 computer's terminal.

*****************************************************************************************)

var  (* See definitions in PDASYS2 source code *)

  DARK,
  THE_DATA,
  TEMP_DATA : external array[1..1024] of integer;



procedure HP_PLOT;

  var

    POINT,             (* Index to data arrays *)
    FIRST_TO_PLOT,     (* First point to plot *)
    LAST_TO_PLOT,      (* Last point to plot *)
    Y_MIN,             (* Minimum Y value *)
    Y_MAX,             (* Maximum Y value *)
    X_RANGE : integer; (* Range of pixels to plot *)



begin

  Y_MAX := 2548;  (* Set YMAX to the ADC full scale of 2048 plus 500 *)
  Y_MIN := 0;

  write('Enter first point to be plotted : ');
  readln(FIRST_TO_PLOT);
  write('Enter last point to be plotted : ');
  readln(LAST_TO_PLOT);

  for POINT := 1 to 1024 do
    TEMP_DATA[POINT] := THE_DATA[POINT] - DARK[POINT] + 500;  (* Generate dark corrected spectrum *)

  X_RANGE := LAST_TO_PLOT-FIRST_TO_PLOT;

  write('Turn on aux port and hit return');
  readln;
```

```
(* Set plotter scale *)
 write(chr(27),'.IB1;;17:',chr(27),'.N;19:');
  write('SC',-5 * X_RANGE div 100 ,',', X_RANGE + 5 * X_RANGE div 100,',',Y_MIN -5 * (Y_MAX-Y_MIN) div 100,',',
        Y_MAX + 5 * (Y_MAX-YMIN) div 100,';');

(* Move pen to first point and lower to paper *)
  write('PU,');
  write(FIRST_TO_PLOT,',',TEMP_DATA[FIRST_TO_PLOT],',');
  write('PD,');

  for POINT := FIRST_TO_PLOT to LAST_TO_PLOT do
    write(POINT,',',TEMP_DATA[POINT],',');        (* Plot data *)

  write('PU,');  (* Lift pen *)
  writeln;

  readln  (* Read carriage return input after aux port is turned off *)

end;

modend.
```

```
module CAL;

(*****************************************************************************************

                    Module: CALMOD.SRC
                       By: S.W. McGeorge
                     Date: August 1984

    This module is an overlay invoked in response to the 'C' (Calibrate) option
from PDASYS2.  After prompting the user for a threshold value the program finds
any peaks exceeding that threshold.  A second order polynomial fit is performed
on the three peak diodes of each peak and the fractional diode (also referred to
as subdiode) corresponding to the curve maximum is calculated.  The peak subdiodes
are recorded in an array called PEAK_LIST which is a global array variable.  This
list is subsequently used when control is transferred back to the PDASYS2 to
calibrate the spectrum and report the wavelengths of the lines found.

    The algorithm for the orthogonal polynomial curve fit was based on the method
described in "Design and Analysis of Experiments" by D.C. Montgomery John Wiley and Sons,
New York (1976).  ( Call number QA279.M66)

*****************************************************************************************)

const

  FACTOR = 0.66666667;  (* This factor is a constant derived from the equation used to
                           calculate orthogonal model parameters *)

var  (* See definitions in PDASYS2 *)

  PEAK_COUNT : external integer;

  THE_DATA,
  TEMP_DATA,
  DARK      : external array[1..1024] of integer;
  TEMP_LIST : external array[1..50] of integer;

  PEAK_LIST,
  INTENSITY_LIST : external array[1..50] of real;


(* This function furnishes an estimate of the intensity of the interpolated subdiode *)
function Y_ESTIMATE(SUB_DIODE,POLY_0,POLY_1,POLY_2: real) : real;

begin
  Y_ESTIMATE := POLY_0 + POLY_1*SUB_DIODE + (POLY_2*3)*(sqr(SUB_DIODE) - FACTOR)
end;
```

```
procedure CALIBRATE;

 var

   POINT,              (* Index to data arrays *)
   Y_MAX,              (* Used to determine maximum diode of each peak *)
   THRESHOLD,          (* Threshold value above baseline for peak search *)
   I,J,                (* General counting variables *)
   SUM,                (* Sum of diode intensities for a given peak *)
   COEFF_1,            (* Intermediate coefficients for orthogonal parameters *)
   COEFF_2: integer;

   LINEAR    : array[1..3] of integer;  (* Linear coefficients of polynomial *)
   QUADRATIC : array[1..3] of integer;  (* Quadratic coefficients of polynomial *)

   POLY_0,             (* POLY_0 - POLY_2 are model parameters for polynomial *)
   POLY_1,
   POLY_2,
   SUB_DIODE,          (* Fractional diode used to determine peak subdiode *)
   OLD_ESTIMATE,       (* OLD_ESTIMATE and NEW_ESTIMATE are used to find peak subdiode *)
   NEW_ESTIMATE : real;


begin

  for POINT := 1 to 1024 do
    TEMP_DATA[POINT] := THE_DATA[POINT] - DARK[POINT];  (* Generate dark corrected spectrum *)

  write('Enter threshold:');
  readln(THRESHOLD);

  PEAK_COUNT := 0;
  POINT := 1;

  while POINT < 1024 do
    begin
      while TEMP_DATA[POINT] < THRESHOLD do  (* Search for diode > THRESHOLD *)
        POINT := POINT + 1;

      YMAX := TEMP_DATA[POINT];

      while TEMP_DATA[POINT + 1] > YMAX do  (* Find maximum value for this peak *)
        begin
          POINT := POINT + 1;
          YMAX := TEMP_DATA[POINT]
        end;

      if POINT < 1024 then
        begin
          PEAK_COUNT := PEAK_COUNT + 1;   (* Increment peak count *)
          TEMP_LIST[PEAK_COUNT] := POINT  (* Record peak diode *)
        end;
```

```
    if PEAK_COUNT < 50 then    (* Continue if less than 50 peaks found so far *)
      while TEMP_DATA[POINT + 1] > THRESHOLD do
        POINT := POINT + 1
    else
      POINT := 1024;
    POINT := POINT + 1
  end;

if PEAK_COUNT = 0 then
  writeln('No peaks found')
else
  begin
    for I := 1 to PEAK_COUNT - 1 do
      if TEMP_LIST[I] > TEMP_LIST[I + 1] - 5 then  (* Report potential overlaps *)
        writeln('Pontential overlap between peak ',I,' and peak ',I + 1);

(* Assign orthogonal coefficients to arrays *)
    LINEAR[1] := -1; LINEAR[2] := 0; LINEAR[3] := 1;
    QUADRATIC[1] := 1; QUADRATIC[2] := -2; QUADRATIC[3] := 1;

    for I := 1 to PEAK_COUNT do
      begin
        COEFF_1 := 0; COEFF_2 := 0; SUM := 0;

        for J := 1 to 3 do  (* Determine intermediate polynomial parameters *)
          begin
            POINT := TEMP_LIST[I] +J - 2;
            SUM := SUM + TEMP_DATA[POINT];
            COEFF_1 := COEFF_1 + LINEAR[J] * TEMP_DATA[POINT];
            COEFF_2 := COEFF_2 + QUADRATIC[J] * TEMP_DATA[POINT];
          end;

       (* Calculate orthogonal model parameters *)
        POLY_0 := SUM/3;
        POLY_1 := COEFF_1/6;
        POLY_2 := COEFF_2/18;

       (* Start peak interpolation one full diode before peak diode *)
        SUB_DIODE := -1;
        OLD_ESTIMATE := 0;
        NEW_ESTIMATE := Y_ESTIMATE(SUB_DIODE,POLY_0,POLY_1,POLY_2);

        while NEW_ESTIMATE > OLD_ESTIMATE do  (* Increment subdiode by 0.1 until maximum intensity
                                                 estimate is reached *)
          begin
            OLD_ESTIMATE := NEW_ESTIMATE;
            SUB_DIODE := SUB_DIODE + 0.01;
            NEW_ESTIMATE := Y_ESTIMATE(SUB_DIODE,POLY_0,POLY_1,POLY_2)
          end;

        PEAK_LIST[I] := TEMP_LIST[I] + SUB_DIODE;  (* Record peak subdiode *)
        INTENSITY_LIST[I] := OLD_ESTIMATE          (* Record estimate of peak intensity *)

       end
```

```
        end
    end;
modend.
```

```
module DIS;

(*****************************************************************************

                    Module: DISMOD.SRC
                       By: S.W. McGeorge
                     Date: August 1984

    This overlay is invoked by the option 'D' (Display) from PDASYS2.  The procedure
permits the listing of dark, raw analyte and corrected analyte data by diode or by
wavelength.  To use the wavelength option the Calibrate routine must be run first
or an error is flagged.  The output from this routine is sent to the screen,
however, a copy of the output can be routed to the printer by responding appropriately
to the prompt at the end of the module.

*****************************************************************************)

var   (* See definitions in PDASYS2 *)

  CAL_DIODE,
  INTERCEPT,
  MIN_WAVELEN,
  MAX_WAVELEN,
  CAL_WAVELEN : external real;

  DARK,
  THE_DATA : external array[1..1024] of integer;


  external procedure PRINT(FORMAT:char;FIRST_DIODE,LAST_DIODE:integer); (* Procedure to send information
                                                                          to the printer *)

procedure DISPLAY;

const  (* See PDASYS2 *)

  SLOPE = -5.05E-8;

var
  POINT,                (* Index to data arrays *)
  IO_RES,               (* Status of I/O operations *)
  PEAK_DIODE,           (* Center diode to be displayed when D(iode) option selected *)
  NUM_DIODES,           (* Number of diodes surrounding center diode to be displayed *)
  LAST_DIODE,           (* Last diode to display *)
  LINE_COUNT,           (* Keeps track of the number of lines of information sent to screen*)
  FIRST_DIODE : integer; (* First diode to display *)

  RD,                  (* Reciprocal dispersion *)
  REGION,              (* Width of wavelength region to display when W(avelength) option selected *)
  WAVELEN,
  LOW_WAVELEN,         (* Low boundary of wavelength region *)
  HIGH_WAVELEN : real;  (* High boundary of wavelength region *)

  QUERY,          (* Variable for single letter responses *)
  FORMAT : char;  (* Format='D' for diode display, ='W' for wavlength display *)
```

```
begin

    write('Display Wavelength or Diode region ? ');
    readln(QUERY);

    if (QUERY = 'W') or (QUERY = 'w') then
      begin
        if INTERCEPT = 0 then  (* INTERCEPT is non-zero only if Calibrate has been executed *)
          begin
            writeln('Error: Run calibration procedure first.');
            exit
          end;
        FORMAT := 'W';
        write('Enter wavelength of line : ');
        readln(WAVELEN);
        if (WAVELEN < MIN_WAVELEN) or (WAVELEN > MAX_WAVELEN) then
          begin
            writeln('Error: Wavelength not in current window.');
            exit
          end;
        write('Enter width of region in nm :');
        readln(REGION);

        LOW_WAVELEN := WAVELEN - REGION/2;
        HIGH_WAVELEN := WAVELEN + REGION/2;

        if LOW_WAVELEN < CAL_WAVELEN then   (* Find diode corresponding to LOW_WAVELEN *)
          if LOW_WAVELEN < MIN_WAVELEN then
            FIRST_DIODE := 1
          else
            FIRST_DIODE := round(CAL_DIODE - (CAL_WAVELEN - LOW_WAVELEN)/0.02)
        else
          FIRST_DIODE := round(CAL_DIODE + (LOW_WAVELEN - CAL_WAVELEN)/0.02);

        if HIGH_WAVELEN > CAL_WAVELEN then  (* Find diode corresponding to HIGH_WAVELEN *)
          if HIGH_WAVELEN > MAX_WAVELEN then
            LAST_DIODE := 1024
          else
            LAST_DIODE := round(CAL_DIODE + (HIGH_WAVELEN - CAL_WAVELEN)/0.02)
        else
          LAST_DIODE := round(CAL_DIODE - (CAL_WAVELEN - HIGH_WAVELEN)/0.02);

      end
    else
      begin
        FORMAT := 'D';
        write('Enter peak diode : ');
        readln(PEAK_DIODE);
        write('Enter number of diodes to display : ');
        readln(NUM_DIODES);

        FIRST_DIODE := PEAK_DIODE - NUM_DIODES div 2;
        if FIRST_DIODE < 0 then
          FIRST_DIODE := 1;
        LAST_DIODE := FIRST_DIODE + NUM_DIODES - 1
```

```
      end;

  (* Output data to screen. Include wavelength information if requested earlier *)
    writeln;
    write('Diode');
    if FORMAT = 'W' then
      write('  Wavelength');
    writeln('  Dark Value  Raw Value  Corrected Value');
    writeln;
    LINE_COUNT := 0;
    POINT := FIRST_DIODE;
    while POINT <= LAST_DIODE do
      begin
        while (LINE_COUNT < 19) and (POINT <= LAST_DIODE) do (* Data is listed 19 lines at a time *)
          begin
            write(POINT:5);
            if FORMAT = 'W' then
              begin
                RD := INTERCEPT + (POINT - CAL_DIODE)*SLOPE;
                write(CAL_WAVELEN + RD*(POINT - CAL_DIODE):11:3)
              end;
            writeln(DARK[POINT]:10,THE_DATA[POINT]:11,THE_DATA[POINT] - DARK[POINT]:14);
            POINT := POINT + 1;
            LINE_COUNT := LINE_COUNT + 1
          end;
        write('Hit return to continue');
        readln;
        LINE_COUNT := 0
      end;
    writeln;

    write('Print results  (Y or N)? ');
    readln(QUERY);
    if (QUERY = 'Y') or (QUERY = 'y') then
      PRINT(FORMAT,FIRST_DIODE,LAST_DIODE)

end;

.endend.
```

```
module LIST;

(*****************************************************************************************

                Module: LSTMOD.SRC
                   By: S.W. McGeorge
                 Date: August 1984

    This module is linked with the display overlay DISMOD and permits the printing
of the same information furnished by the 'D' (Display) option on the printer.

*****************************************************************************************)

var  (* See PDASYS2 *)

  DARK,
  THE_DATA : external array[1..1024] of integer;

  INTERCEPT,
  CAL_DIODE,
  CAL_WAVELEN : external real;


procedure PRINT(FORMAT:char;FIRST_DIODE,LAST_DIODE:integer);

const

  SLOPE = -5.05E-8;

var

  POINT : integer;     (* Index to data arrays *)

  RD : real;           (* Reciprocal dispersion *)

  LIST_FILE : text;    (* 'Filename' of list device *)

  TITLE : string[120]; (* Title for printout *)


begin

  assign(LIST_FILE,'LST:');
  rewrite(LIST_FILE);

  write('Title for listing? ');
  readln(TITLE);
  writeln(LIST_FILE,TITLE);
  writeln(LIST_FILE);

  write(LISTFILE,'Diode');
  if FORMAT = 'W' then
    write(LIST_FILE,'  Wavelength');
  writeln(LIST_FILE,'  Dark Value   Raw Value  Corrected Value');
  writeln(LIST_FILE);
```

```
    for POINT := FIRST_DIODE to LAST_DIODE do  (* Print data *)
      begin
        write(LIST_FILE,POINT:5);
        if FORMAT = 'W' then
          begin
            RD := INTERCEPT + (POINT - CAL_DIODE)*SLOPE;
            write(LIST_FILE,CAL_WAVELEN + RD*(POINT - CAL_DIODE):11:3)
          end;

        writeln(LIST_FILE,DARK[POINT]:10,THE_DATA[POINT]:11,THE_DATA[POINT] - DARK[POINT]:14);
        writeln(LIST_FILE)
      end

  end;

  modend.
```

```
1 REM*************************************************************************
2 REM
3 REM              PROGRAM: PDASYS2B.DOC
4 REM                   BY: S.W. MCGEORGE
5 REM                 DATE: 4 FEBRUARY 1985 (DOCUMENTATION)
6 REM
7 REM     THIS DOCUMENTATION DESCRIBES THE USER INTERFACE FOR THE AIM COMPUTER
8 REM WHEN THE PDA DETECTOR IS OPERATED UNDER SYSTEM 2.  THE PROGRAM FILE IS
9 REM CALLED PDASYS2.BAS.  ROUTINES CALLED BY PDASYS2.BAS INCLUDE THE ASSEMBLER
10 REM PROGRAMS PDAINITZ.ASM, PDASCAN2.ASM, CSELECT.ASM AND PDABLURT.ASM.
11 REM     THIS PROGRAM IS ALMOST IDENTICAL TO ITS PREDECESSOR PDASYS1.BAS.
12 REM THEREFORE ONLY THOSE ASPECTS UNIQUE TO THIS PROGRAM WILL BE DOCUMENTED
13 REM BELOW.
14 REM
15 REM*************************************************************************
20 REM
30 REM MAIN PROGRAM
40 REM
60 INPUT"DATA ACQ.(Y/N)";Q$
70 IF Q$="Y" GOTO 100
80 POKE248,255
90 GOTO 110
100 POKE248,0
110 INPUT"# OF PIXELS";P
115 P=P-1
120 PH=INT(P/256):PL=P-256*PH
130 POKE 246,PL:POKE 247,PH
140 INPUT"DSID WAIT REQ'D";QD$
150 IF QD$="N" GOTO 190
160 POKE 224,255
170 GOTO 200
190 POKE 224,0
200 POKE4,0:POKE5,32:X=USR(0)   :REM PDAINITZ.ASM
204 POKE240,8
206 TMIN=0.058
208 F=17.857
210 REM
530 INPUT"COMMAND";C$
540 IF C$="SCAN" THEN GOSUB 600
550 IF C$="BLURT" THEN GOSUB 1410
560 IF C$="CSELECT" THEN GOSUB 2000
580 IF C$="QUIT" THEN STOP
590 GOTO 530
592 REM*************************************************************************
594 REM "SCAN" SUBROUTINE ACQUIRES 1 OR MORE SPECTRA AT GIVEN INTEGRATION TIME
596 REM USING PDASCAN2.ASM
598 REM
600 INPUT"INT. TIME(SEC)";IT
630 IF IT>TMIN THEN T=(IT-TMIN)*1000:GOTO 680
670 T=0
680 FOR C=1 TO 5                :REM THIS SEGMENT ADJUSTS THE
681 IF T/C > 65535 THEN NEXT C  :REM  FREQUENCY THAT CONTROLS
682 T=INT(T/C)                  :REM  THE RANGE OF INTEGRATION
683 C=498*C                     :REM  TIMES THAT CAN BE USED.
684 CH=INT(C/256)               :REM THE MAXIMUM INTEGRATION
```

```
685 CL=C-CH*256                 :REM  TIME ALLOWED IS 5.46 MINUTES.
686 POKE 36868,CL               :REM 36868,36869 ARE THE LBYTE,HBYTE LOCATIONS
687 POKE 36869,CH               :REM  OF TIMER 2 OF VIA 1.
689 IH=INT(T/256)
690 IL=INT(T-IH*256+.5)
700 POKE244,IL:POKE245,IH
710 IF QD$="N" GOTO 790
720 INPUT"DSID WAIT PERIOD";WP
725 IF WP<0.058 THEN WP=0.058
730 WP=WP*1000-58
740 WH=INT(WP/256):WL=WP-WH*256
750 POKE 225,WL:POKE 226,WH
790 INPUT"# OF SCANS";NS        :REM PDASYS2 CAN GENERATE MULTIPLE SCANS
800 POKE243,NS
860 POKE4,0:POKE5,34:X=USR(0)   :REM JUMP TO PDASCAN2.ASM
890 INPUT"CONTINUE";Q$
900 IF Q$="Y" GOTO 600
930 RETURN
1400 REM*************************************************************************
1402 REM BLURT SUBROUTINE.  ACCESSES PDABLURT.ASM
1403 REM
1410 INPUT"BLURT FREQ.(MHZ)";BF
1420 IF BF=1 THEN POKE 241,56: GOTO 1470
1430 IF BF=.5 THEN POKE241,52: GOTO 1470
1440 IF BF=.25 THEN POKE 241,48: GOTO 1470
1450 PRINT BF;"IS NOT A BLURT FREQ."
1460 GOTO 1410
1470 INPUT"RUN LETTER";R$
1480 INPUT"SCAN TYPE";SCAN$
1490 INPUT"# OF BLURT REPS";BR
1500 IF BR>48 GOTO 1490
1510 POKE 243,BR
1520 INPUT"PEAK DIODE";PD
1530 INPUT"# OF DIODES TO ACQ.";ND
1540 IF ND>128 GOTO 1530
1550 IF ND<15 GOTO 1530
1560 NP=PD+INT(ND/2+.5)
1570 PH=INT(NP/256): PL=NP-PH*256
1580 POKE 246,PL: POKE 247,PH
1590 B=1035-ND
1600 BH=INT(B/256): BL=B-BH*256
1610 POKE 249,BL: POKE 250,BH
1620 POKE 251,0
1630 POKE 254,0: POKE 255,48
1640 POKE 252,ND
1650 POKE 4,0: POKE 5,35
1660 X=USR(0)
1670 DVEC=12288
1680 EXT=100
1690 FOR I=1 TO BR
1700 FD$=D$+":"+DATE$+"."+R$+RIGHT$(STR$(EXT+I),2)
1730 SCAN$="BLURT"
1740 PRINT DATE$
1750 PRINT BF*1000
1760 PRINT SCAN$
```

```
1770 PRINT M1
1780 IT=0
1790 PRINT IT
1800 D=PD-INT(ND/2)
1810 FOR J=DVEC TO DVEC+(ND-1)*2 STEP 2
1820 PRINT D;PEEK(J)+PEEK(J+1)*256
1830 D=D+1
1840 NEXT J
1850 DVEC=DVEC+256
1870 NEXT I
1880 INPUT"REPEAT";Q$
1890 IF Q$="Y" GOTO 1410
1900 RETURN
1990 REM*************************************************************************
1992 REM CLOCK FREQUENCY SELECTION SUBROUTINE. INVOKES CSELECT.ASM
1994 REM
2000 INPUT"READOUT FREQ(KHZ)";F$
2010 FLAG=0
2020 IF VAL(F$) < 125 GOTO 2100
2030 IF F$="1000" THEN POKE 240,24 : GOTO 2200
2040 IF F$="500" THEN POKE 240,20 : GOTO 2200
2050 IF F$="250" THEN POKE 240,16 : GOTO 2200
2060 IF F$="125" THEN POKE 240,12 : GOTO 2200
2070 IF F$="EXT" THEN POKE 240,4 : GOTO 2200
2080 IF F$="GND" THEN POKE 240,0 : GOTO 2200
2090 GOTO 2000
2100 F=VAL(F$)
2110 FLAG=1
2120 N=INT(125/F-1.5)
2130 IF N >= 0 GOTO 2160
2140 PRINT "FREQ NOT AVAILABLE"
2150 GOTO 2000
2160 IF N > 255 GOTO 2140
2170 POKE 242,N
2180 F=125/(N+2)
2190 POKE 240,8
2200 IF FLAG=1 GOTO 2220
2210 F=VAL(F$)
2220 PRINT "ACTUAL READOUT RATE = ";F;"KHZ"
2230 IF F <= 10 GOTO 2290
2240 PRINT"READOUT RATE IS TOO"
2250 PRINT"FAST FOR DATA ACQ."
2260 INPUT"CONTINUE (Y/N)";Q$
2270 IF Q$ = "Y" GOTO 2290
2280 GOTO 2000
2290 POKE 4,0: POKE 5,33
2300 X=USR(0):REM CSELECT.ASM
2310 TMIN=1038/(F*1000)
2320 RETURN
2325 REM*************************************************************************
2330 END
```

```
;*************************************************************
;
;              PROGRAM: PDAINIT2.ASM
;                  BY: S.W. MCGEORGE
;                DATE: 4 NOVEMBER 1984
;
;    THIS PROGRAM INITIALIZES THE PDA AT FOR A READOUT RATE OF
; 17.85 KHZ AND SETS UP VIA1 TO COUNT INTEGRATION PULSES AS WELL AS
; GENERATE START CONVERT PULSES.  VIA3 HANDLES THE PDA LOGIC
; INTERFACE AS IN PDAINIT1.ASM.
;
;*************************************************************
;
        * = $2000        ;PROGRAM START AT $2000
;
; VIA REGISTER LOCATIONS
;
        DDRB1 = $9002
        T1CL1 = $9004
        T1CH1 = $9005
        ACR1  = $900B
        PCR1  = $900C
;
        DRB3  = $9020
        DDRB3 = $9022
        DDRA3 = $9023
        T1CL3 = $9024
        T1CH3 = $9025
        ACR3  = $902B
        PCR3  = $902C
;
; INITIALIZE VIA 1 FUNCTIONS
;
        LDA     #$B0
        STA     DDRB1   ;PB0-3 FOR INPUT, PB4,5 FOR OUTPUT.
        LDA     #$A1    ;CA1 DETECTS RISING EDGE,
        STA     PCR1    ; CB2 TO GENERATE CONVERT PULSE.
        LDA     #$E0
        STA     ACR1    ;ENABLE PB7 PULSE GEN., PB6 PULSE COUNT
;
; INITIALIZE VIA 3 FUNCTIONS
;
        LDA     #$FF
        STA     DDRA3   ;PA0-7 FOR OUTPUT
        LDA     #$BF
        STA     DDRB3   ;PB0-5 FOR OUTPUT
        LDA     #$E0
        STA     ACR3    ;PB6 FOR PULSE COUNTING, PB7 CLOCK GEN.
        LDA     #$BC
        STA     PCR3    ;CA2 SET LOW,CB2 PULSE MODE
        LDA     #$05
        STA     T1CL3
        LDA     #$00
        STA     T1CH3   ;START 17.857 KHZ CLOCK ON PB7
        LDA     #$08
```

```
        STA     DRB3    ;SELECT PB7 AS CLOCK SOURCE
;
; INITIATE VIA #1 FOR GENERATION AND COUNTING OF 1 MS INTERRUPTS
;
        LDA     #$F2
        STA     TC1L1
        LDA     #$01
        STA     TC1H1   ;START PULSES
;
        RTS
        END
```

```
;*********************************************************
;
;            PROGRAM: PDASCAN2.ASM
;                 BY: S.W. MCGEORGE
;               DATE: 4 NOVEMBER 1984
;
;    THIS PROGRAM IS CALLED BY PDASYS2.BAS WHICH ACTS
; AS THE USER INTERFACE.  THE PROGRAM DETECTS A START PULSE,
; COUNTS OUT A USER SPECIFIED NUMBER OF DIODES AND FIRES THE
; DSID SOLENOID.  THE READOUT CLOCK IS THEN TURNED OFF FOR
; A USER SPECIFIED PERIOD WHICH ALLOWS TIME FOR THE
; SAMPLE PROBE TO STABILIZE IN THE PLASMA AND HEAT UP TO
; THE TEMPERATURE REQUIRED FOR VAPORIZATION OF THE SAMPLE.
;    AFTER THIS DSID WAIT PERIOD THE PDA IS READ OUT TO RESET
; ALL PIXELS AND THE CLOCK IS AGAIN TURNED OFF, THIS TIME FOR
; AN INTEGRATION PERIOD TO CAPTURE THE TRANSIENT SIGNAL.  THE
; WAIT PERIOD AND INTEGRATION PERIOD ARE DETERMINED BY
; EMPLOYING MULTIPLE READOUTS WITH ZERO WAIT AND INTEGRATION
; PERIODS AND PLOTTING MULTIPLE SCANS USING PDA3D, A PROGRAM
; WHICH DISPLAYS WAVELENGTH VS. INTENSITY VS. TIME IN A 3-
; DIMENSIONAL PLOT.
;   THE S-100 SYSTEM RUNNING UNDER R.L. SING'S SOFTWARE
; DETECTS END OF CONVERSION STATUS AND ACQUIRES THE DATA
; DIRECTLY USING THE 12-BIT ADC SUBSYSTEM.  THE ADC HARDWARE
; HAS BEEN MODIFIED SUCH THAT BNC CONNECTOR #4 IS CONNECTED
; TO THE START CONVERT LINE ENABLING THE AIM TO GENERATE
; CONVERSIONS AT THE APPROPRIATE TIME USING VIA1.  THIS ROUTINE
; ALSO DIFFERS FROM PDASCAN1.ASM IN THAT UP TO 255 CONSECUTIVE
; SCANS CAN BE GENERATED SO THAT TEMPORAL DATA CAN BE ACQUIRED
; FROM THE DSID EXPERIMENT.
;
;*********************************************************
;
; VIA REGISTER LOCATIONS
;
      DRB1  = $9000
      TC2L1 = $9008   ; T2 OF VIA1 COUNTS .1 MS INTEGRATION
      TC2H1 = $9009   ;  PULSES FOR STOPPED CLOCK MODE.
      ACR1  = $900B
      PCR1  = $900C
      IFR1  = $900D   ;
;
      DRB3  = $9020   ; PORT B CONN. TO PDA LOGIC
      DRA3  = $9021   ; PORT A  "   "   "   "
      TC2L3 = $9028   ; T2 OF VIA3 COUNTS SAMPLE PULSES
      TC2H3 = $9029   ;  GENERATED BY PDA
      IFR3  = $902D   ;
;
; PAGE ZERO LOCATIONS
;
      WAITF = $E0     ; DSID WAIT FLAG (=255 FOR WAIT)
      WAITL = $E1     ; LO BYTE, WAIT PERIOD
      WAITH = $E2     ; HI BYTE, WAIT PERIOD
      CC1   = $F0     ; CLOCK CODE (PB2,3,4)
      REPS  = $F3     ; # OF CONSECUTIVE SCANS
```

```
        INTL  = $F4     ; LOW BYTE OF INTEGRATION COUNT
        INTH  = $F5     ; HIGH  "  "       "       "
        PIXLO = $F6     ; LOW BYTE - NUMBER OF PIXELS TO READOUT
        PIXHI = $F7     ; HIGH BYTE    "    "            "
        RFLAG = $F8     ; REPEAT FLAG (=0 FOR ACQ, =$FF FOR LOOP)
        PSCAN = $FD     ; NUMBER OF PRESCANS BEFORE DATA ACQUISITION
        DATA  = $FE     ; LOW BYTE FOR INDIRECT INDEXED ADDRESSING
                        ;" TO DATA VECTOR ($FF CONTAINS HIGH BYTE)
        * = $2200
;
        LDX     PIXLO
        STX     TC2L3
        LDY     PIXHI
        LDA     DRA3    ;CLEAR CA1 FLAG
STRT1   LDA     IFR3
        AND     #$02
        BEQ     STRT1   ;WAIT FOR FIRST START PULSE
        LDA     DRA3    ;CLEAR CA1 FLAG
;
        STY     TC2H3   ;LOAD TC2 VIA3 WITH PIXEL COUNT
;
SCAN1   LDA     IFR3
        AND     #$20
        BEQ     SCAN1   ;CHECK FOR END OF READOUT
;
        LDA     #$AC
        STA     PCR1    ;FIRE DSID
;
        LDA     WAITF
        BEQ     LOOP    ; IF WAIT FLAG=0 SKIP WAIT ROUTINE
;
        LDA     DRB3
        AND     #$E3    ;SELECT CLOCK CODE 000 (GND)
        STA     DRB3    ;STOP CLOCK
;
        LDA     WAITL
        STA     TC2L1
        LDA     WAITH
        STA     TC2H1   ;LOAD TIMER 2, VIA1 WITH DSID WAIT PERIOD
;
WAIT    LDA     IFR1
        AND     #$20
        BEQ     WAIT    ;WAIT FOR END OF WAIT PERIOD
;
        LDA     DRB3
        ORA     CC1
        STA     DRB3    ;RESTART CLOCK FOR READOUT PERIOD
;
STRT2   LDA     IFR3
        AND     #$02
        BEQ     STRT2   ;WAIT FOR SECOND START PULSE
        LDA     DRA3    ;CLEAR CA1 FLAG
;
        LDA     PIXLO
        STA     TC2L3
```

```
        LDA     PIXHI
        STA     TC2H3   ;LOAD TC2, VIA3 WITH PIXEL COUNT
;
RDOUT   LDA     IFR3
        AND     #$20
        BEQ     RDOUT   ;RESET PDA PIXELS
;
LOOP    LDA     DRB3
        AND     #$E3    ;SELECT CLOCK CODE 000 (GND)
        STA     DRB3    ;STOP CLOCK
;
        LDA     INTL
        STA     TC2L1
        LDA     INTH
        STA     TC2H1   ;LOAD TC2, VIA1 WITH INTEGRATION TIME
;
INT     LDA     IFR1
        AND     #$20
        BEQ     INT     ;WAIT FOR END OF INTEGRATION PERIOD
;
        LDA     DRB3
        ORA     CC1
        STA     DRB3    ;RESTART READOUT CLOCK FOR DATA ACQ.
;
        STX     TC2L3
;
STRTN   LDA     IFR3
        AND     #$02
        BEQ     STRTN   ;WAIT FOR NEXT START PULSE
        LDA     DRA3    ;CLEAR CA1 FLAG
;
        STY     TC2H3   ;LOAD TC2 VIA3 WITH PIXEL COUNT
;
        LDA     DRB1
SAMPL   LDA     IFR3
        AND     #$10
        BEQ     SAMPL   ;WAIT FOR A SAMPLE PULSE (PIXEL READOUT)
        STA     IFR3    ;CLEAR CB1 FLAG
;
        AND     #00
        STA     DRB1    ;TRIGGER CONVERSION
CONT    LDA     IFR3
        AND     #$20
        BEQ     SAMPL   ; CHECK FOR END OF SCAN
;
        DEC     REPS
        BNE     LOOP    ; RESCAN IF REPS>0, ELSE RETURN
        LDA     #$AE
        STA     PCR1
        RTS
        END
```

Flow Chart of System 1 Support Software

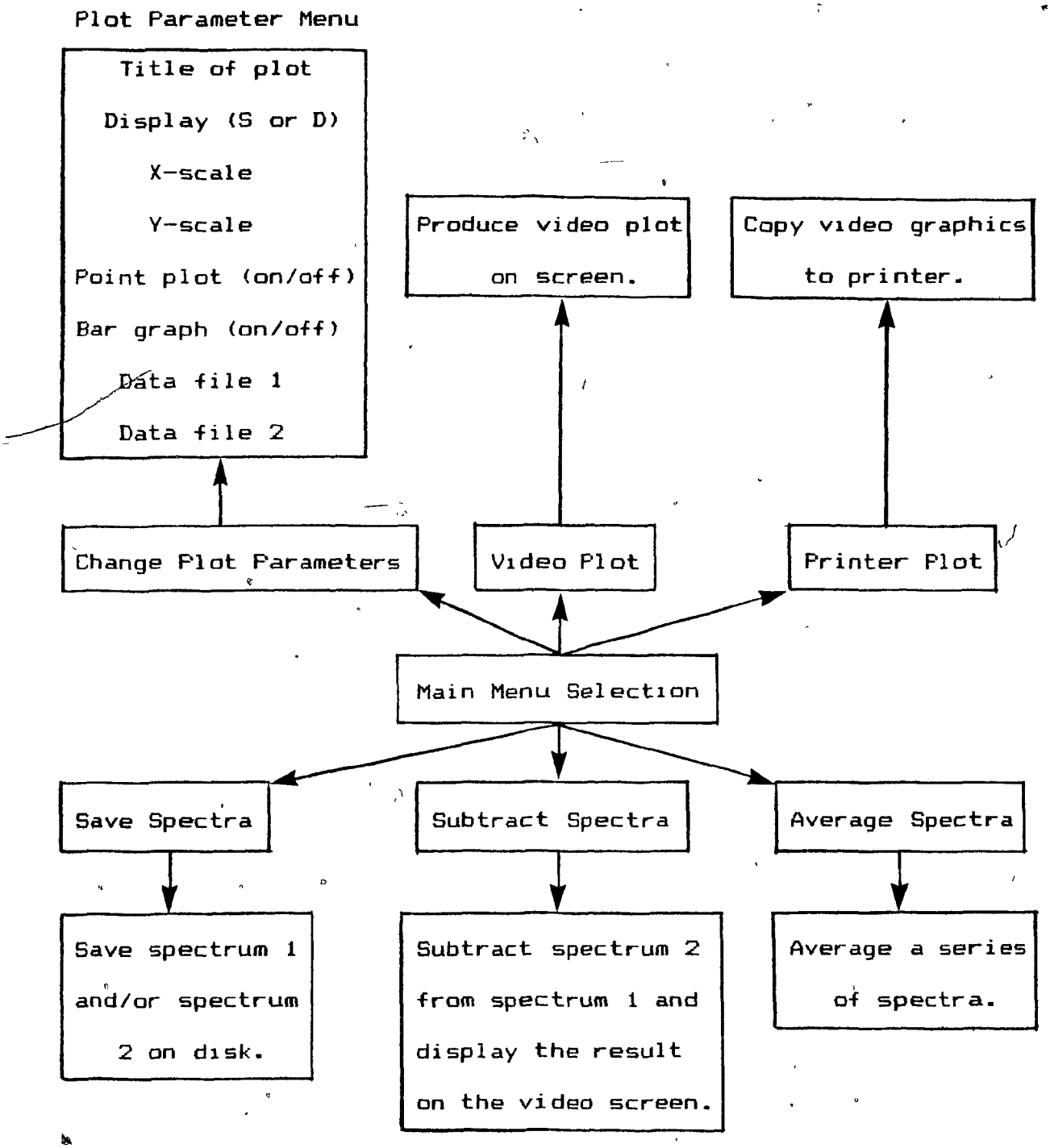

Appendix K - Page Zero Locations

ADDR Hex	ADDR Dec	Function	System
E0	224	DSID wait flag (0=no; 255=yes)	SYS2
E1	225	Low byte of DSID wait period.	"
E2	226	High byte of DSID wait period.	"
F0	240	Clock code 1 - Readout clock.	SYS1/2
F1	241	Clock code 2 - Blurt clock.	"
F2	242	Low byte of timer 1, VIA 3 - Determines PB7 Freq	"
F3	243	Number of sequential scans or Blurts.	"
F4	244	Low byte of integration count.	"
F5	245	High byte of integration count.	"
F6	246	Low byte of number of pixels to readout.	"
F7	247	High byte of number of pixels to readout.	"
F8	248	Repeat flag (0=Acquisition; 255=Infinite loop)	SYS1
F9	249	Low byte of Blurt count.	SYS1/2
FA	250	High byte of Blurt count.	"
FB	251	Index into data vector for spectrum storage.	SYS1
FC	252	Number of diodes to acquire for Blurt mode.	SYS1/2
FD	253	Number of prescans.	SYS1
FE	254	Low byte for indirect address of data vector.	"
FF	255	High byte for indirect address of data vector.	"

```
program profile1(input,output);
(* This program calculates integrated response profiles for an
   ideal image whose width is anywhere from 1 to 50 microns.

   The image is first centred on a diode and the response is
   calculated for diode 0,1 and 2.  Diodes -1 and -2 are not
   dealt with because their response will just be the mirror
   image of diodes 1 and 2.

   After each set of diode responses has been determined, the image
   is translated to the 'right' by 1 micron.

   The output consists of reporting the responses for each diode
   as a function of image translation, as well as the ratio of
   response 0 to response 1.  *)

const m1=0.04165; (* m1 is the result of integrating 0.0833x dx
                     which is the slope of the geometry function G(x) *)

const m2=2.083;   (* m2 is slope of y-intercept vs. diode plot for G(x) *)

const b2=1.542;   (* b2 is intercept of y-intercept vs. diode plot for
                     G(x).  The y-intercept for a diode (d) is
                     +-|m2*d+b2.  m2 is -ve for left zone, +ve for
                     right zone. *)
var a,b,c:real;
var i,n,diode:integer;
var image_width:real;
var left_image_boundary,right_image_boundary:real; (* delimits image *)
var diode_left_boundary,diode_right_boundary:real; (* delimits diode *)
var left_diode_boundary,right_diode_boundary:real; (* edge of left/right
                                                      adjacent diode *)
var b1_left,b1_right:real;
var iteration:array[0..2,0..50] of real; (* records integrated response of
                                            diodes over all image positions *)
external function left_zone(m1,left_image_boundary,right_image_boundary,
        left_diode_boundary,diode_left_boundary,b1_left:real):real;
external function central_zone(left_image_boundary,right_image_boundary,
        diode_left_boundary,diode_right_boundary:real):real;
external function right_zone(m1,left_image_boundary,right_image_boundary,
        right_diode_boundary,diode_right_boundary,b1_right:real):real;
begin
  write('image width in microns? ');
  readln(image_width);
  write('number of iterations? ');
  readln(i);
  left_image_boundary:=-image_width/2;
  right_image_boundary:=image_width/2;
```

```
for n:=0 to 1 do
  begin
    for diode:=0 to 2 do
    begin
      diode_left_boundary:=diode*25.0-6.5;
      diode_right_boundary:=diode*25.0+6.5;
      left_diode_boundary:=diode*25.0-18.5;
      right_diode_boundary:=diode*25.0+18.5;
      b1_left:=-m2*diode+b2;
      b1_right:=m2*diode+b2;


      a:=left_zone(m1,left_image_boundary,right_image_boundary,
                  left_diode_boundary,diode_left_boundary,b1_left);
      b:=central_zone(left_image_boundary,right_image_boundary,
                  diode_left_boundary,diode_right_boundary);
      c:=right_zone(m1,left_image_boundary,right_image_boundary,
                  right_diode_boundary,diode_right_boundary,b1_right);

      iteration[diode,n]:=a+b+c;

    end; (* End of 'diode' loop. *)

    left_image_boundary:=left_image_boundary+1;
    right_image_boundary:=right_image_boundary+1; (* Shift image 1 micron. *)

  end; (* End of 'iteration' loop. *)

  writeln('iteration':10,'diode 0':9,'diode 1':9,'diode 2':9,
        'diode 0/diode 1':18);

  for n:=0 to 1 do
  begin
    write(n:5,'      ');
    for diode:=0 to 2 do write(iteration[diode,n]/image_width:5:3,'    ');
    if iteration[1,n] > 0 then
    writeln(iteration[0,n]/iteration[1,n]:11:3)
    else writeln(' ');
  end;
end. (* End of program 'profile1'. *)
```

```
module lzone1;

(* This module calculates the integrated response of the left
   zone of a given diode.  All variables are declared in the
   mainline program. *)


function left_zone(m1,left_image_boundary,right_image_boundary,
                   left_diode_boundary,diode_left_boundary,b1_left:real):real;
begin
     left_zone:=0;
     if left_image_boundary <= left_diode_boundary then
       if ((right_image_boundary < diode_left_boundary) and
          (right_image_boundary > left_diode_boundary)) then
         left_zone:=(m1*sqr(right_image_boundary)+
                     b1_left*right_image_boundary)
                   - (m1*sqr(left_diode_boundary)+
                     b1_left*left_diode_boundary)
       else if right_image_boundary >= diode_left_boundary then
         left_zone:=(m1*sqr(diode_left_boundary)+
                     b1_left*diode_left_boundary)
                   - (m1*sqr(left_diode_boundary)+
                     b1_left*left_diode_boundary)
            else left_zone:=0
     else
       if left_image_boundary < diode_left_boundary then
         if right_image_boundary < diode_left_boundary then
           left_zone:=(m1*sqr(right_image_boundary)+
                       b1_left*right_image_boundary)
                     - (m1*sqr(left_image_boundary)+
                       b1_left*left_image_boundary)
         else
           left_zone:=(m1*sqr(diode_left_boundary)+
                       b1_left*diode_left_boundary)
                     - (m1*sqr(left_image_boundary)+
                       b1_left*left_image_boundary);
end;
(* Completes integration of G(x)P(x)dx for left zone. *)

modend.
```

```
module czone1;

(* This module calculates the integrated response of the central zone
   of a given diode.  All variables are declared in the mainline program.*)

function central_zone(left_image_boundary,right_image_boundary,
                      diode_left_boundary,diode_right_boundary:real):real;
begin
     central_zone:=0;

     if left_image_boundary <= diode_left_boundary then
       if ((right_image_boundary < diode_right_boundary) and
          (right_image_boundary > diode_left_boundary)) then
         central_zone:=right_image_boundary-diode_left_boundary
       else if right_image_boundary >= diode_right_boundary then
         central_zone:=diode_right_boundary-diode_left_boundary
           else central_zone:=0
     else
       if right_image_boundary < diode_right_boundary then
         central_zone:=right_image_boundary-left_image_boundary
       else if left_image_boundary < diode_right_boundary then
         central_zone:=diode_right_boundary-left_image_boundary;
end;

(* Completes integration of G(x)P(x)dx for central zone. *)

modend.
```

```
module rzone1;

(* This module calculates the integrated response of the right zone
   of a given diode.  All variables are declared in the mainline program. *)

function right_zone(m1,left_image_boundary,right_image_boundary,
                    right_diode_boundary,diode_right_boundary,
                    b1_right:real):real;
begin
     right_zone:=0;

     if left_image_boundary <= diode_right_boundary then
       if ((right_image_boundary < right_diode_boundary) and
          (right_image_boundary > diode_right_boundary)) then
         right_zone:=(-m1*sqr(right_image_boundary)+
                      b1_right*right_image_boundary)
                   - (-m1*sqr(diode_right_boundary)+
                      b1_right*diode_right_boundary)
       else if right_image_boundary >= right_diode_boundary then
         right_zone:=(-m1*sqr(right_diode_boundary)+
                      b1_right*right_diode_boundary)
                   - (-m1*sqr(diode_right_boundary)+
                      b1_right*diode_right_boundary)
            else right_zone:=0
     else
       if right_image_boundary < right_diode_boundary then
         right_zone:=(-m1*sqr(right_image_boundary)+
                      b1_right*right_image_boundary)
                   - (-m1*sqr(left_image_boundary)+
                      b1_right*left_image_boundary)
       else if ((left_image_boundary > diode_right_boundary) and
               (left_image_boundary < right_diode_boundary)) then
         right_zone:=(-m1*sqr(right_diode_boundary)+
                      b1_right*right_diode_boundary)
                   - (-m1*sqr(left_image_boundary)+
                      b1_right*left_image_boundary);
end;

(* Completes integration of G(x)P(x)dx for right zone. *)

modend.
```

```
program profile2(input,output);
(* This program calculates integrated response profiles for two
   closely spaced, ideal images.  The width of the two images
   and the spacing between them are user input parameters.

   The images are first centred on a diode and the response is
   calculated for diode 0,1 and 2.  Diodes -1 and -2 are not
   dealt with because their response will just be the mirror
   image of diodes 1 and 2.

   After each set of diode responses has been determined, the image
   pair is translated to the 'right' by 1 micron.

   The output consists of reporting the responses for each diode
   as a function of image translation, as well as the ratio of
   response 0 to response 1.  *)

const m1=0.04165; (* m1 is the result of integrating 0.0833x dx
                     which is the slope of the geometry function G(x) *)

const m2=2.083;   (* m2 is slope of y-intercept vs. diode plot for G(x) *)

const b2=1.542;   (* b2 is intercept of y-intercept vs. diode plot for
                     G(x).  The y-intercept for a diode (d) is
                     +-|m2*d+b2.  m2 is -ve for left zone, +ve for
                     right zone. *)
var iteration,n,diode:integer;
var image_width,image_separation:real;
var image1_left_boundary,image1_right_boundary:real; (* delimits image1 *)
var image2_left_boundary,image2_right_boundary:real; (* delimits image2 *)
var diode_left_boundary,diode_right_boundary:real; (* delimits diode *)
var left_diode_boundary,right_diode_boundary:real; (* edge of left/right
                                                      adjacent diode *)
var b1_left,b1_ri, t:real;
var integrated_response:array[0..2,0..50] of real; (* records integrated
                                                      response of diodes over
                                                      all image positions*)
external function left_zone(m1,left_image_boundary,right_image_boundary,
        left_diode_boundary,diode_left_boundary,b1_left:real):real;
external function central_zone(m1,left_image_boundary,right_image_boundary,
        diode_left_boundary,diode_right_boundary:real):real;
external function right_zone(m1,left_image_boundary,right_image_boundary,
        right_diode_boundary,diode_right_boundary,b1_right:real):real;
begin
  write('image width in microns? ');
  readln(image_width);
  write('number of iterations? ');
  readln(n);
  write('image separation in microns?');
  readln(image_separation);

  image1_left_boundary:=-image_separation/2-image_width/2;
  image1_right_boundary:=-image_separation/2+image_width/2;
  image2_left_boundary:=image_separation/2-image_width/2;
  image2_right_boundary:=image_separation/2+image_width/2;
```

```
for iteration:=0 to n do
begin
  for diode:=0 to 2 do
  begin
    diode_left_boundary:=diode*25.0-6.5;
    diode_right_boundary:=diode*25.0+6.5;
    left_diode_boundary:=diode*25.0-18.5;
    right_diode_boundary:=diode*25.0+18.5;
    b1_left:=-m2*diode+b2;
    b1_right:=m2*diode+b2;

    integrated_response[diode,iteration]:=left_zone(m1,image1_left_boundary,
    image1_right_boundary,left_diode_boundary,diode_left_boundary,b1_left)+
                                central_zone(m1,image1_left_boundary,
    image1_right_boundary,diode_left_boundary,diode_right_boundary)+
                                right_zone(m1,image1_left_boundary,
    image1_right_boundary,right_diode_boundary,diode_right_boundary,b1_right)+
                                left_zone(m1,image2_left_boundary,
    image2_right_boundary,left_diode_boundary,diode_left_boundary,b1_left)+
                                central_zone(m1,image2_left_boundary,
    image2_right_boundary,diode_left_boundary,diode_right_boundary)+
                                right_zone(m1,image2_left_boundary,
    image2_right_boundary,right_diode_boundary,diode_right_boundary,b1_right);

    end; (* End of 'diode' loop. *)

    image1_left_boundary:=image1_left_boundary+1;
    image1_right_boundary:=image1_right_boundary+1; (* Shift image 1 micron.
*)
    image2_left_boundary:=image2_left_boundary+1;
    image2_right_boundary:=image2_right_boundary+1;

  end; (* End of 'iteration' loop. *)

  writeln('iteration':10,'diode 0':9,'diode 1':10,'diode 2':10,
       'IRR0':8,'IRR1':8);

  for iteration:=0 to n do
  begin
    write(iteration:5,'      ');
    for diode:=0 to 2 do
      write(integrated_response[diode,iteration]/(2*image_width):5:3,'     ');
    if integrated_response[1,iteration] > 0 then

  write(integrated_response[0,iteration]/integrated_response[1,iteration]:
       2:3)

    else writeln(' ');

    if integrated_response[2,iteration] > 0 then

  writeln(integrated_response[1,iteration]/integrated_response[2,iteration]:
       10:3)
```

```
    else writeln(' ')
  end
end. (* End of program 'profile2'. *)
```

```
module lzone2;

(* This module calculates the integrated response of the left
   zone of a given diode.  All variables are declared in the
   mainline program. *)

function left_zone(ml,image_left_boundary,image_right_boundary,
                   left_diode_boundary,diode_left_boundary,bl_left:real):real;
begin
     left_zone:=0;
     if image_left_boundary <= left_diode_boundary then
       if ((image_right_boundary < diode_left_boundary) and
          (image_right_boundary > left_diode_boundary)) then
         left_zone:=(ml*sqr(image_right_boundary)+
                     bl_left*image_right_boundary)
                   - (ml*sqr(left_diode_boundary)+
                     bl_left*left_diode_boundary)
       else if image_right_boundary >= diode_left_boundary then
         left_zone:=(ml*sqr(diode_left_boundary)+
                     bl_left*diode_left_boundary)
                   - (ml*sqr(left_diode_boundary)+
                     bl_left*left_diode_boundary)
          else left_zone:=0
     else
       if image_left_boundary < diode_left_boundary then
         if image_right_boundary < diode_left_boundary then
           left_zone:=(ml*sqr(image_right_boundary)+
                       bl_left*image_right_boundary)
                     - (ml*sqr(image_left_boundary)+
                       bl_left*image_left_boundary)
         else
           left_zone:=(ml*sqr(diode_left_boundary)+
                       bl_left*diode_left_boundary)
                     - (ml*sqr(image_left_boundary)+
                       bl_left*image_left_boundary);
end;
(* Completes integration of G(x)P(x)dx for left zone. *)

modend.
```

```
module czone2;

(* This module calculates the integrated response of the central zone
   of a given diode.  All variables are declared in the mainline program.*)

function central_zone(ml,image_left_boundary,image_right_boundary,
                      diode_left_boundary,diode_right_boundary:real):real;
begin
      central_zone:=0;

      if image_left_boundary <= diode_left_boundary then
        if ((image_right_boundary < diode_right_boundary) and
           (image_right_boundary > diode_left_boundary)) then
          central_zone:=image_right_boundary-diode_left_boundary
        else if image_right_boundary >= diode_right_boundary then
          central_zone:=diode_right_boundary-diode_left_boundary
            else central_zone:=0
      else
        if image_right_boundary < diode_right_boundary then
          central_zone:=image_right_boundary-image_left_boundary
        else if image_left_boundary < diode_right_boundary then
          central_zone:=diode_right_boundary-image_left_boundary;
end;

(* Completes integration of G(x)P(x)dx for central zone. *)

modend.
```

```
module rzone2;

(* This module calculates the integrated response of the right zone
   of a given diode.  All variables are declared in the mainline program. *)

function right_zone(ml,image_left_boundary,image_right_boundary,
                    right_diode_boundary,diode_right_boundary,
                    bl_right:real):real;
begin
      right_zone:=0;

      if image_left_boundary <= diode_right_boundary then
        if ((image_right_boundary < right_diode_boundary) and
           (image_right_boundary > diode_right_boundary)) then
          right_zone:=(-ml*sqr(image_right_boundary)+
                       bl_right*image_right_boundary)
                    - (-ml*sqr(diode_right_boundary)+
                       bl_right*diode_right_boundary)
        else if image_right_boundary >= right_diode_boundary then
          right_zone:=(-ml*sqr(right_diode_boundary)+
                       bl_right*right_diode_boundary)
                    - (-ml*sqr(diode_right_boundary)+
                       bl_right*diode_right_boundary)
             else right_zone:=0
      else
        if image_right_boundary < right_diode_boundary then
          right_zone:=(-ml*sqr(image_right_boundary)+
                       bl_right*image_right_boundary)
                    - (-ml*sqr(image_left_boundary)+
                       bl_right*image_left_boundary)
        else if ((image_left_boundary > diode_right_boundary) and
                 (image_left_boundary < right_diode_boundary)) then
          right_zone:=(-ml*sqr(right_diode_boundary)+
                       bl_right*right_diode_boundary)
                    - (-ml*sqr(image_left_boundary)+
                       bl_right*image_left_boundary);
end;

(* Completes integration of G(x)P(x)dx for right zone. *)

modend.
```

```
program profile3(input,output);
(* This program is a specialized version of PROFILE2.SRC which
   calculates integrated response and integrated response ratio
   data for two closely spaced, ideal images.  The image widths
   range from 5 to 30 microns in steps of 5 microns and the image
   separations range from 2 to 50 microns in increments of 2
   microns.

   The images are first centred on a diode and the response is
   calculated for diode 0,1 and 2.  Diodes -1 and -2 are not
   dealt with because their response will just be the mirror
   image of diodes 1 and 2.

   After each set of diode responses has been determined, the image
   pair is translated to the 'right' by 1 micron. 50 translations
   are carried out for each image width/image separation case.

   The output consists of reporting the responses for each diode
   as a function of image translation, as well as the ratio of
   response 0 to response 1 and of response 1 to response 2.  *)

const m1=0.04165; (* m1 is the result of integrating 0.0833x dx
                     which is the slope of the geometry function
                     G(x) *)

const m2=2.083;   (* m2 is slope of y-intercept vs. diode plot for
                     G(x) *)

const b2=1.542;   (* b2 is intercept of y-intercept vs. diode plot for
                     G(x).  The y-intercept for a diode (d) is
                     +-)m2*d+b2.  m2 is -ve for left zone, +ve for
                     right zone. *)
var iteration,n,diode:integer;
var image_width,image_separation:real;
var image1_left_boundary,image1_right_boundary:real; (*delimits image1*)
var image2_left_boundary,image2_right_boundary:real; (*delimits image2*)
var diode_left_boundary,diode_right_boundary:real; (* delimits diode *)
var left_diode_boundary,right_diode_boundary:real; (* edge of left/right
                                                      adjacent diode *)
var b1_left,b1_right:real;
var integrated_response:array[0..2,0..50] of real; (* records integrated
                                                      response of diodes
                                                      over all image
                                                      positions*)
external function left_zone(m1,left_image_boundary,right_image_boundary,
                            left_diode_boundary,diode_left_boundary,
                            b1_left:real):real;
external function central_zone(m1,left_image_boundary,
                               right_image_boundary,diode_left_boundary,
                               diode_right_boundary:real):real;
external function right_zone(m1,left_image_boundary,
                             right_image_boundary,right_diode_boundary,
                             diode_right_boundary,b1_right:real):real;
```

```
begin
 n:=50;
 image_width:=10;

 while image_width <= 30 do
  begin
   image_separation:=2;
   while image_separation <= 50 do
    begin
     image1_left_boundary:=-image_separation/2-image_width/2;
     image1_right_boundary:=-image_separation/2+image_width/2;
     image2_left_boundary:=image_separation/2-image_width/2;
     image2_right_boundary:=image_separation/2+image_width/2;

     for iteration:=0 to n do
      begin
       for diode:=0 to 2 do
        begin
         diode_left_boundary:=diode*25.0-6.5;
         diode_right_boundary:=diode*25.0+6.5;
         left_diode_boundary:=diode*25.0-18.5;
         right_diode_boundary:=diode*25.0+18.5;
         b1_left:=-m2*diode+b2;
         b1_right:=m2*diode+b2;

         integrated_response[diode,iteration]:=
          left_zone(m1,image1_left_boundary,image1_right_boundary,
                    left_diode_boundary,diode_left_boundary,b1_left)+
          central_zone(m1,image1_left_boundary,image1_right_boundary,
                       diode_left_boundary,diode_right_boundary)+
          right_zone(m1,image1_left_boundary,image1_right_boundary,
                    right_diode_boundary,diode_right_boundary,b1_right)+
          left_zone(m1,image2_left_boundary,image2_right_boundary,
                    left_diode_boundary,diode_left_boundary,b1_left)+
          central_zone(m1,image2_left_boundary,image2_right_boundary,
                       diode_left_boundary,diode_right_boundary)+
          right_zone(m1,image2_left_boundary,image2_right_boundary,
                    right_diode_boundary,diode_right_boundary,b1_right);

        end; (* End of 'diode' loop. *)

       image1_left_boundary:=image1_left_boundary+1;
       image1_right_boundary:=image1_right_boundary+1; (* Shift image
                                                          1 micron. *)
       image2_left_boundary:=image2_left_boundary+1;
       image2_right_boundary:=image2_right_boundary+1;

      end; (* End of 'iteration  loop. *)

     writeln('Image width = ',image_width:3:1);
     writeln('Image separation = ',image_separation:3:1);
     writeln;

     writeln('iteration':10,'diode 0':9,'diode 1':10,'diode 2':10,
             'IRR0':8,'IRR1':10);
```

```
      for iteration:=0 to n do
       begin
        write(iteration:5,'    - ');
        for diode:=0 to 2 do
         write(integrated_response[diode,iteration]/
              (2*image_width):5:3,'    ');
        if integrated_response[1,iteration] > 0 then
         write(integrated_response[0,iteration]/
              integrated_response[1,iteration]:2:3)
        else write('     ');
        if integrated_response[2,iteration] > 0 then
         writeln(integrated_response[1,iteration]/
                 integrated_response[2,iteration]:10:3)
        else writeln
       end;

      writeln(chr(12));
      image_separation:=image_separation+2
     end; (* End separation loop *)

    image_width:=image_width+5
   end; (* End image_width loop *)

end. (* End of program 'profile3'. *)
```

Appendix M - Three Dimensional Plotting and Spectrum Acquisition Software

```
program PLOT_3D;

(* This program acquires up to ten 1024 point PDA spectra and
   plots the series in 3-D. *)

const
     X_OFFSET = 10;
     Y_OFFSET = 96;

type

     DATA_ARRAY = array[1: 10240] of integer;

var
    I,io_res,
    NUM_PER_SCAN,
    NUM_SCANS,
    NUM_POINTS,
    FIRST_TO_PLOT,
    LAST_TO_PLOT,
    X_SHIFT,
    Y_SHIFT,
    Y_MIN,
    Y_MAX,
    X_RANGE,
    Y_TEMP      : integer;
    THE_DATA    : DATA_ARRAY;
    DARK        : array[1:1024] of integer;
    DATA_FILE     : File;
    DARK_FILE     : File;
    DATE        : string[8];
    COM_CH,DARK_CH : char;
    EXT   : string[3];


external procedure GET_PDA(THE_DATA.:integer; NUM_PTS : integer);


function Y(SCAN,POINT:integer):integer;
   begin
     Y := THE_DATA[(SCAN - 1) *NUM_PER_SCAN + POINT];
   end;
```

```
procedure PLOT_IT;

var
POINT,
SCAN,
FRONT_SCAN,
BACK_SCAN : integer;

begin
        Y_MAX := 2548;
        Y_MIN := 0;

        write('Enter number of scans : ');
        readln(NUM_SCANS);
        write('Enter number of points per scan :');
        readln(NUM_PER_SCAN);

        write('Enter first point to  be plotted : ');
        readln(FIRST_TO_PLOT);
        write('Enter last point to be plotted : ');
        readln(LAST_TO_PLOT);

        for SCAN := 1 to NUM_SCANS do
          for POINT := 1 to NUM_PER_SCAN do
            THE_DATA[(SCAN-1)*NUM_PER_SCAN + POINT] := Y(SCAN,POINT)-
                                                       DARK[POINT] +
                                                       500;
        for BACK_SCAN := NUM_SCANS downto 2 do
          for FRONT_SCAN := 1 to (BACK_SCAN - 1) do
            begin
              Y_SHIFT := (BACK_SCAN-FRONT_SCAN)*Y_OFFSET;
              X_SHIFT := (Back_scan-FRONT_SCAN)* X_OFFSET;
              for POINT := FIRST_TO_PLOT to (LAST_TO_PLOT-((BACK_SCAN-FRONT_SCAN) * X_OFFSET)) do
                if (Y(BACK_SCAN,POINT)+Y_SHIFT) < Y(FRONT_SCAN,POINT+X_SHIFT) then
                  setbit(THE_DATA[(BACK_SCAN-1) *NUM_PER_SCAN+POINT],15);

              writeln('Scan ',BACK_SCAN, ' has had features hidden by scan ', FRONT_SCAN, ' removed');

            end;

        X_RANGE := (LAST_TO_PLOT-FIRST_TO_PLOT) + NUM_SCANS * X_OFFSET;

        Y_MAX := Y_MAX + NUM_SCANS * Y_OFFSET;
        write('Turn on aux port and hit return');
        readln;
        write(chr(27),'.I81;;17:',chr(27),'.N;19:');
        write('SC',-5 * X_RANGE div 100 ,',', X_RANGE + 5 * X_RANGE div 100,',',
              Y_MIN -5 * (Y_MAX-Y_MIN) div 100,',',Y_MAX + 5 * (Y_MAX-YMIN) div
              100,';');
```

```
                for SCAN := 1 to NUM_SCANS do
                  begin
                    X_SHIFT := (SCAN-1)*X_OFFSET;
                    Y_SHIFT := (SCAN-1)*Y_OFFSET;
                    write('PU',1+X_SHIFT,',',Y(SCAN,1)+YSHIFT,',');

                    for POINT := FIRST_TO_PLOT to LAST_TO_PLOT do
                     begin
                       if tstbit(Y(SCAN,POINT),15) then
                          begin
                            clrbit(THE_DATA[(SCAN-1) *NUM_PER_SCAN+POINT],15);
                            write('PU',POINT+XSHIFT,',',Y(SCAN,POINT)+YSHIFT,',');
                          end
                        else
                          write(POINT+XSHIFT,',',Y(SCAN,POINT)+YSHIFT,'PD,');
                     end;
                  end;
   READLN;

          end;

begin

write('Enter date for experimental data (e.g. FEB22/84) :');
readln(DATE);

repeat

write('Do you wish to Acquire, Dark, Plot, Save, Load ,^C ?');
readln(COMCH);

case COMCH of

'D','d' : begin
            write('Load or Acquire dark');
            readln(DARK_CH);
            if (DARK_CH = 'L') or (DARK_CH = 'l') then
              begin
                assign(DARK_FILE,concat('B:',DATE,'.DRK'));
                reset(DARK_FILE);

                blockread(DARK_FILE,DARK,IO_RES, 2048, -1 );
                if IO_RES <> 0 then
                  writeln('Error loading dark ');
              end
            else
              begin

                write('Ready to acquire dark scan, press return when ready');
                readln;

                writeln('Waiting for dark scan');

                GETPDA(addr(DARK),1024);
```

```
                assign(DARK_FILE,concat('B:',DATE,'.DRK'));
                rewrite(DARK_FILE);

                blockwrite(DARK_FILE,DARK,IO_RES, 2048,-1 );
                if IO_RES <> 0 then
                  writeln('Error saving dark ');
              end;

            close(DARK_FILE,IORES);

            if IO_RES = 255 then
              writeln('Error closing dark');

          end;

'A','a' : begin

            write('Enter number of points coming:');
            readln(NUM_POINTS);

            GETPDA(addr(THE_DATA),NUM_POINTS);

            writeln('Data Acquired');

          end;

'P','p' : PLOT_IT;

'S','s' : begin

            write('Enter data set extension :');
            readln(EXT);

            assign(DATA_FILE,concat('B:',DATE,'.',EXT));
            rewrite(DATA_FILE);

            blockwrite(DATA_FILE,THE_DATA,IO_RES,10240 * 2,-1);
            if I <> 0 then
              begin
                Writeln('Error in writing file');
                exit;
              end;

           close(DATA_FILE,IO_RES);
           if IO_RES = 255 then
             writeln('Error closing file');

          end;

'L','l' : begin

            write('Enter data set extension :');
            readln(EXT);

            assign(DATA_FILE,concat('B:',DATE,'.',EXT));
```

```
            reset(DATA_FILE);

            blockread(DATA_FILE,THE_DATA,IO_RES,10240 * 2,-1);
            if I <> 0 then
              begin
                Writeln('Error in reading file');
                exit;
              end;
            close(DATA_FILE,IO_RES);
            if IO_RES = 255 then
              writeln('Error closing file');
           end;

'' : exit;

else
writeln('Improper selection try again');

end;

until false;
end.
```